SELECTIVE CRITERIA

IN

WERNER CLATHRATES

A thesis submitted to the

UNIVERSITY OF CAPE TOWN

in fulfilment of the requirements for the degree of

MASTER OF SCIENCE

by

LAURENCE LAVELLE

B.Sc.(Hons) (Cape Town)

Department of Physical Chemistry

University of Cape Town

Rondebosch

7700

Republic of South Africa

August 1988

ACKNOWLEDGEMENTS

I would like to thank:

Professor L. R. Nassimbeni, for his supervision, patience and good humour.

Dr M. Niven, for her advice and friendly words and to Professor M. Caira for proof-reading.

Mike Taylor for assistance with the programs and to my colleagues in the longroom who accepted my working hours.

Rob Austin who unexpectedly offered the use of his personal computer.

Tanya, family and friends for their love and support.

Financial assistance from the University of Cape Town and the C.S.I.R.

This work is dedicated to my parents, as a token of my appreciation for the education that they have given me.

PUBLICATIONS

We have submitted the following papers based on this thesis and other related work:

1. To Acta Crystallographica: Studies in Werner Clathrates. Part 12. Structure and thermal analysis of bis(isothiocyanato)tetra (4-phenylpyridine)nickel(II).benzene (1:4).
Laurence Lavelle, Luigi R. Nassimbeni, Margaret L. Niven and Michael W. Taylor*.

2. To the Journal of the Chemical Society, Dalton Transactions: Studies in Werner Clathrates. Part 13. Structures of bis(isothiocyanato)tetra(4-vinylpyridine)nickel(II) with systematically changing cyclic hydrocarbons.
Laurence Lavelle, Luigi R. Nassimbeni* and Margaret L. Niven.

ABSTRACT

We have elucidated the structures of a series of Werner Clathrates with systematically changing guest molecules.
The host is the inorganic coordination compound bis(isothiocyanato)tetra(4-vinylpyridine)nickel(II), $[Ni(NCS)_2(4\text{-}ViPy)_4]$. The guests are mixtures of tetrahydrofuran and the cyclic hydrocarbons: cyclohexane, cyclohexene, 1,3-cyclohexadiene, 1,4-cyclohexadiene and benzene.

Host to guest ratios were elucidated by density and proton nuclear magnetic resonance spectroscopy. The thermal characteristics of the compounds were analysed by thermogravimetric analysis and differential thermal analysis.

The structures of two related compounds $[Ni(NCS)_2(Py)_4]$ and $[Ni(NCS)_2(Py)_4]$.nbenzene were also studied.

CONTENTS PAGE

CHAPTER 1

INTRODUCTION

1.1 Host-guest compounds.

The first mention of the word Clathrate as a contemporary scientific term was by H. M. Powell in 1948[1.1]. This term was used to describe crystalline compounds in which molecules of one component form an enclosing structure around smaller molecules of a second type. Clathrate originates from the Latin word `clathratus´ meaning enclosed or protected by cross bars of a grating. This is a most apt description as today there is much work being done to elucidate the nature of these secondary interactions which act as cross bars. This has led to the need of a more precise terminology.

Inclusion compounds fall under the general class of compounds that are porous on the molecular scale and in some cases at the atomic scale, where the enclosing structure is the host within which the smaller guest molecules reside. These structures are classified by:

a) the host-guest type and their interaction

When their interaction is a coordination, the structure is called a complex, as in the crown ethers and cryptands. As a result of a relatively strong binding force these complexes retain their identity in solution. When the guest is retained by steric barriers, that is,

when their interaction is at the level of van der Waals forces, the structure is called a clathrate, as in the β-hydroquinones, Hofmann's compound, the cyclodextrins, Dianin's compound and the Werner Clathrates. Here the binding force is weaker and often without direction, hence these clathrates normally lose their identity in solution. It is noted that this loss of identity in solution occurs to varying degrees as salts of the general formula $M[Al_2R_6X]$ (host)[1.2] and aromatic molecules (guest) form more ordered structures than is usually observed in the liquid phase. These inclusion compounds are called Liquid Clathrates. Since all host-guest structures cannot be classified as either complexes or clathrates, the borderline cases must be treated as complex/clathrate hybrids. Structures which demonstrate a certain degree of coordinative properties but have a dominant clathrate character, are called coordinatoclathrates. Structures which demonstrate a certain degree of clathrate properties but have a dominant coordinative character, are called clathratocomplexes. The majority of the crown ether complexes with neutral guest molecules are examples of clathratocomplexes.

b) the topology of the host-guest structure

With this criterion there are two major distinctions: intramolecular and extramolecular host-guest structures. The intramolecular structures are inclusion compounds which operate via any sort of host cavity (cavitate). Thus, we have the following topologies for cavitates displaying increasing encapsulation: two-dimensional open layer (intercalate), sandwich (coronate) and ring structures

(podate); one-dimensional open channel structures (tubulates); pocket like host arrangements (aediculate) and, finally, totally enclosed cage structures (cryptates). The extramolecular structures are addition compounds (adducts) which do not contain a host cavity. Typical examples of adducts are charge transfer and hydrogen-bonded complexes.

c) the number of various components forming the structure[1.3].

In this last division further clarification is obtained by specifying the total number of individual components (in a chemical sense) involved in the respective host-guest compound. Finally a more precise classification is the ratio of host to guest in the host-guest unit.

As already used for the crown ethers[1.4], it is possible to distinguish between a structure with host only and the host-guest structure by using the terminology -and and -ate respectively. Thus for a guest free structure the terms clathrand, tubuland and cavitand are used and similarly for their respective host-guest structures clathrate, tubulate and cavitate.

The above guidelines are useful when describing a host-guest structure, and are sufficiently flexible to allow varying degrees of description or classification.

The following is a brief description of host-guest compounds with characteristics similar to the Werner Clathrates which are discussed in greater detail in section 1.2. In the Werner Clathrates the nature of the host-host, host-guest and guest-guest interaction is at the

van der Waals level.

The following are not included: zeolites, cyclodextrins, crown ethers and cryptands. The zeolites are industrially versatile and form a large section as inclusion compounds. These macromolecular compounds are completely stable (crystal remains intact) in the absence of guest molecules owing to the partly covalent and partly ionic bonding of the host atoms. The fundamental building units in natural zeolites are tetrahedra SiO_4 and AlO_4 and are tectosilicates, that is they are formed by the linking together of these tetrahedra to give three-dimensional anionic networks in which each oxygen of a given tetrahedron is shared between this tetrahedron and one of four others. The cyclodextrins are macrocyclic bioorganic compounds (covalently linked α-1,4-D-glucopyranose units) and the crown ethers and cryptands have a coordination between the host and guest, classifying them as complexes as mentioned earlier.

The β-hydroquinone/hydrogen sulphide cryptato-clathrate (3:1) was prepared by Wohler[1.5] in 1849. However it was not until the pioneering X-ray work of Palin and Powell[1.6, 1.7] in 1947 that the true nature of the β-hydroquinone structures was determined.

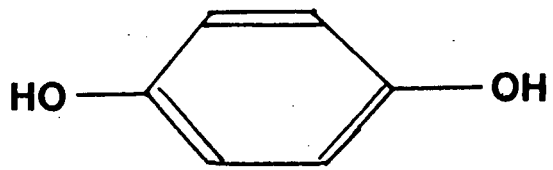

Figure 1.1 β-Hydroquinone

β-Hydroquinone forms discrete spherical cages by the linking of the molecules through their OH-groups. Six oxygen atoms of six different

molecules form hydrogen-bonded hexagons which completely enclose one small guest molecule per cavity, e.g. Ar, Kr, C_2H_2, HCl.

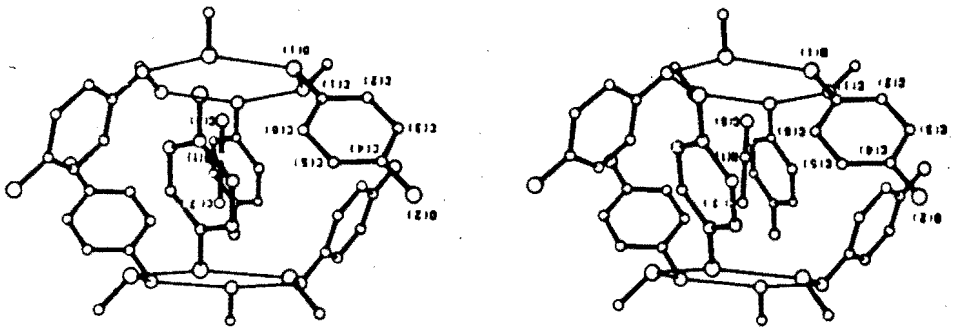

Figure 1.2 A stereo drawing showing a CH_3NC guest molecule trapped inside a cage in the structure of β-hydroquinone. Hydrogens omitted[1.20].

Powell further showed that if larger molecules are included, the hydroquinone lattice is distorted to form oblong cavities. This distortion increases in the series CH_3OH, SO_2, CO_2 and CH_3CN. This provides an experimental system to test the theoretical models of host-guest interaction with minimal guest-guest interaction.

Hofmann's benzene compound $Ni(CN)_2NH_3.C_6H_6$ (1:2) was reported in 1897[1.8] and is the prototype of the Hofmann-type and analogous cryptates formed by various combinations between ammine- or amine-metal(II)tetracyanometallate(II) hosts and aromatic guest molecules. About half a century later Powell and Rayner[1.9, 1.10] determined its structure.

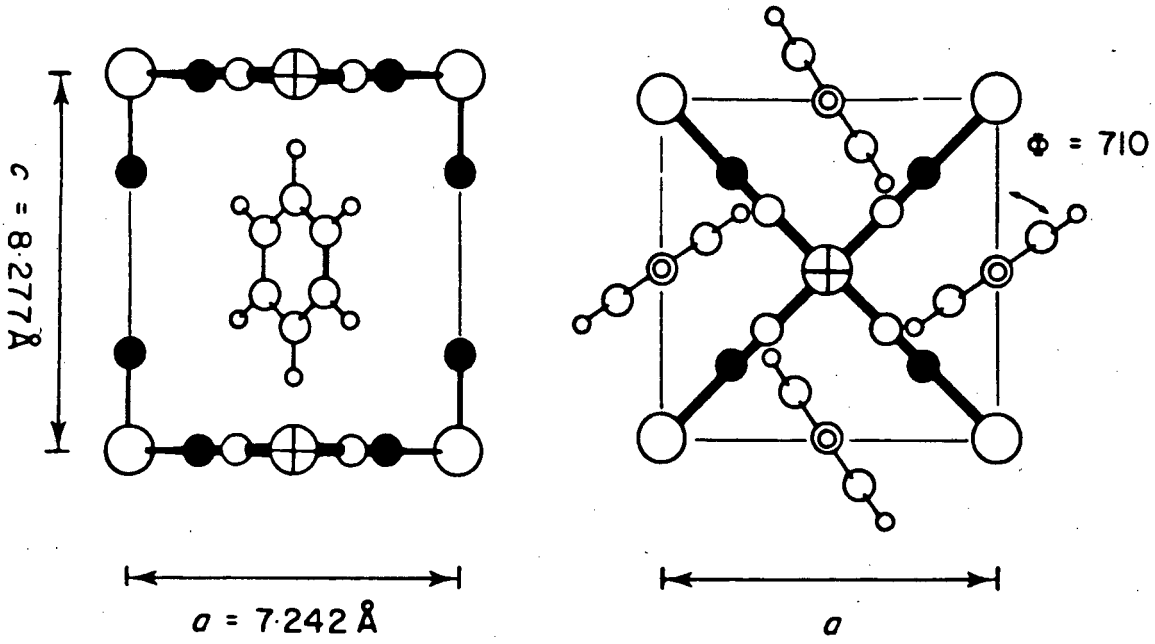

Figure 1.3 Structure of Hofmann's benzene cryptate $Ni(NH_3)_2Ni(CN)_4.2C_6H_6$[1.11]. Large open circle, six coordinate Ni; crossed large circle, square planar Ni; solid circle, N; open circle, C; small open circle, H. Protons of NH_3 are not shown.

There are two kinds of nickel(II) atoms: one exhibits square planar coordination (tetracyanonickelate(II)), and the other has an octahedral array of nitrogen atoms about it - four from the tetracyanonickelate(II) moieties and two from the trans ammine ligands. This forms a layered structure of extended metal complex sheets with the ammonia molecules protruding above and below the sheets giving rise to cavities. The benzene guest lies within these cavities, perpendicular to the sheets. Hosts of the Hofmann type can include five- or six-membered aromatic molecules without bulky substituents (alkyl, halo, nitro, etc.). When a unidentate or bidentate amine with bulky substituents is introduced into the host structure, the substituents occupy the cavity partly or wholly in

place of a guest molecule. According to the number of cavities (0, 1, 2 and 3) occupied by substituents the number of guest molecules in the general formula may vary stepwise from 2, 3/2, 1 to 1/2.
The inclusion of benzene into Hofmann's host was applied to the purification of benzene[1.12]; the benzene recovered from Ni-Ni-Bz showed $n_4^{20} = 1.5011$, $d_4^{20} = 0.87904$, and a melting point of 5.535 °C.
A patent has been issued[1.13] for the recovery of benzene from hydrocarbon stocks using Hofmann's clathrate[1.14].

Dianin's compound 4-p-hydroxyphenyl-2,2,4-trimethylchroman was first prepared by A. P. Dianin in 1914[1.15] when he reported its remarkable ability to retain certain organic solvents tightly, and in fixed amounts. Subsequently it has been shown to have a wide enclathrating ability, for example with argon, sulphur dioxide, iodine, ammonia, decalin, glycerol, sulphur hexafluoride and di-t-butylnitroxide[1.16]. Its molecular structure was determined in the mid-fifties by Baker and coworkers, who also prepared over fifty analogues[1.17, 1.18]. It contains an hexagonal unit of hydrogen bonded OH groups, as in the β-hydroquinones, but the cavity formed is larger. The guest molecules usually exhibit disorder and the number of guests occupying each cavity is dependent on their size. The cavity size can be varied by various changes, for example, by removing one of the geminal dimethyl groups, by replacing the ether oxygen with sulphur to form the respective thiachroman, or by replacing the OH group with SH.
Highly toxic organo-mercurials such as dimethylmercury may be handled with comparative safety in the form of their clathrates with thiachroman[1.19].

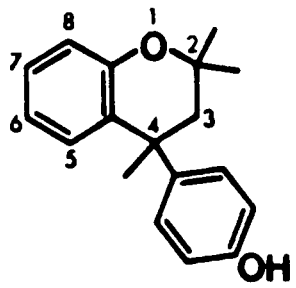

Figure 1.4 Dianin's compound, 4-p-hydroxyphenyl-2,2,4-trimethylchroman.

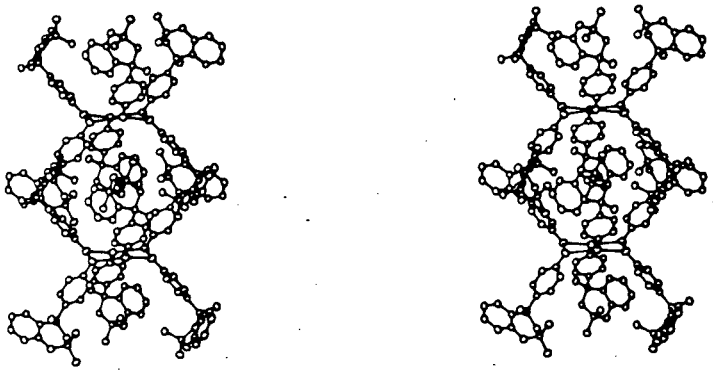

Figure 1.5 Stereoview of Dianin's compound as chloroform cryptate. Guest not shown[1.20].

1.2 Werner Clathrates.

Named after the pioneer of coordination chemistry, Alfred Werner, these compounds comprise host molecules of general formula MX_2L_4 where: M is a divalent transition metal cation, e.g. Mn^{2+}, Fe^{2+}, Co^{2+}, Ni^{2+}, Cu^{2+}, Zn^{2+}

X is an anionic ligand, e.g. NCS^-, NCO^-, CN^-, NO_3^-, NO_2^-, halogen

L is an electrically neutral substituted pyridine, 1-arylalkylamine or isoquinoline.

Many different host complexes may be constructed by using these constituents, and even more if the possibility for isomerism and/or complexation by more than one type L ligand is taken into account. Interest in the enclathrating ability of these hosts was stimulated by Schaeffer and coworkers, who announced in 1957 a new method of separating aromatics from petroleum fractions[1.21]. Since then the host $[Ni(NCS)_2(4\text{-}MePy)_4]$ has received the most attention, with its wide enclathrating ability ranging from noble gases to condensed aromatics in cavities of layer, channel or cage shape. Its chromatographic abilities (1981)[1.22] and the thermodynamics of clathration (1982)[1.23] have been studied. The physico-chemical behaviour of these clathrates has been reviewed by Lipkowski (1984)[1.24].

By suitable choice of solvent the host can be made to crystallise as a compact clathrand, called the α-phase or as a clathrate to form the various phases β, γ, δ, ...etc. These latter phases arise from the different host-guest ratios and from the varied sizes and shapes of the guest molecules.

As typified by the above 4-MePy host, the substituted pyridine hosts which have been studied in this laboratory (bis4-MePy,bis4-PhPy [1.25, 1.33]; 4-PhPy[1.26, 1.30, 1.31]; 3-MePy[1.26]; 3,5-diMePy[1.26]; 4-ViPy [1.27, 1.29, 1.32]; 4-EtPy[1.28]; 4-t-ButylPy[1.34]; 4-BenzylPy[1.34]) all have irregular octahedral coordination. Owing to `overcrowding´ around the metal there are non-bonding repulsive interactions among the ligands which allows only certain stable conformations. It is the substituents on the ortho position of the pyridine (hydrogen in the above hosts) which determine the extent of this repulsive interaction[1.26]. It is found that the most common is the `propeller´ conformation where the four pyridine rings are twisted from the coplanar arrangement. The isothiocyanate groups are bonded via the nitrogen to the metal and are trans to each other, with the M-Ncs-Cs bond angle ranging from 153° to 180° .

The wide enclathrating ability of these hosts has been thought to depend largely on the free rotation of the pyridine rings about their Ni-N bonds, allowing the host to adopt a suitable conformation and accommodate the guest. Presently this seems doubtful as the host 3,5-dimethyl pyridine has been found to crystallise as the clathrand only, while conformational energy studies (using the program EENY[1.34]) show the 3,5-dimethyl pyridine as having rotational freedom of approximately 40° about its Ni-N bond[1.26]. On the basis of spectral data, charge transfer interactions between host and guest have been reported[1.36]. However further studies have enabled re-interpretation of the spectral data solely in terms of steric interactions (that is, host-guest interaction at the energy magnitude of the van der Waals forces)[1.37, 1.38]. Other steric factors to take into account are the size and shape of the substituents on the pyridine ring resulting in poor packing and hence allowing guest occupation. The size and shape of the guests that are to fit in these cavities is another factor, taking note of the further restriction that may arise when the cavity imposes a symmetry condition. Finally the solubilities of all the respective components prior to crystallisation and the conditions under which crystallisation occurs must be taken into account.

1 REFERENCES

1.1 H. M. Powell: J. Chem. Soc. 61 (1948).

1.2 Inclusion Compounds, edited by J. L. Atwood, J. E. D. Davies, D. D. MacNicol; Academic Press, New York, vol. 1, chapter 9 (1984).

1.3 E. Weber and H. P. Josel: J. Incl. Phenom. 1, 79 (1983).

1.4 E. Weber and F. Vogtle: Inorg. Chem. Acta. L65, 45 (1980).

1.5 F. Wohler: Justus Liebigs Ann. Chem. 69, 297 (1849).

1.6 D. E. Palin and H. M. Powell: J. Chem. Soc. 208 (1947).

1.7 D. E. Palin and H. M. Powell: J. Chem. Soc. 815 (1948).

1.8 K. A. Hofmann and F. A. Kuspert: Z. Anorg. Chem. 15, 204 (1897).

1.9 H. M. Powell and J. H. Rayner: Nature 163, 566 (1949).

1.10 H. M. Powell and J. H. Rayner: J. Chem. Soc. 319 (1952).

1.11 Inclusion Compounds, edited by J. L. Atwood, J. E. D. Davies, D. D. MacNicol; Academic Press, New York, vol. 1, chapter 2 (1984).

1.12 R. F. Evans, O. Ormrod, B. B. Goalby and L. A. K. Staveley: J. Chem. Soc. 3346 (1950).

1.13 U. S. Patent: 2, 732, 413 (1956).

1.14 Inclusion Compounds, edited by J. L. Atwood, J. E. D. Davies, D. D. MacNicol; Academic Press, New York, vol. 1, chapter 2 (1984).

1.15 A. P. Dianin: J. Russe. Phys. Chem. Soc. 46, 1310 (1914).

1.16 Inclusion Compounds, edited by J. L. Atwood, J. E. D. Davies, D. D. MacNicol; Academic Press, New York, vol. 2, chapter 1 (1984).

1.17 W. Baker, A. J. Floyd, J. F. W. McOmie, G. Pope, A. S. Weaving and J. H. Wild: J. Chem. Soc. 2010 (1956).

1.18 W. Baker, J. F. W. McOmie and A. S. Weaving: J. Chem. Soc. 2018 (1956).

1.19 R. J. Cross, J. J. McKendrick and D. D. MacNicol: Nature 245, 146 (1973).

1.20 Inclusion Compounds, edited by J. L. Atwood, J. E. D. Davies, D. D. MacNicol; Academic Press, New York, vol. 2, chapter 1 (1984).

1.21 W. D. Schaeffer, W. S. Dorsey, D. A. Skinner and J. Christian: J. Am. Chem. Soc. 79, 5870 (1957).

1.22 W. Kemula, D. Sybliska and J. Lipkowski: J. Chromatogr. 218, 465 (1981).

1.23 J. Lipkowski, P. Starzewski and W. Zielenkiewicz: Pol. J. Chem. 56, 349 (1982).

1.24 Inclusion Compounds, edited by J. L. Atwood, J. E. D. Davies, D. D. MacNicol; Academic Press, New York, vol. 1, chapter 3 (1984).

1.25 D. R. Bond, G. E. Jackson and L. R. Nassimbeni: S. Afr. J. Chem. 36, 19 (1983).

1.26 L. R. Nassimbeni, S. Papanicolaou and M. H. Moore: J. Incl. Phenom. 4, 31 (1986).

1.27 M. H. Moore, L. R. Nassimbeni, M. L. Niven and M. W. Taylor: Inorg. Chem. Acta. 115, 211 (1986).

1.28 M. H. Moore, L. R. Nassimbeni and M. L. Niven: J. Chem. Soc. Dalton Trans. 2125 (1987).

1.29 M. H. Moore, L. R. Nassimbeni and M. L. Niven: Inorg. Chem. Acta. 131, 45 (1987).

1.30 L. R. Nassinbeni, M. L. Niven and M. W. Taylor: Inorg. Chem. Acta. 132, 67 (1987).

1.31 L. R. Nassimbeni, M. L. Niven and M. W. Taylor: J. Chem. Soc. Dalton Trans. In Press.

1.32 L. R. Nassimbeni, M. L. Niven and A. P. Suckling: Inorg. Chem. Acta. Submitted.

1.33 L. R. Nassimbeni, M. L. Niven and M. W. Taylor: J. Coord. Chem. Submitted.

1.34 L. R. Nassimbeni, M. L. Niven and M. W. Taylor: Acta. Cryst. C Submitted.

1.35 W. D. S. Motherwell: EENY Potential Energy Program, Univ. Chem. Laboratories, Cambridge (1974).

1.36 P. de Radzitzky and J. Hanotier: Indstr. Eng. Chem. Process Design Devpt. 1, 10 (1962).

1.37 Z. Borkowska, J. Lipkowski, B. Moszynska and W. Wolfram: J. Mol. Struc. 12, 265 (1972).

1.38 B. Moszynksa, J. Lipkowski and A. Janowski: J. Mol. Struc. 19, 347 (1973).

CHAPTER 2

Aims of the Research Project

With a carefully devised experimental system the object is to narrow down the number of variables in order to assist in the interpretation of the results. With this in mind, what characteristics does the host $[Ni(NCS)_2(4\text{-}ViPy)_4]$ select when enclathrating different guests?
We therefore sought to investigate a series of clathrates where, with a given host, the guest entity was changed systematically.
We thus chose a series of cyclic hydrocarbons each having a skeleton of six carbon atoms, but where the number of double bonds varied from zero to three:- cyclohexane, cyclohexene, 1,3-cyclohexadiene, 1,4-cyclohexadiene and benzene.

As the host was found to be insoluble in cyclohexane, cyclohexene, 1,3-cyclohexadiene and 1,4-cyclohexadiene the solvent tetrahydrofuran was used. Previous studies had shown THF not to be included when used as a solvent with other guests (ortho-, meta-, para-xylene, chloroform[2.1] and ortho-bromo iodobenzene[2.2]).

The complete nomenclature used in this thesis is as follows.

THF=tetrahydrofuran

STRUCTURE

number	name	
1	HANE	= [Ni(NCS)$_2$(4-ViPy)$_4$](1.78THF)(0.22cyclohexane)
2	HENE	= [Ni(NCS)$_2$(4-ViPy)$_4$](1.76THF)(0.24cyclohexene)
3	DIEN3	= [Ni(NCS)$_2$(4-ViPy)$_4$](0.48THF)(0.52 1,3-cyclohexadiene)
4	DIEN4	= [Ni(NCS)$_2$(4-ViPy)$_4$](0.36THF)(1.04 1,4-cyclohexadiene)
5	THF/BEN	= [Ni(NCS)$_2$(4-ViPy)$_4$](0.35THF)(1.05benzene)
6	BEN	= [Ni(NCS)$_2$(4-ViPy)$_4$](3benzene)
I	T	= [Ni(NCS)$_2$(4-ViPy)$_4$](2THF)
7	PY	= [Ni(NCS)$_2$(Py)$_4$]
II	PYBEN	= [Ni(NCS)$_2$(Py)$_4$](nbenzene)

where: the numbers 1 to 7 represent solved structures

: I on the basis of isomorphous test with structures 1 and 2

: II on the basis of unit cell parameters.

Structures 7 and II are not part of the above main theme but are an extension of it with the host [Ni(NCS)$_2$(Py)$_4$].

2 REFERENCES

2.1 M. H. Moore, L. R. Nassimbeni, M. L. Niven and M. W. Taylor: Inorg. Chem. Acta. 115, 211 (1986).

2.2 L. Lavelle: B.Sc. (Honours) Project, 1986, unpublished results.

CHAPTER 3

Experimental and Computational Procedures

3.1 Preparation of $[Ni(NCS)_2(4\text{-}ViPy)_4]$ and $[Ni(NCS)_2(Py)_4]$ complexes.

All reagents and solvents (except for 4-vinylpyridine, 1,3-cyclohexadiene and 1,4-cyclohexadiene) used were analytically pure and supplied by SARchem, Johannesburg. The 4-vinylpyridine, 1,3-cyclohexadiene and 1,4-cyclohexadiene were obtained from the Aldrich Chemical Company, Germany. Unless stated otherwise all procedures, i.e. bench work; crystal formation; visual observation, photography and mounting of crystals are at room temperature, 293 to 303 K.

Host powder complexes were prepared by the method of Schaeffer et al[3.1] as follows:

A green transparent solution of $Ni(NCS)_2$ (8.4mmole) was made by dissolving nickel chloride, $NiCl_2.6H_2O$ (2.00g, 8.4mmole) and potassium thiocyanate, KSCN (1.64g, 16.8mmole) in glass distilled water (20ml). The pyridine/vinylpyridine (36.9mmole, 10% excess) was added dropwise to the green solution (approximately 5 minutes) with constant stirring. An immediate fine pale blue precipitate formed (host powder complex). After all the ligand was added stirring was continued for an additional 30 minutes to ensure complete reaction. The precipitate was filtered (Buchi Apparatus), washed with glass distilled water (3x10ml), air dried for 30 minutes and placed in a desiccator for 24 hours.

3.2 Crystal growth.

a) for the series HANE, HENE, DIEN3, DIEN4 and THF/BEN:
A stock solution of $[Ni(NCS)_2(4\text{-}ViPy)_4]$ was prepared by dissolving 10.70g of the complex in 50ml of tetrahydrofuran giving a saturated solution of 29.0×10^{-3} mole fraction complex, neglecting any loss owing to a very small amount of undissolved complex and the formation of complex equilibria in solution. With the object of crystal formation it is usually desirable to work with saturated solutions. Prior to crystal preparation a suitable volume of stock solution was centrifuged to remove any colloidal particles; this method was used as it was far more efficient than filtering.
The method of layering or liquid diffusion[3.2] is the layering of two liquids varying sufficently in density to allow initial formation of two distinct layers, while being miscible with each other to allow gradual mixing by diffusion. As the complex is soluble in only one of these liquids, crystal formation results.
Using a Pasteur pipette, 2.5ml of stock solution was layered with equal volumes of cyclohexane, cyclohexene, 1,3-cyclohexadiene, 1,4-cyclohexadiene and benzene. The vials were then stoppered and left to stand undisturbed.
The compound number and code name are in brackets.
With the cyclohexane (1 HANE) and cyclohexene (2 HENE) crystals could be seen at the interface after aproximately fifteen minutes. The rapid formation of these clearly defined crystals (crystal blue, cyclohexane clear) led me to attempt filming the crystallisation (Teaching Methods Unit, U. C. T.). Owing to insufficient detail (magnification) no fruitful results were obtained.

With the 1,3-cyclohexadiene (3 DIEN3) dark blue crystals formed after three days at the bottom of the vial.
With the 1,4-cyclohexadiene (4 DIEN4) and benzene (5 THF/BEN) dark blue crystals formed at the bottom of the vials after the stoppers were removed to allow evaporation. The time taken for crystal formation is not specific (approx. 10-14 days) as the stoppered tubes were left for some time until it became obvious that no crystals would form. The above procedure was attempted as crystal formation under similar conditions would be desirable when comparing the outcome. The complex is sufficiently soluble in 1,4-cyclohexadiene and benzene for crystallisation not to occur without solvent evaporation.

b) for BEN and T:
$[Ni(NCS)_2(4\text{-ViPy})_4]$ was dissolved in benzene until a saturated solution was obtained; this was centrifuged giving a clear blue solution. Approximately 8ml was placed in a vial, covered with perforated plastic film and left to stand. After sufficient benzene had evaporated (three days) blue crystals (6 BEN) formed at the bottom of the vial.
Except for the complex being dissolved in tetrahydrofuran the above procedure was followed giving blue crystals (I T) after 5 days at the bottom of the vial.

c) for PY and PYBEN:
$[Ni(NCS)_2(Py)_4]$ was dissolved in tetrahydrofuran and benzene with the same procedures as above for slow evaporation. Light blue crystals formed at the bottom of the vials after three days for the

tetrahydrofuran solution (7 PY) and six days for the benzene solution (II PYBEN).

Photographs of the above crystals are presented in section 6.3.

3.3 Density.

Using the method of flotation the host:total guest stoichiometry was determined by careful measurement of the single crystal densities. Cyclohexane (d_4^{20}=0.778), carbontetrachloride (d_4^{20}=1.594) and 1,2-dichlorobenzene (d_4^{20}=1.305) were used, as their densities are suitable and the crystals are sufficiently stable in these liquids to allow measurement. The procedure was to obtain approximate densities with suitable mixtures of one of the above liquids. A new crystal was used (owing to loss of guest) for each approximation until the final crystal was suspended in solution. Using an Anton Paar digital densitometer, DMA 35, the density of each crystal was determined to +/- 0.01 g. cm^{-3}. The densities of different crystals from the same vial were determined at least three times.

The observed densities and corresponding host:total guest ratios are given in section 4.2.

For previous structures with the vinylpyridine as host the observed densities correlated well with the calculated densities with a host:guest ratio of 1:1 or 1:2.

For the series of crystals 1 HANE, 2 HENE, 3 DIEN3, 4 DIEN4 and 5 THF/BEN this was not the case. As the observed densities could not be reconciled with any simple ratio of host to single guest, we analysed the clathrates by proton nuclear magnetic resonance.

3.4 Proton nuclear magnetic resonance spectroscopy.

Spectra for the series of crystals 1 HANE, 2 HENE, 3 DIEN3, 4 DIEN4 and 5 THF/BEN were recorded on a Brucker WH-90 spectrometer. From each vial a single large crystal was removed from its mother liquor, dabbed dry and dissolved in $CDCl_3$. The spectra were repeated with each crystal being `washed' with two or three drops of $CDCl_3$ and then dissolved in $CDCl_3$. This was to eliminate the possibility of surface contamination by the mother liquor. The spectra are shown in section 4.1.

Conditions for each run.

Frequency:	90.02 MHz
Lock compound:	TMS
Number of scans:	250
Pulse width:	1 sec
Repeat rate:	2 sec
Sweep width:	1.2 kHz
Data points (FID):	8 K
Input filter:	0.05 Hz
Frequency offset:	4 kHz

3.5 Single crystal X-ray diffractometry.

Single crystal diffractometry was employed to elucidate the structures and hence gain futher information on these host-guest compounds.

3.5.1 Crystal preparation.

Only crystals which extinguished uniformly under plane polarised light were selected. Most of the crystals had to be cut to a suitable size; dimensions are listed in the tables of crystal data, section 4.3. All the crystals had to be kept in contact with mother liquor otherwise they decomposed (structure destroyed owing to loss of guest). This instability posed rather awkward problems. As most of the solvents evaporate readily mother liquor had to be continually dropped on to the crystals. The crystals were mounted with mother liquor in sealed Lindemann capillary tubes (0.5mm diameter). Sealing was carried out with wax as glue reacted with the mother liquor and rendered the crystal not suitable for analysis and a naked flame to seal the glass ignited the solvent. For compound 6 the crystal moved while being irradiated with X-rays. A glass fibre (rounded at one end by flame, so as not to damage the crystal) was inserted into the capillary tube, placed flush against the crystal and sealed. The same was done for the other end.

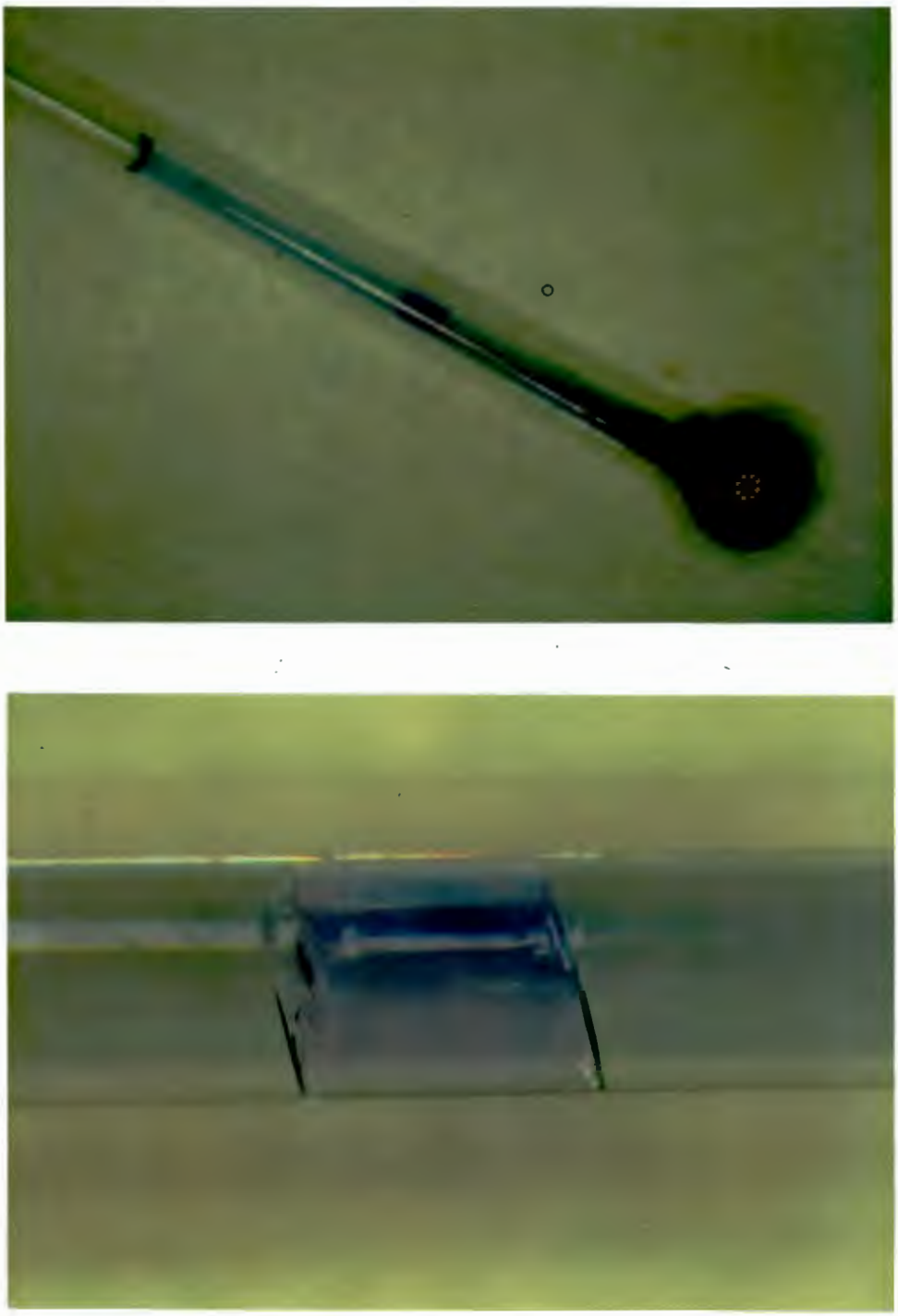

Photographs of crystal in a Lindemann tube.

3.5.2 Data collection.

Accurate cell parameters were determined by least-squares analysis of 24 reflections measured in the range $16^{\circ} \leq \theta \leq 17^{\circ}$ automatically located and centred on an Enraf-Nonius CAD4 diffractometer with graphite monochromated MoK_{α} radiation (λ=0.7107 Å, Philips PW1730 generator, 50KV, 20mA). Intensity data were collected at 294K in the ω-2θ scan mode with a final acceptance limit of 20σ at 20°/min in ω and a maximum recording time of 40s. The intensity variation of three standard reflections was monitored every hour to ascertain both instrumental stability and crystal decomposition. Recentring was carried out every 100 measured reflections. All intensities were corrected for Lorentz-polarisation and an empirical absorption correction[3.3] was applied to each data set.

3.6 Computation.

All computations were performed on a Sperry 1100 main-frame computer at the University of Cape Town. The following programs were utilised.

SHELX-76[3.4]: This program was used for crystallographic data reduction, structure solution and refinement. All structures were solved by the heavy atom method and subsequent difference Fourier syntheses. Features of this program that were utilised include data reduction, rejection of systematic absences, full-matrix least-squares refinement of the atomic parameters, bond length constraints and refinement, analysis of variance and automatic optimisation of weighting schemes, Fourier synthesis with peak search and structure

factor listings. Hydrogen atoms were geometrically positioned with respect to their parent carbons and allowed to ride on the carbon atoms to which they were bonded. The C-H bond distances were fixed at 1.00 Å with the temperature factors of hydrogens linked. No hydrogens were included for the guest molecules.

For structures 3, 4, and 5 the guests were constrained to a regular pentagon and hexagon, as appropriate.

When atoms on special positions were treated anisotropically, symmetry restrictions were applied according to Peterse and Palm[3.5]

The agreement between observed (Fo) and calculated (Fc) structure factors is expressed by the conventional residual R, defined as:

$$R = \frac{\Sigma||Fo| - |Fc||}{\Sigma|Fo|} = \frac{\Sigma|\triangle F|}{\Sigma|Fo|}$$

or as a weighted index:

$$R_w = \frac{\Sigma\, w^{1/2}|\triangle F|}{\Sigma\, w^{1/2}|Fo|}$$

where $w = 1/[\sigma^2(Fo) + gFo^2]$. The value of g was chosen to give the smallest variation of $\left(\frac{\Sigma w \Delta^2}{w\sigma^2}\right)$ with $\sqrt{Fo/Fmax}$. An analysis of variance computed after the final refinement cycle gives an indication of the effectiveness of the weighting scheme. A resulting low value for the discrepancy index R is indicative of a correctly refined structure. For these clathrate compounds, R is typically 10% with intensity data collected at 294K. This relatively high value is due to the fact that the guest moieties often display disorder.

Atomic radii used in the program were those of Pauling[3.6]. Scattering factors for all non-hydrogen atoms were from Cromer and Mann[3.7] and those for the hydrogen atoms from Stewart et al[3.8]. The program SHELX 400 was used to handle the large number of parameters for structure 6.

PARST[3.9]: This was used for all molecular geometry calculations, in particular calculations of torsion angles[3.10], weighted least-squares planes (e.s.d.s after Stanford and Waser[3.11]) and intermolecular contacts.

PLUTO[3.12]: This was used to draw individual molecules and to study their molecular packing. Hydrogens were not included in these diagrams.

OPEC[3.13]: This was used to map precisely the sizes and shapes of the guest cavities. The program is based on standard molecular geometries and atomic radii established by Bondi[3.14] and provides a method of computing molecular volume.

ALCHEMY[3.15]: This was used to calculate the coordinates of a cyclohexane and cyclohexene molecule. These coordinates were used in the program MULTAN.

MULTAN[3.16]: The MULTAN 78 program NORMAL was used to calculate the spherically averaged molecular scattering factor for cyclohexane and cyclohexene molecules. This was used as a possible model for the disordered guests in structures 1 and 2, respectively.

3.7 Thermal analysis.

Thermal analysis of the crystals was performed to confirm the presence (quantitatively) or absence of guest, the temperature of guest release from the clathrate, and the breakdown of the host complex.

All thermograms were carried out on a Stanton-Redcroft Thermal Analyser (STA 780), operating at a heating rate of 10 °C/min and a nitrogen flow rate of 60ml/min, with inert alumina (Al_2O_3) as the reference material.

In the sample holder assembly (figure 3.1) each platinum crucible sits directly on top of its thermocouple. This allows direct measurement of the furnace temperature only. The lag between furnace and sample temperature was obtained by running a series of standards and plotting the furnace temperature at which melting occurred ($T_{furnace}$) versus the known melting point (T_{melt}). This gave an excellent calibration line with:

$$\text{sample temperature} = 1.05(\text{furnace temperature}) - 51.45\ ^{\circ}C \qquad I$$

All quoted sample temperatures were corrected by equation I.

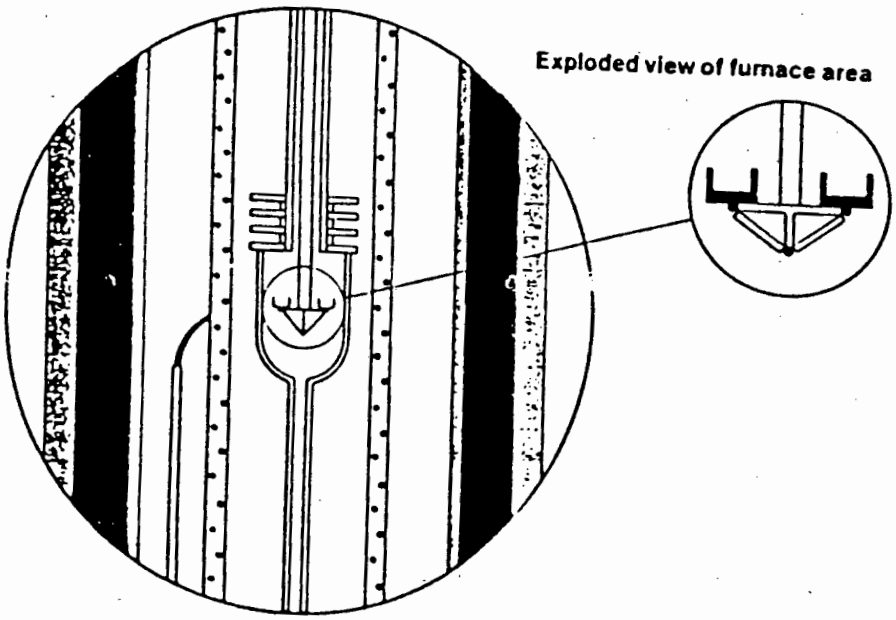

Figure 3.1 Sample holder assembly of the Stanton Redcroft STA-780 simultaneous TG/DTA system[3.17].

3 REFERENCES

3.1 W. D. Schaeffer, W. S. Dorsey, D. A. Skinner and J. Christian: J. Am. Chem. Soc. 79, 5870 (1957).

3.2 C. Orvig: J. Chem. Ed. 62, 82 (1985).

3.3 A. C. T. North, D. C. Phillips and F. S. Mathews: Acta Cryst. A24, 351 (1968).

3.4 G. M. Sheldrick: SHELX-76 program system in Computing in Crystallography edited by H. Schenk, R. Olthof-Hazekamp, H. van Koningsveld and G. C. Bassi; Delft Univ. Press, 34 (1978).

3.5 W. J. A. M. Peterse and J. H. Palm: Acta Cryst. 20, 147 (1966).

3.6 L. Pauling: The Nature of The Chemical Bond, Cornell Univ. Press, Ithaca, New York.

3.7 D. T. Cromer and J. B. Mann: Acta Cryst. A24, 321 (1968).

3.8 R. F. Stewart, E. R. Davidson and W. T. Simpson: J. Chem. Phys. 42, 3175 (1965).

3.9 M. Nardelli: Comput. Chem. 7, 95 (1983).

3.10 W. Klyne and V. Prelog: Experientia 16, 521 (1960).

3.11 G. Stanford and J. Waser: Acta Cryst A28, 213 (1972).

3.12 W. D. S. Motherwell: PLUTO program for plotting molecular and crystal structures. Cambridge Univ., England, unpublished.

3.13 A. Gavezzotti: OPEC Organic Packing Energy Calculations Program, J. Am. Chem. Soc. 105, no.16, 5220 (1983).

3.14 A. Bondi: J. Phys. Chem. 68, 441 (1964).

3.15 ALCHEMY, Tripos Associates Inc., 6548 Clayton Road, St. Louis, Missouri, 63117.

3.16 P. Main, S. E. Hull, L. Lessinger, G. Germain, J. P. Declercq and M. M. Woolfson: MULTAN 78, A System of Computor Programs for the Automatic Solution of Crystal Structures from X-ray Diffraction Data (Univ. of York, England and Univ. of Louvain, Belgium) (1978).

3.17 M. E. Brown: Getting Started in Thermal Analysis, Rhodes Univ., South Africa (1985).

CHAPTER 4

Characterisation and Structure Determination

4.1 Proton nuclear magnetic resonance spectroscopy.

The difference between the guest ratios for the `washed´ and `unwashed´ crystals was within experimental error. The spectra of the `washed´ crystals were used to determine the guest ratios.
The paramagnetic nature of the Ni^{2+} ion causes shifting of the 4-vinylpyridine ligand resonances from their normal resonance positions. As shown in spectrum 8, 4-vinylpyridine has multiple peaks between $\delta 5$ and $\delta 9$. Intergration of the broad and shifted 4-vinylpyridine ligands in spectra 1 to 5 to determine the host:total guest ratio gave poor correlation with the density measurements and variation from spectrum to spectrum.

Please see spectra for identification of peaks. Spectra have been reduced to A4 size.
The corresponding peaks for the pure compounds[4.1] are given in brackets. The ratio of guest 1 (variable) to guest 2 (THF) were reproducible, however, and yielded the following results. All nmr peaks are quoted in δ.

1 HANE: A peak at 1.40, 12H (1.42) for cyclohexane and 1.96, 4H (1.83) for THF and their respective integrations gave a ratio of cyclohexane to THF, 1:8.

2 HENE: A peak at 5.64, 2H (5.69) for cyclohexene and 3.64, 4H (3.70) for THF and their respective integrations gave a ratio of cyclohexene to THF, 1:7. These peaks were chosen owing to peak overlap in the vicinity of 2.00.

3 DIEN3: A peak at 5.82, 4H (5.80) for 1,3-cyclohexadiene and 3.70, 4H (3.70) for THF and their respective integrations gave a ratio of 1,3-cyclohexadiene to THF, 1.1:1.

4 DIEN4: A peak at 5.68, 4H (5.68) for 1,4-cyclohexadiene and 1.92, 4H (1.83) for THF and their respective integrations gave a ratio of 1,4-cyclohexadiene to THF, 2.9:1.

5 THF/ BEN : A peak at 7.36, 6H (7.40) for benzene and 1.88, 4H (1.83) for THF and their respective integrations gave a ratio of benzene to THF, 3:1.

Spectrum 6 is of host powder dissolved in tetrahydrofuran and shows the characteristic peaks of the previous spectra, that is, a peak at 1.98, 4H (1.83) and 3.64, 4H (3.70) for tetrahydrofuran and the broad peaks at 3.00, 9.78 and 10.38 for the 4-vinylpyridine ligands.

Spectrum 7 is of host powder in $CDCl_3$ and confirms the positions of the 4-vinylpyridine ligands.

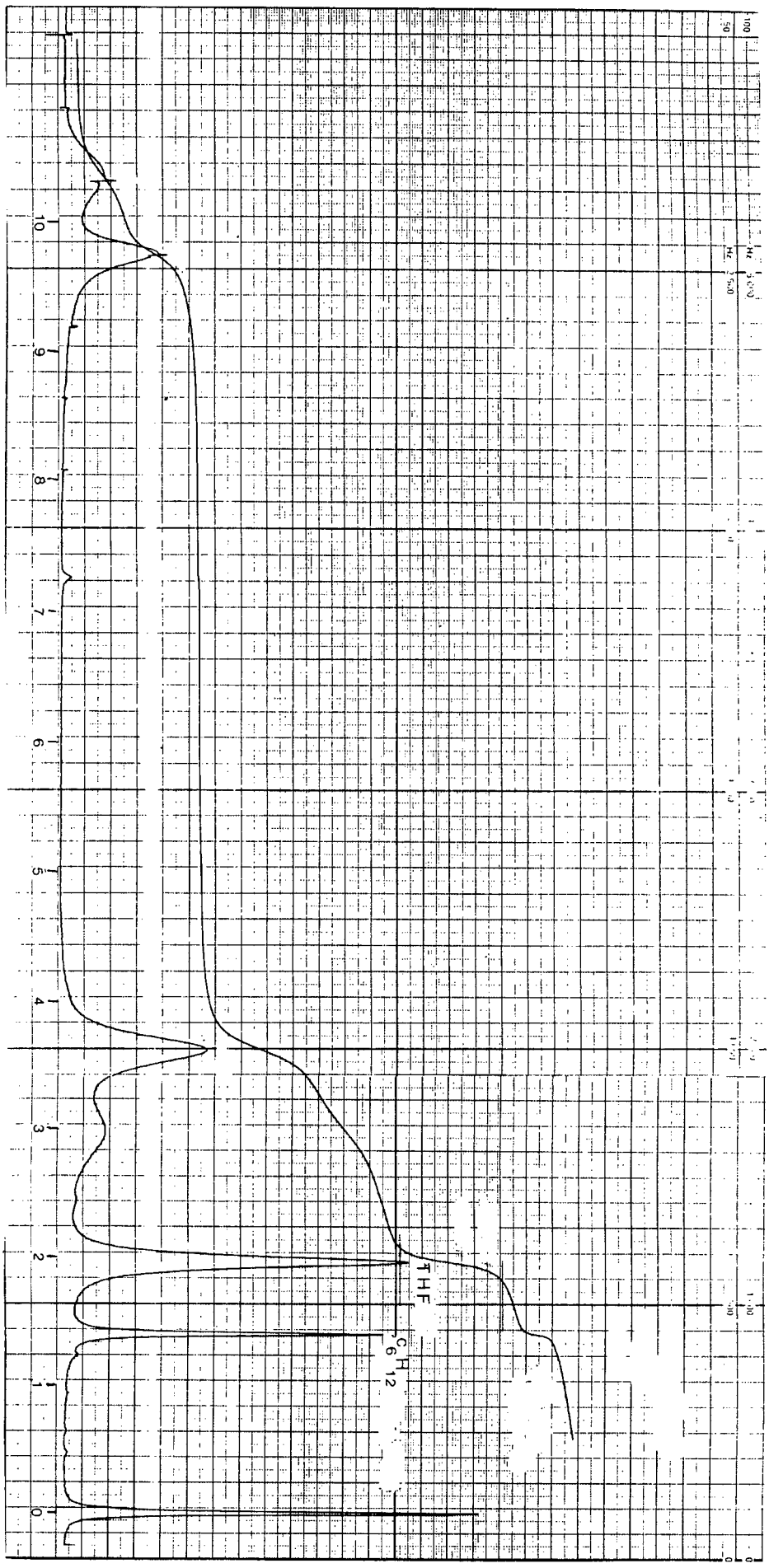

Spectrum 1: 1 HNR

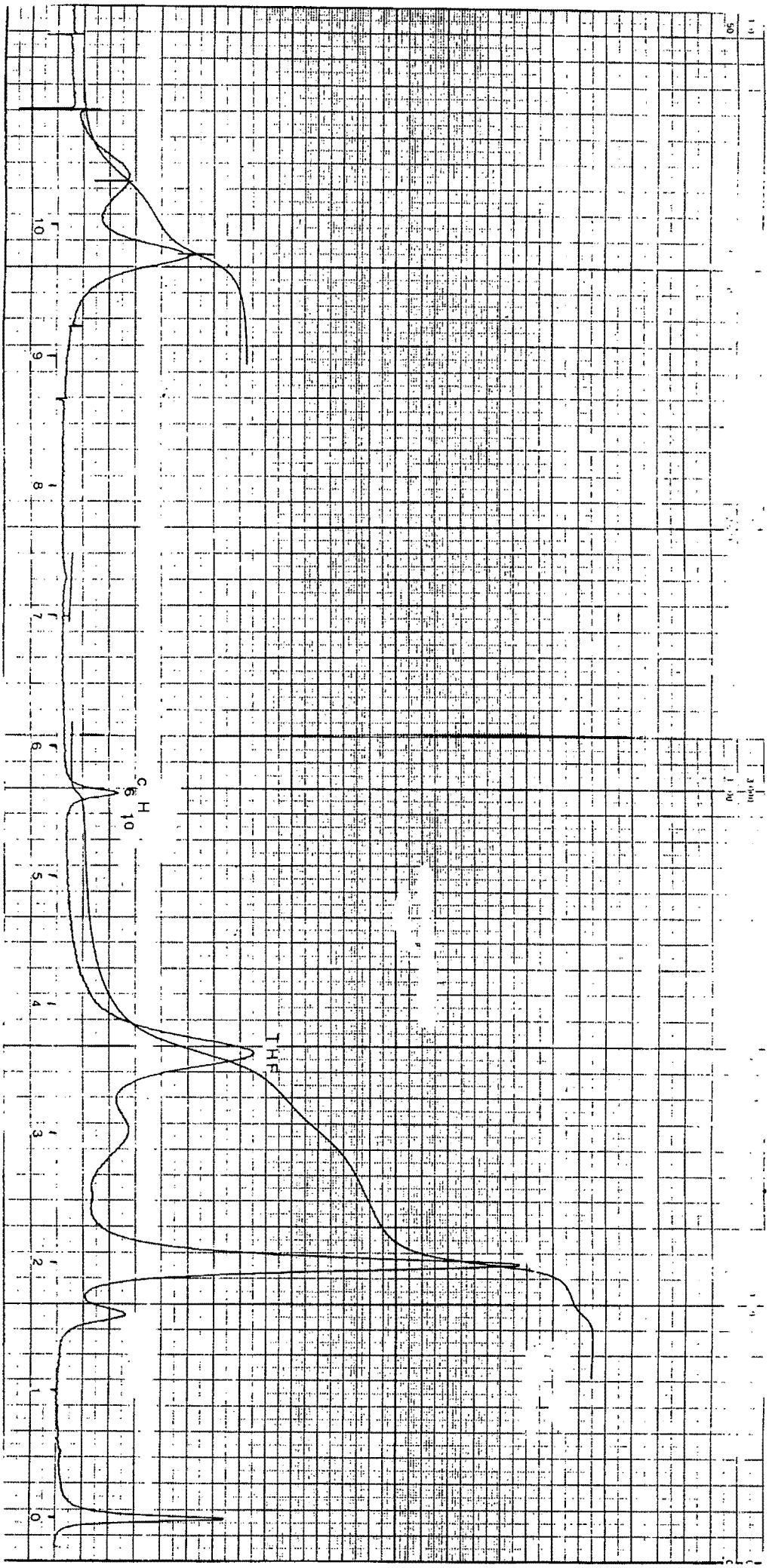

Spectrum 2: 22 HENK

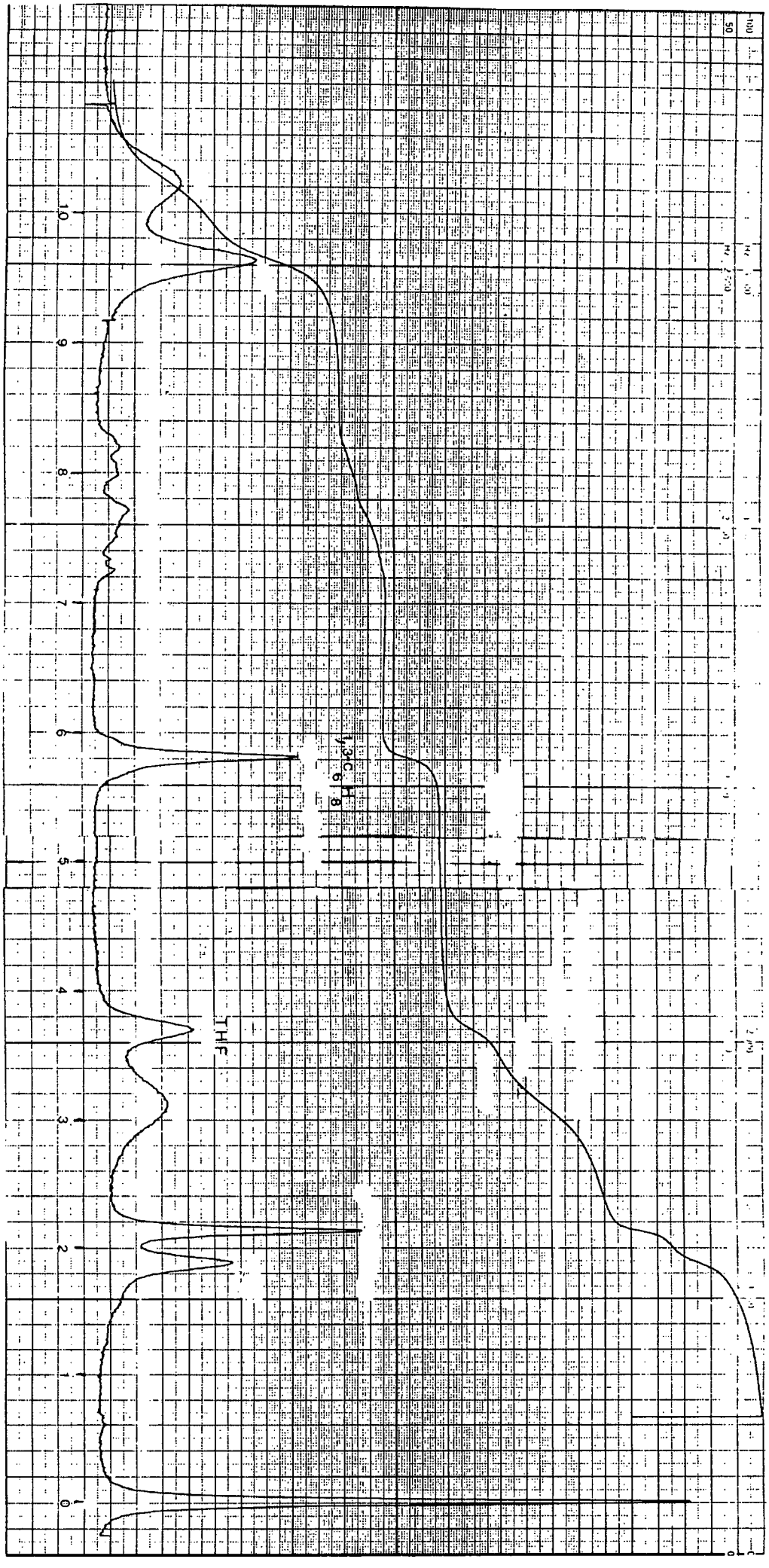

Spectrum 3: 3 DIEN3

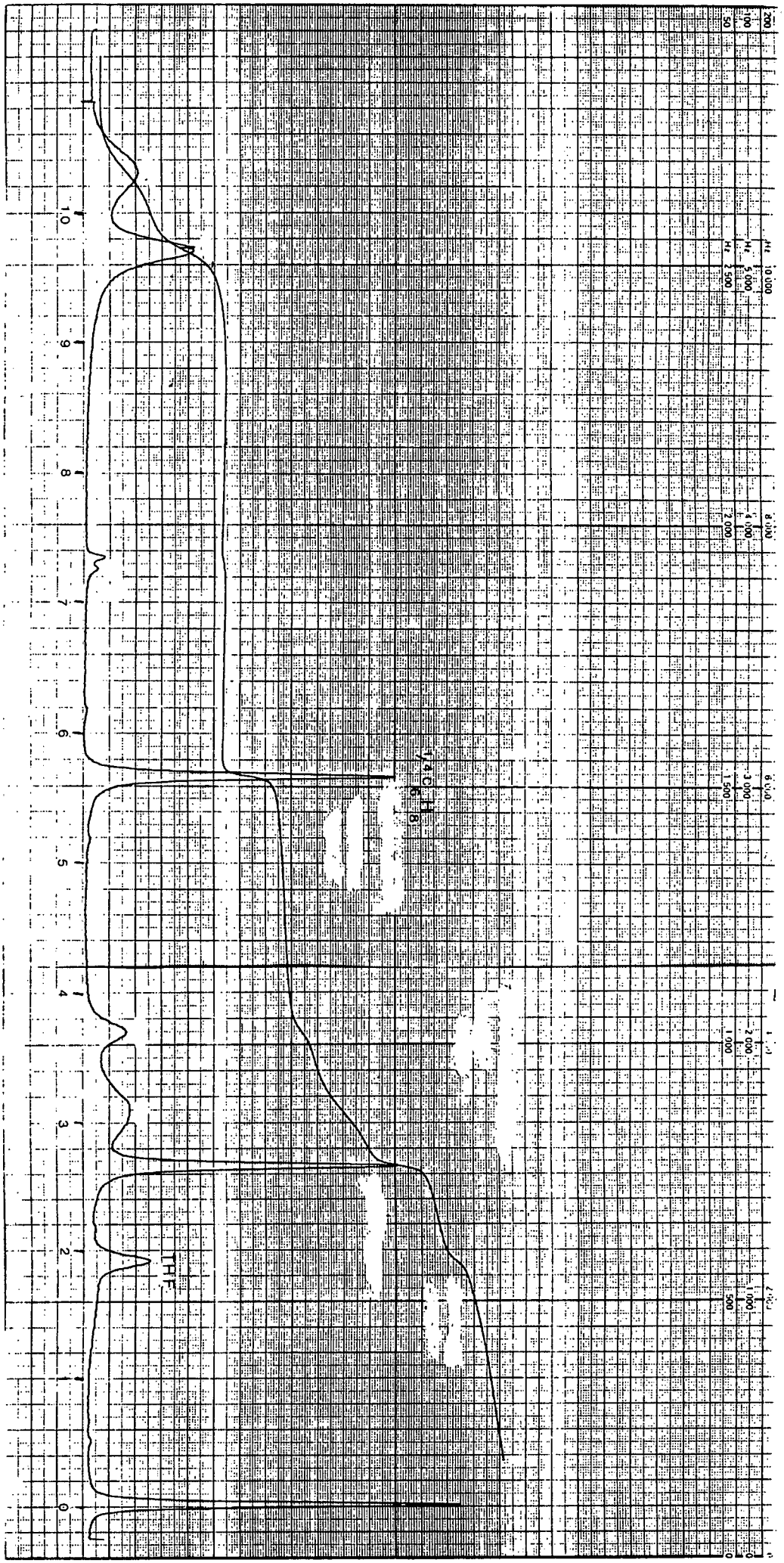

Spectrum 4: 4 DIEN4

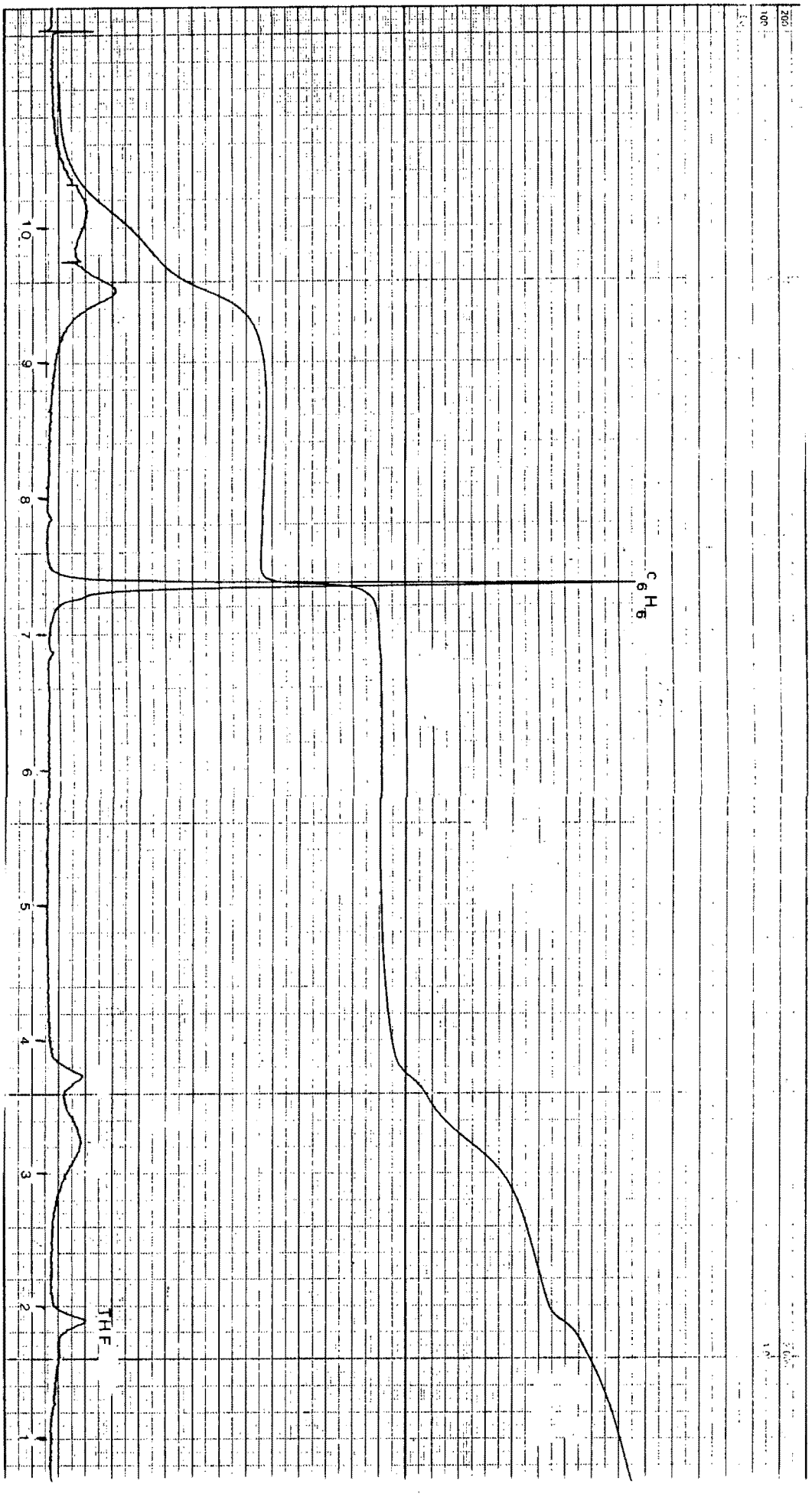

Spectrum 5: 5 THF/BEN

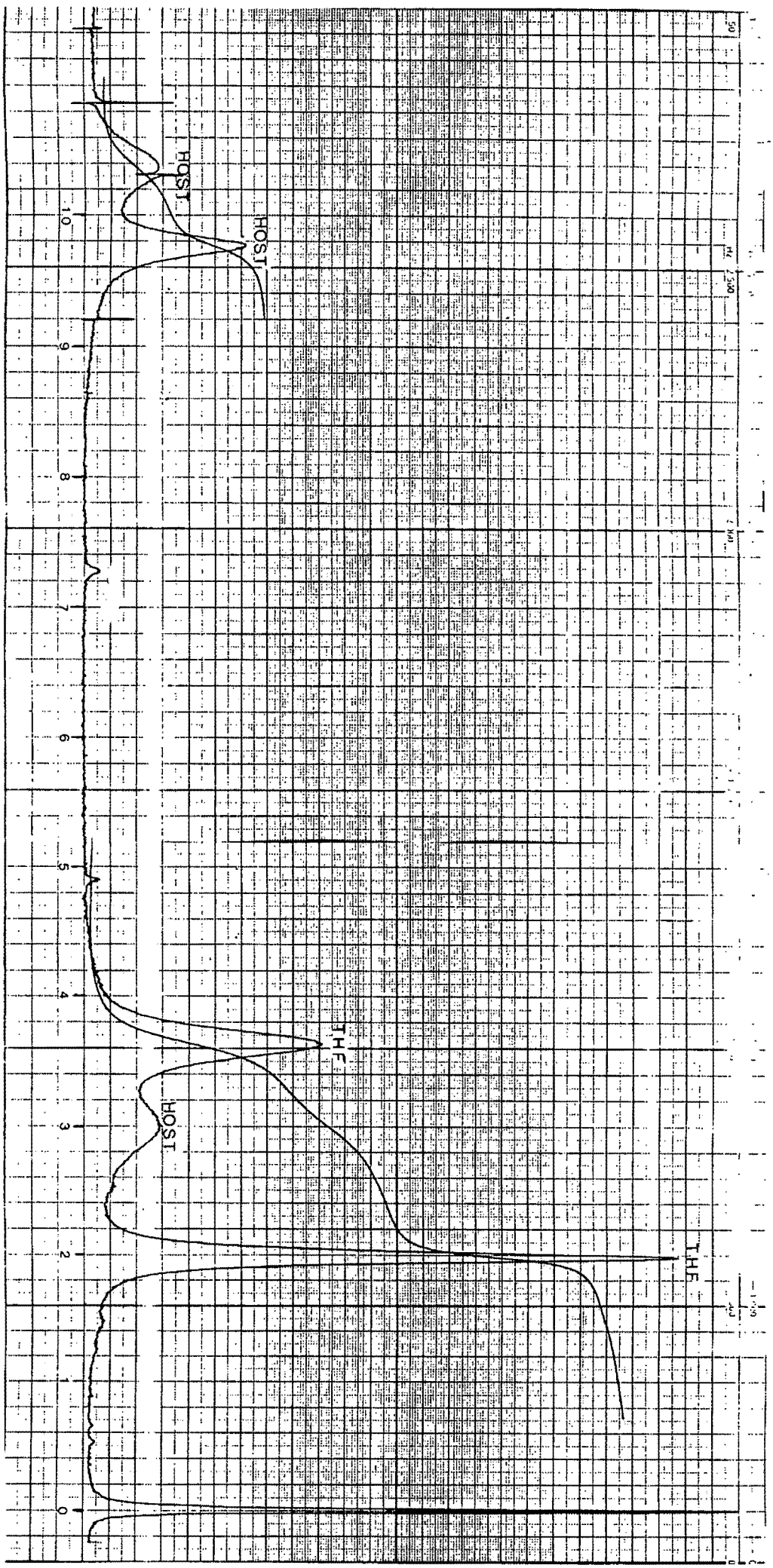

Spectrum 6: HOST in THF

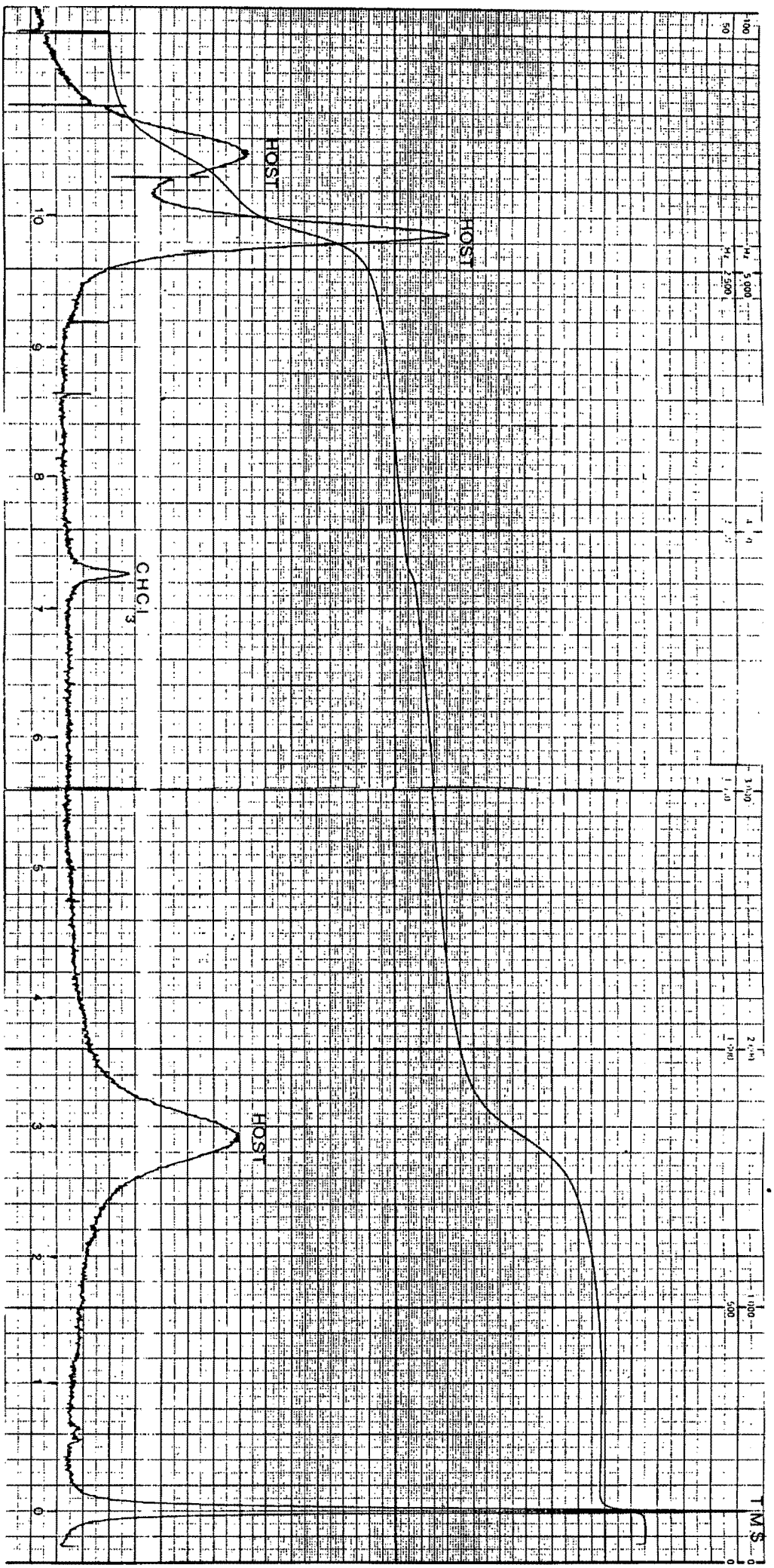

Spectrum 7: HOST in $CDCl_3$ only

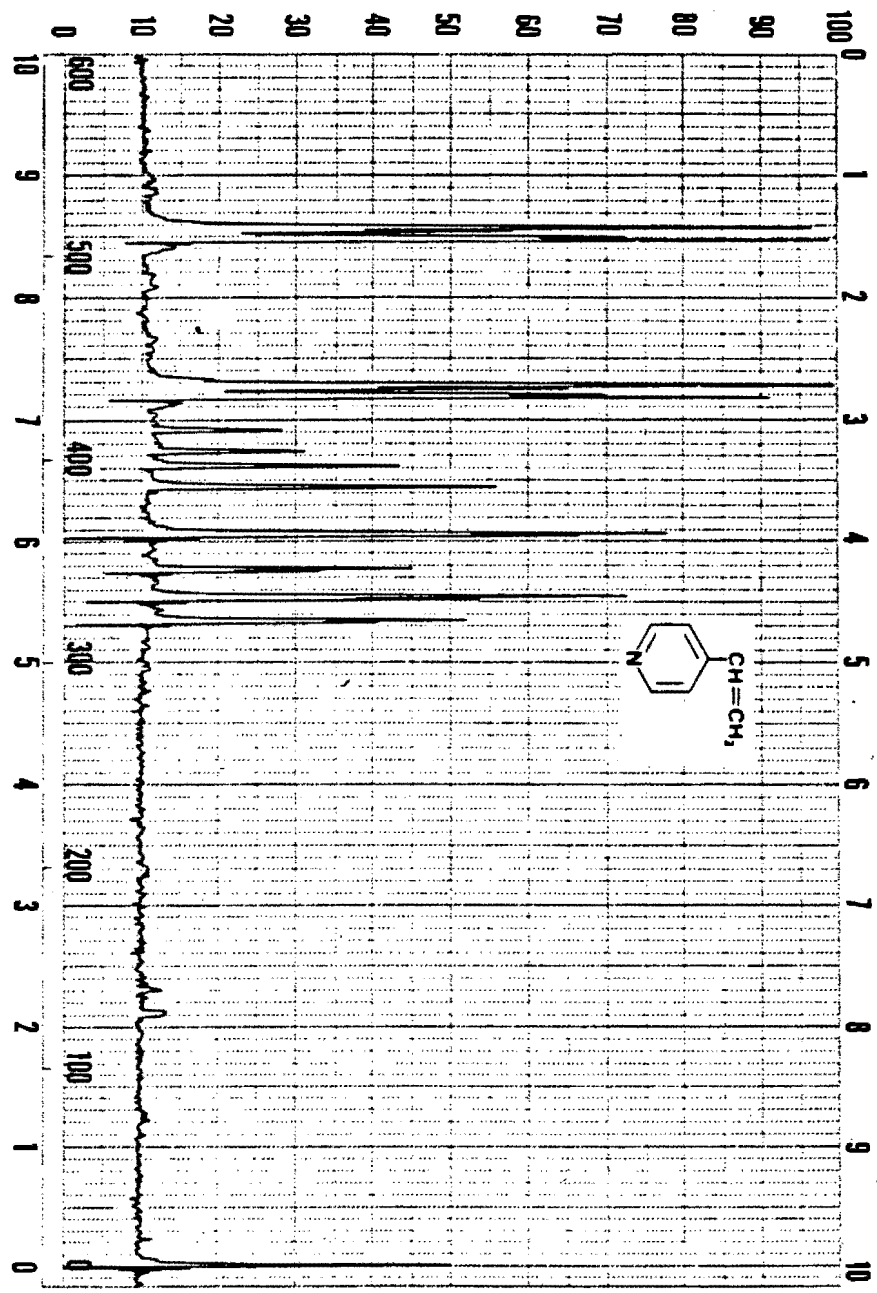

Spectrum 8: 4-vinylpyridine

4.2 Density.

For the series of crystals 1 to 5 once the ratios of the guests were known from their ^1H N.M.R., the correct host:total guest ratio could be calculated using the measured densities of the respective crystals. The following equation was used:

$$Z_H(M_H) + Z_G[N_{G1}(M_{G1}) + N_{G2}(M_{G2})] = N\ D_m\ Vol\ X\ 10^{-24}$$

where, Z_H :Number of host molecules per unit cell

Z_G :Number of guest molecules per unit cell

N_{G1} :Ratio of guest type one

N_{G2} :Ratio of guest type two

M_H :Molecular weight of host in g. mol^{-1}

M_{G1} :Molecular weight of guest type one in g. mol^{-1}

M_{G2} :Molecular weight of guest type two in g. mol^{-1}

N :Avogadro constant, $6.023\ X\ 10^{23}$

D_m :Measured density in g. cm^{-3}

Vol :Volume of unit cell in $Å^3$

The number of host molecules per unit cell was obtained from the crystal structure analysis, and supported by volume calculations. (THF=tetrahydrofuran)

1 HANE; Z_H = 4

M_H = 595.42

M_{G1} = 72.12

M_{G2} = 84.16

D_m = 1.21

Vol = 4087.49

giving Z_G = 8

N_{G1}:N_{G2}

THF:cyclohexane

0.89:0.11

host:total guest

1:2

2 HENE; Z_H = 4

M_{G2} = 82.15

D_m = 1.20

Vol = 4096:44

giving Z_G = 8

N_{G1}:N_{G2}

THF:cyclohexene

0.88:0.12

host:total guest

1:2

3 DIEN3; Z_H = 8

M_{G2} = 80.14

D_m = 1.18

Vol = 7556.31

giving Z_G = 8

N_{G1}:N_{G2}

THF:1,3-cyclohexadiene

0.48:0.52

host:total guest

1:1

4 DIEN4; Z_H = 8 N_{G1}:N_{G2}

M_{G2} = 80.14 THF:1,4-cyclohexadiene

Dm = 1.25 0.26:0.74

Vol = 7471.62

giving Z_G = 11 host:total guest

1:1.4

5 THF/BEN; Z_H = 8 N_{G1}:N_{G2}

M_{G2} = 78.12 THF:benzene

Dm = 1.25 0.25:0.75

Vol = 7457.61

giving Z_G = 11 host:total guest

1:1.4

The following crystals contain one type of guest.

6 BEN; Z_H = 2

M_G = 78.12

Dm = 1.17

Vol = 2360.82

giving Z_G = 6 host:guest

1:3

I T; Z_H = 4 from isomorphus test with structure 1

M_G = 72.12

Dm = 1.21

Vol = 4068.40

giving Z_G = 8 host:guest

1:2

7 Py; Z_H = 4

M_H = 490.17

Dm = 1.41

Vol = 2312.23

No guest, α-phase, $[Ni(NCS)_2(Py)_4]$.

4.3 X-Ray diffraction studies.

Single-crystal diffractometry was employed to elucidate the structures of 1 HANE, 2 HENE, 3 DIEN3, 4 DIEN4, 5 THF/BEN, 6 BEN, 7 PY and the unit cell parameters of I T (including isomorphous test) and II PYBEN.

For structures 1, 2, 3, 4, 5, 6 the final model employed anisotropic thermal parameters for the heavy atoms, (Ni, S) and isotropic ones for the rest. For structure 7 all atoms, except the hydrogens, were treated anisotropically as there were sufficient reflections to allow this refinement. No guest hydrogens were included and the host hydrogens were subjected to constrained refinement, riding at 1.00 Å from their parent carbon atoms, with a common isotropic temperature factor.

An absorption correction was applied to all data collections. For structures 1 and 2 there was significant crystal decay which was compensated by a decay correction.

Crystal data and experimental details of the data collections are in tables 4.3.1 to 4.3.4.

TABLE 4.3.1 CRYSTAL DATA, EXPERIMENTAL AND REFINEMENT PARAMETERS OF:

Crystal Data

Compound	1	2
Molecular Formula	$C_{38.44}H_{44.88}N_6O_{1.78}NiS_2$	$C_{38.44}H_{44.48}N_6O_{1.76}NiS_2$
Mr/gmol^{-1}	742.31	742.07
Space Group	Pbcn	Pbcn
a/Å	9.976(6)	9.987(7)
b/Å	20.630(25)	20.614(4)
c/Å	19.861(4)	19.898(4)
V/Å^3	4087.49	4096.44
Z	4	4
Host:G1:G2	1:1.78:0.22	1:1.76:0.24
Dm/gcm^{-3}	1.21	1.20
μ (MoK$_\alpha$)/cm^{-1}	5.67	5.66
F(000)	1566.99	1564.75

Data Collection

Compound	1	2
Crystal dimensions/mm	.25 x .5 x .74	.42 x .5 x .55
Scan mode	$\omega - 2\theta$	$\omega - 2\theta$
Scan width, $\Delta\omega$/°	1.00 + 0.35tanθ	1.05 + 0.35tanθ
Vertical aperture length/mm	6	6
Aperture width/mm	1.50 + 1.05tanθ	1.20 + 1.05tanθ
Final acceptance limit	20σ at 20min^{-1}in ω	20σ at 20min^{-1}in ω
Max recording time/s	40	40
Total number of unique reflections	2606	2497
Total number of 'observed' reflections [with $I_{rel} > 2\sigma I_{rel}$]	1461	1304
Crystal stability/%	17.2	32.4
Decay correction:		
Min. correction factor	1.00013	1.00035
Max. correction factor	1.09891	1.21554
Ave. correction factor	1.04634	1.09387

Final Refinement

Number of variables	97	97
$R=\Sigma\|\|F_o\| - \|F_c\|\| / \Sigma\|F_o\|$	0.087	0.084
$R=\Sigma w^{1/2}\|\|F_o\| - \|F_c\|\| / \Sigma w^{1/2}\|F_o\|$	0.100	0.096
Weighting scheme w	$(\sigma^2F)^{-1}$	$(\sigma^2F)^{-1}$

TABLE 4.3.2 CRYSTAL DATA, EXPERIMENTAL AND REFINEMENT PARAMETERS OF:

Crystal Data

Compound	3	4
Molecular Formula	$C_{35.04}H_{38}N_8O_{0.48}NiS_2$	$C_{37.68}H_{39.2}N_8O_{0.36}NiS_2$
Mr/gmol^{-1}	671.71	704.70
Space Group	$I4_1/a$	$I4_1/a$
a/Å	16.898(3)	16.986(4)
b/Å	16.898(3)	16.986(4)
c/Å	26.463(6)	25.896(15)
V/Å^3	7556.31	7471.62
Z	8	8
Host:G1:G2	1:0.48:0.52	1:0.36:1.04
Dm/gcm^{-3}	1.18	1.25
μ (MoK$_\alpha$)/cm^{-1}	6.08	6.17
F(000)	2816.54	3045.82

Data Collection

Compound	3	4
Crystal dimensions/mm	.5 x .5 x .56	.47 x .5 x .53
Scan mode	$\omega - 2\theta$	$\omega - 2\theta$
Scan width, $\Delta\omega$/°	$1.00 + 0.35\tan\theta$	$1.00 + 0.35\tan\theta$
Vertical aperture length/mm	6	6
Aperture width/mm	$1.20 + 1.05\tan\theta$	$1.40 + 1.05\tan\theta$
Final acceptance limit	20σ at 20min^{-1} in ω	20σ at 20min^{-1} in ω
Max recording time/s	40	40
Total number of unique reflections	2628	3002
Total number of 'observed' reflections [with $I_{rel} > 2\sigma I_{rel}$]	1698	2025
Crystal stability/%	8.7	3.2

Final Refinement

Number of variables	88	88
$R=\Sigma\|\|F_o\| - \|F_c\|\| / \Sigma\|F_o\|$	0.120	0.103
$R=\Sigma w^{1/2}\|\|F_o\| - \|F_c\|\| / \Sigma w^{1/2}\|F_o\|$	0.125	0.112
Weighting scheme w	$(\sigma^2 F)^{-1}$	$(\sigma^2 F)^{-1}$

TABLE 4.3.3 CRYSTAL DATA, EXPERIMENTAL AND REFINEMENT PARAMETERS OF:

Crystal Data

Compound	5	I
Molecular Formula	$C_{37.70}H_{37.1}N_6O_{0.35}NiS_2$	$C_{38}H_{44}N_6O_2NiS_2$
M_r/gmol^{-1}	702.69	739.71
Space Group	$I4_1/a$	Pbcn
a/Å	17.102(10)	9.937(4)
b/Å	17.102(10)	20.634(4)
c/Å	25.498(8)	19.842(8)
V/Å^3	7457.61	4068.40
Z	8	4
Host:G1:G2	1:0.35:1.05	1:2:0
Dm/gcm^{-3}	1.25	1.21
μ (MoK_α)/cm^{-1}	6.17	6.17
F(000)	2944.70	1560

Data Collection

Compound	5
Crystal dimensions/mm	.5 x .5 x .56
Scan mode	$\omega - 2\theta$
Scan width, $\triangle\omega$/°	$0.85 + 0.35\tan\theta$
Vertical aperture length/mm	6
Aperture width/mm	$1.15 + 1.05\tan\theta$
Final acceptance limit	20σ at $20 min^{-1} in \omega$
Max recording time/s	40
Total number of unique reflections	2823
Total number of 'observed' reflections [with $I_{rel} > 2\sigma I_{rel}$]	2200
Crystal stability/%	5.9

Final Refinement

Number of variables	88
$R=\Sigma\|\|F_o\| - \|F_c\|\| / \Sigma\|F_o\|$	0.118
$R=\Sigma w^{1/2}\|\|F_o\| - \|F_c\|\| / \Sigma w^{1/2}\|F_o\|$	0.132
Weighting scheme w	$(\sigma^2 F)^{-1}$

TABLE 4.3.4 CRYSTAL DATA, EXPERIMENTAL AND REFINEMENT PARAMETERS OF:

Crystal Data

Compound	6	7
Molecular Formula	$C_{48}H_{46}N_6NiS_2$	$C_{22}H_{20}N_6NiS_2$
Mr/gmol^{-1}	860.02	490.17
Space Group	$P\bar{1}$	C2/c
a/Å	10.432(24)	12.410(6)
b/Å	11.155(9)	12.922(2)
c/Å	21.581(7)	15.102(5)
α/°	78.70(5)	-
β/°	82.60(7)	107.30(4)
γ/°	74.09(13)	-
V/Å^3	2360.82	2312.23
Z	2	4
Host:Guest	1:3	-
Dm/gcm^{-3}	1.17	1.41
μ (MoK_α)/cm^{-1}	4.92	9.78
F(000)	872.0	1016.0

Data Collection

Compound	6	7
Crystal dimensions/mm	.53 x .56 x .56	.44 x .47 x .5
Scan mode	$\omega - 2\theta$	$\omega - 2\theta$
Scan width, $\Delta\omega$/°	$0.95 + 0.35\tan\theta$	$1.03 + 0.35\tan\theta$
Vertical aperture length/mm	6	6
Aperture width/mm	$1.20 + 1.05\tan\theta$	$1.06 + 1.05\tan\theta$
Final acceptance limit	20σ at $20\,min^{-1}$ in ω	20σ at $20\,min^{-1}$ in ω
Max recording time/s	40	40
Total number of unique reflections	3985	1930
Total number of 'observed' reflections [with $I_{rel} > 2\sigma I_{rel}$]	3427	1775
Crystal stability/%	6.9	1.8

Final Refinement

Number of variables	293	144
$R = \Sigma\|\|F_o\| - \|F_c\|\| / \Sigma\|F_o\|$	0.078	0.028
$R = \Sigma w^{1/2}\|\|F_o\| - \|F_c\|\| / \Sigma w^{1/2}\|F_o\|$	0.085	0.033
Weighting scheme w	$(\sigma^2 F)^{-1}$	$(\sigma^2 F)^{-1}$

4.4 Solution and refinement of structures with $[Ni(NCS)_2(4\text{-}ViPy)_4]$ as host.

4.4.1 1 HANE: $[Ni(NCS)_2(4\text{-}ViPy)_4](1.78THF)(0.22CYCLOHEXANE)$

Pbcn; a=9.976(6)Å, b=20.630(25)Å, c=19.861(4)Å, Z=4.

The conditions from the diffractometer intensity data for non-extinction of reflections were determined as:

hk0 : k = 2n (0k0 : k = 2n)

h0l : h + l = 2n (h00 : h = 2n)

0kl : l = 2n (00l : l = 2n)

which define the orthorhombic space group as Pcnb. To transform to Pbcn (as is customary), k and l were interchanged.

The matrix 1 0 0 0 0 -1 0 1 0 was applied to h k l respectively.

A Patterson vector map was computed to locate the coordinates of the nickel atom (heaviest atom). From the vector grid for the space group Pbcn the nickel atom was located at the Wyckoff special position c.

For all structures, when the relative intensities are given, they are in decending order as in the Patterson map.

Relative Intensity	u	v	w	Vector Position
999	.00	.00	.00	0, 0, 0
556	.50	.50	.00	1/2, 1/2, 0
451	.00	.37	.50	0, 2y, 1/2
275	.50	.87	.50	1/2, 2y +1/2, 1/2

giving y = 0.185 for the nickel atom.

The first electron density difference map based on the Ni atom position yielded the isothiocyanate ligand and two of the nitrogens from the vinyl pyridine ligands. Subsequent electron density difference maps yielded all the remaining non-hydrogen atoms of the vinyl pyridine ligands.

With the nickel atom sitting on the twofold axis the positions of all the host non-hydrogen atoms were determined as one isothiocyanate, two half vinyl pyridines and a full vinyl pyridine ligand. For the atoms of the two half vinyl pyridine rings that sit on the twofold axis their positions are allowed to refine in the y-direction only (0, y, .25) with site occupancy 0.5, that is N11, C14, C17, N21, C24, C27. For C17 and C27 this symmetry restriction is somewhat ideal as the thermal motion of these vinyl carbons results in higher temperature factors. Temperature factors (U) for C17 and C27 are 0.16 and 0.17 $Å^2$ respectively in comparison with an average value of 0.10 $Å^2$ for the pyridine ring atoms. Temperature factors are quoted from the final structure factor calculation. This symmetry restriction also resulted in variation of the bond lengths along the twofold axis for distances C14-C17 and C24-C27 which resulted in variation of the vinyl bonds C17-C18 and C27-C28 respectively. See Appendix A for bond lengths. C18 and C28 of the vinyl groups have site occupancy 0.5 as they are disordered about the twofold axis.

Anisotropic treatment of the heavy atoms (Ni, S) coupled with the insertion of hydrogen atoms gave an R of 17%. This yielded several peaks of electron density greater than 1 electron/$Å^3$ confirming the presence of guest. As it was known that both tetrahydrofuran and cyclohexane were present in the ratio 0.89:0.11 (from nmr) modelling of these residual peaks with THF was attempted. As no acceptable bond

lengths and angles were obtained, a difference electron density map was calculated and contoured in the region:

0.00 to 0.55 for x

0.20 to 0.72 for y

-0.20 to 0.32 for z (fractional coordinates)

As the guests are at general positions (Wyckoff position d) one guest molecule needs to be located for every half host molecule. The above contoured region was transferred onto perspex sheets with the appropiate scaling to facilitate the matching of the electron density peaks with a model. These peaks could be matched with a model of THF.

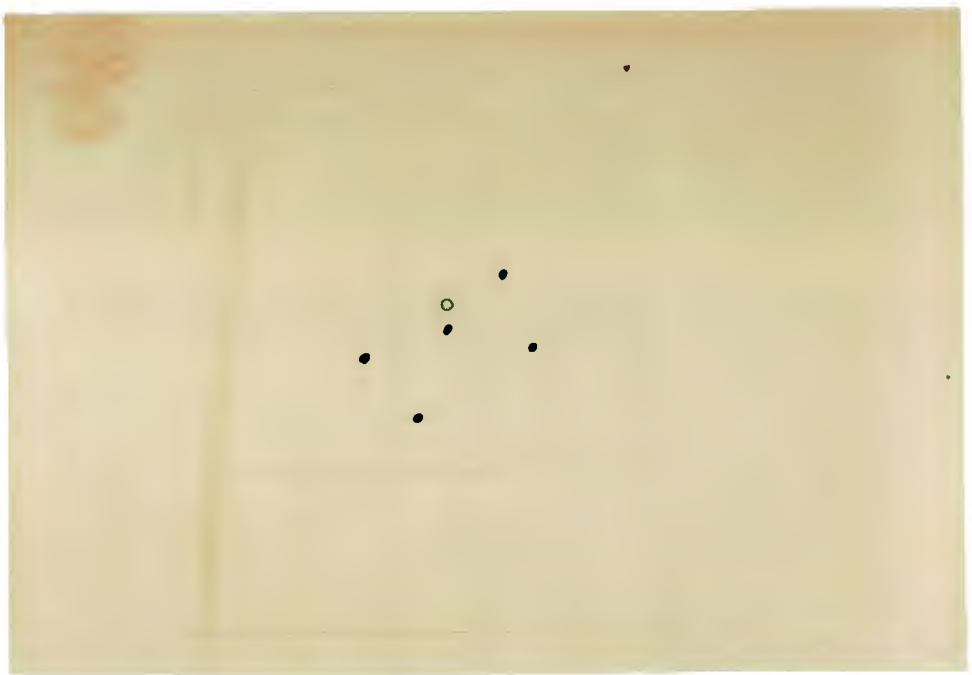

Photograph of peaks only, representing the THF atoms. Oxygen atom not identified.

These positions were inserted with three bond lengths constrained at 1.46 Å, the average of all the THF bonds, and three positions fixed, to allow the best possible refining of the model. The site occupancy of these atoms was fixed at 0.89.

In order to take the electron density of the cyclohexane into account a model of its molecular scattering factor was attempted. The program ALCHEMY[4.2] was used to obtain the coordinate input to NORMAL of MULTAN[4.3]. An approximation of the scattering factor with sin θ/λ was then obtained in the form suitable for SHELX[4.4];

$$f(x) = a_1e^{-bx} + a_2e^{-bx} + a_3e^{-bx} + C.$$

The scattering factors obtained from MULTAN were plotted as a function of sin θ/λ. A calculation from statistical methods was used to fit the approximating function to the calculated curves[4.5]. As the shape of the approximating curve is derived from the addition of normal distribution functions, it cannot take into account any maxima or minima other than at sin $\theta/\lambda = 0$. The curve fit needs to be best in the range $0 < \sin \theta/\lambda < 0.5$, as this is the range in which the reflections were collected.

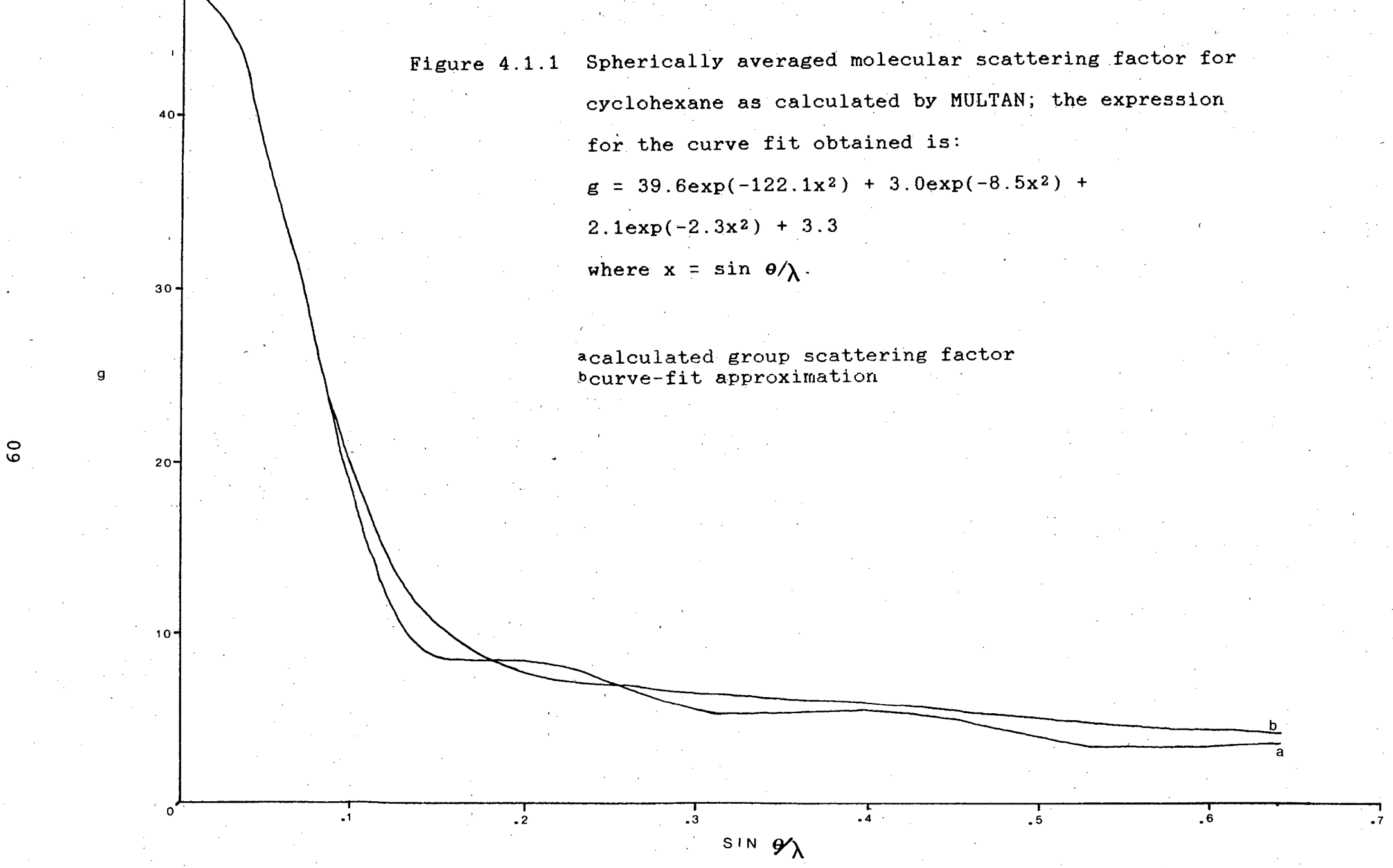

Figure 4.1.1 Spherically averaged molecular scattering factor for cyclohexane as calculated by MULTAN; the expression for the curve fit obtained is:

$g = 39.6\exp(-122.1x^2) + 3.0\exp(-8.5x^2) + 2.1\exp(-2.3x^2) + 3.3$

where $x = \sin\theta/\lambda$.

[a]calculated group scattering factor
[b]curve-fit approximation

This spherically averaged group was placed at the centre of the THF guest molecule with a site occupancy of 0.11, and refined isotropically. This was considered a poor model owing to its unrealistic temperature factor (1.20 $Å^2$) and a slight increase of R to 9.1% and was not included in the final structure refinement. The final least squares refinement converged to R = 8.7%, Rw = 10.0% with the weighting scheme $w = 1/(\sigma^2(F_o) + 0.002F_o^2)$, and one residual peak of 0.6 $e/Å^3$ in the vicinity of the THF molecule as a result of not including the cyclohexane. The analysis of variance (Appendix B) computed after the final cycle showed that this weighting scheme was satisfactory. All fractional atomic coordinates and thermal parameters are listed in table 4.1.1.

Bond lengths, angles and torsion angles are in Appendix A.

Observed and calculated structure factors are in Appendix C.

Table 4.1.1 Fractional atomic coordinates (x 10**4)
and Thermal Parameters (A**2 x 10**3)
with e.s.d. s in parentheses for Compound HANE.

Atom	x/a	y/b	z/c	Uiso/Uequiv(*)
Ni(1)	0(0)	1839(1)	2500(0)	72(1) *
N(1)	-1851(8)	1846(4)	2020(4)	82(2)
C(1)	-2851(11)	1864(5)	1773(6)	92(3)
S(1)	-4292(4)	1888(3)	1404(2)	178(3) *
N(11)	0(0)	804(6)	2500(0)	85(3)
C(12)	-540(11)	462(6)	2002(6)	102(3)
C(13)	-514(12)	-216(6)	2000(6)	109(4)
C(14)	0(0)	-564(9)	2500(0)	106(5)
C(17)	0(0)	-1202(15)	2500(0)	163(9)
C(18)	-201(35)	-1718(17)	2145(20)	171(14)
N(21)	0(0)	2873(6)	2500(0)	83(3)
C(22)	1114(11)	3205(5)	2361(5)	96(3)
C(23)	1113(12)	3887(6)	2368(5)	106(4)
C(24)	0(0)	4219(9)	2500(0)	108(5)
C(27)	0(0)	4924(15)	2500(0)	168(10)
C(28)	-635(46)	5329(21)	2401(25)	207(19)
N(41)	-960(7)	1839(4)	3462(4)	80(2)
C(42)	-2046(11)	1500(5)	3557(6)	93(3)
C(43)	-2622(11)	1428(6)	4224(6)	102(4)
C(44)	-2024(11)	1761(5)	4732(6)	94(3)
C(45)	-964(12)	2124(6)	4615(6)	107(4)
C(46)	-411(11)	2169(5)	3982(6)	95(3)
C(47)	-2525(17)	1680(9)	5447(9)	154(6)
C(48)	-3482(19)	1304(9)	5661(9)	166(6)
C(1G)	2837(0)	4710(0)	-282(0)	474(32)
C(2G)	3788(0)	4290(0)	104(0)	567(38)
C(3G)	3416(0)	3852(0)	672(0)	349(19)
C(4G)	1940(0)	3918(0)	625(0)	380(22)
C(5G)	1804(0)	4532(0)	228(0)	410(27)

Anisotropic atoms have thermal parameters (A**2 x 10**3) of the form :

EXP(-2*PI**2(U11*H**2*(A*)**2+...+2*U12*H*K*(A*)*(B*)+...)

Atom	U11	U22	U33	U23	U13	U12
Ni(1)	75(1)	75(1)	67(1)	0(0)	-10(1)	0(0)
S(1)	106(3)	263(6)	165(4)	-54(4)	-61(3)	38(3)

4.4.2 2 HENE: $[Ni(NCS)_2(4\text{-ViPy})_4](1.76THF)(0.24CYCLOHEXENE)$

Pbcn; a=9.987(7)Å, b=20.614(4)Å, c=19.898(4)Å, Z=4.

The conditions from the diffractometer intensity data for non-extinction of reflections were the same as the previous structure, thus defining the space group as Pcnb which was transformed to Pbcn. The positions of the nickel and isothiocyanate atoms from structure 1 were used for initial phasing. Subsequent difference electron maps showed the remaining host atoms to be isomorphous with structure 1, with slight variations for the vinyl atoms owing to their thermal motion.

The difference Fourier map obtained after refinement of the host atoms (R=14%) showed several peaks with electron density greater than 1 e/Å^3, confirming the presence of guest. As the ratio of THF to cyclohexene was 0.88:0.12 modelling of these residual peaks with THF was again attempted. This did not yield any solution and the same region as for structure 1 was contoured and transferred onto perspex sheets. The electron density peaks corresponded with the atom positions of a THF model. These positions were inserted and refined as for structure 1 with site occupancy 0.88. The same procedure was followed to take the scattering matter of cyclohexene into account. Owing to its unrealistic temperature factor, the molecular scattering model was not included in the final structure refinement.

The final least squares refinement converged to R = 8.4%, Rw = 9.6% with the weighting scheme $w = 1/(\sigma^2(F_o) + 0.002F_o^2)$, and a residual peak of 0.4 e/Å^3. The analysis of variance (Appendix B) computed after the final cycle showed that this weighting scheme was satifactory. All fractional atomic coordinates and thermal parameters

are listed in table 4.2.1.

Bond lengths, angles and torsion angles are in Appendix A.

Observed and calculated structure factors are in Appendix C.

Table 4.2.1 Fractional atomic coordinates (x 10**4) and Thermal Parameters (A**2 x 10**3) with e.s.d. s in parentheses for Compound HENE.

Atom	x/a	y/b	z/c	Uiso/Uequiv(*)
Ni(1)	0(0)	1842(1)	2500(0)	73(1) *
N(1)	-1838(9)	1844(4)	2029(4)	91(3)
C(1)	-2866(11)	1862(5)	1785(6)	94(3)
S(1)	-4283(4)	1884(3)	1404(3)	181(3) *
N(11)	0(0)	791(6)	2500(0)	86(3)
C(12)	-550(11)	463(6)	2010(6)	98(3)
C(13)	-554(12)	-202(6)	2009(6)	108(4)
C(14)	0(0)	-558(10)	2500(0)	113(5)
C(17)	0(0)	-1300(17)	2500(0)	179(10)
C(18)	-219(40)	-1578(22)	2062(25)	197(16)
N(21)	0(0)	2875(6)	2500(0)	88(3)
C(22)	1101(12)	3207(5)	2355(5)	97(3)
C(23)	1106(13)	3880(6)	2358(6)	108(4)
C(24)	0(0)	4219(10)	2500(0)	116(5)
C(27)	0(0)	4924(19)	2500(0)	188(11)
C(28)	-635(63)	5328(28)	2490(30)	268(30)
N(41)	-941(8)	1823(4)	3460(4)	84(2)
C(42)	-2041(11)	1491(5)	3570(6)	96(3)
C(43)	-2597(12)	1414(6)	4206(6)	101(4)
C(44)	-2039(12)	1742(6)	4736(6)	100(4)
C(45)	-919(12)	2113(6)	4624(6)	107(4)
C(46)	-411(11)	2151(6)	3982(6)	98(4)
C(47)	-2569(18)	1693(8)	5471(8)	145(5)
C(48)	-3486(21)	1297(9)	5635(10)	181(7)
C(1G)	2659(0)	4657(0)	-206(0)	432(27)
C(2G)	2080(0)	4677(0)	507(0)	306(16)
C(3G)	2980(0)	4288(0)	979(0)	499(35)
C(4G)	3299(0)	3799(0)	499(0)	475(21)
C(5G)	3834(0)	4226(0)	2(0)	592(40)

Anisotropic atoms have thermal parameters (A**2 x 10**3) of the form :

EXP(-2*PI**2(U11*H**2*(A*)**2+...+2*U12*H*K*(A*)*(B*)+...)

Atom	U11	U22	U33	U23	U13	U12
Ni(1)	78(1)	70(1)	71(1)	0(0)	-11(1)	0(0)
S(1)	111(3)	257(6)	176(4)	-63(4)	-63(3)	42(3)

4.4.3 3 DIEN3: $[Ni(NCS)_2(4\text{-ViPy})_4](0.48THF)(0.52\ 1,3\text{-CYCLOHEXADIENE})$ $I4_1/a$; a=16.898(3)Å, c=26.463(6)Å, Z=8.

The conditions from the diffractometer intensity data for non-extinction of reflections were determined as:

hkl : h + k + l = 2n

hk0 : h, k = 2n

0kl : k + l = 2n

hhl : l = 2n

00l : l = 4n

h00 : h = 2n

$h\bar{h}0$: h = 2n

which defines the tetragonal space group $I4_1/a$. All of the $I4_1/a$ structures (3, 4 and 5) are reported with respect to the second origin choice at $\bar{1}$[4.6]. With the unit cell volume the number of host molecules (as defined by the nickel position) must be 8, out of a choice of 16, 8 or 4. With this restriction the vector grids for Wyckoff positions e and d were constructed to solve the Patterson.

Relative Intensity	u	v	w	Vector Position
999	.00	.00	.00	0, 0, 0
813	.50	.50	.50	1/2, 1/2, 1/2
306	.00	.00	.34	0, 0, 2z +1/4
295	.00	.50	.75	0, 1/2, 3/4
206	.50	.00	.09	1/2, 0, 2z

giving z = 0.045 for the nickel atom.

With the z coordinate being a general position this defined the nickel position as Wyckoff special position e. The nickel was positioned at 1/2, 1/4, .545 with site occupancy 0.5. Subsequent difference electron density maps yielded the remaining atoms in the asymmetric unit; nickel with site occupancy 0.5 on the twofold axis, one isothiocynate and two 4-vinylpyridine ligands with full site occupancy on general positions. With anisotropic treatment of the heavy atoms and insertion of hydrogen atoms the R was 15%. Confirming the presence of guest were 5 peaks of electron density greater than 1 e/Å^3. These peaks were in a disordered array about the center of inversion, Wyckoff position d, confirming the density of host to guest 1:1. Owing to the statistical disorder of the two guests no chemical model could be obtained. A difference electron density map was calculated and contoured in the region:

0.00 to 0.60 for x

0.10 to 0.40 for y

0.60 to 0.90 for z

and transferred onto perspex sheets with an appropriate scaling.

Photographs of the contoured region with the colour scale:

black = 40

blue = 60

green = 80

red = 100 where 1 e/Å^3 = 61

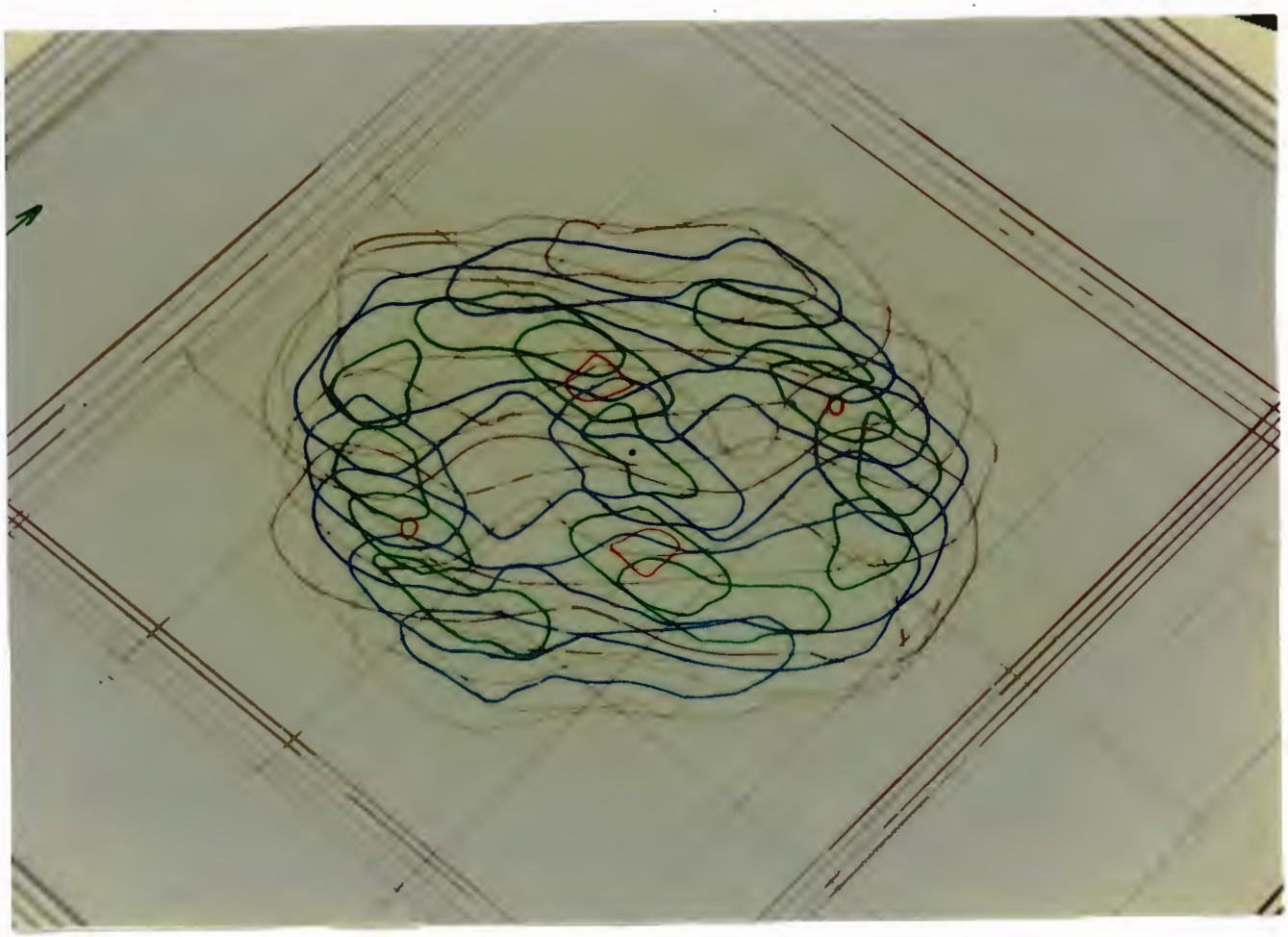

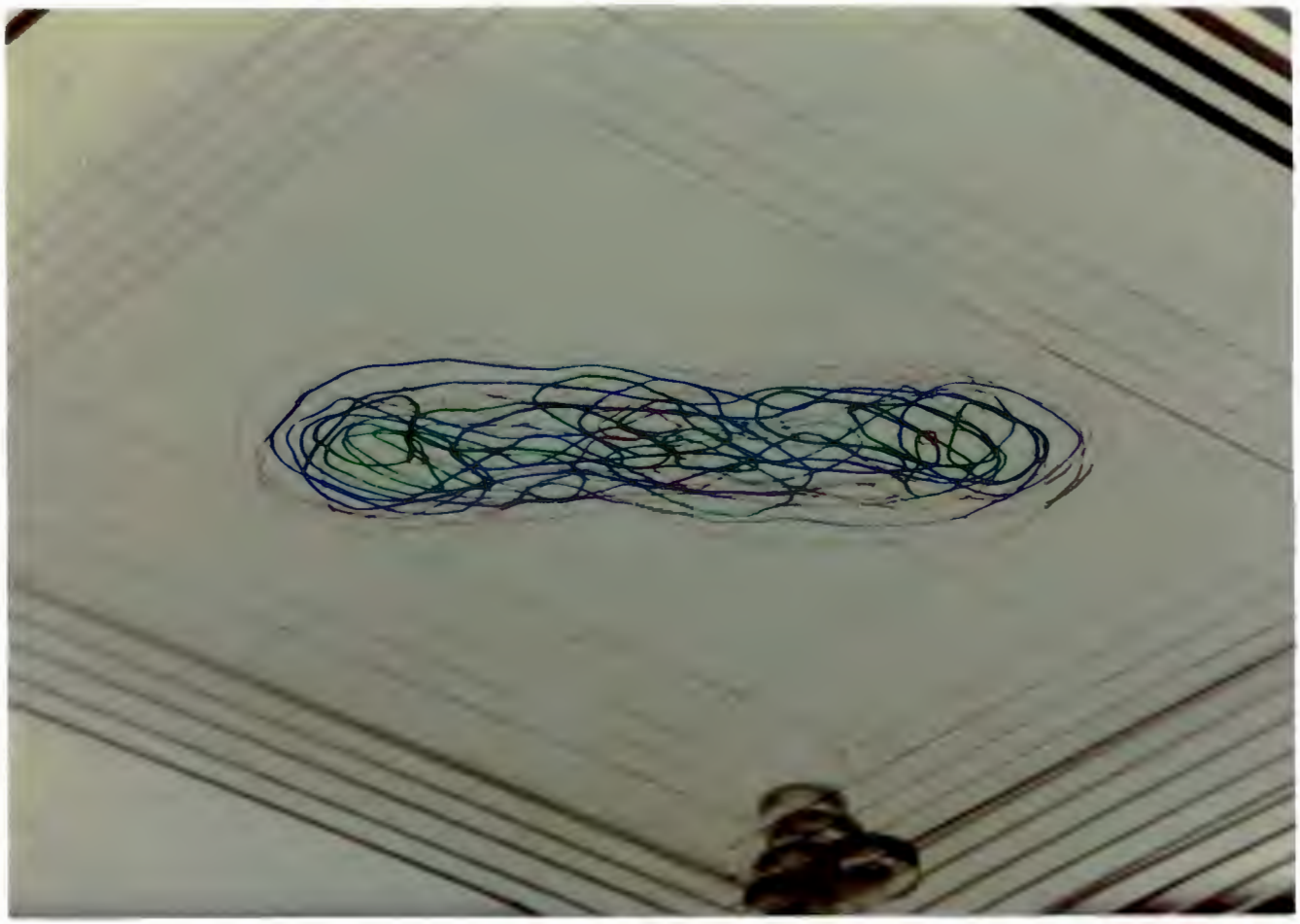

The centre of inversion (1/2, 1/2, 3/4) is at the centre of the electron-dense region which is a disc shape. This contouring was most informative as it showed the presence of electron density both around and through the centre of inversion which was unexpected. The six atoms of 1,3-cyclohexadiene (1,3C_6H_8) and the five atoms of THF (with one atom being fixed at the center of inversion) were chosen so as to coinside with the peaks and give a suitable chemical model. For the 1,3C_6H_8 the atoms were given a site occupancy of 0.26 and for THF 0.24, thereby taking into account the density, nmr analysis and centre of inversion. The average of their bond lengths was calculated, 1.47 Å and 1.49 Å respectively, and used to fix the distance between successive atoms. These positions were allowed to refine taking into account the puckered conformations of the guests. This model was not accepted as R increased to 30%.

The original positions were used but this time the bond lengths (as above) were fixed and constrained to a regular hexagon and pentagon respectively. This approximation of the guest modelling was acceptable as the R decreased and the average temperature factor for the guest atoms was 0.34 $Å^2$, a high but acceptable value for disordered guests of these compounds. As will be shown in section 5.3 the channels are large enough to allow guest motion.

Only after structures 4 and 5 were solved and found to be isomorphous with previous $I4_1/a$ structures of this host, was it realised that this structure (3) was also isomorphous. When referring to these structures as being isomorphous it is with respect to the host atoms only. Some may or may not be isomorphous with respect to the guest, as the guests usually sit at the $\bar{1}$ or $\bar{4}$ sites depending on their geometry. With the nickel atom at 0.50, 0.25, 0.54 for all these

structures, the sulphur for structure 3 was at 0.25, 0.13, 0.53 and for structures 4 and 5 at approximately 0.25, 0.37, 0.55. This showed the NCS ligand to be slewed by 90° for structure 3 with respect to the NCS ligands of structures 4 and 5. To have a proper comparison of structures 3, 4 and 5 and to confirm all the host atoms as being isomorphous, the unit cell of structure 3 was transformed by the matrix 1 0 0 0 -1 0 0 0 1. The guest input atoms were correspondingly transformed. The refinement values quoted below are for the transformed structure.

The final least squares refinement converged to R = 12.0%, Rw = 12.5% with the weighting scheme $w = 1/(\sigma^2(F_o) + 0.022592F_o^2)$, and one significant residual peak of 1.1 e/Å^3 at 0.249, 0.203, 0.816 which is in the vicinity of the guest atoms. This peak may be attributed to the planar condition imposed on the non planar guests. The analysis of variance (Appendix B) computed after the final cycle showed the weighting scheme to be satisfactory. All fractional atomic coordinates and thermal parameters are listed in table 4.3.1. Bond lengths, angles and torsion angles are in Appendix A. Observed and calculated structure factors are in Appendix C.

Table 4.3.1 Fractional atomic coordinates (x 10**4)
and Thermal Parameters (A**2 x 10**3)
with e.s.d. s in parentheses for Compound DIEN3.

Atom	x/a	y/b	z/c	Uiso/Uequiv(*)
Ni(1)	5000(0)	2500(0)	5441(1)	61(1) *
N(1)	4017(5)	3242(5)	5428(3)	74(2)
C(1)	3363(7)	3421(7)	5425(4)	74(3)
S(1)	2443(2)	3660(3)	5411(2)	123(2) *
N(11)	5502(5)	3218(5)	6020(3)	69(2)
C(12)	5033(7)	3515(7)	6387(4)	77(3)
C(13)	5332(7)	3946(7)	6781(5)	82(3)
C(14)	6173(7)	4050(7)	6820(5)	80(3)
C(15)	6600(7)	3735(7)	6458(5)	83(3)
C(16)	6278(7)	3346(7)	6070(4)	74(3)
C(17)	6543(8)	4433(8)	7260(5)	94(4)
C(18)	6215(10)	4629(11)	7672(7)	130(5)
N(21)	4448(5)	1802(5)	4868(3)	63(2)
C(22)	4063(6)	2169(7)	4477(4)	76(3)
C(23)	3735(7)	1767(7)	4081(4)	77(3)
C(24)	3759(6)	936(6)	4074(4)	70(3)
C(25)	4144(7)	573(7)	4468(4)	76(3)
C(26)	4466(6)	1030(6)	4858(4)	69(3)
C(27)	3423(9)	493(10)	3654(6)	109(4)
C(28)	3126(14)	675(14)	3275(9)	166(8)
GC1	2673	2223	7320	340
GC2	3473	1981	7472	340
GC3	3780	2200	7972	340
GC4	3285	2663	8321	340
GC5	2484	2905	8169	340
GC6	2178	2686	7669	340
GC11	2403	2368	7362	
GC22	3220	2044	7408	340
GC33	3533	2271	7914	340
GC44	2910	2736	8180	340
GC55	2212	2796	7839	340
				340

Anisotropic atoms have thermal parameters (A**2 x 10**3) of the form

EXP(-2*PI**2(U11*H**2*(A*)**2+...+2*U12*H*K*(A*)*(B*)+...)

Atom	U11	U22	U33	U23	U13	U12
Ni(1)	65(1)	54(1)	65(1)	0(0)	0(0)	0(1)
S(1)	79(2)	107(3)	181(4)	0(3)	-5(2)	20(2)

4.4.4 4 DIEN4: [Ni(NCS)$_2$(4-ViPy)$_4$](0.36THF)(1.04 1,4-CYCLOHEXADIENE)

I4$_1$/a; a=16.986(4)Å, c=25.896(15)Å, Z=8.

The nickel atom was located by interpreting the Patterson map and the remaining atoms were found in subsequent electron density maps. With all the host atoms located and anisotropic treatment of the heavy atoms, the R was 13%. Again residual peaks in the vicinity of the inversion centre (1/2, 1/2, 3/4) did not satisfy any chemical model. A difference electron density map was calculated and contoured in the same region as for structure 3, and transferred onto perspex sheets with an appropriate scaling. The electon density had the same general shape of a disc as in structure 3 but was much more diffuse. This greater spread of electron density was supportive of the measured crystal density which gave a host to total guest ratio 1:1.4. To make sure these voids were able to accommodate two guests the volume of the cavities was determined using the program OPEC[4.7]. These cavities are discussed in section 5.3 and are large enough to accommodate two guests that are disordered about the inversion centre, with this disorder being carried through to the $\bar{4}$ site, thus forming a channel filled with guest in the ratio 1:1.4 (host:guest). The six atoms of 1,4-cyclohexadiene (1,4C$_8$H$_8$) were given site occupancy 0.52 and the five atoms of THF were given site occupancy 0.18, thus taking into account the density, nmr and centre of inversion. Their average bond lengths, 1.47 Å and 1.49 Å respectively, were used to fix the distance between successive atoms, which were allowed to refine taking into account the puckered conformations. Again this refinement was unsuccessful and a regular hexagon and pentagon were employed as models.

The final least squares refinement converged to R = 10.3%, Rw = 11.2% with the weighting scheme $w = 1/(\sigma^2(F_o) + 0.004659F_o^2)$, and one significant residual peak of 1.3 e/Å^3 at 0.193, 0.208, 0.764 which is in the vicinity of the guest atoms and may have occurred owing to the approximate nature of the models. The analysis of variance (Appendix B) computed after the final cycle showed that this weighting scheme was satisfactory. All fractional atomic coordinates and thermal parameters are listed in table 4.4.1.

Bond lengths, angles and torsion angles are in Appendix A.

Observed and calculated structure factors are in Appendix C.

Table 4.4.1 Fractional atomic coordinates (x 10**4)
and Thermal Parameters (A**2 x 10**3)
with e.s.d. s in parentheses for Compound DIEN4.

Atom	x/a	y/b	z/c	Uiso/Uequiv(*)
Ni(1)	5000(0)	2500(0)	5477(1)	60(1) *
N(1)	4010(4)	3234(4)	5464(2)	69(2)
C(1)	3372(5)	3403(5)	5480(3)	75(2)
S(1)	2463(2)	3687(2)	5508(2)	125(2) *
N(11)	5486(4)	3216(4)	6068(3)	68(2)
C(12)	5020(6)	3520(5)	6435(4)	83(2)
C(13)	5324(6)	3964(6)	6853(4)	93(3)
C(14)	6155(6)	4081(5)	6889(3)	82(2)
C(15)	6609(6)	3775(5)	6517(4)	84(2)
C(16)	6256(5)	3339(5)	6118(3)	77(2)
C(17)	6533(7)	4488(6)	7309(5)	110(3)
C(18)	6182(10)	4675(11)	7747(7)	165(6)
N(21)	4442(4)	1820(3)	4890(2)	64(2)
C(22)	4079(5)	2162(5)	4486(3)	72(2)
C(23)	3733(5)	1771(5)	4087(3)	75(2)
C(24)	3751(5)	954(5)	4083(3)	70(2)
C(25)	4129(5)	592(5)	4490(3)	73(2)
C(26)	4457(5)	1014(5)	4880(3)	70(2)
C(27)	3442(7)	490(7)	3658(4)	104(3)
C(28)	3145(9)	774(9)	3223(6)	155(5)
GC1	1310	3262	7108	330
GC2	0710	3230	6699	330
GC3	0591	2498	6406	330
GC4	1070	1800	6521	330
GC5	1669	1833	6930	330
GC6	1789	2564	7224	330
GC11	2260	3086	7321	330
GC22	2811	3102	7769	330
GC33	3023	2274	7898	330
GC44	2605	1746	7529	330
GC55	2133	2248	7173	330

Anisotropic atoms have thermal parameters (A**2 x 10**3) of the form :

EXP(-2*PI**2(U11*H**2*(A*)**2+...+2*U12*H*K*(A*)*(B*)+...)

Atom	U11	U22	U33	U23	U13	U12
Ni(1)	62(1)	54(1)	64(1)	0(0)	0(0)	0(1)
S(1)	78(2)	114(2)	183(3)	0(2)	-1(2)	19(2)

4.4.5 5 THF/BEN: $[Ni(NCS)_2(4\text{-ViPy})_4](0.35THF)(1.05\ BENZENE)$

$I4_1/a$; a=17.102(10)Å, c=25.498(8)Å, Z=8.

After location of the nickel atom with a Patterson map and subsequent difference Fourier syntheses all the host atoms were located and found to be isomorphous with structure 4. Again a disordered array of significant residual peaks in the vicinity of the centre of inversion resulted in the same procedure being adopted as for structures 3 and 4. The contoured region was very similar to that of structure 4 with the general shape of a disc with the electron density being diffuse. This larger volume of electron density supported the measured crystal density of host to guest 1:1.4. To confirm that the voids were large enough to accommodate this ratio the program OPEC was used. Again models were used to interpret the three dimensional electron density map by matching high electron density to guest atom positions. The benzene atoms were given site occupancy 0.53 and the THF atoms 0.17 thereby taking into account the density, nmr and centre of inversion. The bond lengths 1.40 Å and 1.49 Å were used to fix successive atoms for benzene and THF respectively. Refinement of these positions without geometric constraint was unsuccessful. A regular hexagon and pentagon with the above bond lengths were used with the positions being allowed to refine, as for structures 3 and 4.

The final least squares refinement converged to R = 11.8%, Rw = 13.2% with the weighting scheme $w = 1/(\sigma^2(F_o) + 0.020285F_o^2)$, and one significant residual peak of 1.6 e/Å^3 at 0.200, 0.205, 0.764 which is in the vicinity of the guest atoms and may have occurred owing to the approximate nature of the models. The analysis of variance (Appendix B) computed after the final cycle showed that this weighting scheme

was satisfactory. All fractional atomic coordinates and thermal parameters are listed in table 4.5.1.
Bond lengths, angles and torsion angles are in Appendix A.
Observed and calculated structure factors are in Appendix C.

The structures that have been discussed (1 to 5) have all had disordered guests. This implies, as with many other clathrates, that the host-guest interaction is weak. Caution should be exercised when locating and refining the guest in a clathrate structure. When the difference electron density map cannot easily be interpreted as representing a single guest, this may well be due to the fact that one has a mixture of two guests and both are disordered. Density measurements may detect the presence of more than one guest, however, density measurements are often considered inaccurate owing to loss of guest. A chemical probe of the crystal contents is therefore needed and in this case nmr was used.

Table 4.5.1 Fractional atomic coordinates (x 10**4)
and Thermal Parameters (A**2 x 10**3)
with e.s.d. s in parentheses for Compound THF/BEN.

Atom	x/a	y/b	z/c	Uiso/Uequiv(*)
Ni(1)	5000(0)	2500(0)	5527(0)	63(1) *
N(1)	4012(4)	3216(4)	5511(2)	77(2)
C(1)	3385(5)	3416(5)	5521(3)	70(2)
S(1)	2479(2)	3711(2)	5542(1)	120(1) *
N(11)	5486(4)	3209(4)	6128(2)	73(2)
C(12)	5025(6)	3531(6)	6489(4)	94(3)
C(13)	5323(6)	3988(6)	6903(4)	99(3)
C(14)	6140(6)	4090(6)	6943(3)	87(2)
C(15)	6585(6)	3781(6)	6574(3)	96(3)
C(16)	6260(5)	3341(5)	6169(3)	81(2)
C(17)	6532(8)	4534(8)	7366(5)	126(4)
C(18)	6154(13)	4648(13)	7793(9)	185(7)
N(21)	4446(3)	1823(3)	4919(2)	66(1)
C(22)	4079(5)	2169(5)	4523(3)	77(2)
C(23)	3744(4)	1779(5)	4111(3)	73(2)
C(24)	3755(5)	987(5)	4101(3)	73(2)
C(25)	4127(5)	600(5)	4523(3)	81(2)
C(26)	4459(4)	1029(4)	4910(3)	69(2)
C(27)	3445(7)	531(7)	3671(4)	104(3)
C(28)	3130(9)	816(10)	3211(6)	155(5)
GC1	2172	3099	7208	340
GC2	1545	3548	7025	340
GC3	0893	3181	6802	340
GC4	0869	2365	6761	340
GC5	1497	1916	6944	340
GC6	2149	2283	7167	340
GC11	2038	2832	7193	340
GC22	2264	3408	7604	340
GC33	2830	3023	7965	340
GC44	2955	2207	7777	340
GC55	2466	2089	7300	340

Anisotropic atoms have thermal parameters (A**2 x 10**3) of the form

EXP(-2*PI**2(U11*H**2*(A*)**2+...+2*U12*H*K*(A*)*(B*)+...)

Atom	U11	U22	U33	U23	U13	U12
Ni(1)	63(1)	61(1)	66(1)	0(0)	0(0)	0(1)
S(1)	76(2)	112(2)	173(3)	0(2)	1(2)	18(1)

4.4.6 6 BEN: $[Ni(NCS)_2(4\text{-}ViPy)_4(3BENZENE)$

PT; a=10.432(24)Å, b=11.155(9)Å, c=21.581(7)Å, α=78.70(5)°, β=82.60(7)°, γ=74.09(13)°, Z=2.

Inspection of the data collection revealed the triclinic space group P1 or PT. The centrosymmetric space group PT was chosen. A Patterson vector map was computed to locate the nickel atom. From the vector grid the nickel atom was located at the Wyckoff general position i.

Relative Intensity	u	v	w	Vector Position
999	.00	.00	.00	0, 0, 0
369	.41	.31	.56	2x, 2y, 2z

giving x=0.205, y=0.155, z=0.280 for the nickel atom.

As the nickel atom is at a general position all the host non-hydrogen atoms(39) were located after subsequent difference electron density maps.

Confirming the density of a host to guest ratio 1:3, guest atoms at general positions and special positions were located. After suitable refinement two benzene rings at general positions were located. This refinement resolved each benzene molecule into two rings superimposed on each other as shown in figure 4.6.1, with a site occupancy 0.5. The temperature factors obtained were consistent with this model.

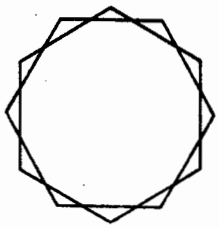

Figure 4.6.1 Superimposed benzene rings showing the positions of the benzene atoms at both general positions.

For the remaining guest molecule three peaks were located around the $\bar{1}$ sites 1/2, 0, 0 (Wyckoff position d) and 0, 0, 0 (Wyckoff position a) and were given full site occupancy. The bond lengths, angles and temperature factors for each of the three peaks gave no indication of disorder around the centre of symmetry. This was the only structure where the guest atoms were able to refine without any approximate models, and be suitably interpreted.

In the last difference electron density map the vinyl atom C28 showed possible disorder. As the pi-system of the vinyl group has a bonding interaction with the pi-system of the pyridine, the vinyl group is always coplanar with the pyridine.
The placing of two C28 atoms with site occupancy 0.5 each resulted in unrealistic bond lengths and angles. The half site occupancy was used as a model of 50% statistical disorder which was inferred from the electron density peaks. In the final refinement the originally located position of C28 with full site occupancy was used. Its unusually high temperature factor of 0.279 $Å^2$ can only be attributed

to thermal motion. In all the previous structures this procedure of testing for statistical disorder of the vinyl group was employed whenever there was evidence of it. In theory this motion or bond bending should be detected as a wag in the infra-red spectrum.

Attempted solution of the structure in space group P1 resulted in extensive correlation in the least-squares matrix and R = 14%, thus substantiating the choice of the centrosymmetric space group $P\bar{1}$.

The final least squares refinement converged to R = 7.8%, Rw = 8.5% with the weighting scheme $w = 1/(\sigma^2(F_o) + .000071F_o^2)$, and no significant residual electron density peaks. The analysis of variance (Appendix B) computed after the final cycle showed that this weighting scheme was satisfactory. All fractional atomic coordinates and thermal parameters are listed in table 4.6.1.
Bond lengths, angles and torsion angles are in Appendix A.
Observed and calculated structure factors are in Appendix C.

Table 4.6.1 Fractional atomic coordinates (x 10**4)
and Thermal Parameters (A**2 x 10**3)
with e.s.d. s in parentheses for Compound BEN.

Atom	x/a	y/b	z/c	Uiso/Uequiv(*)
Ni(1)	2063(1)	1597(1)	2826(0)	73(1) *
N(1)	3660(6)	2117(6)	2261(3)	81(2)
C(1)	4360(7)	2512(7)	1863(4)	72(2)
S(1)	5292(3)	3082(3)	1313(1)	126(2) *
N(2)	452(6)	1090(6)	3352(3)	82(2)
C(2)	-224(8)	578(7)	3698(4)	76(2)
S(2)	-1179(3)	-158(3)	4177(2)	136(2) *
N(11)	1768(6)	3165(5)	3288(3)	74(2)
C(12)	2763(8)	3599(7)	3394(4)	78(2)
C(13)	2648(8)	4607(7)	3678(4)	80(2)
C(14)	1369(8)	5278(8)	3894(4)	82(2)
C(15)	336(9)	4836(8)	3793(4)	95(3)
C(16)	520(8)	3801(8)	3500(4)	90(3)
C(17)	1141(10)	6392(9)	4189(4)	107(3)
C(18)	2017(11)	6847(10)	4367(5)	129(4)
N(21)	782(6)	2754(6)	2117(3)	81(2)
C(22)	-285(9)	2426(8)	1985(4)	97(3)
C(23)	-1112(10)	3165(9)	1513(5)	110(3)
C(24)	-828(10)	4250(10)	1166(5)	113(3)
C(25)	237(10)	4582(9)	1305(5)	111(3)
C(26)	1025(9)	3845(9)	1777(4)	103(3)
C(27)	-1621(14)	5139(14)	647(6)	187(5)
C(28)	-2567(19)	4921(20)	447(10)	280(10)
N(31)	2396(6)	0(5)	2372(3)	72(2)
C(36)	2321(8)	-1134(7)	2710(4)	84(2)
C(35)	2617(8)	-2201(8)	2445(4)	90(3)
C(34)	2983(8)	-2183(8)	1826(4)	87(2)
C(33)	3057(8)	-981(8)	1453(4)	98(3)
C(32)	2762(8)	33(8)	1762(4)	88(2)
C(37)	3297(10)	-3348(10)	1530(5)	123(3)
C(38)	3526(14)	-3418(13)	921(7)	173(5)
N(41)	3370(6)	460(5)	3522(3)	71(2)
C(42)	4648(8)	-95(7)	3339(4)	87(2)
C(43)	5525(8)	-909(7)	3753(4)	82(2)
C(44)	5128(7)	-1200(7)	4378(3)	68(2)
C(45)	3808(7)	-616(7)	4569(4)	77(2)
C(46)	2996(8)	180(7)	4129(4)	73(2)
C(47)	6000(8)	-2079(8)	4844(4)	92(3)
C(48)	7290(10)	-2699(9)	4715(5)	111(3)
C(1G1)	2321(35)	150(31)	7743(17)	132(15)
C(2G1)	1094(36)	1232(49)	7479(18)	144(16)
C(3G1)	948(27)	2492(31)	7595(14)	113(9)
C(4G1)	1872(40)	2895(33)	7927(19)	131(11)
C(5G1)	2993(28)	1896(38)	8194(13)	111(9)
C(6G1)	3093(23)	586(24)	8078(11)	77(7)
C(1G2)	4224(13)	9543(12)	9679(6)	144(4)
C(2G2)	5494(14)	8822(12)	9792(6)	155(4)
C(3G2)	6265(13)	9267(13)	135(6)	155(4)
C(1G3)	-3991(26)	5648(26)	3326(23)	104(9)
C(2G3)	-3579(33)	4816(41)	3905(19)	116(11)
C(3G3)	-3255(33)	3574(37)	4028(18)	133(15)
C(4G3)	-3306(21)	3060(20)	3460(18)	91(7)
C(5G3)	-3757(33)	3887(43)	2859(19)	113(10)
C(6G3)	-3999(33)	5036(43)	2861(19)	121(11)
C(1G4)	293(14)	-305(17)	-580(7)	179(5)
C(2G4)	340(15)	8717(15)	-70(9)	193(6)

Anisotropic atoms have thermal parameters (A**2 x 10**3) of the form :

EXP(-2*PI**2(U11*H**2*(A*)**2+...+2*U12*H*K*(A*)*(B*)+...)

Atom	U11	U22	U33	U23	U13	U12
Ni(1)	54(1)	71(1)	84(1)	0(1)	2(1)	-11(1)
S(1)	118(2)	123(2)	128(2)	9(2)	30(2)	-51(2)
S(2)	119(2)	107(2)	158(3)	-2(2)	62(2)	-34(2)

4.4.7 I T: $Ni(NCS)_2(4\text{-}ViPy)_4(2THF)$

Pbcn; a=9.937(4)Å, b=20.634(4)Å, c=19.842(8)Å, Z=4.

300 Reflections were collected in the range $1 \leq \theta \leq 10$ which gave the same cell parameters and reflection conditions as obtained for structures 1 and 2. We also checked that corresponding reflection intensities of this structure matched (strong, medium and weak) with the intensities of structures 1 and 2. Coupled with the density and thermal analysis it may be assumed that the structure is most likely to be isomorphous, at least with respect to the host. This was expected as structure 1 differs chemically by 11% with respect to guest.

4.5 Solution and refinement of 7 Py: $[Ni(NCS)_2(Py)_4]$

C2/c; a=12.410(6)Å, b=12.922(2)Å, c=15.102(5)Å, β=107.30(4)°, Z=4.

The conditions from the diffractometer intensity data for non-extinction of reflections were determined as:

hkl : h + k = 2n

h0l : h, l = 2n

0k0 : k = 2n

which defines the monoclinic space groups Cc and C2/c.

The space group C2/c was chosen and was subsequently found to be correct; unique axis b, cell choice 1 with the origin at $\bar{1}$ on glide plane c. Previous structures have shown that these complexes usually crystallise in a centrosymmetric space group, for example 6 BEN. A Patterson vector map was computed in order to locate the nickel

atom. After some difficulty the nickel atom was located at Wyckoff special position c (centre of symmetry).

Relative Intensity	u	v	w	Vector Position
999	.00	.00	.00	0, 0, 0
860	.50	.50	.00	1/2, 1/2, 0
534	.00	.50	.50	0, 2y, 1/2
446	.50	.00	.50	2x, 0, 2z + 1/2

The vector position 0, 2y, 1/2 was decided as the 'crucial' one as it had to be solved with a corresponding Patterson peak with the conditions x=0 and z=.5.

The vector position 2x, 0, 2z + 1/2 was used to find x and z, giving the nickel position: x = 0.25, y = 0.25, z = 0.00

This was used for initial phasing (site occupancy 0.5). Subsequent difference electron density maps yielded the remaining atoms of the one isothiocynate and two pyridine ligands with full site occupancy. With all atoms isotropic and no hydrogens the R value was 9% and no significant residual electron density peaks were present. This result concurred with the measured density and absence of guest. Hydrogens were included. As there were sufficient reflections to accommodate anisotropic refinement of all the non hydrogen atoms, this was carried out.

With a final refinement of R = 2.8% for the space group C2/c it was unlikely to be the wrong space group. However solution was attempted in the space group Cc. Owing to the twofold increase in the number of parameters that are refining the host atom positions (the host is no longer sitting on the inversion centre) the refinement should be

better or at least equivalent to that obtained for C2/c. As the refinement could not be reduced below R = 15% with extensive correlation in the least-squares matrix (27 correlation matrix elements greater than 0.5) for the space group Cc, C2/c was considered to be correct. The R value of 15% for Cc must be compared with the equivalent obtained for C2/c with only the Ni and S being treated anisotropically, that is, an R of 7%.

The final least squares refinement in C2/c converged to R = 2.8%, Rw = 3.3% with the weighting scheme $w = 1/(\sigma^2(F_o) + .000228F_o^2)$. The analysis of variance (Appendix B) computed after the final cycle showed that this weighting scheme was satisfactory. All fractional coordinates and thermal parameters are listed in table 4.7.1. Bond lengths, angles and torsion angles are in Appendix A. Observed and calculated structure factors are in Appendix C.

Table 4.7.1 Fractional atomic coordinates (x 10**4)
and Thermal Parameters (A**2 x 10**3)
with e.s.d. s in parentheses for Compound PY.

Atom	x/a	y/b	z/c	Uiso/Uequiv(*)
Ni(1)	2500(0)	2500(0)	0(0)	38(0) *
S(1)	-728(1)	3561(1)	810(0)	66(0) *
N(1)	1135(1)	3280(1)	178(1)	48(1) *
C(1)	358(2)	3401(1)	433(1)	41(1) *
N(11)	1396(1)	1224(1)	-586(1)	44(1) *
C(12)	1746(2)	241(2)	-460(2)	58(1) *
C(13)	1039(3)	-592(2)	-784(2)	70(1) *
C(14)	-55(3)	-411(2)	-1274(2)	77(1) *
C(15)	-419(2)	595(2)	-1433(2)	76(1) *
C(16)	318(2)	1382(2)	-1074(2)	56(1) *
N(21)	2134(1)	3104(1)	-1397(1)	44(1) *
C(22)	1581(2)	3995(2)	-1647(2)	54(1) *
C(23)	1371(2)	4428(2)	-2518(2)	66(1) *
C(24)	1713(2)	3911(2)	-3168(2)	71(1) *
C(25)	2262(2)	2983(2)	-2934(2)	72(1) *
C(26)	2464(2)	2606(2)	-2049(2)	56(1) *

Anisotropic atoms have thermal parameters (A**2 x 10**3) of the form :

EXP(-2*PI**2(U11*H**2*(A*)**2+...+2*U12*H*K*(A*)*(B*)+...)

Atom	U11	U22	U33	U23	U13	U12
Ni(1)	35(0)	37(0)	41(0)	-1(0)	12(0)	2(0)
S(1)	63(0)	62(0)	85(1)	0(0)	42(0)	8(0)
N(1)	44(1)	51(1)	52(1)	-1(1)	17(1)	7(1)
C(1)	45(1)	32(1)	44(1)	0(1)	9(1)	4(1)
N(11)	44(1)	40(1)	51(1)	-4(1)	17(1)	-1(1)
C(12)	61(1)	45(1)	69(2)	-6(1)	21(1)	0(1)
C(13)	84(2)	46(1)	88(2)	-12(1)	36(2)	-9(1)
C(14)	82(2)	68(2)	86(2)	-23(2)	32(2)	-34(2)
C(15)	56(1)	78(2)	85(2)	-16(2)	10(1)	-18(1)
C(16)	46(1)	55(1)	63(2)	-4(1)	9(1)	-3(1)
N(21)	40(1)	47(1)	43(1)	0(1)	11(1)	-2(1)
C(22)	53(1)	54(1)	53(1)	6(1)	13(1)	4(1)
C(23)	58(1)	74(2)	62(2)	21(1)	12(1)	3(1)
C(24)	60(2)	102(2)	48(1)	18(1)	10(1)	-10(2)
C(25)	71(2)	99(2)	48(1)	-10(2)	22(1)	-6(2)
C(26)	56(1)	64(2)	47(1)	-11(1)	14(1)	-1(1)

4.6 II PYBEN: [Ni(NCS)$_2$(Py)$_4$(nBENZENE)].

As determined by the diffractometer, the unit cell was found with parameters: a=16.270(4)Å, b=16.273(8)Å, c=21.309(7)Å, β=112.42(2)°. This monoclinic cell was sufficiently different from the α-phase to be considered as a clathrate. Owing to crystal decay the poor data collection did not enable solution of this structure. Successive attempts confirmed the instability of these crystals. As this was not part of the main theme of this work, data collection at low temperature was not attempted.

As the host powder had been dissolved in benzene, the only possible guest is benzene. As both the pyridine ligand and the benzene have the same high symmetry this structure is interesting. In addition if any py-py interactions play a role in the selectivity of Werner Clathrates towards aromatic guests, the lack of complication (no steric hindrance by substituents) in this structure may provide futher information.

Providing less steric hindrance is the host [Ni(Cl)$_2$(Py)$_4$], but it is not sufficiently soluble in benzene to yield crystals.

4 REFERENCES

4.1 The Aldrich Library of N.M.R. Spectra, edition II, Vol. 1 and 2 (1983).

CHAPTER 5

Discussion of Structures

5.1 Host molecule conformation.

Both $[Ni(NCS)_2(4\text{-}ViPy)_4]$ and $[Ni(NCS)_2(Py)_4]$ crystallise as discrete mononuclear molecules. Each nickel atom is coordinated to six donor ligands via a nitrogen atom with the isothiocyanate ligands trans to each other. The majority of the bond lengths involving the vinyl carbon atoms fall within the typical range for complexes of this type[5.1].

For $[Ni(NCS)_2(4\text{-}ViPy)_4]$ the variation in the bond lengths for each type of bond is reported in table 5.1.1 and an illustration of the typical environment of the nickel atom is shown in figure 5.1.1. In structures 1 to 6 the host conformation is similar. Figure 5.1.2 represents a typical example.

TABLE 5.1.1 Variation in and average bond lengths (Å) with estimated standard deviations in parentheses for the host complex of structures 1 to 6.

Bond	Varies		Average Length[c]
	from[a]	to[a]	
Ni-Ncs	2.053(7) [6]	2.094(8) [1]	2.08
Ni-Npy	2.05(1) [1][b]	2.204(8) [1][b]	2.13
Ncs-Cs	1.12(1) [4]	1.15(1) [6]	1.14
Cs-S	1.583(8) [6]	1.630(9) [5]	1.62
Nring-Cring	1.29(1) [1][b]	1.37(1) [1][b]	1.34
Cring-Cring	1.30(2) [1][b]	1.49(2) [1][b]	1.38
Cring-Cvinyl	1.26(4) [1][b]	1.56(2) [1][b]	1.45
Cvinyl-Cvinyl	1.04(5) [1][b]	1.38(2) [5]	1.25

[a] Number in brackets refers to the structure.

[b] Varying substantially owing to symmetry condition, see section 5.2.

[c] Average of all bond lengths.

For structures 1 to 5 there is no systematic variation in the bond lengths of the host except for the Cvinyl-Cvinyl bonds of structures 2 to 5. These average values in Å are 1.15, 1.22, 1.32 and 1.33 respectively. As there is no vinyl group-guest interaction (less than the sum of the van der Waals radii, see packing diagrams) this bond length variation appears to bear no relationship to selective guest enclathration. The linking of solid state observations to the liquid state is not realistic. However it is noted that the sphere of solvent molecules must have some contact with the outer vinyl groups.

As previously observed in complexes of this type[5.2, 5.3, 5.4] there is a significant difference between the Ni-N bond distances of the isothiocyanate and pyridine ligands. For structures 1 to 6 the average difference is 0.05 Å. As the propeller conformation of the pyridine ligands is experimentally observed and confirmed by conformational energy studies[5.5], the Ni-N bond differences have been explained in terms of steric effects (interaction of the ortho hydrogens on the pyridine ring).

In each structure the nickel atom is positioned in the molecular plane of the four pyridine nitrogen atoms. Angles subtended at the nickel atom vary from 86.8(2)° to 92.4(3)° for the cis ligands and 176.3(3)° to 180.0(4)° for the trans ligands.

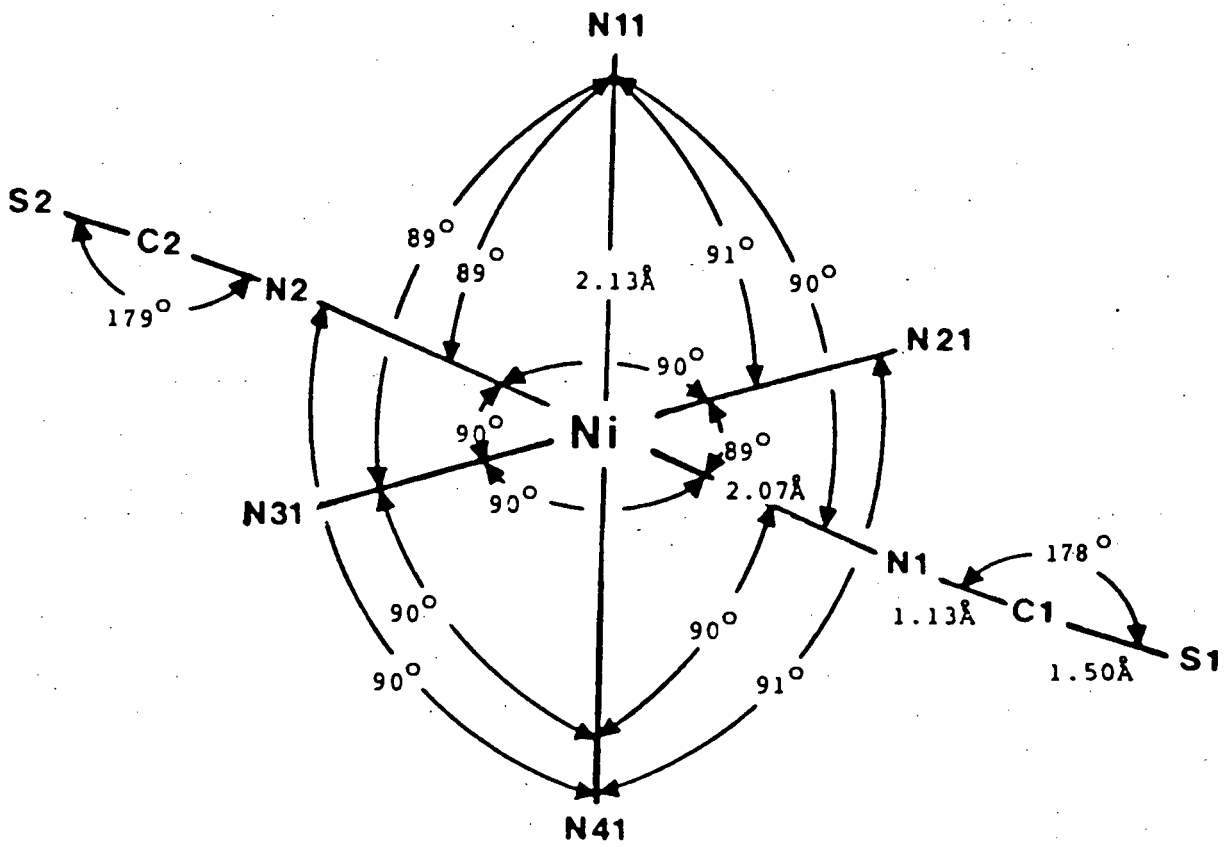

Figure 5.1.1 Typical environment of a nickel atom.

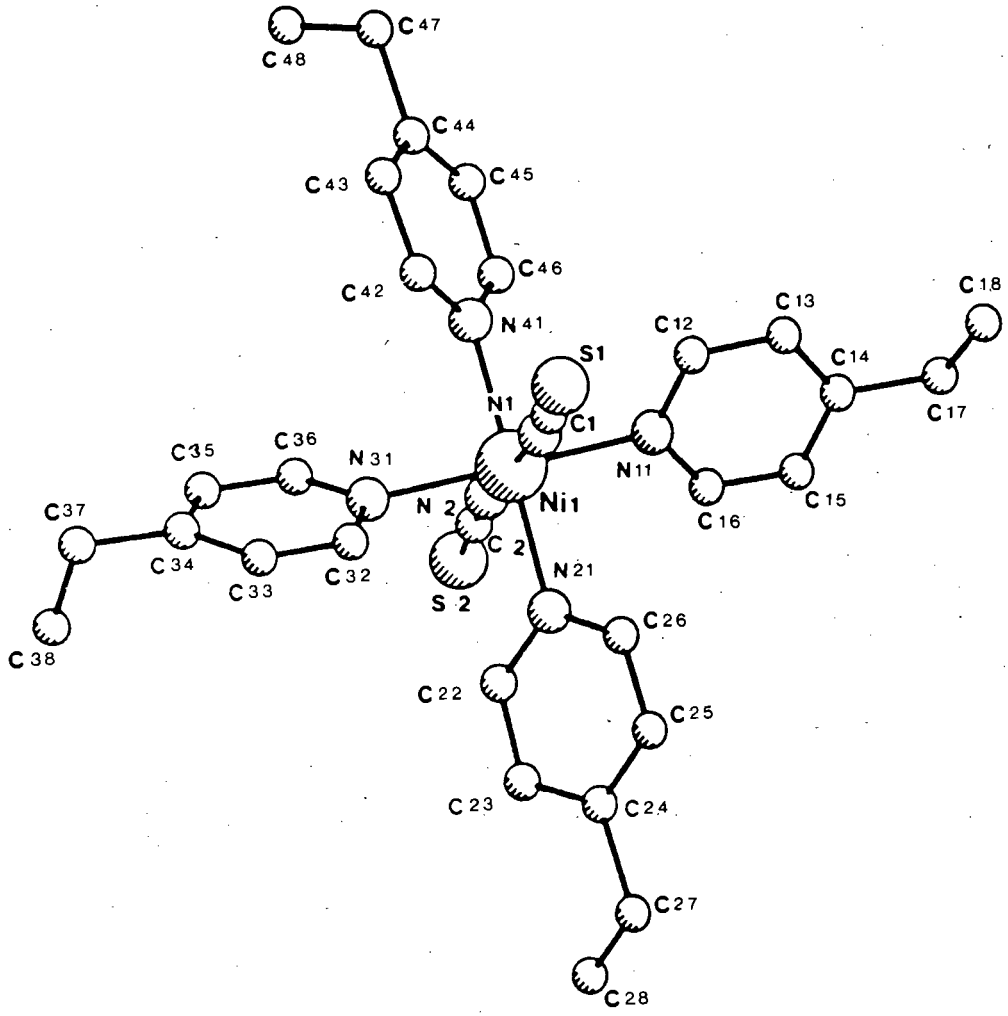

Figure 5.1.2 Perspective view of host conformation with atomic nomenclature.

Previous work[5.6] has shown the isothiocyanate ligands to be linear, a symmetry condition imposed by sitting directly on a diad. In structures 1 to 6 the Ni-Ncs-Cs bond angles range from 158.0(7)° to 166.4(8)° and the Ncs-Cs-S bond angles range from 177(1)° to 179.4(8)°. When the Ni-Ncs-Cs bond angle differs from 180° the conformation of the NCS group around the Ni-N coordination bond plays an important role in determining the overall molecular shape of the host complex. In all the clathrate structures the isothiocyanate ligands are trans, irrespective of whether two-fold or inversion symmetry of the host molecule has imposed this condition. For the α-phase the isothiocyanate ligands are cis with respect to the sulphurs[5.3].

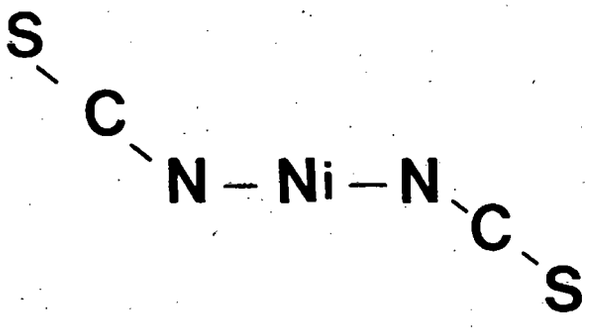

Trans

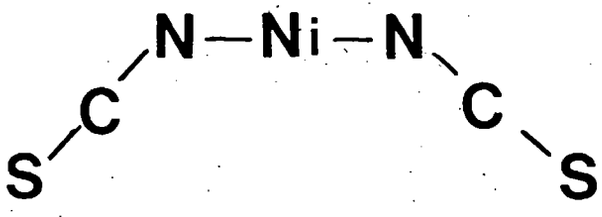

Cis

Figure 5.1.3 Different conformations of the isothiocyanate ligands as found in the clathrates and clathrand respectively.

can be either inside one or more of the atomic spheres (inside the molecule), or outside. The element of volume dv centred at $\underline{s}$ is accordingly labelled as either occupied (by a finite number

representing the packing density) or unoccupied (by 0). By sampling the cell space by systematic variation of s, all the points in the cell can be labelled, and the number of occupied and free points can be obtained. Holes and channels can be seen by visual inspection of the packing density maps; also, local breakdowns of the close packing principle are easily recognised. In all the diagrams obtained from OPEC the 0 's have been deleted to facilitate observation of unoccupied cavities.

5.2 1 HANE and 2 HENE Pbcn.

With the nickel at Wyckoff special position c and two of the 4-vinylpyridine ligands sitting along the diad, the bond lengths and angles warrant further comment. The symmetry conditions imposed on the host are somewhat ideal resulting in the 'observed' bond lengths being different from chemically accepted bond lengths for these complexes. The isothiocyanate ligands are not significantly affected.

HANE: $Ni-N_{py}$ along the diad, both are 2.06(1) Å (shortening).

$Ni-N_{py}$ general position, 2.204(8) Å (lengthening).

$N_{ring}-C_{ring}$ general position, 1.29(1) Å and 1.37(1) Å (shortening and lengthening).

$C_{ring}-C_{ring}$ general position, 1.30(2) Å and 1.50(2) Å (shortening and lengthening)

$C_{ring}-C_{vinyl}$ along the diad, 1.27(4) Å and 1.40(4) Å (shortening).

$C_{vinyl}-C_{vinyl}$ disordered about the diad, 1.05(5) Å and 1.29(3) Å (shortening and lengthening).

The variations in structure 2 are the same but less extreme, only the

Ni-Npy are shown.

HENE: Ni-Npy along the diad, 2.09(1) Å and 2.06(1) Å.

Ni-Npy general position, 2.191(8) Å.

Similarly the nickel's environment with respect to bond angles necessitates further comment as these are significantly different from those observed in structures 3 to 6.

	HANE[a]	HENE[a]
N(11)--Ni(1)--N(21)	180.0(4)°	180.0(3)°

Owing to rings 1 and 2 sitting on the diad.

Showing the host's varying conformation are the torsion angles.

	HANE	HENE
N(1)--Ni(1)--N(41)--C(42)	37.6(9)°	36.1(9)°
N(1)--Ni(1)--N(41)--C(46)	34.7(8)°	35.4(8)°
N(1)--Ni(1)--N(21)--C(22)	42.5(8)°	43.0(8)°
N(1)--Ni(1)--N(11)--C(12)	34.2(8)°	33.6(8)°

The four torsion angles are slightly different from each other showing a non-regular propeller conformation of the host which is observed for all these complexes. The corresponding torsion angles in both structures do not differ significantly (at the 3σ level[5.9]) geometrically, which may be expected as the difference in guest contents is very small.

The program PARST was used to determine if there were any host-guest non bonding interactions. For structure 2 there was one non bonding contact which was shorter than the sum of the respective atoms van der Waals radii.

H23----C3G 2.82 Å < 3.05 Å (sum of van der Waals radii)

However this is not sufficient evidence to account for secondary bonding between the host and guest.
The packing diagrams of the host and guest (hydrogens omitted) as obtained by PLUTO are shown in figure 5.2.1. The disorder of the terminal vinyl carbon atoms about the diad can be seen. The packing view down the x axis shows a) the propeller conformation of the 4-vinylpyridine ligands b) the clearly defined geometry of the ligands (90°)
c) the isothiocyanate ligands running almost parallel to the a axis.

Both structures are almost identical with structure 1 being used for illustrative purposes.
On the basis of previous work[5.3, 5.10] these structures may be regarded as β-phases with a three dimensional network of cavities interconnected by channels. These channels run parallel to the x axis and the z axis as shown by the packing diagrams (OPEC hydrogens included) with the host atoms only. Observation of the diagram at x = 0.0 shows the channels parallel to the x axis located around 0, 1/2, 0 and 0, 1/2, 1/2, inversion centres, Wyckoff special position b; and 0, 0, 0 and 0, 0, 1/2, inversion centres, Wyckoff special position a. Observation of the diagram at x = 0.25 shows the channels

and interlinked cavities running parallel to the z axis.
Observation of the packing diagram (figure 5.2.2) with host and guest at x = 0.0 shows the guest occuping the channels around 0, 0, 0 and 0, 0, 1/2 with the channels around Wyckoff special position b remaining empty. This gives four THF molecules in the unit cell (with their atoms on general positions) but related by a centre of symmetry. Observation of the host-guest packing diagram at x = 0.25 shows two new guests which sit in the cavities (linked by channels) in the vicinity of 0.25, 0.4, 0.0 and 0.25, 0.54, 0.5. These two guests generate the remaining two guests by the $\bar{1}$ sites at 1/2, 1/2, 0 and 1/2, 1/2, 1/2. Thus all the guest atom positions are on general positions with four THF molecules being related by four inversion centres at Wyckoff special position a to generate the remaining four THF molecules.
The remaining unoccupied voids about the inversion centres, Wyckoff special position b are smaller than the occupied voids but could accomodate the remaining cyclic hydrocarbon (11% cyclohexane in HANE and 12% cyclohexene in HENE).
However, a difference electron density map contoured in this region, showed a very low value of the electron density, less than 0.4 $e^-/Å^3$, and so we can effectively regard these sites as unoccupied.

Figure 5.2.1 Molecular packing in structure 1.

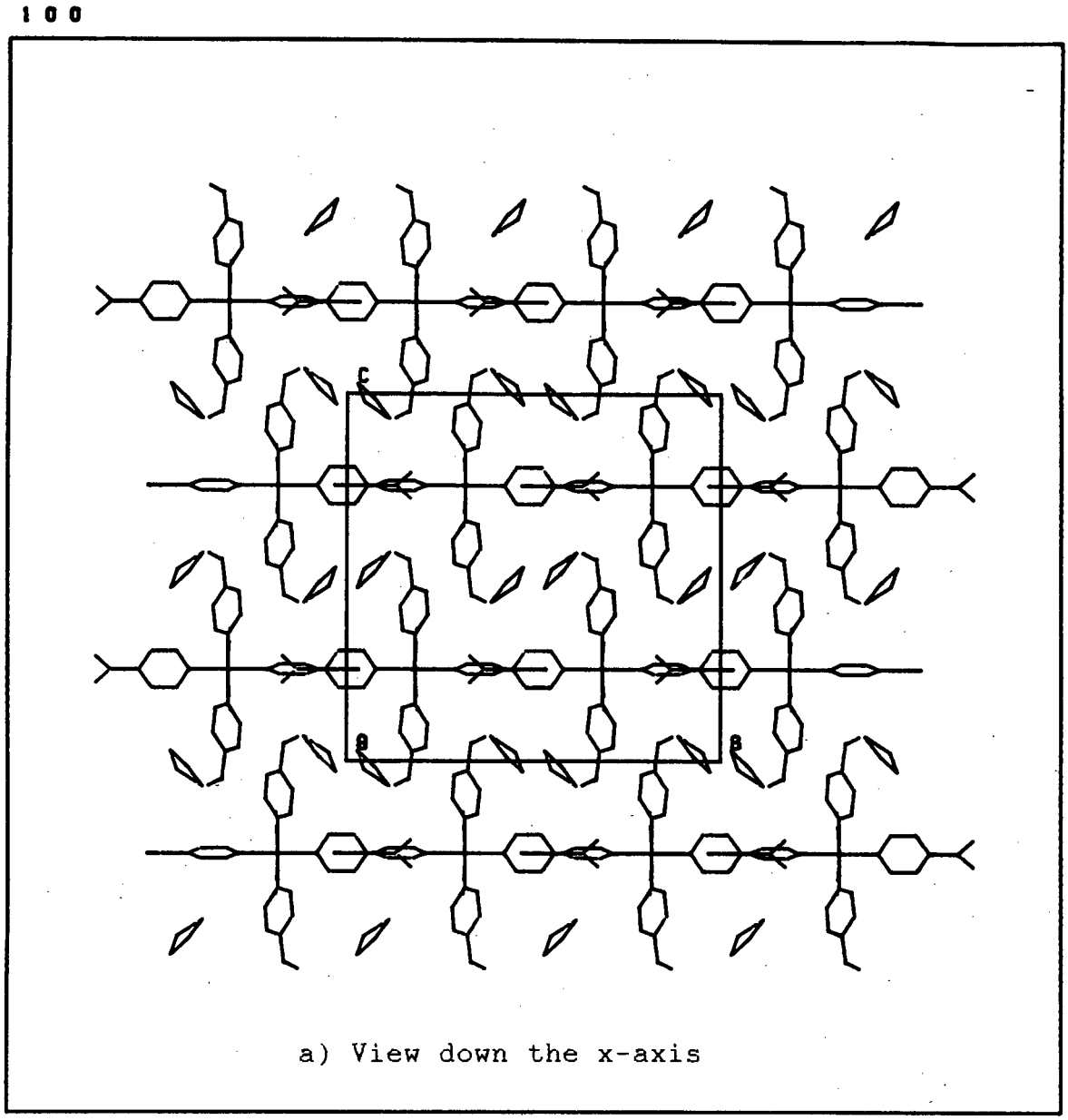

a) View down the x-axis

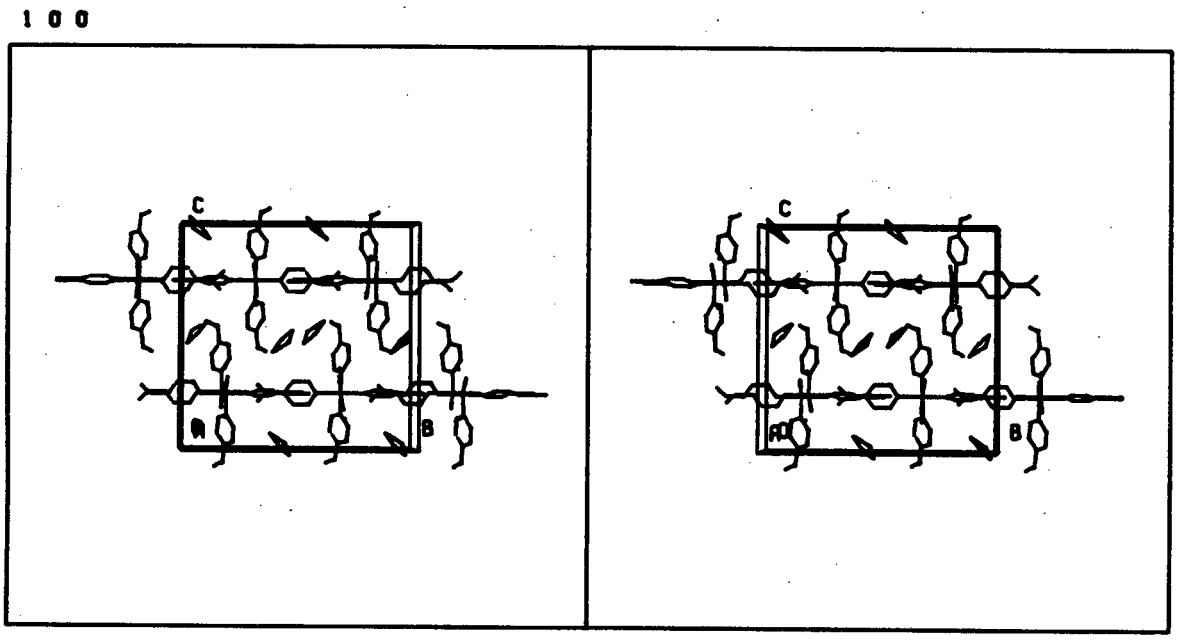

b) Stereo view down the x-axis

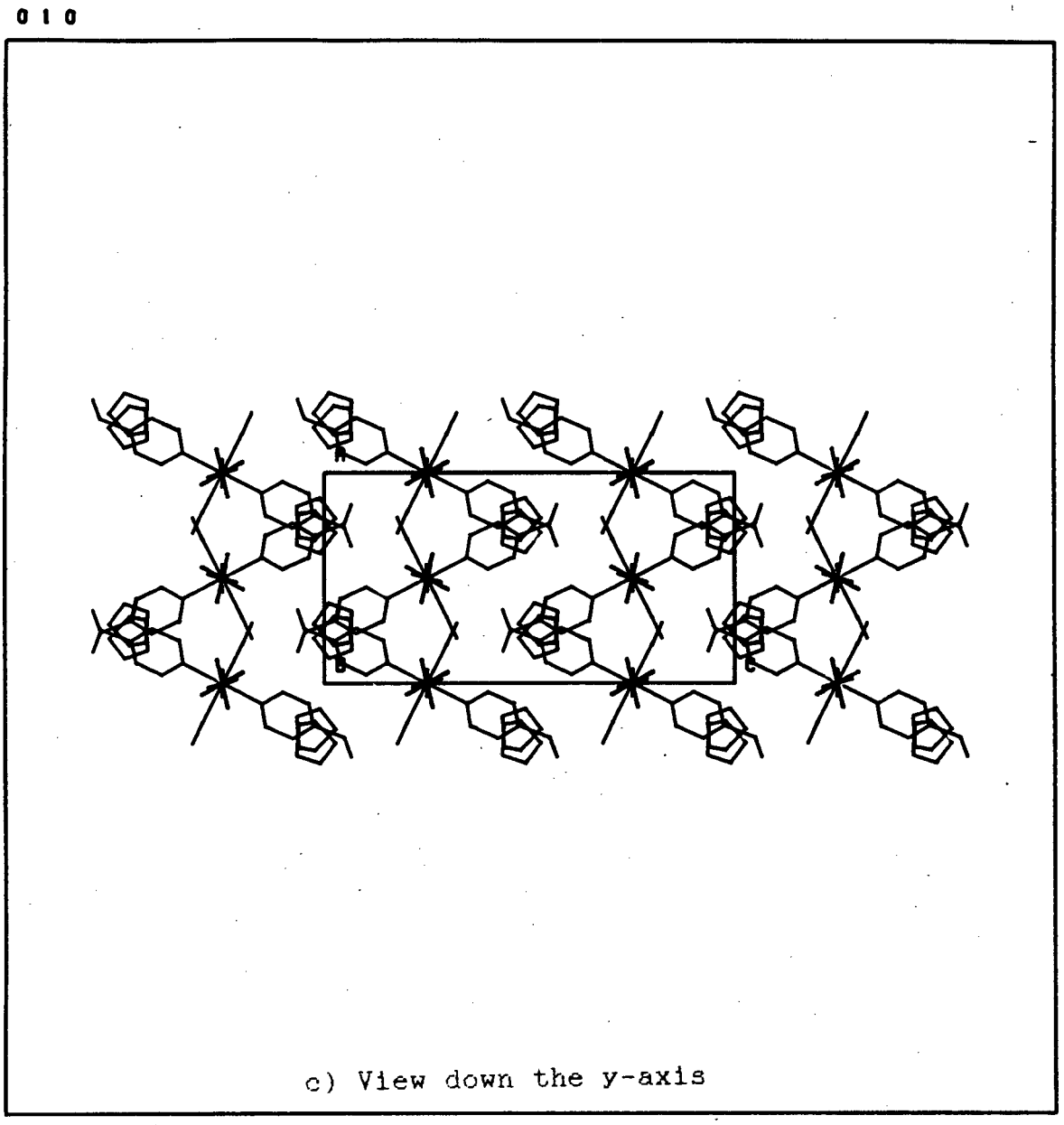

c) View down the y-axis

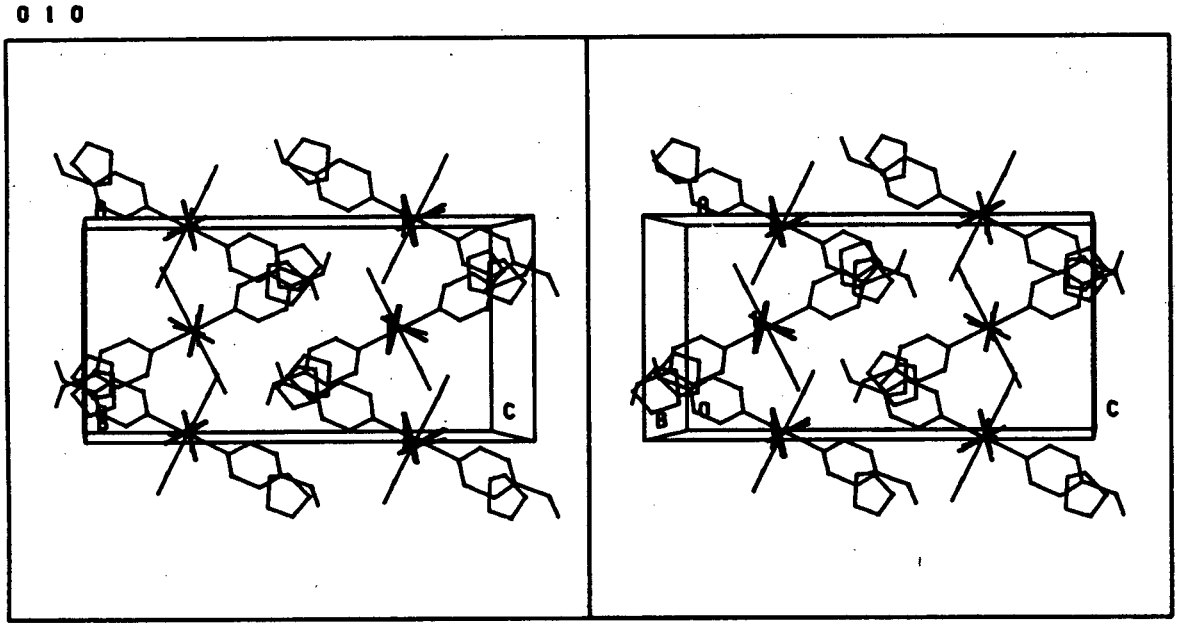

d) Stereo view down the y-axis

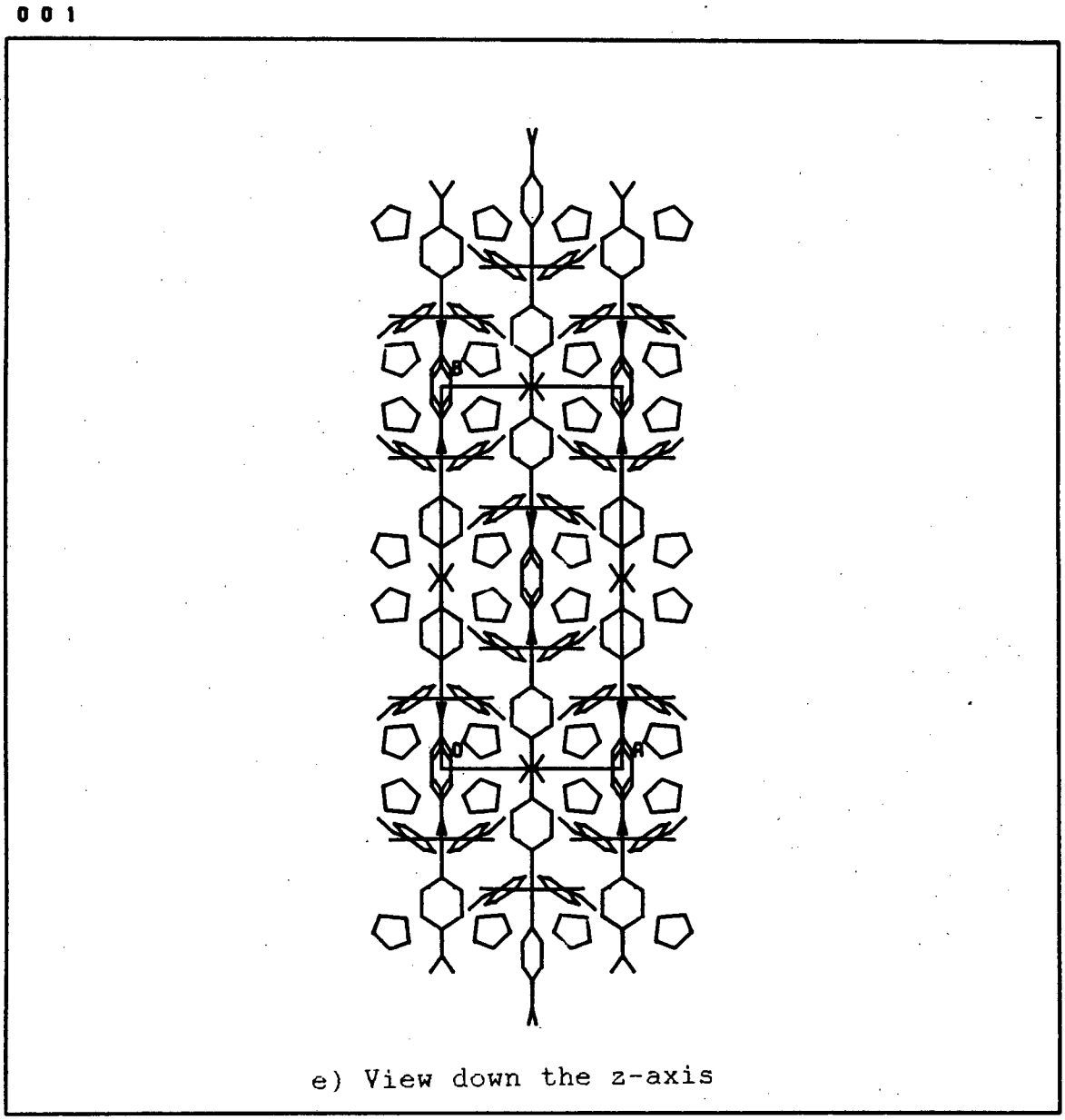

e) View down the z-axis

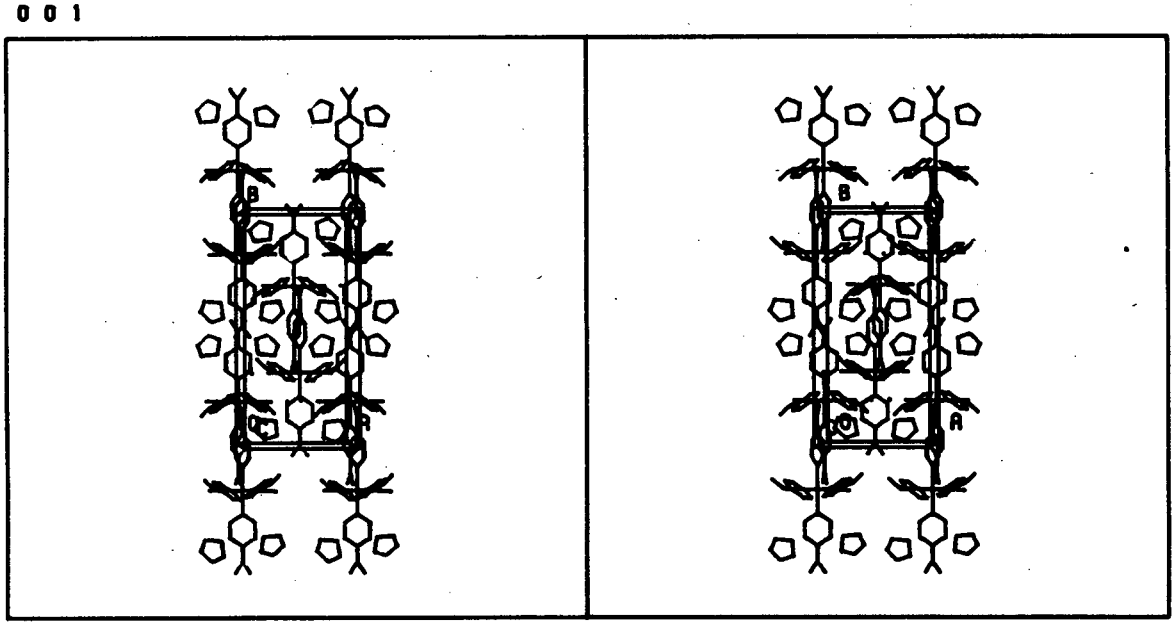

f) Stereo view down the z-axis

Figure 5.2.2 Packing diagrams of structure 1 as obtained from OPEC. Each cross-section is a representation of the unit cell, i.e. drawn to scale. {All OPEC diagrams are drawn to scale.}

a) Host only

b) Host and guest

Asymmetric unit $0 \leq x \leq \frac{1}{4}$; $0 \leq y \leq \frac{1}{4}$; $0 \leq z \leq \frac{1}{4}$

HOST

Z ⟶ (000 .053 .106 .158 .211 .264 .317 .370 .422 .475 .528 .581 .634 .686 .739 .792 .845 .898 .950 1.003)

X=.00

Y ↓

Y	000	.053	.106	.158	.211	.264	.317	.370	.422	.475	.528	.581	.634	.686	.739	.792	.845	.898	.950	1.003
.000			22	100	100	100	100	72					73	100	100	100	100	22		
.020			19	100	100	100	100	69					79	100	100	100	100	27		
.040			27	100	100	100	100	77					75	100	100	100	100	23		
.060			25	100	100	100	100	75					61	100	100	100	99	9		
.080			13	100	100	100	100	63					31	100	100	100	75			
.100			0	83	100	100	100	38					2	91	100	100	40			
.120			0	49	96	100	83	16					24	100	100	100	69			
.140	10	41	74	97	92	100	91	68	37	30			47	100	100	100	91			12
.160	65	100	100	100	100	100	100	100	100	98	20		56	100	100	100	100	6		71
.180	94	100	100	100	100	100	100	100	100	100	49		57	100	100	100	100	8	6	97
.200	100	100	100	100	100	100	100	100	100	100	67		50	100	100	100	94		23	100
.220	100	100	100	100	98	100	98	100	100	100	89		31	100	100	100	75		45	100
.240	100	100	100	97	90	100	90	100	100	100	95	13	84	100	98	100	95	47	50	100
.260	100	100	100	93	100	100	93	100	100	100	83	54	100	92	19	60	100	95	45	100
.280	68	77	100	66	100	100	77	90	96	67	41	77	100	99	11	63	100	100	35	69
.300		6	42	27	100	100	75	24	28			88	100	100	22	74	100	100	36	
.320		11	3	29	100	100	78		11	2		88	100	100	23	74	100	100	37	
.340	1	73	34	23	100	100	73	1	75	31		79	100	100	13	65	100	100	28	2
.360	6	95	57	17	100	100	67	8	96	54		58	100	88		43	100	96	8	10
.380	6	94	56	27	100	100	77	8	96	53		17	91	42	10	10	86	56		10
.400		70	33	35	100	100	85	1	73	29			5	15	94	55	4	1		2
.420		9	2	38	100	100	90		9	2				53	100	95	4			
.440				36	100	100	87							73	100	100	22			
.460				30	100	100	81							81	100	100	29			
.480				36	100	100	89							84	100	100	32			
.500				38	100	100	90							90	100	100	36			
.520				33	100	100	83							90	100	100	36			
.540				30	100	100	81							81	100	100	29			
.560				22	100	100	73							88	100	100	33			
.580				5	95	100	52				2	9		90	100	100	36	2	9	
.600	1		1	4	56	93	15	5			30	72	1	86	100	100	34	33	70	
.620	10		56	86	10	10	43	91	17		54	96	8	78	100	100	26	57	94	5
.640	10	8	97	100	43	1	88	100	57		54	96	8	68	100	100	16	57	94	6
.660	2	28	100	100	64	14	100	100	78		32	74	1	74	100	100	22	35	72	
.680		38	100	100	73	24	100	100	88		2	11		79	100	100	28	3	11	
.700		37	100	100	73	23	100	100	87			28	24	75	100	100	27	42	6	
.720	69	35	100	100	63	12	99	100	77	41	67	96	89	77	100	100	66	100	77	68
.740	100	45	95	100	60	19	93	100	53	84	100	100	100	93	100	100	93	100	100	100
.760	100	49	48	96	100	99	100	84	12	95	100	100	100	90	100	90	98	100	100	100
.780	100	44		75	100	100	100	30		90	100	100	100	98	100	98	100	100	100	100
.800	100	22		95	100	100	100	47		68	100	100	100	100	100	100	100	100	100	94
.820	97	6	8	100	100	100	100	55		50	100	100	100	100	100	100	100	100	100	64
.840	70		7	100	100	100	100	55		21	98	100	100	100	100	100	100	100	100	64
.860	12			92	100	100	100	46			31	57	89	91	100	92	97	74	41	10
.880				69	100	100	100	24					16	84	100	96	48			
.900				41	100	100	91	1					38	100	100	100	83			
.920				76	100	100	100	30					64	100	100	100	99	12		
.940			10	99	100	100	100	60					75	100	100	100	100	24		
.960			24	100	100	100	100	74					78	100	100	100	100	26		
.980			27	100	100	100	100	78					70	100	100	100	100	18		
1.000			22	100	100	100	100	72					73	100	100	100	100	22		

Z →

X = .125

Y ↓

Y \ Z	.000	.053	.106	.158	.211	.264	.317	.370	.422	.475	.528	.581	.634	.686	.739	.792	.845	.898	.950	1.003
.000					37	100	100	65						8	79	100	100	14		
.020					25	100	100	63						32	99	100	100	35		
.040				1	47	100	100	83						41	100	100	100	45		
.060					56	100	100	98	1					43	100	100	100	42		
.080		2	31	63	63	100	100	97	1					33	100	100	99	22		
.100	24	66	95	100	87	100	100	80						28	100	87	38		1	27
.120	92	100	100	100	78	86	97	31						41	100	98	25	9	73	94
.140	100	100	100	100	72	84	99	20						61	100	100	56	38	100	100
.160	100	100	100	100	93	100	100	43						82	100	100	70	32	100	100
.180	100	100	100	100	100	100	100	57	6					83	100	100	71	64	100	100
.200	100	100	100	100	99	100	100	78	39					65	99	100	60	72	100	100
.220	100	100	100	100	74	95	100	92	58					17	66	99	39	52	83	100
.240	100	100	100	100	79	92	89	85	65						6	59	91	64	43	100
.260	99	100	100	85	99	100	27	73	62	3						82	100	98	40	100
.280	73	98	92	68	100	100	45	32	79	68					16	99	100	100	35	77
.300	6	21	5	60	100	100	60	18	96	99	41	76	13		30	100	100	100	43	8
.320				63	100	100	63	37	100	100	88	100	56	2	32	100	100	100	43	
.340				60	100	100	60	79	100	100	98	100	85	12	22	100	100	100	33	
.360				56	100	100	57	88	100	100	100	100	87	13	4	93	100	99	13	
.380				63	100	100	63	88	100	100	100	100	69	3	8	42	95	68		
.400				63	100	100	63	77	100	100	95	100	41	13	92	54	13	5		
.420				52	100	100	55	55	100	97	57	98	13	50	100	94	4			
.440				31	100	100	38	16	94	39	6	33		70	100	100	22			
.460				3	88	100	28		11	2				79	100	100	30			
.480					90	100	45							77	100	100	28			
.500				15	100	100	68							66	100	100	17			
.520				26	100	100	80							44	100	90	1			
.540				27	100	100	81							45	100	73		3	10	
.560	18	27	13	19	100	100	73							81	100	83		63	93	14
.580	61	92	63	3	93	100	52						7	99	100	98	15	98	100	58
.600	95	100	91	3	51	92	17	16					18	100	100	100	46	100	100	95
.620	100	100	100	26	1	15	77	97	24				18	100	100	100	58	100	100	100
.640	100	100	100	52		45	100	100	64				11	100	100	100	49	100	100	100
.660	98	100	100	50		67	100	100	85				15	100	100	100	42	100	100	98
.680	90	97	96	15		77	100	100	93				18	100	100	100	29	98	100	89
.700	70	57	52			75	100	100	93		21	9	17	100	100	100	8	67	100	66
.720	27					51	100	100	83	29	98	95	67	95	100	90	3	65	87	22
.740						32	99	100	61	74	100	100	98	86	100	71	29	98	15	
.760						28	77	94	24	87	100	100	100	95	76	99	76	99	14	
.780					35	92	84	17	76	95	100	100	100	100	71	100	95	90	10	
.800				16	97	100	99	37	100	100	100	100	100	100	98	100	96	60	6	
.820				32	100	100	100	40	98	100	100	100	100	100	100	100	97	11		
.840				31	100	100	100	28	95	100	100	100	100	100	93	100	88			
.860				12	96	100	99	12	83	100	100	100	100	100	60	100	65			
.880					86	100	76		42	83	100	100	100	99	66	98	73	2		
.900					73	100	62	18		6	47	87	100	89	96	100	100	30		
.920					78	100	100	73				8	63	42	99	100	100	46		
.940					88	100	100	94						14	96	100	100	46		
.960				1	85	100	100	98						14	85	100	100	32		
.980				3	74	100	100	86						2	74	100	100	12		
1.000					37	100	100	65						8	79	100	100	14		

Z ⟶ X=.25

Y ↓

Y	.000	.053	.106	.158	.211	.264	.317	.370	.422	.475	.528	.581	.634	.686	.739	.792	.845	.898	.950	1.003
.000																				
.020																				
.040														12	45					
.060		33	33	6										52	98	12		14	34	
.080	36	96	99	95	51									67	100	32		71	98	35
.100	92	100	100	100	93	1	26	4						65	100	46	5	97	100	92
.120	100	100	100	100	100	43	99	58						52	100	47	15	100	100	100
.140	100	100	100	100	100	89	100	94	3					38	100	34	16	100	100	100
.160	100	100	100	100	98	99	100	100	19					46	100	40	12	100	100	100
.180	100	100	100	100	91	100	100	100	27					59	100	48	15	100	100	100
.200	100	100	100	100	66	100	100	100	25					69	100	40	18	100	100	100
.220	100	100	85	91	16	93	100	100	14					64	100	22	10	99	100	100
.240	94	92	9	6	9	65	100	86	9	6	33	3		37	88	61	75	77	98	95
.260	17	22			82	62	85	60	97	94	100	48	6	2	29	98	100	40	8	20
.280				12	99	73		54	100	100	100	92	92	51	50	100	100	59		
.300				18	100	90	1	63	100	100	100	100	100	94	70	100	100	71		
.320				9	98	96	4	59	100	100	100	100	100	100	91	100	100	72		
.340				1	90	90	1	56	100	100	100	100	100	100	97	100	100	64		
.360					83	84		61	100	100	100	100	100	100	89	100	100	45		
.380				4	95	96	5	60	100	100	100	100	100	100	58	83	94	11		
.400				14	100	95	4	49	100	96	95	100	100	100	42	12	19			
.420				16	100	82		21	99	67	62	100	99	83	9					
.440				4	95	62			35	12	10	50	14							
.460					39	18														
.480																				
.500																				
.520																				
.540														12	45					
.560		33	33	6										52	98	12		14	34	
.580	36	96	99	95	51									67	100	32		71	98	35
.600	92	100	100	100	93	1	26	4						65	100	46	5	97	100	92
.620	100	100	100	100	100	43	99	58						52	100	47	15	100	100	100
.640	100	100	100	100	100	89	100	94	3					38	100	34	16	100	100	100
.660	100	100	100	100	98	99	100	100	19					46	100	40	12	100	100	100
.680	100	100	100	100	91	100	100	100	27					59	100	48	15	100	100	100
.700	100	100	100	100	66	100	100	100	25					69	100	40	18	100	100	100
.720	100	100	85	91	16	93	100	100	14					64	100	22	10	99	100	100
.740	94	92	9	6	9	65	100	86	9	6	33	3		37	88	61	75	77	98	95
.760	17	22			82	62	85	60	97	94	100	48	6	2	29	98	100	40	8	20
.780				12	99	73		54	100	100	100	92	92	51	50	100	100	59		
.800				18	100	90	1	63	100	100	100	100	100	94	70	100	100	71		
.820				9	98	96	4	59	100	100	100	100	100	100	91	100	100	72		
.840				1	90	90	1	56	100	100	100	100	100	100	97	100	100	64		
.860					83	84		61	100	100	100	100	100	100	89	100	100	45		
.880				4	95	96	5	60	100	100	100	100	100	100	58	83	94	11		
.900				14	100	95	4	49	100	96	95	100	100	100	42	12	19			
.920				16	100	82		21	99	67	62	100	99	83	9					
.940				4	95	62			35	12	10	50	14							
.960					39	18														
.980																				
1.000																				

Z ⟶

X = .375

Y ↓

	.000	.053	.106	.158	.211	.264	.317	.370	.422	.475	.528	.581	.634	.686	.739	.792	.845	.898	.950	1.003
.000				15	100	100	68							66	100	100	17			
.020				26	100	100	80							44	100	90	1			
.040				27	100	100	81							45	100	73		3	10	
.060	18	27	13	19	100	100	73							81	100	83		63	93	14
.080	61	92	63	3	93	100	32						7	99	100	98	15	98	100	58
.100	95	100	91	3	51	92	17	16					18	100	100	100	46	100	100	93
.120	100	100	100	26	1	15	77	97	24				18	100	100	100	58	100	100	100
.140	100	100	100	52		45	100	100	64				11	100	100	100	49	100	100	100
.160	98	100	100	50		67	100	100	85				15	100	100	100	42	100	100	98
.180	90	97	96	15		77	100	100	93				18	100	100	100	29	98	100	89
.200	70	57	52			75	100	100	93		21	9	17	100	100	100	8	67	100	66
.220	27					61	100	100	83	29	98	95	67	95	100	90	3	65	87	22
.240						32	99	100	61	74	100	100	98	86	100	71	29	98	15	
.260						28	77	94	24	87	100	100	100	95	76	99	76	99	14	
280					35	92	84	17	76	95	100	100	100	100	71	100	95	90	10	
.300				16	97	100	99	37	100	100	100	100	100	100	98	100	96	60	6	
.320				32	100	100	100	40	98	100	100	100	100	100	100	100	97	11		
.340				31	100	100	100	28	95	100	100	100	100	100	93	100	88			
.360				12	96	100	99	12	83	100	100	100	100	100	60	100	65			
.380					86	100	76		42	83	100	100	100	99	66	98	73	2		
.400					73	100	62	18		6	47	87	100	89	96	100	100	30		
.420					78	100	100	73				8	63	42	99	100	100	46		
.440					88	100	100	94						14	96	100	100	46		
.460				1	85	100	100	98						14	85	100	100	32		
.480				3	74	100	100	86						2	74	100	100	12		
.500					37	100	100	65						8	79	100	100	14		
.520					25	100	100	63						32	99	100	100	35		
.540				1	47	100	100	83						41	100	100	100	45		
.560					56	100	100	98	1					43	100	100	100	42		
.580		2	31	63	63	100	100	97	1					33	100	100	99	22		
.600	24	66	95	100	87	100	100	80						28	100	87	38		1	27
.620	92	100	100	100	78	86	97	31						41	100	98	25	9	73	94
.640	100	100	100	100	72	84	99	20						61	100	100	56	38	100	100
.660	100	100	100	100	93	100	100	43						82	100	100	70	52	100	100
.680	100	100	100	100	100	100	100	97						83	100	100	71	64	100	100
.700	100	100	100	100	99	100	100	78	39					65	99	100	60	72	100	100
.720	100	100	100	100	74	95	100	92	58					17	66	99	39	52	83	100
.740	100	100	100	100	79	92	89	85	65						6	59	91	64	43	100
.760	99	100	100	85	99	100	27	73	62	3						82	100	98	40	100
.780	73	98	92	68	100	100	45	32	79	68					16	99	100	100	35	77
.800	6	21	5	60	100	100	60	18	96	99	41	76	13		30	100	100	100	43	8
.820				63	100	100	63	37	100	100	88	100	56	2	32	100	100	100	43	
.840				60	100	100	60	78	100	100	98	100	85	12	22	100	100	100	33	
.860				56	100	100	57	88	100	100	100	100	87	13	4	93	100	99	13	
.880				63	100	100	63	88	100	100	100	100	69	3	8	42	95	68		
.900				63	100	100	63	77	100	100	95	100	41	13	92	54	13	5		
.920				52	100	100	55	55	100	97	57	98	13	30	100	94	4			
.940				31	100	100	38	16	94	59	6	33		70	100	100	22			
.960				3	88	100	28		11	2				79	100	100	30			
.980					90	100	45							77	100	100	28			
1.000				15	100	100	68							66	100	100	17			

HOST and GUEST

Z ⟶ X=.00

Y ↓

	.000	.053	.106	.158	.211	.264	.317	.370	.422	.475	.528	.581	.634	.686	.739	.792	.845	.898	.950	1.003
.000	9		22	100	100	100	100	72		5	5		73	100	100	100	100	22		9
.020	82	7	19	100	100	100	100	69		43	75	2	79	100	100	100	100	27	36	80
.040	100	36	27	100	100	100	100	77		82	99	22	75	100	100	100	100	23	74	100
.060	100	50	25	100	100	100	100	75	2	95	100	37	61	100	100	100	99	9	89	100
.080	100	51	13	100	100	100	100	63	3	96	100	53	31	100	100	100	75	13	93	100
.100	100	38		83	100	100	100	38		84	100	85	4	91	100	100	40	43	99	100
.120	88	10		49	96	100	83	16		48	94	91	29	100	100	100	69	49	96	86
.140	19	41	74	97	92	100	91	88	57	33	30	65	47	100	100	100	91	29	61	21
.160	65	100	100	100	100	100	100	100	100	98	22	9	56	100	100	100	100	9	8	71
.180	94	100	100	100	100	100	100	100	100	100	49		57	100	100	100	100	8	6	97
.200	100	100	100	100	100	100	100	100	100	100	67		50	100	100	100	94		23	100
.220	100	100	100	100	98	100	98	100	100	100	89		31	100	100	100	75		45	100
.240	100	100	100	97	90	100	90	100	100	100	95	13	84	100	98	100	95	47	50	100
.260	100	100	100	93	100	100	93	100	100	100	83	54	100	92	19	60	100	95	45	100
.280	68	77	100	66	100	100	77	90	96	67	41	77	100	99	11	63	100	100	35	69
.300		6	42	27	100	100	75	24	28			88	100	100	22	74	100	100	36	
.320		11	3	29	100	100	78		11	2		88	100	100	23	74	100	100	37	
.340	1	73	34	23	100	100	73	1	75	31		79	100	100	13	65	100	100	28	2
.360	6	95	57	17	100	100	67	8	96	94		58	100	88		43	100	96	8	10
.380	6	94	56	27	100	100	77	8	96	53		17	91	42	10	10	86	56		10
.400		70	33	35	100	100	85	1	73	29			5	15	94	55	4	1		2
.420		9	2	38	100	100	90		9	2				53	100	95	4			
.440	4	3		36	100	100	87			7				73	100	100	22			5
.460	7	5		30	100	100	81			11				81	100	100	29			8
.480				36	100	100	89							84	100	100	32			
.500				38	100	100	90							90	100	100	36			
.520				33	100	100	83							90	100	100	36			
.540	8			30	100	100	81				11			81	100	100	29		5	7
.560	5			22	100	100	73				7			88	100	100	35		3	4
.580				5	95	100	52				2	9		90	100	100	36	2	9	
.600	1		1	4	56	93	15	5			30	72	1	86	100	100	34	33	70	
.620	10		56	86	10	10	43	91	17		54	96	8	78	100	100	26	57	94	5
.640	10	8	77	100	43	1	88	100	57		54	96	8	68	100	100	16	57	94	6
.660	2	28	100	100	64	14	100	100	78		32	74	1	74	100	100	22	35	72	
.680		38	100	100	73	24	100	100	88		2	11		79	100	100	28	3	11	
.700		37	100	100	73	23	100	100	87			28	24	75	100	100	27	42	6	
.720	69	35	100	100	63	12	99	100	77	41	67	96	89	77	100	100	66	100	77	68
.740	100	45	95	100	60	19	93	100	53	84	100	100	100	93	100	100	93	100	100	100
.760	100	47	48	96	100	99	100	84	12	95	100	100	100	90	100	90	98	100	100	100
.780	100	44		75	100	100	100	30		90	100	100	100	98	100	98	100	100	100	100
.800	100	22		95	100	100	100	49		68	100	100	100	100	100	100	100	100	100	100
.820	97	6	0	100	100	100	100	55		50	100	100	100	100	100	100	100	100	100	94
.840	70	0	9	100	100	100	100	55	9	22	98	100	100	100	100	100	100	100	100	64
.860	21	61	28	92	100	100	100	47	66	29	33	57	89	91	100	92	97	74	41	19
.880	86	96	48	69	100	100	100	28	91	94	48		16	84	100	96	48		10	88
.900	100	97	42	41	100	100	91	4	86	100	83		38	100	100	100	83		39	100
.920	100	93	13	76	100	100	100	30	54	100	95	2	64	100	100	100	99	12	52	100
.940	100	80	10	99	100	100	100	60	38	100	95	2	75	100	100	100	100	24	51	100
.960	100	74	24	100	100	100	100	74	24	99	81		78	100	100	100	100	26	37	100
.980	80	35	27	100	100	100	100	78	2	76	42		70	100	100	100	100	18	8	83
1.000	9		22	100	100	100	100	72		5	5		73	100	100	100	100	22		9

Z →

X = .25

Y ↓

	.000	.053	.106	.158	.211	.264	.317	.370	.422	.475	.528	.581	.634	.686	.739	.792	.845	.898	.950	1.003
.000	100	99	18					8	99	100	100	63						59	100	100
.020	100	68						17	100	100	100	84						38	100	100
.040	84	4						17	100	100	100	96	9	12	45			6	88	79
.060	9	33	33	6				6	99	100	100	100	43	52	98	12		14	45	7
.080	36	96	99	95	51				80	100	100	100	64	67	100	32		71	98	35
.100	92	100	100	100	93	1	26	4	35	98	100	100	73	65	100	46	5	97	100	92
.120	100	100	100	100	100	43	99	58		48	100	100	72	52	100	47	15	100	100	100
.140	100	100	100	100	100	89	100	94	3	27	100	100	63	38	100	34	16	100	100	100
.160	100	100	100	100	98	99	100	100	19	6	95	100	41	46	100	40	12	100	100	100
.180	100	100	100	100	91	100	100	100	27		47	78	6	59	100	48	15	100	100	100
.200	100	100	100	100	66	100	100	100	25					69	100	40	18	100	100	100
.220	100	100	85	91	16	93	100	100	14					64	100	22	10	99	100	100
.240	94	92	9	6	9	65	100	86	9	6	33	3		37	88	61	75	77	98	95
.260	17	22			82	62	85	60	97	94	100	48	6	2	29	98	100	40	8	20
.280				12	99	73		34	100	100	100	92	92	51	50	100	100	59		
.300				18	100	90	1	63	100	100	100	100	100	94	70	100	100	71		
.320	9	80	42	9	98	96	4	59	100	100	100	100	100	100	91	100	100	72		12
.340	48	100	90	4	90	90	1	56	100	100	100	100	100	100	97	100	100	64		54
.360	72	100	100	18	83	84		61	100	100	100	100	100	100	89	100	100	45		78
.380	89	100	100	32	95	96	5	60	100	100	100	100	100	100	58	83	94	11	7	93
.400	100	100	100	42	100	95	4	49	100	96	95	100	100	100	42	12	19	4	83	100
.420	100	100	100	36	100	82		21	99	67	62	100	99	83	9			35	100	100
.440	100	100	93	7	95	62			36	30	10	50	14					37	100	100
.460	100	100	58		39	18			42	99	36							67	100	100
.480	100	100	39						83	100	95	22						68	100	100
.500	100	99	18					8	99	100	100	63						59	100	100
.520	100	68						17	100	100	100	84						38	100	100
.540	84	4						17	100	100	100	96	9	12	45			6	88	79
.560	9	33	33	6				6	99	100	100	100	43	52	98	12		14	45	7
.580	36	96	99	95	51				80	100	100	100	64	67	100	32		71	98	35
.600	92	100	100	100	93	1	26	4	35	98	100	100	73	65	100	46	5	97	100	92
.620	100	100	100	100	100	43	99	58		48	100	100	72	52	100	47	15	100	100	100
.640	100	100	100	100	100	89	100	94	3	27	100	100	63	38	100	34	16	100	100	100
.660	100	100	100	100	98	99	100	100	19	6	95	100	41	46	100	40	12	100	100	100
.680	100	100	100	100	91	100	100	100	27		47	78	6	59	100	48	15	100	100	100
.700	100	100	100	100	66	100	100	100	25					69	100	40	18	100	100	100
.720	100	100	85	91	16	93	100	100	14					64	100	22	10	99	100	100
.740	94	92	9	6	9	65	100	86	9	6	33	3		37	88	61	75	77	98	95
.760	17	22			82	62	85	60	97	94	100	48	6	2	29	98	100	40	8	20
.780				12	99	73		34	100	100	100	92	92	51	50	100	100	59		
.800				18	100	90	1	63	100	100	100	100	100	94	70	100	100	71		
.820	9	80	42	9	98	96	4	59	100	100	100	100	100	100	91	100	100	72		12
.840	48	100	90	4	90	90	1	56	100	100	100	100	100	100	97	100	100	64		54
.860	72	100	100	18	83	84		61	100	100	100	100	100	100	89	100	100	45		78
.880	89	100	100	32	95	96	5	60	100	100	100	100	100	100	58	83	94	11	7	93
.900	100	100	100	42	100	95	4	49	100	96	95	100	100	100	42	12	19	4	83	100
.920	100	100	100	36	100	82		21	99	67	62	100	99	83	9			35	100	100
.940	100	100	93	7	95	62			36	30	10	50	14					37	100	100
.960	100	100	58		39	18			42	99	36							67	100	100
.980	100	100	39						83	100	95	22						68	100	100
1.000	100	99	18					8	99	100	100	63						59	100	100

5.3 3 DIEN3, 4 DIEN4 and 5 THF/BEN $I4_1/a$.

In all three structures the nickel is positioned at 1/2, 1/4, 0.55 being Wyckoff special position e. With respect to the host they are all isomorphous (slight variations) with bond lengths and angles being chemically acceptable for these complexes. None of the ligands lie on the diad as shown in figure 5.3.1.

In these three structures the guest contents vary significantly. If the ability of the host's pyridine ligands in varying their conformation plays a major role in its enclathrating ability, this should be detected in comparing the torsion angles.

	DIEN3	DIEN4	THF/BEN
N(1)--Ni(1)--N(21)--C(22)	41.6(8)°	43.7(6)°	42.6(6)°
N(1)--Ni(1)--N(21)--C(26)	40.0(8)°	40.6(6)°	41.3(6)°
N(1)--Ni(1)--N(11)--C(12)	39.1(8)°	37.7(7)°	35.2(7)°
N(1)--Ni(1)--N(11)--C(16)	33.5(9)°	32.8(7)°	34.0(7)°

In conjunction with the isomorphous nature of these structures the torsion angles do not vary significantly (at the 3σ level[5.9]) to account for the selectivity of the guests included nor the host:total guest ratio.

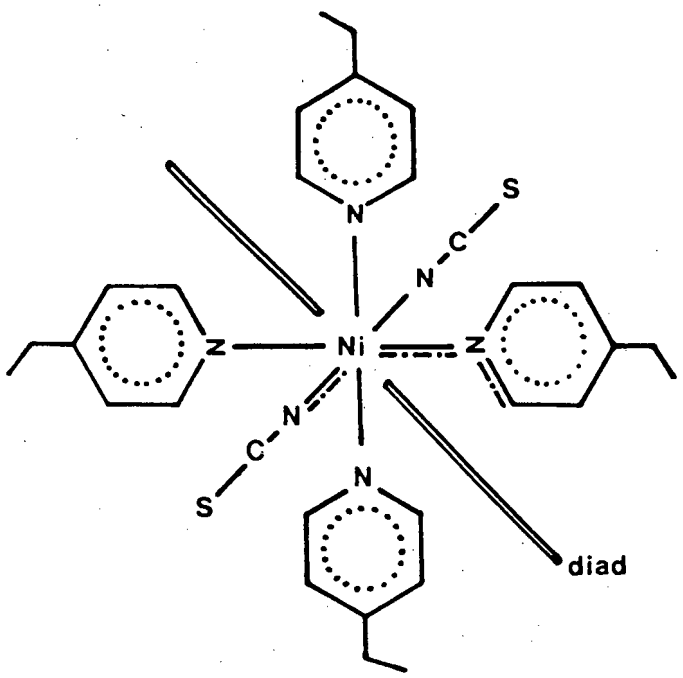

Figure 5.3.1 Illustration of the ligands about the diad showing two 4-vinylpyridines and one isothiocyanate ligand as the asymmetric unit.

These three structures crystallise in the same manner as the traditional β-phase structures of $[Ni(NCS)_2(4\text{-}MePy)_4]$. These structures have a three-dimensional system of cavities interconnected by channels. These channels run parallel to the y axis and the x axis as shown by the packing diagrams in figure 5.3.2 (OPEC, hydrogens included) with the host atoms only. Observation of the packing diagram of the unit cell section at y = 0.0 clearly shows the channels parallel to the y axis, located at 0, 0, 1/2 and 1/2, 0, 0. These are inversion centres, Wyckoff special position d. Observation of the packing diagram at y = 0.25 shows the channel/cavity parallel to the x axis. This void is extremely large and includes the inversion centre at 3/4, 1/4, 3/4 and the $\bar{4}$ sites at 0, 1/4, 5/8 and 1/2, 1/4, 7/8, Wyckoff special position b. Note the small voids at 0, 1/4, 1/8 and 1/2, 1/4, 3/8 which are $\bar{4}$ sites, Wyckoff special position a.

The packing diagrams of the host (hydrogens omitted) as obtained by PLUTO are shown in figure 5.3.3. These diagrams are very similar for structures 3, 4 and 5 with structure 4 being used for illustrative purposes.

Each structure is described separately with respect to the host-guest packing. In each structure the guests are disordered owing to the mixture of two guest types and the symmetry of 1,3-cyclohexadiene and 1,4-cyclohexadiene not coinciding with the site symmetry. There is also very little host-guest interaction to minimise the guests' thermal motion.

Figure 5.3.2 Packing diagrams of structures 4 and 5 as obtained from OPEC (Host only).

Asymmetric unit $0 \leq x \leq \frac{1}{4}$; $0 \leq y \leq \frac{1}{4}$; $0 \leq z \leq 1$

STRUCTURE 4

X ⟶ Y = .00

Z ↓

	.000	.077	.154	.231	.308	.385	.462	.539	.616	.693	.770	.847	.924	1.001
.000	19	63	14	45	80					79	47	13	63	19
.020	42	4	33	22	22				1	89	58	51	99	41
.040	48	7	94	59						76	46	67	100	47
.060	46	22	100	78					47	35	7	68	100	45
.080	31	24	100	80				2	93	50	8	83	100	30
.100	4	11	97	70				5	78	56	46	100	78	3
.120			58	60		2		1	85	41	66	100	60	
.140			15	30	23	89	19		20	5	70	100	64	
.160	6	26	20		64	100	58		26	1	75	100	54	6
.180	21	64	75	8	83	100	77	28	99	37	81	99	26	22
.200	15	65	100	73	87	100	81	58	100	67	69	85	1	15
.220		68	100	98	88	100	76	69	100	80	27	38		
.240	4	96	100	98	68	100	56	66	100	98	28	61	54	5
.260	28	100	100	76	20	80	15	51	100	100	68	99	97	28
.280	48	100	100	35	54	8		21	99	100	87	100	100	49
.300	46	99	100	40	99	38	1	34	96	97	67	100	100	43
.320	29	76	85	34	100	75	2	41	86	39	35	100	100	28
.340	11	12	16	26	100	98	8	12	38	2	17	100	98	10
.360		4	21	21	100	100	16			38	6	69	62	
.380		38	89	18	100	99	12		19	83	17	1		
.400		52	99	12	92	98	34		58	99	21			
.420		46	96	4	41	99	78		72	100	31			
.440		13	51	24	19	100	93	1	70	100	30			
.460			27	93	22	100	93	4	51	97	12			
.480			41	99	16	95	78	15	10	36	27	4		
.500			31	93	3	45	40	39	46	3	93	32		
.520			3	27	36	10	15	77	95	16	99	42		
.540				11	96	52	3	92	100	22	92	28		
.560				28	100	72	1	92	100	20	23	51	14	
.580				30	100	74		77	99	42	3	95	47	
.600				20	99	60		33	95	93	11	99	54	
.620			1	17	83	20		11	99	100	19	88	39	
.640		60	69	6	39			15	100	100	22	21	4	
.660	9	98	100	18	2	37	12	7	98	100	27	16	13	10
.680	27	100	100	36	38	86	42	2	73	100	35	84	77	28
.700	43	100	100	69	96	97	34	1	36	99	40	100	99	43
.720	48	100	100	87	100	100	22		8	54	35	100	100	49
.740	28	97	99	68	100	100	52	15	80	20	75	100	100	28
.760	6	53	61	27	98	100	68	55	100	68	98	100	96	5
.780			37	28	79	100	70	75	100	88	98	100	69	
.800	16		84	70	65	100	59	81	100	87	72	100	66	15
.820	22	25	99	82	36	99	30	76	100	83	8	74	64	22
.840	6	53	100	76	1	26		57	100	65		19	27	6
.860		63	100	71	4	20		19	89	24	29	15		
.880		58	100	67	40	87	1		2		59	60		
.900	3	77	100	47	55	99	6				69	98	12	3
.920	28	99	83	9	48	94	3				79	100	25	30
.940	43	100	69	7	35	47					77	100	23	45
.960	46	100	68	45	77						58	94	8	47
.980	40	99	52	57	90	1				22	22	33	4	41
1.000	19	63	14	45	80					79	47	13	63	19

X ⟶ Y =.0833

Z ↓

Z \ X	.000	.077	.154	.231	.308	.385	.462	.539	.616	.693	.770	.847	.924	1.001
.000	100	12	37	81	45				66	100	90	50	100	100
.020	100	19	90	59					75	100	91	74	100	100
.040	96	37	100	91				10	96	100	85	92	100	95
.060	73	48	100	100	9			43	100	100	84	100	100	71
.080	63	61	100	100	41			61	100	99	57	100	100	62
.100	89	99	100	100	75			83	100	95	55	100	100	89
.120	91	100	100	100	82		8	99	100	88	73	100	99	91
.140	78	100	100	100	71	56	45	100	100	72	96	100	80	80
.160	75	100	100	97	47	100	93	100	100	49	100	100	61	77
.180	84	100	100	75	43	100	100	100	93	30	100	100	45	85
.200	92	100	100	79	50	100	100	93	43	17	100	100	38	92
.220	84	81	76	67	45	100	100	18		2	90	98	13	85
.240	50	35	24	23	27	100	89	2			35	79	81	51
.260	43			5	64	88	54	64	7	41	2	75	100	41
.280	60	7		43	100	60	36	99	60	97	20	94	100	59
.300	92	86	7	64	100	82	48	100	100	100	32	99	100	91
.320	100	100	50	73	100	91	38	100	100	100	27	91	100	100
.340	93	100	78	68	100	99	42	100	100	100	71	71	100	93
.360	65	100	99	69	100	100	64	100	100	100	100	45	63	65
.380	55	100	100	65	100	100	92	100	100	100	100	34		56
.400	35	100	100	57	97	100	90	97	99	100	100	26		36
.420	13	100	100	65	87	100	97	27	97	100	85	3		14
.440	1	90	100	97	85	100	100	26	97	100	57			1
.460		55	100	100	80	100	100	48	83	100	42			
.480		27	100	100	69	100	100	60	48	94	16			
.500		17	100	100	47	96	100	59	13	62	84	7		
.520		4	95	100	48	81	100	56	58	99	100	35		
.540			80	100	43	47	100	49	80	100	100	49		
.560			59	99	23	7	51	13	77	100	100	50		
.580			14	49	16	68	6	2	49	97	100	37		
.600					66	97	71	51	6	48	90	9		
.620				27	98	99	97	88	13	15	9			
.640			1	60	100	100	100	96	21	17				
.660		36	43	63	100	100	100	93	3	2		5	4	
.680		74	83	45	99	100	100	87				71	63	
.700	5	83	91	13	99	100	100	91			10	98	95	4
.720	14	72	81	30	100	100	100	95			36	100	100	13
.740	44	34	38	30	100	100	100	79			63	100	100	43
.760	100	31		14	99	100	73	25	56	7	79	100	100	100
.780	100	48			83	100	62	25	99	33	78	100	100	100
.800	100	45			57	100	50	35	100	43	60	100	100	100
.820	100	40			24	93	19	27	99	39	91	100	100	100
.840	100	47	3			9		5	66	26	100	100	100	100
.860	100	53	31						1	12	99	100	100	100
.880	100	41	26	7	2						75	100	96	100
.900	83	12	17	84	50						22	95	76	83
.920	4	8	88	100	86					44	21	53	33	4
.940	43	29	100	100	97	3			13	98	70	4	24	42
.960	93	35	100	100	97	3			32	100	91	7	91	93
.980	100	20	94	100	84				50	100	95	35	100	100
1.000	100	12	37	81	45				66	100	90	50	100	100

X ⟶ Y = .1667

Z ↓

Z \ X	.000	.077	.154	.231	.308	.385	.462	.539	.616	.693	.770	.847	.924	1.001
.000	96	89	100	99	58				50	100	94	41	100	96
.020	92	32	41	19	5			2	90	100	70	67	100	92
.040	79	72	26		3			18	100	100	52	93	100	78
.060	51	73	47	13		10		26	100	100	67	100	100	50
.080	32	23	55	74	2	83	32	41	100	100	73	100	100	31
.100	25	49	84	96	17	99	55	82	100	97	55	100	100	24
.120	52	100	100	98	19	99	63	99	100	57	34	100	98	52
.140	72	100	100	90	3	77	54	100	100	32	19	99	72	73
.160	99	100	100	97	20	69	95	100	100	23	34	72	38	99
.180	100	100	100	100	63	96	100	100	92	5	45	60	65	100
.200	100	100	100	100	81	100	100	99	74	28	27	38	74	100
.220	100	100	100	100	69	99	100	100	100	85	2	4	65	100
.240	100	100	100	97	23	85	100	100	100	99	17	4	75	100
.260	100	100	100	65		30	97	100	100	100	69	37	100	100
.280	100	100	100	38	5	16	99	100	100	100	99	69	100	100
.300	100	89	60	6	55	33	100	100	100	100	100	80	100	100
.320	100	100	48	6	83	34	100	100	100	100	99	62	100	100
.340	95	100	72	3	74	40	73	100	100	100	67	22	99	95
.360	65	100	80		66	99	49	100	100	100	43	30	83	66
.380	63	100	94	14	81	100	58	91	100	100	58	57	98	63
.400	41	100	100	56	92	100	66	31	59	100	53	58	99	41
.420	3	86	100	77	92	100	80	5	33	88	28	37	79	3
.440		74	100	83	80	100	95	32	75	31	1	2	9	
.460		65	100	92	53	100	100	57	70	2		3		
.480		42	100	99	41	99	100	50	47	28	15			
.500		6	92	100	48	86	100	87	100	99	95	13		
.520			91	100	55	67	100	100	100	100	100	43		
.540			87	100	74	53	99	100	100	100	100	57		
.560			69	100	100	99	99	100	100	100	100	57		
.580			24	67	96	100	100	100	100	100	100	45		
.600					93	100	100	100	96	98	97	16		
.620				10	98	100	100	100	61	18	22			
.640				35	100	100	100	100	62					
.660				40	100	100	100	100	54					
.680				18	99	100	100	97	18					
.700					76	100	100	66						
.720					16	92	98	35						
.740						21	30	3						
.760	20											10	25	20
.780	83	1										62	96	82
.800	99	19									29	98	100	99
.820	100	65									67	100	100	100
.840	100	98	7							1	88	100	100	100
.860	100	100	16								84	100	100	100
.880	100	97	26	21	7						59	100	100	100
.900	100	96	98	98	63						45	100	100	100
.920	100	100	100	100	93	1				61	77	100	100	100
.940	100	100	100	100	100	10			91	99	100	100	99	100
.960	100	100	100	100	99	9			48	100	99	42	85	100
.980	100	100	100	100	92	1			44	100	99	27	100	100
1.000	96	89	100	99	58				50	100	94	41	100	96

X →

Y = .25

Z ↓

Z \ X	.000	.077	.154	.231	.308	.385	.462	.539	.616	.693	.770	.847	.924	1.001
.000	100	100	47		64	34			33	64		46	100	100
.020	100	100	79	5	98	92	5	4	91	98	6	78	100	100
.040	100	100	92	12	100	100	26	25	100	100	13	91	100	100
.060	100	100	94	18	100	100	39	38	100	100	19	93	100	100
.080	83	100	97	23	100	100	85	84	100	100	23	97	100	83
.100	23	93	99	16	92	100	93	93	100	93	16	99	94	24
.120		55	100	24	66	100	96	96	100	68	22	100	56	
.140		13	95	14	49	100	100	100	100	51	13	95	15	
.160	14	3	39	15	16	96	100	100	96	17	14	40	4	13
.180	81	39	69	56	4	61	100	100	62	4	55	70	39	82
.200	100	92	100	70	80	76	100	100	76	81	68	100	92	100
.220	100	100	100	70	99	99	100	100	99	99	70	100	100	100
.240	100	100	100	66	99	100	100	100	100	99	66	100	100	100
.260	100	100	100	66	98	100	100	100	100	98	66	100	100	100
.280	100	99	99	72	97	100	100	100	100	98	71	99	99	100
.300	100	99	72	55	99	94	97	97	94	99	55	72	96	100
.320	100	98	19	12	88	34	70	71	33	88	13	18	98	100
.340	100	100	64		40	13	11	11	13	41		63	100	100
.360	100	100	96	5	59	61			60	60	4	96	100	100
.380	95	100	100	20	70	95	11	11	95	71	19	100	100	96
.400	92	100	100	47	60	100	56	55	100	61	46	100	100	94
.420	73	100	100	64	54	100	90	89	100	55	63	100	100	73
.440	24	97	100	67	45	100	100	100	100	46	66	100	97	24
.460		73	100	62	42	100	100	100	100	43	61	100	74	
.480		46	100	54	29	100	100	100	100	30	53	100	47	
.500		4	70	23	6	89	100	100	90	6	22	71	5	
.520					31	79	100	100	79	32				
.540					63	97	100	100	97	65				
.560					66	99	100	100	99	68				
.580					59	99	100	100	99	60				
.600					42	99	100	100	99	43				
.620					36	98	99	99	78	37				
.640					16	72	64	65	71	17				
.660						8	16	17	8					
.680														
.700														
.720														
.740														
.760														
.780														
.800														
.820														
.840	32	2	6									6	2	32
.860	74	59	57									56	59	74
.880	98	98	85	1								84	98	98
.900	100	99	88	3							4	87	99	100
.920	100	99	98	14							13	98	99	100
.940	100	100	98	21							19	98	100	100
.960	100	100	94	20							19	93	100	100
.980	100	99	58	6							6	57	98	100
1.000	100	100	47		64	34			33	64		46	100	100

X ⟶ Y=.33

Z ↓

	.000	.077	.154	.231	.308	.385	.462	.539	.616	.693	.770	.847	.924	1.001
.000	95	100	42	93	100	51				58	99	100	89	96
.020	91	100	69	69	100	91	2			5	19	41	32	92
.040	77	100	94	51	100	100	19			3		25	73	78
.060	48	100	100	67	100	100	27		10		13	47	74	50
.080	30	100	100	74	100	100	42	31	84	2	73	56	23	31
.100	24	100	100	55	97	100	83	53	99	18	96	85	49	24
.120	53	97	100	35	56	100	99	63	99	20	98	100	100	52
.140	74	71	99	20	30	100	100	55	78	2	89	100	100	73
.160	99	39	71	35	22	100	100	95	70	19	97	100	100	99
.180	100	67	59	46	4	91	100	100	97	62	100	100	100	100
.200	100	75	37	28	28	73	99	100	100	82	100	100	100	100
.220	100	66	3	2	84	100	100	100	99	69	100	100	100	100
.240	100	75	4	15	99	100	100	100	86	23	97	100	100	100
.260	100	100	39	68	100	100	100	97	31		64	100	100	100
.280	100	100	69	99	100	100	100	100	17	5	37	100	100	100
.300	100	100	81	100	100	100	100	100	34	55	6	59	88	100
.320	100	100	62	99	100	100	100	100	34	83	7	47	100	100
.340	95	99	23	65	100	100	100	74	40	75	3	71	100	95
.360	68	82	31	42	100	100	100	49	99	67		79	100	66
.380	64	98	58	57	100	100	92	57	100	82	13	93	100	63
.400	41	98	60	51	100	60	32	65	100	93	55	100	100	41
.420	3	78	39	27	88	33	5	79	100	93	75	100	87	3
.440		9	2	1	30	74	32	94	100	81	82	100	75	
.460			3		2	69	57	100	100	53	91	100	67	
.480				15	28	47	49	100	99	41	99	100	44	
.500			12	95	99	100	87	100	87	47	100	93	6	
.520			42	100	100	100	100	100	69	53	100	93		
.540			55	100	100	100	100	99	54	73	100	89		
.560			56	100	100	100	100	99	99	100	100	70		
.580			44	100	100	100	100	100	100	97	67	25		
.600			15	97	98	96	100	100	100	94				
.620				22	18	60	100	100	100	98	11			
.640						61	100	100	100	100	36			
.660						53	100	100	100	100	41			
.680						17	96	100	100	99	19			
.700							64	100	100	77				
.720							34	98	93	17				
.740							2	29	21					
.760	19	25	10											20
.780	81	96	62											82
.800	98	100	98	30									17	99
.820	100	100	100	68									64	100
.840	100	100	100	90	2							6	98	100
.860	100	100	100	84	1							14	100	100
.880	100	100	100	60						7	21	25	97	100
.900	100	100	100	47						62	98	99	96	100
.920	100	100	100	77	62	1			1	92	100	100	100	100
.940	100	99	100	100	99	23			8	99	100	100	100	100
.960	100	85	41	99	100	41			8	99	100	100	100	100
.980	100	100	26	99	100	46				91	100	100	100	100
1.000	95	100	42	93	100	51				58	99	100	89	96

X ⟶ Y=.4167

Z ↓

Z \ X	.000	.077	.154	.231	.308	.385	.462	.539	.616	.693	.770	.847	.924	1.001
.000	100	100	32	89	100	67				44	82	38	10	100
.020	100	100	76	89	100	77					58	91	19	100
.040	94	100	93	85	100	96	11				89	100	38	95
.060	70	100	100	84	100	100	45			8	99	100	50	71
.080	61	100	100	57	99	100	63			39	100	100	62	62
.100	89	100	100	56	94	100	85			74	100	100	99	89
.120	92	99	100	74	87	100	99	9		81	100	100	100	91
.140	81	79	100	96	72	100	100	46	57	70	100	100	100	80
.160	78	60	100	100	50	100	100	93	100	47	97	100	100	77
.180	86	43	100	100	30	92	100	100	100	44	74	100	100	85
.200	94	38	100	100	18	42	92	100	100	50	78	100	100	92
.220	86	12	98	91	2		16	100	100	46	66	76	80	85
.240	52	80	79	36			1	88	100	28	22	25	34	51
.260	40	100	77	2	42	7	64	54	39	65	6			41
.280	58	100	95	19	97	60	99	38	58	100	43		7	59
.300	91	100	100	34	100	100	100	49	81	100	66	6	85	91
.320	100	100	93	25	100	100	100	39	90	100	74	48	100	100
.340	93	100	72	70	100	100	100	41	99	100	69	76	100	93
.360	66	63	44	100	100	100	100	64	100	100	70	99	100	65
.380	58		32	100	100	100	100	92	100	100	65	100	100	56
.400	37		25	100	100	99	97	90	100	98	56	100	100	36
.420	15		3	85	100	99	28	97	100	88	64	100	100	14
.440	2			55	100	98	25	100	100	85	97	100	92	1
.460				41	100	84	47	100	100	80	100	100	56	
.480				15	93	49	59	100	100	69	100	100	29	
.500			6	83	62	14	58	100	77	46	100	100	18	
.520			34	100	99	59	55	100	82	46	100	96	4	
.540			48	100	100	80	48	100	48	42	100	81		
.560			49	100	100	77	12	52	7	22	99	61		
.580			36	100	97	50	2	6	67	16	49	15		
.600			8	89	49	6	50	72	97	68				
.620				8	15	14	87	97	99	99	28			
.640					17	21	96	100	100	100	61	1		
.660		4	6		1	3	92	100	100	100	65	43	37	
.680		62	72				86	100	100	99	46	82	75	
.700	3	95	99	11			90	100	100	99	14	90	84	4
.720	12	100	100	37			93	100	100	100	31	80	74	13
.740	42	99	100	64			77	100	100	100	32	37	34	43
.760	100	100	100	80	6	58	25	72	100	99	16		31	100
.780	100	100	100	79	32	99	26	61	100	84			46	100
.800	100	100	100	61	42	100	36	49	100	58			43	100
.820	100	100	100	91	38	99	28	18	93	25			38	100
.840	100	100	100	100	26	66	6		9			3	45	100
.860	100	100	100	99	13	1						31	52	100
.880	100	97	100	76						2	8	26	39	100
.900	83	76	96	23						49	85	17	11	83
.920	4	32	54	20	45					84	100	89	8	4
.940	42	24	4	69	98	14			2	96	100	100	30	42
.960	91	91	7	89	100	34			2	96	100	100	36	93
.980	100	100	35	94	100	51				82	100	94	20	100
1.000	100	100	32	89	100	67				44	82	38	10	100

STRUCTURE 5

x ⟶ y=.00

z ↓

	.000	.077	.154	.231	.308	.385	.462	.539	.616	.693	.770	.847	.924	1.001
.000	14	70	16	58	81					80	59	15	71	14
.020	39	4	38	35	44					80	62	50	100	38
.040	47	14	97	48					5	54	38	64	100	46
.060	43	31	100	68					74	32	1	63	100	42
.080	26	33	100	70				3	97	51	8	81	99	25
.100	2	20	99	60				2	96	50	42	100	70	2
.120		1	67	49		18	14	14	46	24	60	100	58	
.140			16	25	38	99	91	85	4		63	100	61	
.160	5	17	11		72	100	100	100	70	10	63	100	50	5
.180	25	63	57	1	87	100	100	100	100	51	67	97	21	26
.200	29	73	99	54	91	100	100	100	100	71	52	67		30
.220	28	65	100	96	86	100	100	100	100	90	20	18		28
.240	96	95	100	100	70	100	100	100	100	100	44	52	63	96
.260	100	100	100	92	18	69	77	94	100	100	70	99	100	100
.280	100	100	100	49	27	2	15	31	99	100	85	100	100	100
.300	100	100	100	33	90	22	6	49	97	88	59	100	100	100
.320	100	100	95	25	99	67	3	45	77	20	40	100	100	100
.340	100	88	42	14	99	96	5	9	23	1	25	100	100	100
.360	100	40	1	15	100	100	13			37	5	85	90	100
.380	26	24	67	12	99	99	10		28	79	10	11	9	26
.400		48	97	5	89	97	26		68	97	12			
.420		49	98	4	39	98	73		82	100	21			
.440		27	76	3	14	99	90		80	100	19			
.460			17	78	18	100	92	3	61	92	5			
.480			32	99	20	95	78	10	15	33	59	10		
.500			32	99	12	52	40	39	53	11	99	33		
.520			9	59	33	16	10	77	95	19	99	33		
.540				4	92	62	3	91	100	19	77	17		
.560				18	99	81		89	98	15	3	75	28	
.580				20	100	83		72	99	40	4	97	50	
.600				11	97	69		25	97	90	5	96	49	
.620	26	9	12	10	79	29		9	99	99	13	66	24	26
.640	100	90	86	6	37			12	100	100	16	1	38	100
.660	100	100	100	26	1	23	9	4	95	99	15	41	87	100
.680	100	100	100	41	19	78	45	4	66	99	26	95	100	100
.700	100	100	100	58	88	97	50	7	21	90	33	100	100	100
.720	100	100	100	85	100	99	32	16	2	27	48	100	100	100
.740	100	100	99	71	100	100	94	77	69	19	91	100	100	100
.760	96	63	53	43	100	100	100	100	100	71	99	100	95	96
.780	29		17	20	89	100	100	100	100	87	95	100	66	28
.800	31		66	53	70	100	100	100	100	93	53	99	73	30
.820	27	19	97	69	50	100	100	100	100	89	1	56	63	26
.840	5	49	100	64	10	70	100	100	100	73		11	17	5
.860		59	100	65		4	84	91	98	39	24	17		
.880		56	100	62	23	67	14	14	18		48	68	2	
.900	1	69	100	44	49	96	3				58	99	21	2
.920	23	99	82	8	50	97	4				69	100	34	25
.940	40	100	64	1	31	75					66	100	32	42
.960	44	100	65	37	55	5					47	97	15	46
.980	37	100	52	60	82					43	36	38	4	38
1.000	14	70	16	58	81					80	59	15	71	14

X ⟶ y=.0833

z ↓	.000	.077	.154	.231	.308	.385	.462	.539	.616	.693	.770	.847	.924	1.001
.000	100	10	33	76	37				65	100	92	53	100	100
.020	100	23	95	48					79	100	91	76	100	100
.040	93	45	100	80				21	99	100	82	93	100	92
.060	70	57	100	95	1			50	100	100	72	100	100	68
.080	60	67	100	100	34			66	100	98	46	100	100	59
.100	87	99	100	100	68		1	91	100	94	57	100	100	87
.120	91	100	100	100	74	2	11	99	100	83	74	100	99	91
.140	80	100	100	100	67	80	80	100	100	60	96	100	80	82
.160	75	100	100	97	51	100	100	100	99	39	100	100	63	77
.180	80	100	100	71	47	100	100	100	83	26	100	100	43	81
.200	90	100	100	74	50	100	100	100	34	17	100	100	37	91
.220	85	83	80	65	44	100	100	100	20	2	91	98	13	86
.240	88	47	30	26	24	100	100	92	4		38	75	68	88
.260	100	47		7	67	77	69	90	11	49	2	72	100	100
.280	100	69		44	100	60	38	99	67	97	17	93	100	100
.300	100	82	1	64	100	81	45	100	100	100	30	100	100	100
.320	100	99	36	73	100	91	33	100	100	100	23	95	100	100
.340	100	100	67	68	100	100	44	100	100	100	67	78	100	100
.360	90	100	96	62	100	100	66	100	100	100	99	52	86	90
.380	58	100	100	62	100	100	91	100	100	100	100	26	2	60
.400	43	100	100	56	98	100	89	97	100	100	100	19		44
.420	17	100	100	56	86	100	97	31	100	100	81	1		18
.440	3	96	100	90	79	100	100	31	100	100	47			4
.460		68	100	100	78	100	100	46	92	100	31			
.480		30	100	100	71	100	100	57	58	90	7			
.500		16	100	100	50	97	100	58	11	56	77	3		
.520		6	98	100	46	84	100	54	51	98	100	29		
.540			83	100	46	55	100	48	76	100	100	46		
.560			68	100	32	7	71	18	78	100	100	48		
.580			31	82	12	41			58	100	100	38		
.600				3	45	93	53	38	14	69	97	13		
.620				9	93	98	94	83	5	12	27			
.640		1	3	48	100	100	99	96	11	6				
.660	7	36	50	60	100	100	100	95	3			25	21	8
.680	48	71	84	52	100	100	100	89			1	86	81	48
.700	65	78	89	17	98	100	100	92			16	99	98	65
.720	49	60	75	17	100	100	100	97			48	100	100	48
.740	61	22	24	26	100	100	100	85			67	100	99	60
.760	100	38		18	100	100	80	36	34	3	75	100	100	100
.780	100	49		3	93	100	77	36	95	27	66	100	100	100
.800	100	45			64	100	82	61	100	41	64	100	100	100
.820	100	42			38	99	57	47	99	42	96	100	100	100
.840	100	49			3	40	6	8	69	25	100	100	100	100
.860	100	51	12						4	4	94	100	99	100
.880	100	35	8	25	9						54	100	93	100
.900	66	7	36	95	60					3	10	85	63	66
.920		13	96	100	87				1	75	42	30	17	
.940	58	29	100	100	97	2			20	99	80		37	57
.960	95	30	100	100	94	1			36	100	93	11	96	94
.980	100	15	91	100	78				54	100	93	37	100	100
1.000	100	10	33	76	37				65	100	92	53	100	100

X ⟶

Y=.1667

Z ↓

Z \ X	.000	.077	.154	.231	.308	.385	.462	.539	.616	.693	.770	.847	.924	1.001
.000	94	74	99	94	44				62	100	91	48	100	94
.020	91	37	31	7	5			5	96	100	61	69	100	91
.040	76	77	27		7			18	100	100	49	95	100	74
.060	47	66	42	10		28	5	24	100	100	67	100	100	46
.080	29	12	57	67	3	91	40	55	100	100	68	100	100	27
.100	24	46	86	93	15	99	57	91	100	92	47	100	100	24
.120	52	100	100	96	14	97	63	100	100	45	29	100	97	52
.140	69	100	100	87	1	70	60	100	100	28	26	100	70	71
.160	96	100	100	94	14	77	96	100	99	17	55	84	27	97
.180	100	100	100	100	58	98	100	91	82	1	64	79	60	100
.200	100	100	100	100	76	100	100	65	76	40	47	62	74	100
.220	100	100	100	100	62	97	100	99	100	88	10	14	69	100
.240	100	100	100	98	27	75	100	100	100	99	20		67	100
.260	100	100	100	69		20	98	100	100	100	74	27	100	100
.280	99	100	100	41	21	22	100	100	100	100	99	62	100	99
.300	78	71	72	15	84	43	100	100	100	100	100	76	100	77
.320	91	99	35	15	98	43	99	100	100	100	97	59	100	91
.340	96	100	66	10	94	45	62	100	100	100	59	30	100	97
.360	68	100	77	1	73	99	45	100	100	100	40	22	87	70
.380	64	100	90	6	77	100	57	91	100	100	54	53	96	64
.400	51	100	100	49	90	100	66	30	60	100	47	60	99	51
.420	12	94	100	74	91	100	76	2	25	88	22	46	88	12
.440		71	100	84	79	100	94	25	69	25		8	25	
.460		66	100	88	53	100	100	56	73	1		6		
.480		50	100	98	35	100	100	53	45	17	5	4		
.500		16	96	100	50	89	100	77	94	96	86	6		
.520			89	100	83	72	100	99	100	100	100	34		
.540			89	100	97	51	91	92	100	100	100	50		
.560			76	100	100	93	83	91	100	100	100	52		
.580			43	99	100	100	100	100	100	100	100	43		
.600			1	38	97	100	100	100	99	100	98	18		
.620				2	96	100	100	100	67	39	36			
.640				24	100	100	100	100	61					
.660				39	100	100	100	100	57					
.680				27	99	100	100	99	29					
.700				2	88	100	100	76						
.720					32	97	99	42						
.740					1	42	50	8						
.760	36													
.780	89	2												
.800	99	28												
.820	100	78												
.840	100	99	10											
.860	100	100	14											
.880	100	96	45	39	13									
.900	100	99	100	100	66									
.920	100	100	100	100	92									
.940	79	100	100	100	99	5								
.960	85	100	100	100	98	3								
.980	99	100	100	100	83									
1.000	94	74	99	94	44									

Z \ X	.000	.077	.154	.231	.308	.385	.462	.539	.616	.693	.770	.847	.924	1.001
.000												21	47	35
.020											4	76	99	88
.040											42	100	100	99
.060											76	100	100	100
.080											88	100	100	100
.100											73	100	100	100
.120											48	100	100	100
.140										14	74	100	100	100
.160									5	89	100	100	100	100
.180									29	100	100	99	91	79
.200									41	100	100	61	86	85
.220									41	100	100	38	100	99
.240									62	100	91	48	100	94

X ⟶ Y=.25

Z ↓

	.000	.077	.154	.231	.308	.385	.462	.539	.616	.693	.770	.847	.924	1.001
.000	99	100	100	100	99	52			51	99	100	100	100	99
.020	100	100	92	72	100	97	9	7	97	100	72	91	100	100
.040	100	100	91	19	100	100	32	31	100	100	19	90	100	100
.060	99	100	92	23	100	100	68	66	100	100	23	92	100	99
.080	77	100	98	23	100	100	88	86	100	100	23	97	100	77
.100	16	90	99	15	89	100	93	93	100	90	15	99	90	16
.120		55	100	22	62	100	98	98	100	64	21	100	57	
.140		15	95	11	44	100	100	100	100	46	11	95	16	
.160	8	2	36	11	10	91	94	94	91	10	10	37	2	8
.180	74	32	64	30	15	47	58	57	47	15	49	65	32	74
.200	99	87	99	67	86	45	12	11	43	87	66	99	87	99
.220	100	100	100	68	99	97	69	68	97	99	68	100	100	100
.240	100	100	100	58	99	100	97	97	100	99	58	100	100	100
.260	96	100	100	59	96	100	100	100	100	97	59	100	100	95
.280	46	93	100	70	96	100	100	100	100	97	70	100	94	46
.300		21	82	58	98	91	95	95	91	99	57	83	21	
.320	31	81	22	12	84	27	62	63	26	84	12	21	81	32
.340	90	100	53		33	14	6	6	14	34		52	100	90
.360	100	100	93	2	56	63			62	58	1	92	100	100
.380	97	100	100	17	68	96	12	11	95	69	15	100	100	97
.400	91	100	100	43	60	100	49	48	100	61	42	100	100	87
.420	78	100	100	64	54	100	87	86	100	55	63	100	100	78
.440	38	99	100	71	43	100	99	99	100	45	70	100	100	38
.460		78	100	69	41	100	100	100	100	42	68	100	79	
.480		54	100	89	76	100	100	100	100	76	89	100	55	
.500		13	86	100	100	100	100	100	100	100	100	87	14	
.520			29	100	100	98	84	83	98	100	100	31		
.540			36	100	100	100	48	47	100	100	100	38		
.560			37	100	100	100	41	40	100	100	100	40		
.580			29	100	100	99	67	66	99	100	100	30		
.600			8	97	100	98	98	98	99	100	97	9		
.620				51	87	99	99	100	99	87	53			
.640					24	88	78	79	88	25				
.660					3	25	22	23	25	3				
.680														
.700														
.720														
.740														
.760														
.780														
.800														
.820	1													1
.840	36	13	19									19	13	36
.860	81	80	72									71	80	81
.880	99	99	95	81	15						14	80	94	99	100
.900	97	98	100	100	56						56	100	100	99	98
.920	45	94	100	100	79						77	100	100	94	45
.940	3	87	100	100	87						87	100	100	88	3
.960	9	91	100	100	86						86	100	100	92	9
.980	71	98	99	100	79						78	100	98	98	70
1.000	99	100	100	100	99	52			51	99	100	100	100	99

Y=.33

Z ↓ / X →	.000	.077	.154	.231	.308	.385	.462	.539	.616	.693	.770	.847	.924	1.001
.000	94	100	49	90	100	64				43	94	99	75	94
.020	90	100	70	60	100	96	5			5	7	31	38	91
.040	73	100	95	48	100	100	20			7		26	78	74
.060	45	100	100	67	100	100	25	4	28		9	41	67	46
.080	26	100	100	68	100	100	56	39	92	4	66	58	12	27
.100	23	100	100	47	92	100	92	56	99	16	92	87	46	24
.120	52	97	100	31	44	100	100	63	98	15	95	100	100	52
.140	72	68	100	27	27	100	100	61	71	1	86	100	100	71
.160	97	27	83	56	16	99	100	96	79	14	94	100	100	97
.180	100	61	77	65		81	91	100	98	58	100	100	100	100
.200	100	74	60	48	39	77	64	100	100	74	100	100	100	100
.220	100	70	13	10	87	100	99	100	98	62	100	100	100	100
.240	100	69		19	99	100	100	100	76	26	98	100	100	100
.260	100	100	28	72	100	100	100	98	20		67	100	100	100
.280	99	100	61	99	100	100	100	100	23	21	40	100	100	99
.300	76	100	76	100	100	100	100	100	44	85	16	72	71	77
.320	91	100	59	96	100	100	100	99	43	99	17	34	99	91
.340	96	100	31	57	100	100	100	63	44	95	11	64	100	97
.360	71	87	23	38	100	100	100	45	99	74	1	76	100	70
.380	65	95	54	53	100	100	92	56	100	78	6	88	100	64
.400	51	99	61	46	100	60	31	65	100	91	47	100	100	51
.420	13	85	47	21	88	26	2	75	100	92	73	100	94	12
.440		24	9		25	68	26	93	100	81	82	100	72	
.460			6	1	1	72	57	100	100	55	88	100	67	
.480			4	5	16	44	53	100	100	35	98	100	51	
.500			5	85	96	94	76	100	90	49	100	96	17	
.520			33	100	100	100	99	100	73	82	100	90		
.540			49	100	100	100	92	91	51	97	100	90		
.560			51	100	100	100	91	82	93	100	100	77		
.580			42	100	100	100	100	100	100	100	99	45		
.600			17	98	100	99	100	100	100	97	39	2		
.620				35	39	66	100	100	100	96	3			
.640						60	100	100	100	100	25			
.660						56	100	100	100	100	41			
.680						28	99	100	100	100	28			
.700							75	100	100	89	2			
.720							41	99	98	33				
.740							8	50	43	1				
.760	35	47	22											35
.780	87	99	77	5									2	88
.800	99	100	100	43									27	99
.820	100	100	100	77									76	100
.840	100	100	100	89	1							8	99	100
.860	100	100	100	74								13	100	100
.880	100	100	100	50						12	39	44	95	100
.900	100	100	100	74	14					65	100	100	99	100
.920	100	100	100	100	89	5				90	100	100	100	100
.940	79	91	99	100	100	30			3	98	100	100	100	79
.960	85	87	60	100	100	43			2	97	100	100	100	85
.980	99	100	58	100	100	43				82	100	100	100	99
1.000	94	100	49	90	100	64				43	94	99	75	94

X ⟶ **Y=.4167**

Z ↓

Z \ X	.000	.077	.154	.231	.308	.385	.462	.539	.616	.693	.770	.847	.924	1.001
.000	100	100	54	92	100	66				36	77	34	9	100
.020	99	100	77	90	100	80					46	95	23	100
.040	90	100	94	81	100	99	22				79	100	46	92
.060	67	100	100	73	100	100	52				94	100	59	68
.080	58	100	100	47	98	100	67			33	100	100	68	59
.100	87	100	100	58	93	100	92	2		67	100	100	99	87
.120	92	99	100	76	82	100	100	12	2	74	100	100	100	91
.140	83	79	100	97	61	100	100	80	80	66	100	100	100	82
.160	78	62	100	100	39	99	100	100	100	51	97	100	100	77
.180	82	42	100	100	26	81	100	100	100	47	70	100	100	81
.200	92	36	100	100	19	33	100	100	100	52	72	100	100	91
.220	87	13	98	92	2	19	100	100	100	45	64	81	82	86
.240	89	67	75	39		3	92	100	100	25	26	31	46	88
.260	100	100	74	2	49	11	89	69	77	67	8		46	100
.280	100	100	94	17	97	67	99	40	59	100	44		68	100
.300	100	100	100	30	100	100	100	46	80	100	66	1	81	100
.320	100	100	97	23	99	100	100	35	91	100	74	35	99	100
.340	100	100	79	66	100	100	100	44	99	100	70	66	100	100
.360	91	86	52	99	100	100	100	66	100	100	62	95	100	90
.380	61	2	24	100	100	100	100	91	100	100	61	100	100	60
.400	46		18	100	100	100	98	88	100	98	56	100	100	44
.420	20		1	80	100	100	32	96	100	87	55	100	100	18
.440	5			45	100	100	31	100	100	80	90	100	97	4
.460				30	100	93	45	100	100	78	100	100	69	
.480				6	89	59	56	100	100	71	100	100	31	
.500			3	76	56	12	57	100	97	49	100	100	17	
.520			28	100	98	52	52	100	85	45	100	99	7	
.540			44	100	100	77	46	100	56	44	100	84		
.560			47	100	100	78	17	71	7	31	100	69		
.580			37	100	100	60			41	12	82	32		
.600			12	96	70	14	37	53	92	46	3			
.620				26	12	5	82	94	98	94	10			
.640					6	11	95	99	99	100	49	3	1	
.660	7	20	25			3	94	100	100	100	62	49	37	8
.680	48	80	87	1			88	100	100	100	53	83	71	48
.700	64	98	99	17			90	100	100	99	18	88	79	65
.720	47	100	100	49			95	100	100	100	18	74	61	48
.740	60	99	100	68			84	100	100	100	27	23	22	60
.760	100	100	100	76	3	34	36	80	100	100	20		36	100
.780	100	100	100	67	26	95	36	77	100	94	4		48	100
.800	100	100	100	65	40	100	62	82	100	65			44	100
.820	100	100	100	97	41	99	48	56	99	39			41	100
.840	100	100	100	100	26	70	9	6	40	4			48	100
.860	100	99	100	95	5	4						12	50	100
.880	100	93	100	55						8	26	8	34	100
.900	65	62	86	10	3					59	96	37	6	66
.920		16	31	40	76	2				86	100	96	13	
.940	56	38		78	99	22			1	96	100	100	31	57
.960	93	96	12	92	100	37				93	100	100	30	94
.980	100	100	38	92	100	56				77	100	91	15	100
1.000	100	100	54	92	100	66				36	77	34	9	100

Figure 5.3.3 Molecular packing in structure 4 (host only)

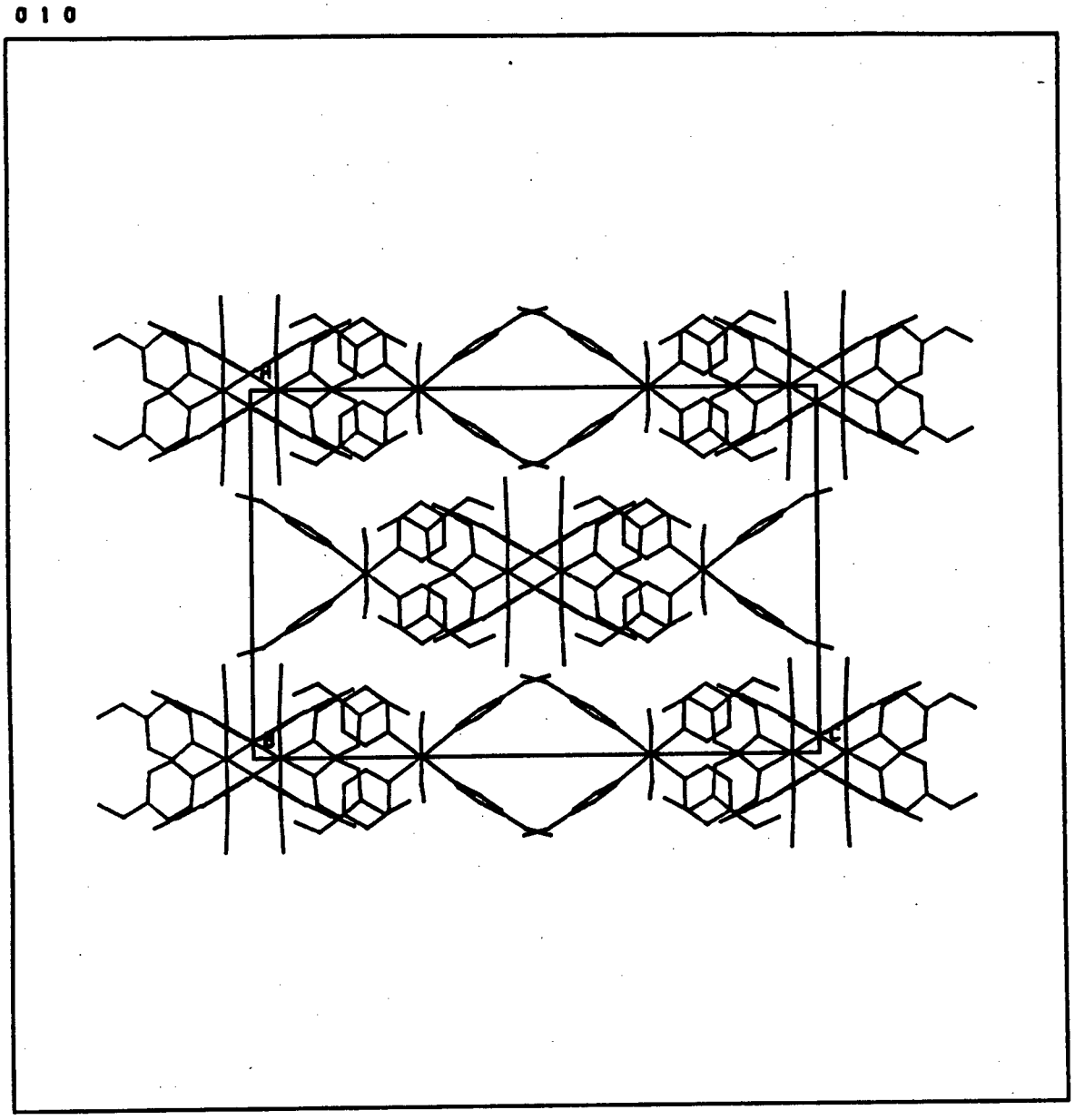

a) View down the y-axis

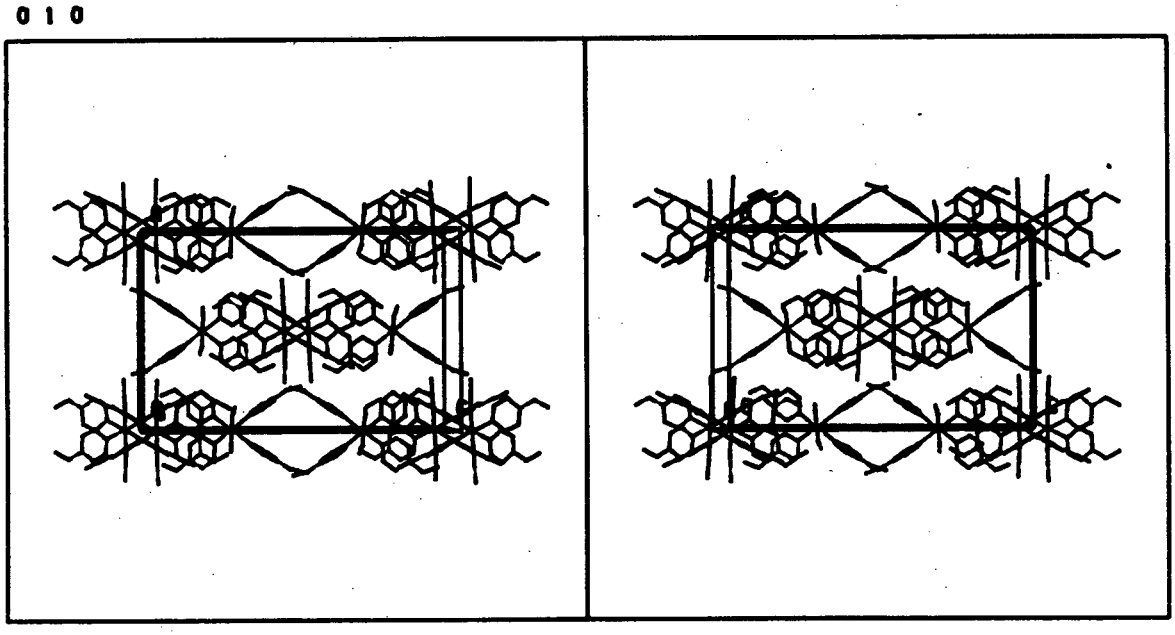

b) Stereo view down the y-axis

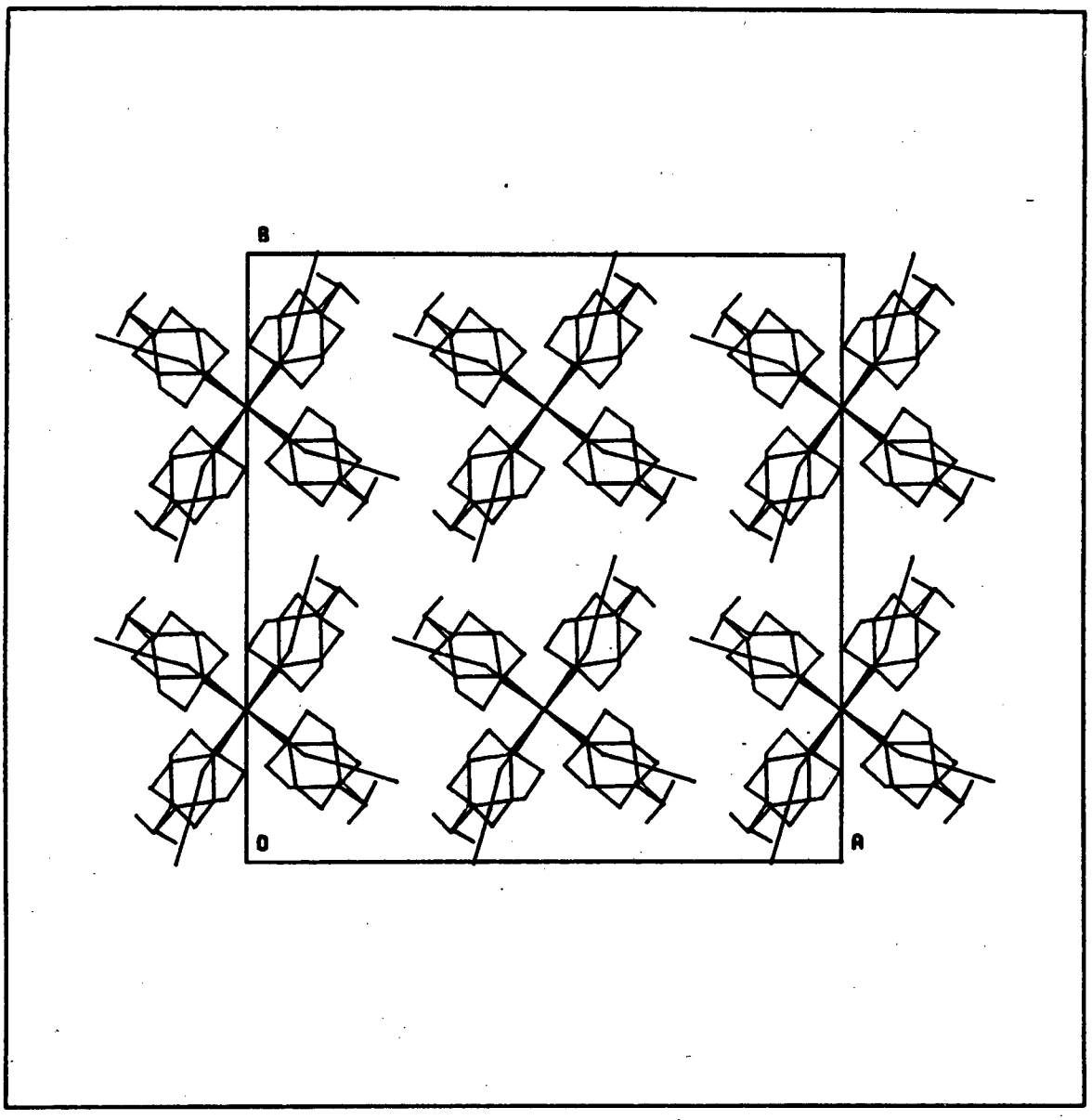

c) View down z-axis

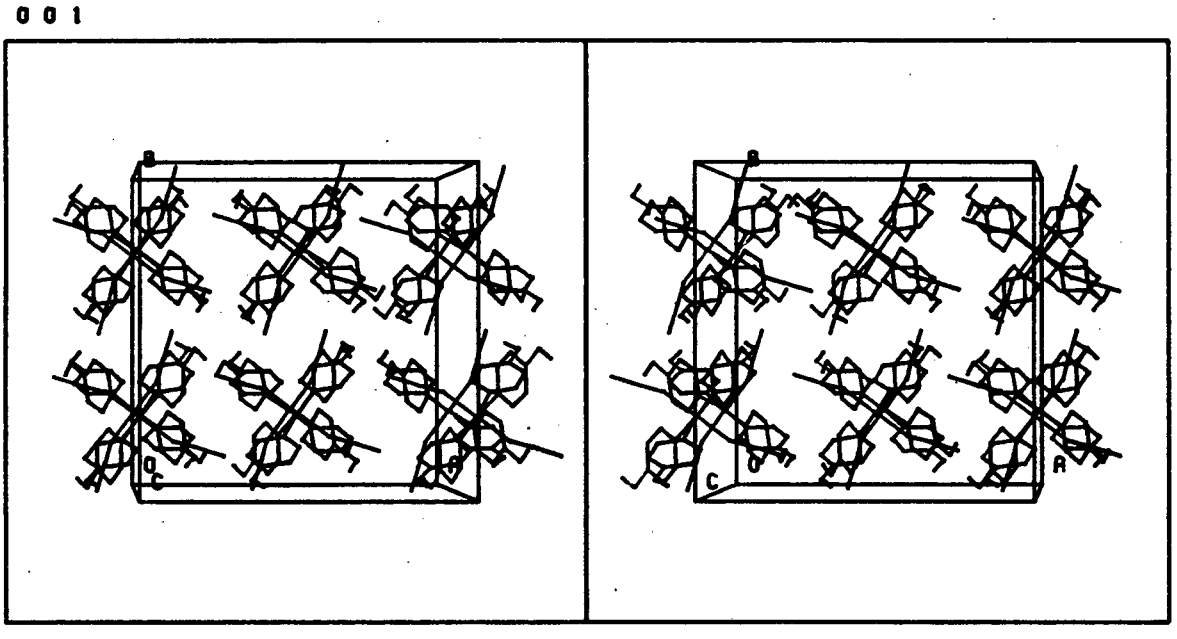

d) Stereo view down the z-axis

DIEN3: As described in section 4.4.3 the guests were placed at Wyckoff special position d, taking into account the host:total guest ratio 1:1. Figure 5.3.4 shows the packing of the guests in the channel with their atoms being disordered about and through the inversion centre. These atoms are shifted by the $\bar{4}$ site at 1/2, 1/4, 7/8 giving another group of atoms disordered about an inversion centre. The guests are in the `channels' at the inversion centres and are connected by the larger `cavities' with the $\bar{4}$ sites. The residual volume is considerable and is discussed in section 5.6.

The program OPEC calculates the volume occupied by the atom input obtained from the solved structure (from the final least squares refinement). Figure 5.3.4 gives an example of the relatively large residual unoccupied cavities, which are also present in the other packing diagrams but to a lesser extent. These residual cavities are rather large to be regarded as poor packing of the host. The implication of interpreting these residual cavities as being vacant implies a vacuum as there is no electron density. These residual cavities may be occupied by guest molecules with low (approx. 10%) site occupancy factor; these guests were not detected in the electron density maps and were left out of the final model of the crystal structure analysis.

Figure 5.3.4 Packing diagram of structure 3, host and guest.

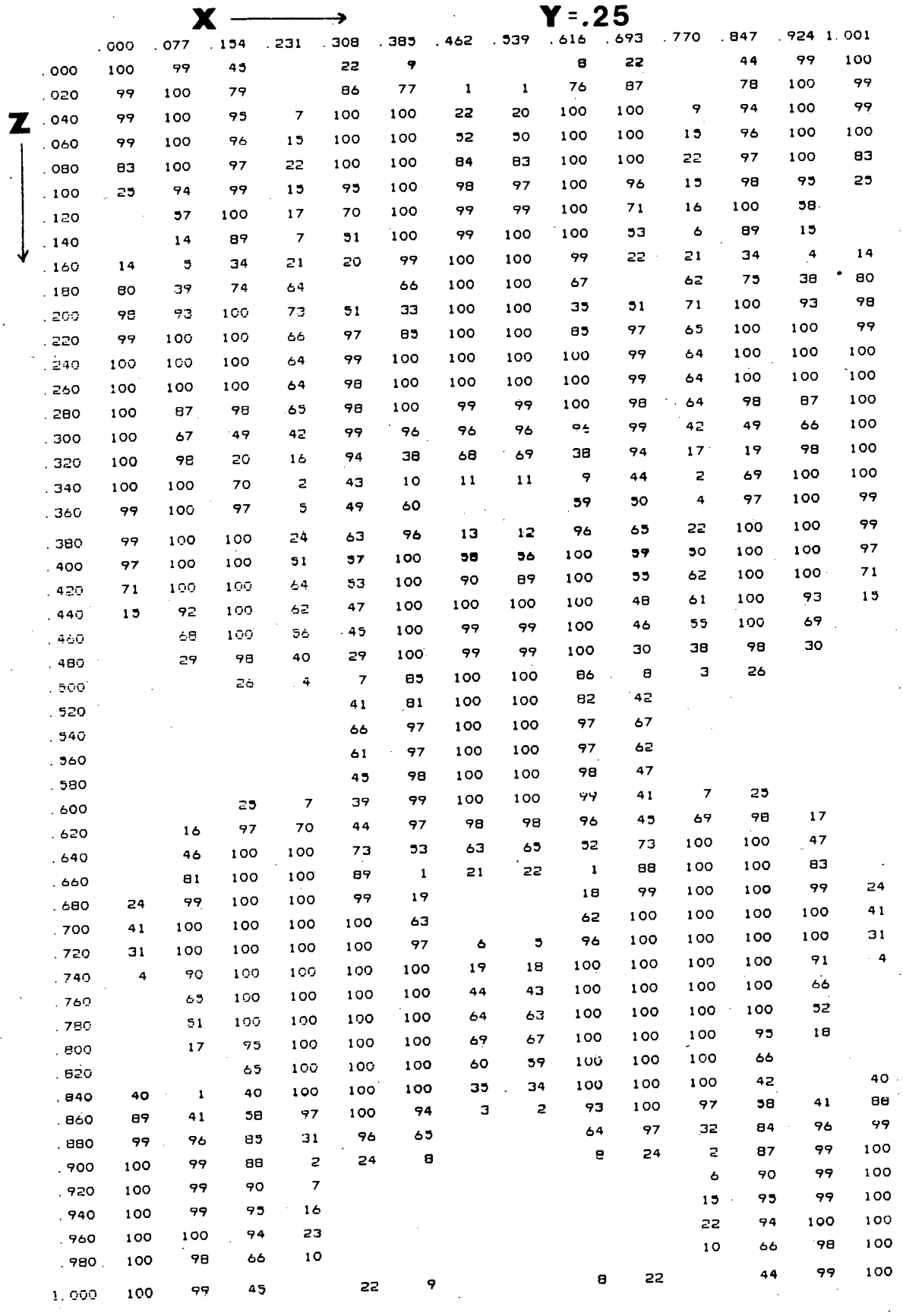

DIEN4: Including the guests, figure 5.3.5 shows the unit cell layered at y = 0.25. The disordered and increased guest contents (host to guest ratio of 1:1.4) fills the channels (centre of symmetry) and the cavities ($\bar{4}$ sites). The size of the channels/cavities is able to accommodate the increased guest contents.

THF/BEN: Including the guests, figure 5.3.6 shows the unit cell layered at y = 0.25 with the same disordering as for DIEN4.
Note the minimal host-guest interaction to the extent of small cavities between the host and guest.

Figure 5.3.5 Packing diagram of structure 4, host and guest.

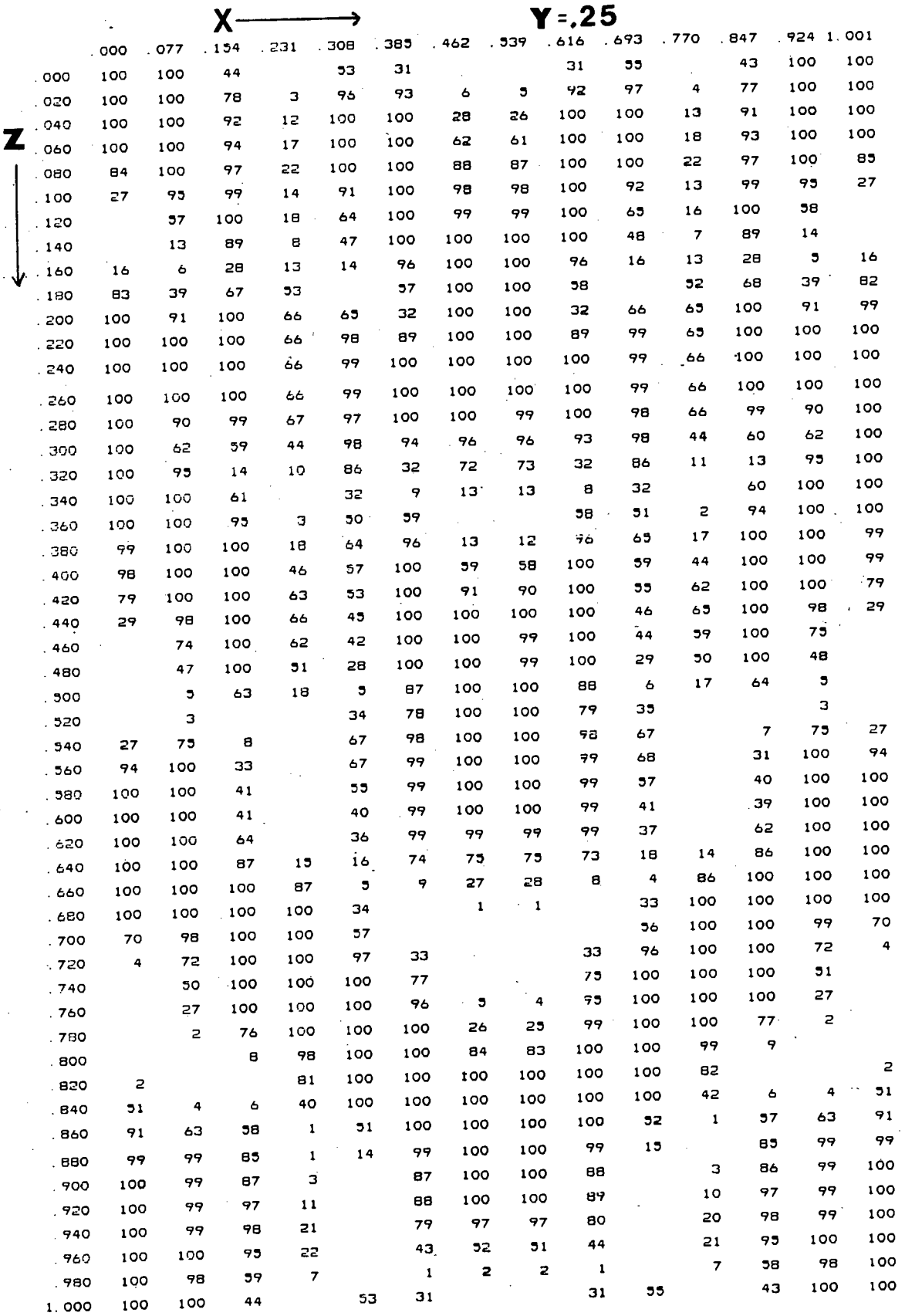

Figure 5.3.6 Packing diagram of structure 5, host and guest.

X ⟶ Y=.25

Z ↓

	.000	.077	.154	.231	.308	.385	.462	.539	.616	.693	.770	.847	.924	1.001
.000	100	100	53		79	50			49	80		52	100	100
.020	100	100	82	8	99	97	8	8	96	100	9	80	100	100
.040	100	100	92	14	100	100	34	32	100	100	15	91	100	100
.060	99	100	94	20	100	100	71	69	100	100	22	92	100	99
.080	77	100	97	21	99	100	90	89	100	100	21	97	100	77
.100	19	91	99	12	88	100	97	93	100	89	11	98	92	19
.120		55	100	16	60	100	98	98	100	61	14	100	56	
.140		14	89	5	41	100	100	100	100	42	5	89	15	
.160	9	3	22	8	7	89	100	100	90	8	8	23	3	9
.180	72	31	58	46	6	41	100	100	41	6	45	59	30	72
.200	98	86	99	63	78	42	100	100	41	79	63	99	85	98
.220	100	100	100	64	99	95	99	100	95	99	64	100	100	100
.240	100	100	100	60	99	100	100	100	100	99	60	100	100	100
.260	100	100	100	61	98	100	100	100	100	98	61	100	100	100
.280	100	95	100	66	96	100	100	99	100	97	66	100	95	100
.300	100	61	76	48	97	90	93	94	90	97	48	77	61	100
.320	100	86	12	6	77	24	61	62	23	77	8	11	85	100
.340	100	100	49		22	9	6	7	8	22		48	100	100
.360	100	100	90	1	47	61			60	47	1	90	100	100
.380	98	100	100	14	62	95	11	11	95	63	12	100	100	99
.400	97	100	100	42	57	100	52	51	100	58	41	100	100	99
.420	83	100	100	62	53	100	87	86	100	54	61	100	100	83
.440	44	100	100	69	44	100	99	99	100	46	67	100	100	45
.460	1	80	100	64	42	100	100	100	100	44	64	100	81	1
.480		53	100	58	32	100	100	99	100	33	57	100	54	
.500		12	86	32	7	93	100	100	94	8	31	86	13	
.520		1	5		19	75	100	100	75	20		5	1	
.540	72	51			54	95	100	100	95	55			51	72
.560	100	90	6		61	98	100	100	99	62		5	89	100
.580	100	89	6		55	99	100	100	99	57		5	88	100
.600	93	60			41	98	100	100	99	42			59	92
.620	42	93	34		36	99	100	100	99	37		33	93	42
.640	90	100	80	22	22	85	87	87	85	23	21	79	100	90
.660	100	100	100	96	15	21	33	34	21	14	95	100	100	100
.680	100	100	100	100	45		3	3		44	100	100	100	100
.700	100	100	100	100	75					74	100	100	100	100
.720	72	100	100	100	96	16			15	96	100	100	100	73
.740	7	65	100	100	100	52			51	100	100	100	65	7
.760		5	95	100	100	89	30	29	88	100	100	96	5	
.780			60	100	100	100	85	84	100	100	100	61		
.800			25	100	100	100	100	100	100	100	100	27		
.820	6		3	89	100	100	100	100	100	100	90	3		5
.840	54	13	16	56	100	100	100	100	100	100	58	16	13	55
.860	92	81	69	6	46	100	94	94	100	46	6	68	82	92
.880	100	99	86	1	1	79	65	64	80	2		84	99	100
.900	100	99	87	5		22	84	85	23		4	86	99	100
.920	100	100	98	10		44	100	100	45		9	97	100	100
.940	100	100	96	17		44	99	99	45		16	95	100	100
.960	100	100	87	15		19	68	69	20		14	86	100	100
.980	100	99	45	3	5		1	1		5	2	44	98	100
1.000	100	100	53		79	50			49	80		52	100	100

5.4 6 BEN PT.

This is the only structure in this study with the nickel at a general position, Wyckoff position i. The bond lengths and angles (Appendix A) are within those normally observed for these complexes. Following the classification of previous work with the 4-EtPy · host[5.11], this structure is a γphase with the host atoms at general positions and the guest molecules located in cavities of $\bar{1}$ symmetry. This structure also has guests at general positions. With a host to guest ratio 1:3, these cavities are large and interlinked by channels. Observation of the packing diagrams show a channel down the x axis and a channel parallel to the z axis. All the guest molecules are well ordered. The benzene molecule being centrosymmetric matches the symmetry of the cavities at the $\bar{1}$ sites.

As with all previous structures the program PARST was used to detect any intermolecular contacts which are less than the sum of their van der Waals radii. For host hydrogen and guest carbon atoms this is a distance of 3.05 Å or less and for host carbon and guest carbon atoms this is a distance of 3.70 Å or less. No intermolecular contacts of this nature were detected. For any pi-pi (charge transfer) interaction between the aromatic rings of the host and guest the interatomic distances must be less than 3.70 Å. As this was not observed a chemical interaction cannot account for the large host to guest ratio.

For any interaction between two atoms (molecules) to be regarded as chemical their interatomic (molecular) distance must be less than the sum of their respective van der Waals radii.

Figure 5.4.1 Molecular packing in structure 6 (host only).

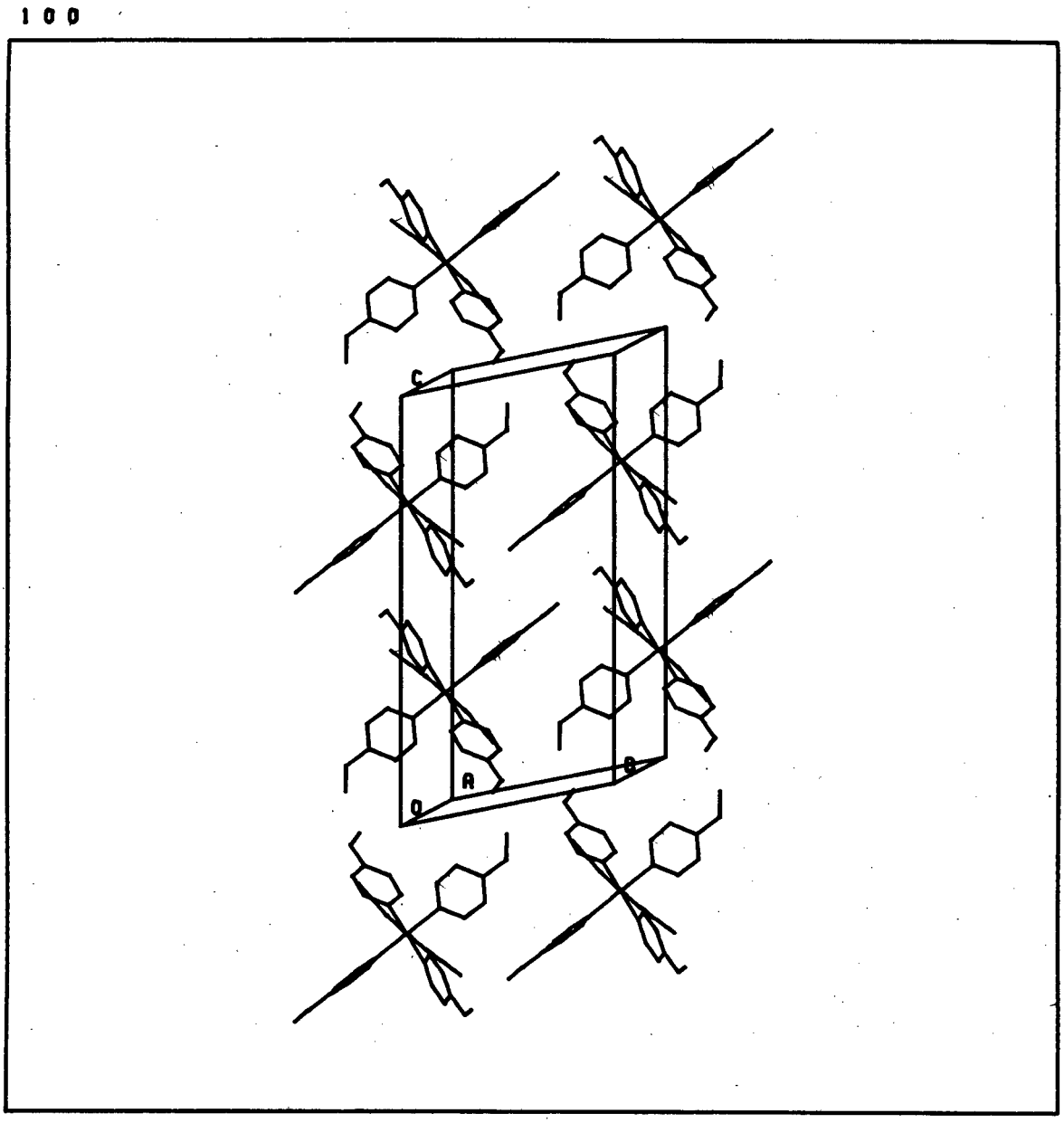

a) View down the x-axis

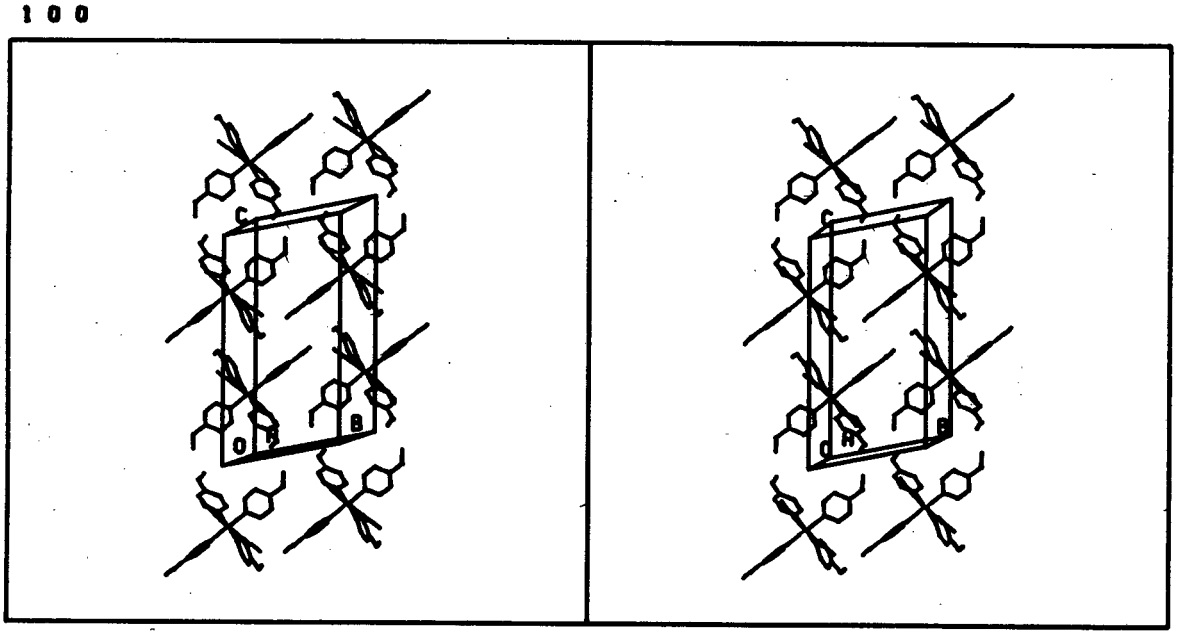

b) Stereo view down the x-axis

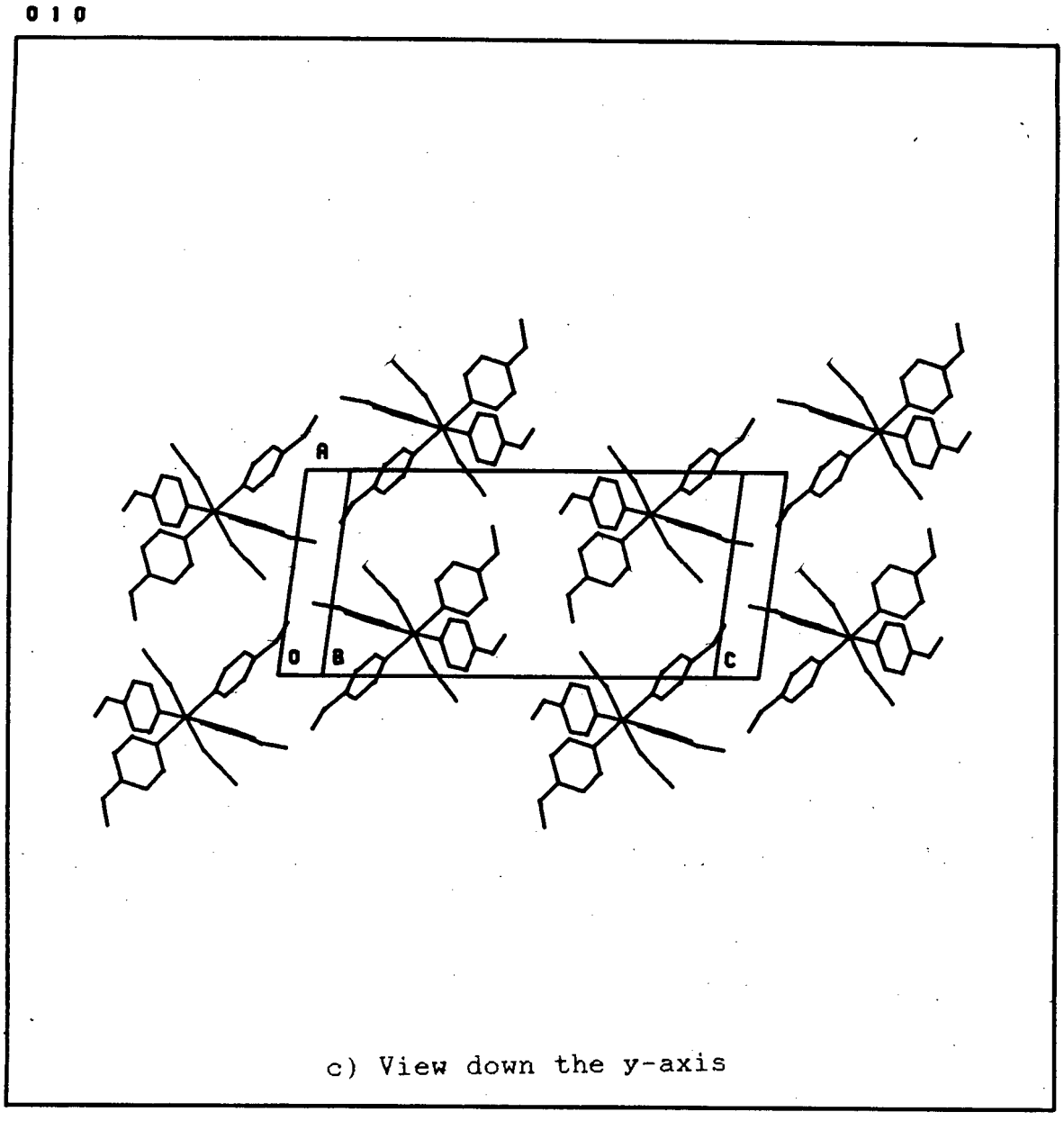

c) View down the y-axis

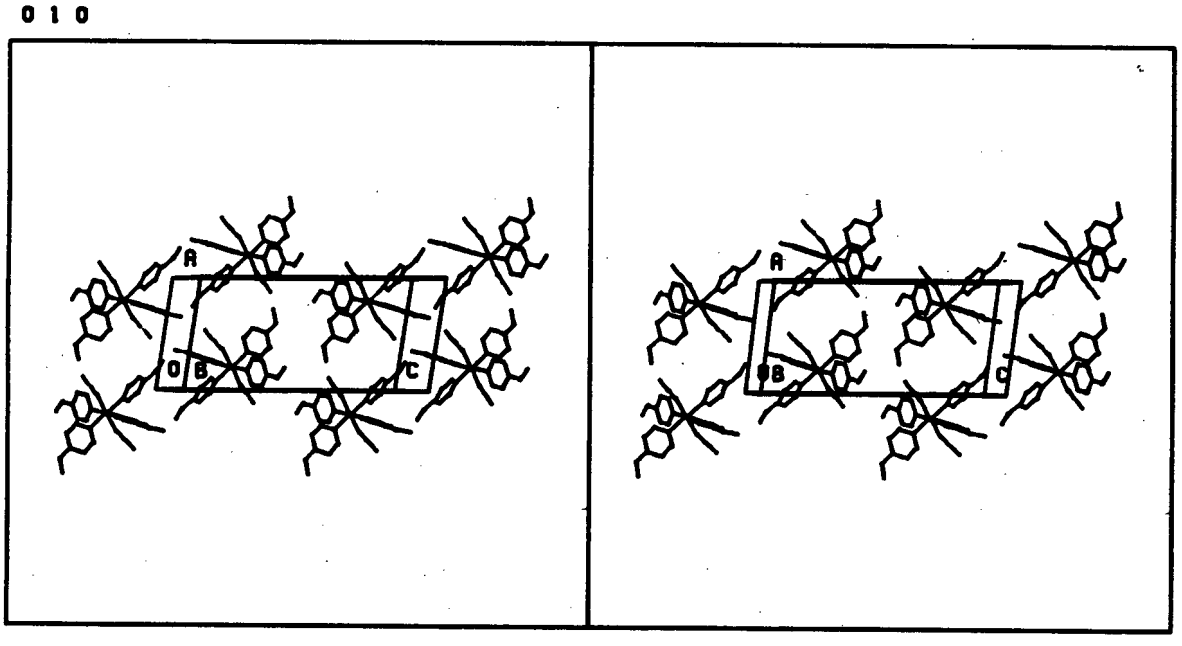

d) Stereo view down the y-axis

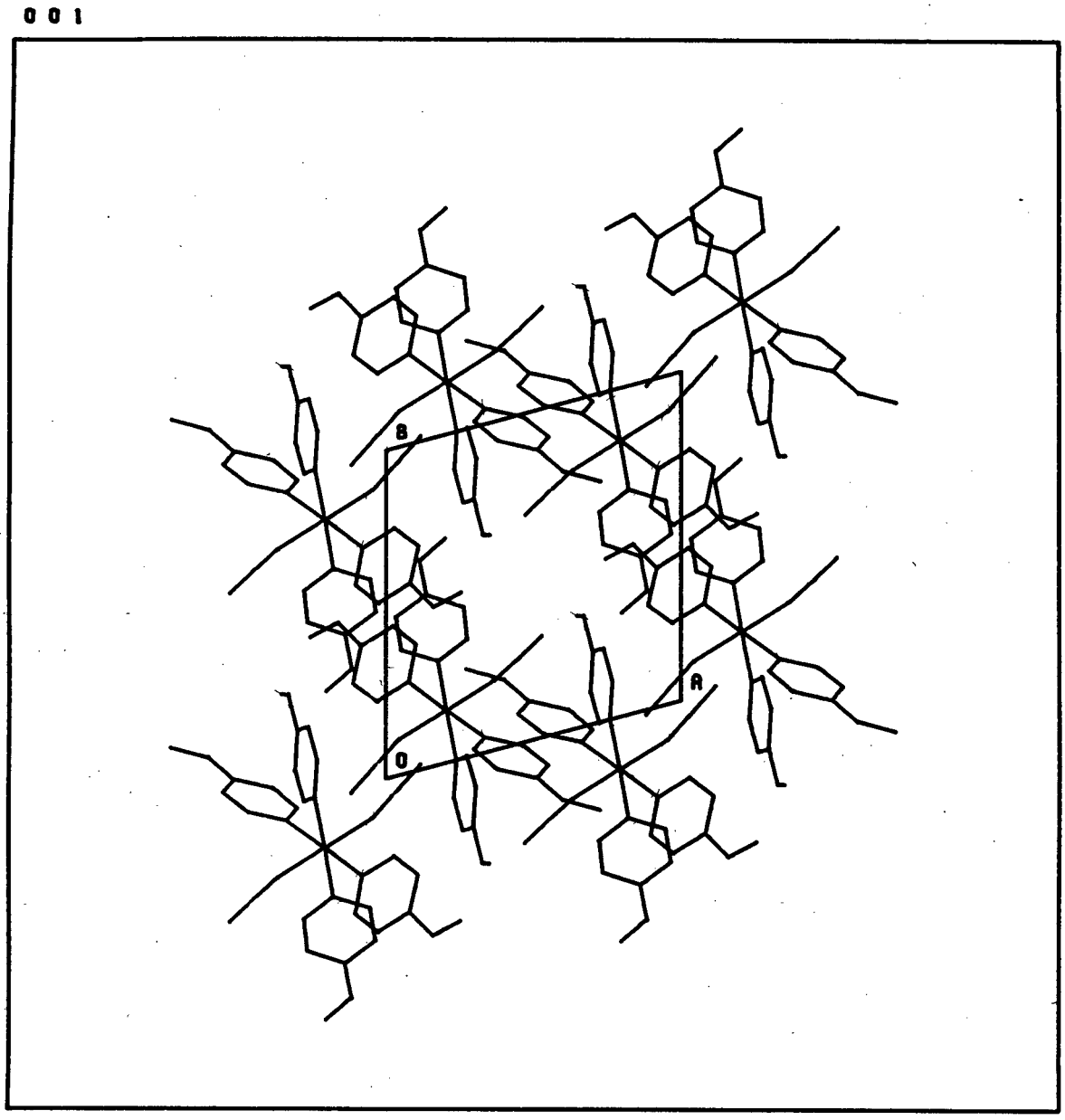

e) View down the z-axis

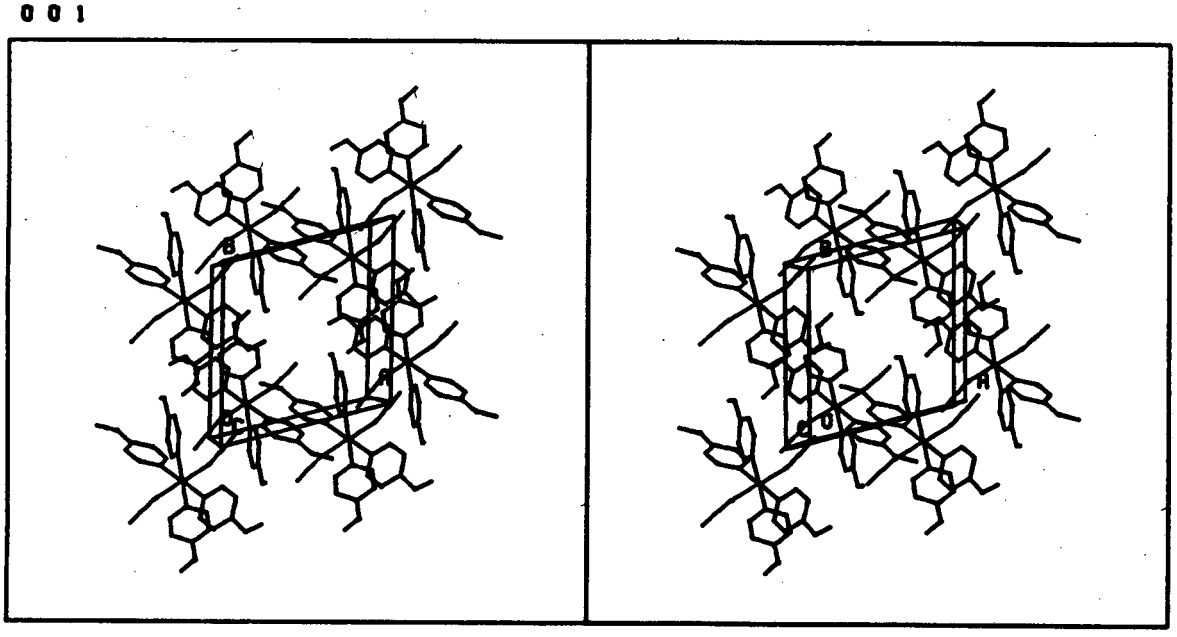

f) Stereo view down the z-axis

Figure 5.4.2 Packing diagram of structure 6, host only.

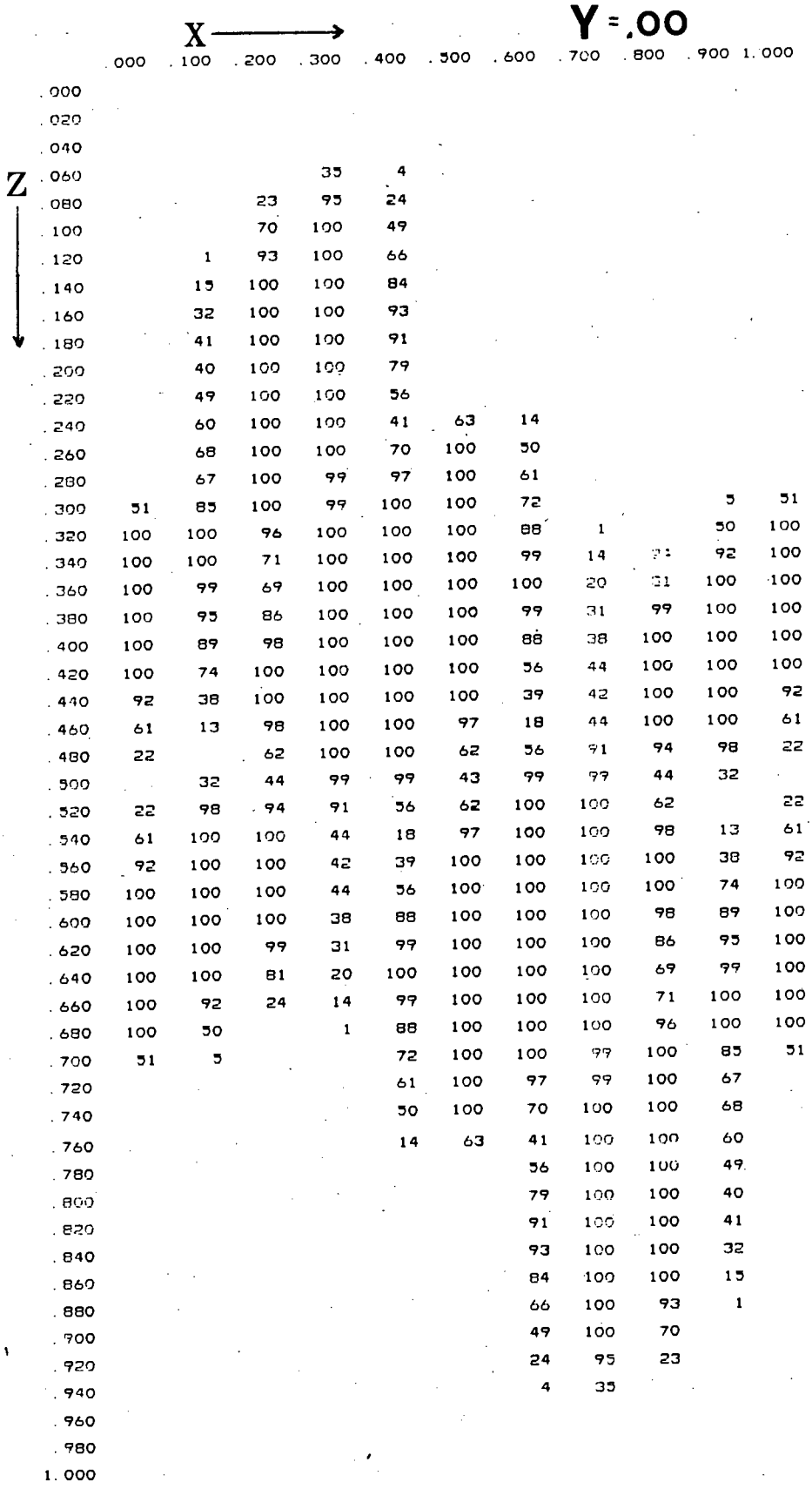

Asymmetric unit $0 \le x \le \frac{1}{2}$; $0 \le y \le 1$; $0 \le z \le 1$

X ⟶ **Y = .25**

Z ↓

Z \ X	.000	.100	.200	.300	.400	.500	.600	.700	.800	.900	1.000
.000											
.020											
.040											
.060						30	46				
.080	10				9	93	99	23		28	10
.100	67				39	100	100	48	50	98	67
.120	95	8		5	85	100	100	70	98	100	95
.140	100	67	18	38	100	100	100	86	100	100	100
.160	100	100	69	63	100	100	100	76	100	100	100
.180	100	100	87	90	100	100	99	35	99	100	100
.200	100	100	99	100	100	100	70		78	100	100
.220	100	100	100	100	100	100	30		51	100	100
.240	100	100	100	100	100	91	5		35	100	100
.260	100	100	100	100	99	37			9	95	100
.280	61	100	100	100	77					27	61
.300	43	100	100	100	95	11					43
.320	72	100	100	100	100	27					72
.340	90	100	100	100	100	23				2	90
.360	85	100	100	100	90	4				4	85
.380	65	100	100	100	53						65
.400	35	80	48	84	14						35
.420	1	6		2	41	32					1
.440				18	95	78					
.460			36	97	100	88					
.480		2	87	100	100	92					
.500		21	100	100	100	98	3	3	63	40	
.520	3	36	100	100	100	96	3	37	100	91	3
.540	75	51	100	100	100	96	8	67	100	100	75
.560	100	72	100	100	100	94	6	82	100	100	100
.580	100	57	99	100	99	75		87	100	100	100
.600	99	23	70	82	69	26		80	100	100	99
.620	73	1	2	6	39	6		58	100	100	73
.640	23				20			13	63	89	23
.660								2	1	5	
.680								65	61		
.700							29	100	99	18	
.720							60	100	100	39	
.740							77	100	100	46	
.760							84	100	100	42	
.780						2	92	100	100	28	
.800						15	100	100	100	12	
.820						23	100	100	99	7	
.840						20	100	100	91		
.860						8	99	100	82		
.880						2	95	100	68		
.900						11	99	100	60		
.920						19	100	100	58		
.940						15	99	100	43		
.960						2	90	98	16		
.980							34	42			
1.000											

Y = .50

Z ↓ / X →	.000	.100	.200	.300	.400	.500	.600	.700	.800	.900	1.000
.000	22	93	100	100	37		37	100	100	93	22
.020	41	22	96	87	5		61	100	100	100	41
.040	60	1	23	15			73	100	100	100	60
.060	100	61					75	100	100	100	100
.080	100	97	7	1	31	1	67	100	100	100	100
.100	100	100	22	9	66	4	44	100	100	100	100
.120	100	100	26	8	54	1	6	75	100	100	100
.140	100	100	34	1	16			8	95	100	100
.160	100	100	61	25	47				72	100	100
.180	100	100	71	59	76				20	84	100
.200	92	98	50	64	70					21	92
.220	41	54	6	34	31						41
.240											
.260											
.280	18	8	12	20							18
.300	91	61	74	96	17					7	91
.320	100	98	99	100	52					33	100
.340	100	100	100	100	87					57	100
.360	100	100	100	100	99					77	100
.380	100	100	100	100	96				4	95	100
.400	100	100	100	100	78				12	100	100
.420	100	100	100	95	30				6	98	100
.440	100	100	98	35	0					66	100
.460	43	93	65							2	43
.480		16	7								
.500											
.520									7	16	
.540	43	2							65	93	43
.560	100	66						35	98	100	100
.580	100	98	6				30	95	100	100	100
.600	100	100	12				78	100	100	100	100
.620	100	95	4			3	96	100	100	100	100
.640	100	77				5	99	100	100	100	100
.660	100	57					87	100	100	100	100
.680	100	33					52	100	99	98	100
.700	91	7					17	96	74	61	91
.720	18							20	12	8	18
.740											
.760											
.780	41						31	34	6	34	41
.800	92	21					70	64	50	98	92
.820	100	84	20				76	59	71	100	100
.840	100	100	72				47	25	61	100	100
.860	100	100	95	8			16	1	34	100	100
.880	100	100	100	75	6	1	54	8	26	100	100
.900	100	100	100	100	44	4	66	9	22	100	100
.920	100	100	100	100	67	1	31	1	7	97	100
.940	100	100	100	100	75					61	100
.960	60	100	100	100	73			15	33	1	60
.980	41	100	100	100	61		5	87	96	22	41
1.000	22	93	100	100	37		37	100	100	93	22

X ⟶ Y = .75

Z ↓

Z \ X	.000	.100	.200	.300	.400	.500	.600	.700	.800	.900	1.000
.000											
.020				42	34						
.040			16	98	90	2					
.060			45	100	99	15					
.080			58	100	100	19					
.100			60	100	99	11					
.120			68	100	95	2					
.140			82	100	99	8					
.160			91	100	100	20					
.180		7	99	100	100	23					
.200		12	100	100	100	15					
.220		28	100	100	92	2					
.240		42	100	100	84						
.260		46	100	100	77						
.280		39	100	100	60						
.300		18	99	100	29						
.320			61	65							
.340		5	1	2							
.360	23	89	63	13			20				23
.380	73	100	100	58		6	59	6	2	1	73
.400	99	100	100	80		26	69	82	70	23	99
.420	100	100	100	87		75	99	100	99	57	100
.440	100	100	100	82	6	94	100	100	100	72	100
.460	75	100	100	67	8	96	100	100	100	51	75
.480	3	91	100	37	3	96	100	100	100	36	3
.500		40	67	3	3	98	100	100	100	21	
.520						92	100	100	87	2	
.540						88	100	97	36		
.560						78	95	18			
.580	1					32	41	2		6	1
.600	35						14	84	48	80	35
.620	65						53	100	100	100	65
.640	85	4				4	90	100	100	100	85
.660	90	2				23	100	100	100	100	90
.680	72					27	100	100	100	100	72
.700	43					11	95	100	100	100	43
.720	61	27					77	100	100	100	61
.740	100	95	9			37	99	100	100	100	100
.760	100	100	35		5	91	100	100	100	100	100
.780	100	100	51		30	100	100	100	100	100	100
.800	100	100	78		70	100	100	100	97	100	100
.820	100	100	99	35	99	100	100	90	87	100	100
.840	100	100	100	76	100	100	100	63	69	100	100
.860	100	100	100	86	100	100	100	38	18	67	100
.880	95	100	98	70	100	100	85	5		8	95
.900	67	98	50	48	100	100	39				67
.920	10	28		23	99	93	9				10
.940					46	30					
.960											
.980											
1.000											

Figure 5.4.3 Packing diagram of structure 6, host and guest.

X ⟶ Y=.00

Z ↓

	.000	.100	.200	.300	.400	.500	.600	.700	.800	.900	1.000
.000	100	70	9	99	100	100	100	99	9	70	100
.020	100	79	5	97	100	100	100	99	12	95	100
.040	100	90		81	100	100	100	96	27	100	100
.060	100	91		62	94	100	100	84	35	100	100
.080	100	81	23	95	60	98	100	60	36	100	100
.100	100	60	70	100	49	66	95	18	25	100	100
.120	98	25	93	100	66	5	44	84	23	91	98
.140	36	15	100	100	84		82	100	64	26	36
.160		32	100	100	93	15	100	100	99	31	
.180		41	100	100	91	29	100	100	100	64	
.200	3	40	100	100	79	33	100	100	100	86	3
.220	16	49	100	100	56	25	100	100	100	99	16
.240	19	60	100	100	41	68	100	100	100	99	19
.260	10	68	100	100	70	100	98	100	100	96	10
.280		67	100	99	97	100	84	100	99	71	
.300	51	85	100	99	100	100	72	56	33	17	51
.320	100	100	96	100	100	100	88	1		50	100
.340	100	100	71	100	100	100	99	14	24	92	100
.360	100	99	69	100	100	100	100	20	31	100	100
.380	100	95	86	100	100	100	99	31	99	100	100
.400	100	89	98	100	100	100	88	38	100	100	100
.420	100	74	100	100	100	100	56	44	100	100	100
.440	92	38	100	100	100	100	39	42	100	100	92
.460	61	13	98	100	100	97	18	44	100	100	61
.480	22		62	100	100	62	56	91	94	98	22
.500		32	44	99	99	43	99	99	44	32	
.520	22	98	94	91	56	62	100	100	62		22
.540	61	100	100	44	18	97	100	100	98	13	61
.560	92	100	100	42	39	100	100	100	100	38	92
.580	100	100	100	44	56	100	100	100	100	74	100
.600	100	100	100	38	88	100	100	100	98	89	100
.620	100	100	99	31	99	100	100	100	86	95	100
.640	100	100	81	20	100	100	100	100	69	99	100
.660	100	92	24	14	99	100	100	100	71	100	100
.680	100	50		1	88	100	100	100	96	100	100
.700	51	17	53	56	72	100	100	99	100	85	51
.720		71	99	100	84	100	97	99	100	67	
.740	10	96	100	100	98	100	70	100	100	68	10
.760	19	99	100	100	100	68	41	100	100	60	19
.780	16	99	100	100	100	25	56	100	100	49	16
.800	3	86	100	100	100	33	79	100	100	40	3
.820		64	100	100	100	29	91	100	100	41	
.840		31	99	100	100	15	93	100	100	32	
.860	36	26	64	100	82		84	100	100	15	36
.880	98	91	23	84	44	5	66	100	93	25	98
.900	100	100	25	18	95	66	49	100	70	60	100
.920	100	100	36	60	100	98	60	95	33	81	100
.940	100	100	35	84	100	100	94	62		91	100
.960	100	100	27	96	100	100	100	81		90	100
.980	100	95	12	99	100	100	100	97	5	79	100
1.000	100	70	9	99	100	100	100	99	9	70	100

X ⟶

Y = .50

Z ↓

Z \ X	.000	.100	.200	.300	.400	.500	.600	.700	.800	.900	1.000
.000	22	93	100	100	37		37	100	100	93	22
.020	41	22	96	87	5		61	100	100	100	41
.040	60	1	23	15			73	100	100	100	60
.060	100	61					75	100	100	100	100
.080	100	97	7	1	31	1	67	100	100	100	100
.100	100	100	22	9	66	4	44	100	100	100	100
.120	100	100	26	8	54		6	75	100	100	100
.140	100	100	34	1	16			8	95	100	100
.160	100	100	61	25	47				72	100	100
.180	100	100	71	59	76				20	84	100
.200	92	98	50	64	70		19	5		21	92
.220	41	54	6	34	31	28	98	63			41
.240						72	100	95	4		
.260					4	96	100	100	17		
.280	18	8	12	20	15	100	100	100	20		18
.300	91	61	74	96	35	100	100	100	17	7	91
.320	100	98	99	100	64	99	100	100	23	33	100
.340	100	100	100	100	87	90	100	100	33	57	100
.360	100	100	100	100	99	88	100	100	49	77	100
.380	100	100	100	100	96	79	100	100	58	95	100
.400	100	100	100	100	78	79	100	100	60	100	100
.420	100	100	100	95	30	73	100	100	39	98	100
.440	100	100	98	35		54	100	94	7	66	100
.460	43	93	65			15	88	44		2	43
.480		16	7				2				
.500											
.520					2				7	16	
.540	43	2		44	88	15			65	93	43
.560	100	66	7	94	100	54		35	98	100	100
.580	100	98	39	100	100	73	30	95	100	100	100
.600	100	100	60	100	100	79	78	100	100	100	100
.620	100	95	58	100	100	79	96	100	100	100	100
.640	100	77	49	100	100	88	99	100	100	100	100
.660	100	57	33	100	100	90	87	100	100	100	100
.680	100	33	23	100	100	99	64	100	99	98	100
.700	91	7	17	100	100	100	35	96	74	61	91
.720	18		20	100	100	100	15	20	12	8	18
.740			17	100	100	96	4				
.760			4	95	100	72					
.780	41			63	98	28	31	34	4	54	41
.800	92	21		5	19		70	64	50	98	92
.820	100	84	20				76	59	71	100	100
.840	100	100	72				47	25	61	100	100
.860	100	100	95	8			16	1	34	100	100
.880	100	100	100	75	6	1	54	8	26	100	100
.900	100	100	100	100	44	4	66	9	22	100	100
.920	100	100	100	100	67	1	31	1	7	97	100
.940	100	100	100	100	75					61	100
.960	60	100	100	100	73			15	23	1	60
.980	41	100	100	100	61		5	87	95	22	41
1.000	22	93	100	100	37		37	100	100	93	22

5.5 7 PY C2/c.

The nickel atom is at 0.25, 0.25, 0.00 which is a centre of symmetry, Wyckoff special position a. The remaining host atoms are at general positions with two pyridine ligands and one isothiocyanate ligand defining the asymmetric unit. This centrosymmetric conformation is of slightly higher energy than the propeller conformation owing to one pair of pyridine ligands being almost coplanar with the isothiocyanate ligands. This can be seen in the packing diagrams. This increased steric interaction accounts for the slightly longer bond lengths (average of all Ni-N bonds) as determined by Guarino et al on the basis of spectroscopic studies[5.12].

	$[Ni(NCS)_2(4\text{-ViPy})_4]$	$[Ni(NCS)_2(Py)_4]$
Ni-N_{cs}	2.08[a]	2.055(2)
Ni-N_{py}	2.13[a]	2.163[a]
	ave: 2.105 A	ave: 2.109 A

[a] Average values.

With significant interatomic contacts less than the sum of the atoms' respective van der Waals radii the host molecules are tightly packed and held together by van der Waals forces. This efficient packing is confirmed by the high density 1.41 $g.cm^{-3}$.

Another significant conformational difference between this α-phase and the 4-ViPy α-phase[5.3] is the isothiocyanate ligands (with respect to the sulphur) trans to each other. This is illustrated by the packing diagrams in figure 5.5.1.

With no vinyl pyridine groups this host is able to pack more efficiently and may result in a poorer ability to enclathrate guests.

We note that this structure had been previously determined by F. Valach, P. Sivy and B. Koren[5.13].
However, we decided that the cell parameters of 7 PY were significantly different from the previously published work.
The crystal data are compared below.

		7 PY	Previously determined[a]
C2/c	a (Å)	12.410(6)	12.434(4)
	b (Å)	12.922(2)	12.944(5)
	c (Å)	15.102(5)	16.461(6)
	β (°)	107.30(4)	118.78(2)
	V (Å^3)	2312.23	2322.1
	Dm (g. cm^{-3})	1.41	1.39
	Dc (g. cm^{-3})	1.41	1.41
	R (%)	2.8	6.3

[a] The nickel is positioned at Wyckoff special position a.

Figure 5.5.1 Molecular packing in structure 7.

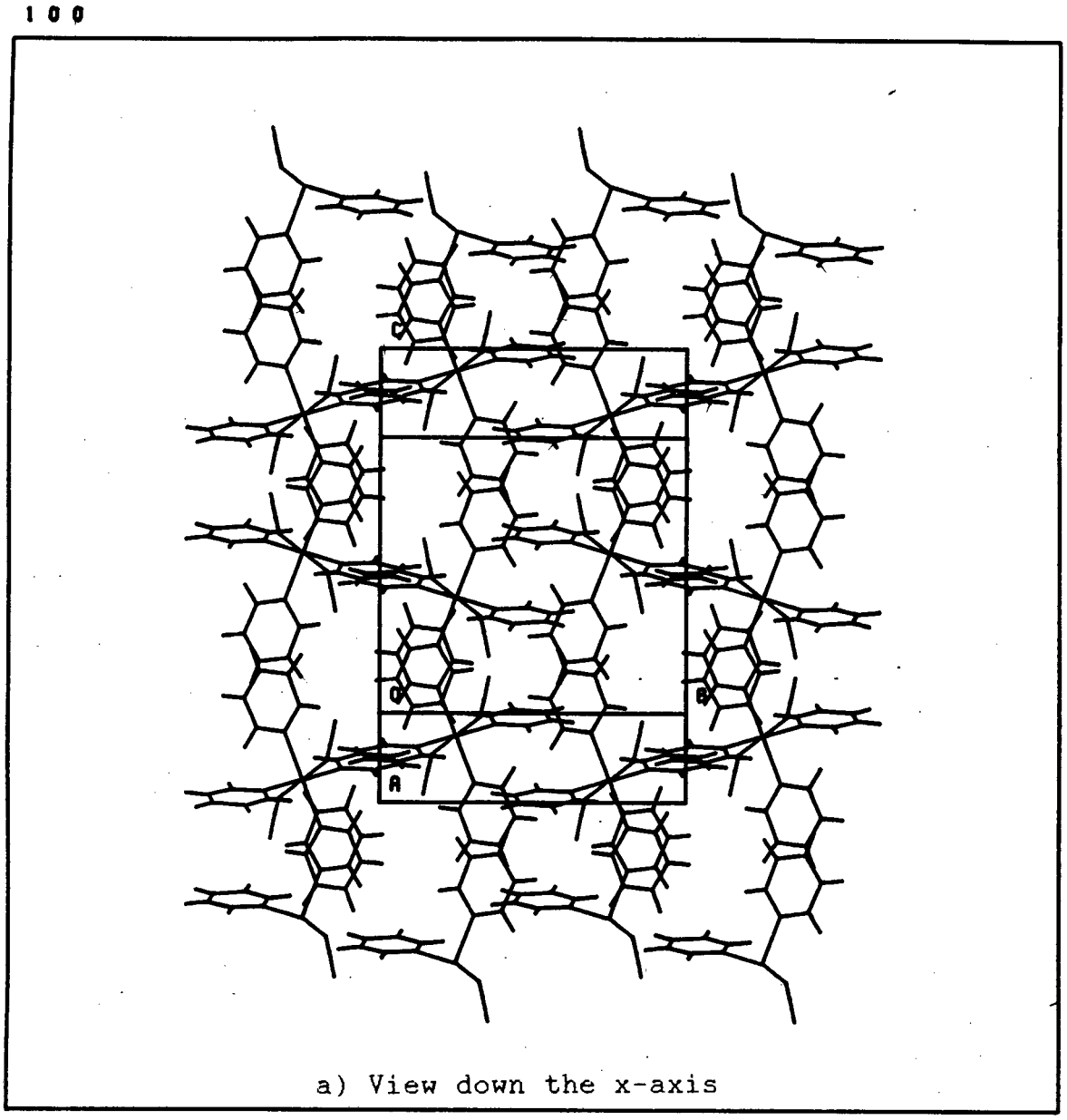

a) View down the x-axis

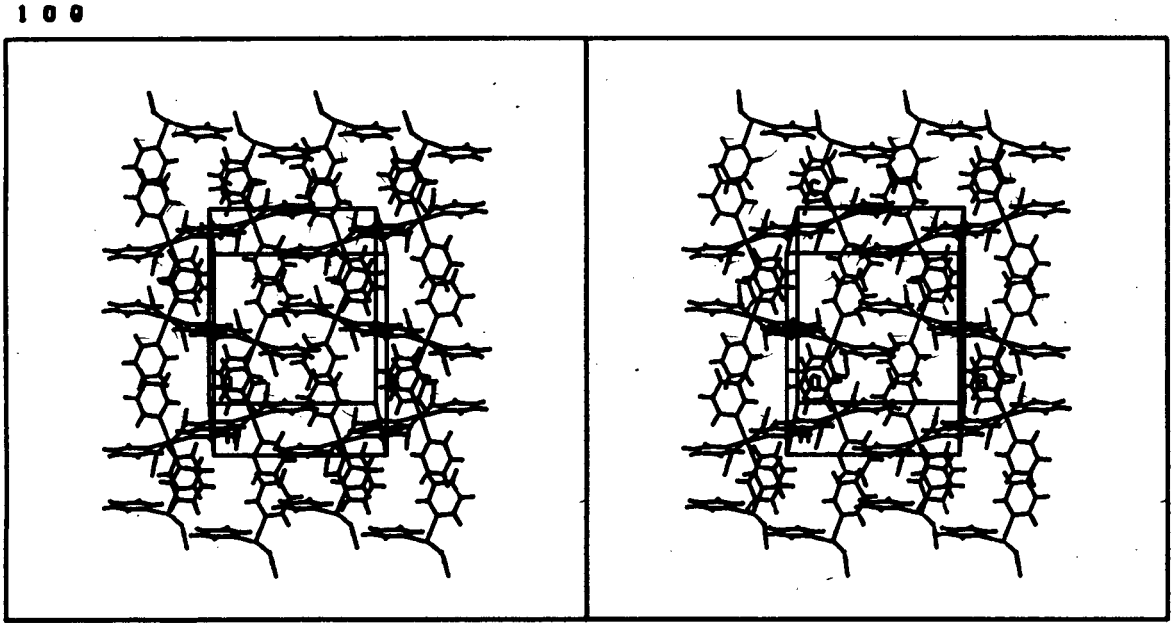

b) Stereo view down the x-axis

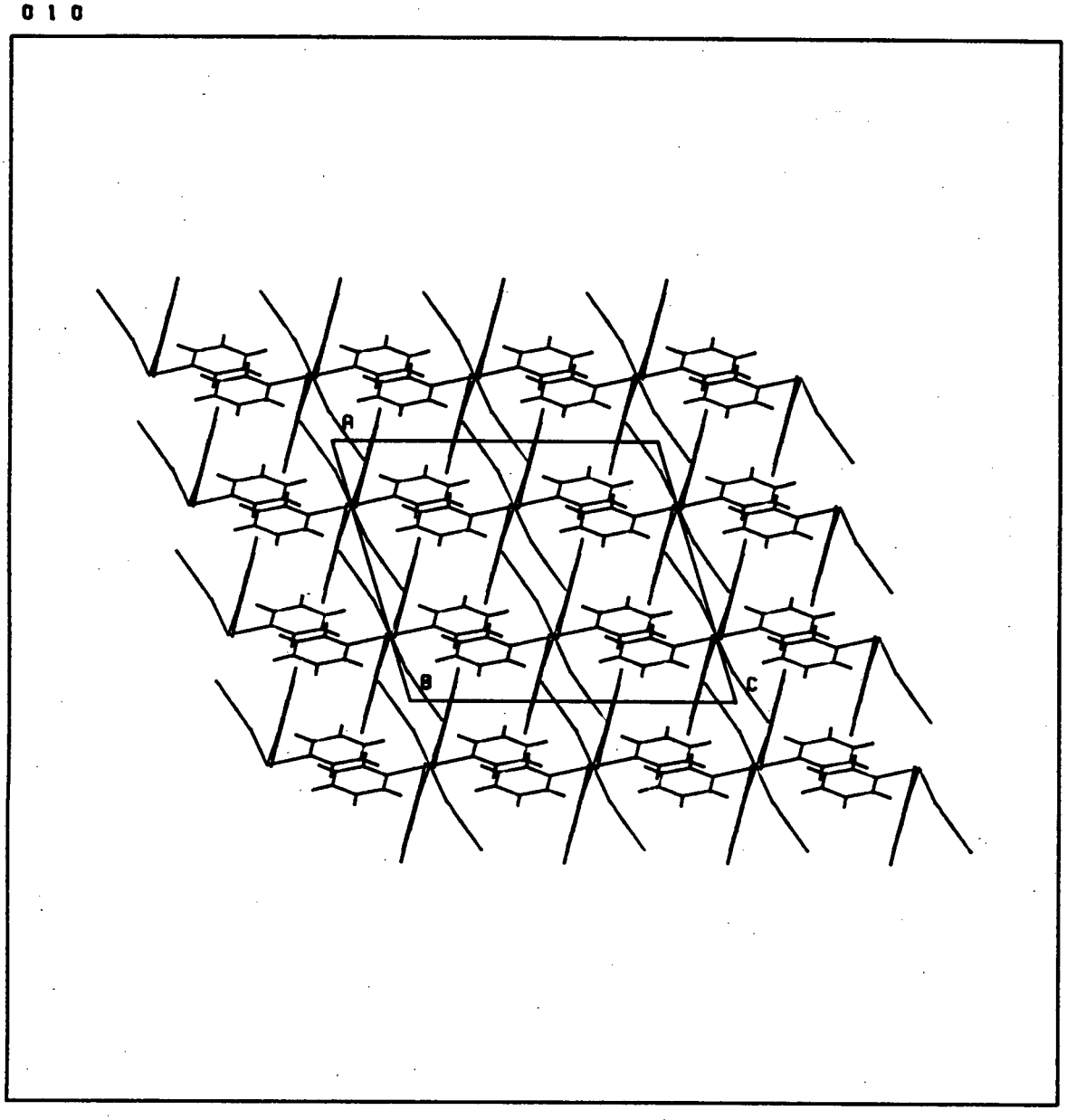

c) View down y-axis

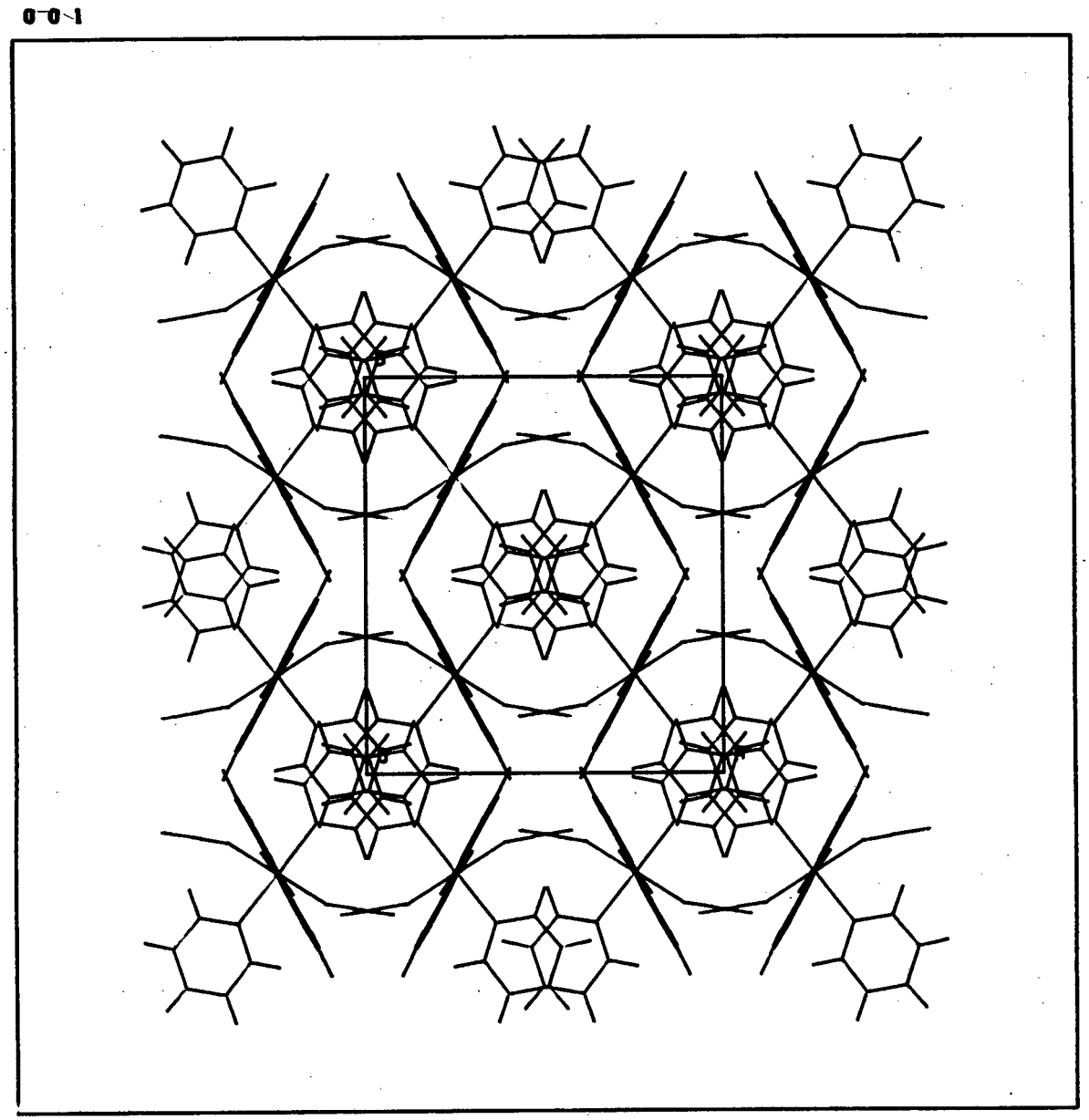

d) View down the z-axis

A rational basis for observation of any secondary bonding interactions between host and guest accounts for the inclusion of guest:- a more stable system is obtained. For observation of secondary bonding the interatomic distance must be less than the sum of their van der Waals radii which should result in the guest being localised in the crystal structure. For structures 1 to 5 neither of these observations is found. The structural analysis shows the host-guest interaction to be minimal and is therefore indicative of a poor selection criterion. As volume considerations of the guests obviously play a role in the selection process, further work with the possible enclathration of guests with: a) an aromatic system b) no highly electronegative atoms c) increasing volume in a symmetrical manner, may yield further information. The guest hexamethylbenzene fulfils these requirements. This proposal is for the time being neglecting any role that solubility may play in the selection process.

5.6 Packing densities and volume comparisons.

Packing densities are expressed as volume of the unit cell/number of non hydrogen atoms in the cell, i.e. as the 'volume per non-hydrogen atom'. This approximate model regards all the non-hydrogen atoms as occuping equal volumes. With these limitations packing densities may be used on a comparative basis for similar type structures. The packing densities of structures 1 to 7, I and the α-phase of $[Ni(NCS)_2(4\text{-}ViPy)_4]$[5.3] are listed in table 5.6.1. With an approximate model care is needed when interpreting the packing densities of these structures, as a high packing volume may indicate disorder of the vinyl group of the host (as in structures 1 and 2) and/or disorder of the guest (as in structures 1 to 5) and/or the presence of completely unoccupied voids (as in structures 1 and 2).

Structures 1, 2 and I have the highest packing volume of 20.8 $Å^3$. Structure 6 with ordered host and guest atoms but a high host to guest ratio of 1:3 has the second highest packing volume of 20.7 $Å^3$ and is indicative of poor packing between the host and guest molecules. Structure 3 has the third highest packing volume of 21.2 $Å^3$ with the $\bar{4}$ sites unoccupied. Structures 4 and 5 with the $\bar{1}$ and $\bar{4}$ sites occupied by guest have a lower packing volume of 19.9 $Å^3$ which is equal to that of the α-phase. The significantly lower packing volume of 18.7 $Å^3$ for structure 7 confirms the tight packing as observed by overlapping van der Waals' radii and the high measured density of 1.41 g. cm^{-3}.

Another way of comparing the packing efficiency of these structures is the comparison of the volume available to the guests and the efficiency with which the guest fills this volume. This is dependent on knowing the volume occupied by a typical host complex. This was obtained by dividing the cell volume of the α-phase by its number of host molecules[5.3]. To calculate the total volume available to guest molecules, the added volume of all the host complexes was subtracted from the experimentally obtained unit cell volume. This total available volume divided by the number of guest molecules per unit cell gives the volume available per guest molecule. These values expressed as vol/guest molecule ($Å^3$) are listed in table 5.6.1 with structure 1 as an example below.

$$\text{vol/guest molecule} = \frac{V_{\text{unit cell}} - (774.4 \times 4)}{8}$$

$$= 123.7\ Å^3.$$

The theoretical volume for each guest type was calculated using the volumes of appropriate fragments as determined by Kitaigorodsky[5.14]. Taking the molecular ratios of the guests into account for structures 1 to 5 the theoretical volumes `per guest´ were calculated. These values are listed in table 5.6.1 with structure 1 as an example below.

volume of THF = 78.4 Å^3

volume of cyclohexane = 102.6 Å^3

volume `per guest´ = (78.4 x 0.89) + (102.6 x 0.11)

= 81.1 Å^3.

The most efficient packing of the guests in the `available volumes´ is unity. Again structure 1 serves as an example:

$$\text{packing efficiency per void per guest} = \frac{\text{volume `per guest´}}{\text{`available volume´}} = \frac{81.1}{123.7} = 0.66$$

or as percentage packing efficiency per void per guest = 66%; these values are listed in table 5.6.1. Again care is needed when interpreting these various packing values, as the total volume not occupied by host does not necessary imply that it is available for guest occupation. It is interesting to note that the volume of each guest ratio pair (or volume `per guest´) is fairly constant for structures 1 to 5.

TABLE 5.6.1 PACKING DENSITIES AND VOLUME COMPARISONS

STRUCTURE	PACKING DENSITY(vol/non H atom)Å^3	VOL/GUEST MOLECULE Å^3
α phase	19.9	-
1 HANE	20.8	123.7
2 HENE	20.8	124.9
3 DIEN3	21.2	170.1
4 DIEN4	19.9	116.0
5 THF/BEN	19.9	114.8
6 BEN	20.7	135.3
7 PY	18.7	-
I T	20.8	121.4

STRUCTURE	VOL `PER GUEST'[a]Å^3	% PACKING EFFICIENCY PER VOID PER GUEST	TOTAL VOL OF GUEST PER HOST Å^3
1 HANE	81.1	66	162.2
2 HENE	80.7	65	161.4
3 DIEN3	86.0	51	86.0
4 DIEN4	89.2	77	124.9
5 THF/BEN	85.8	75	120.1
6 BEN	88.2[b]	65	264.6
I T	78.4[b]	65	156.8

[a]Obtained from theoretical volumes of guest molecules, see section 7.1 - properties of guests.

[b]Only one guest type and is therefore the theoretical volume.

With structure 7 PY being an α-phase the volume occupied per host complex may be calculated.

$$\frac{\text{Volume of unit cell}}{4} = 578.1 \text{ Å}^3$$

The volume of a vinyl group (Kitaigorodsky) is 31.8 Å^3.

Difference in volume between the 4-ViPy and the Py hosts:

$$4 \times 31.8 \text{ Å}^3 = 127.2 \text{ Å}^3$$

Volume occupied per Py host taking the additional volume of the vinyl groups into account:

$$578.1 + 127.2 = 705.3 \text{ Å}^3 = \text{Py*}$$

Although the volume used for the vinyl group is a minimum value, the difference in the volumes occupied by the host complexes is substantial.

volume 4-ViPy host = 774.4 Å^3

volume Py* host = 705.3 Å^3 (-)

69.1 Å^3

This again confirms the tight packing for structure 7 PY with extensive overlapping of the van der Waals radii.

5 REFERENCES

5.1 Inclusion Compounds, edited by J. L. Atwood, J. E. D. Davies, D. D. MacNicol; Academic Press, New York, vol. 1, chapter 3 (1984).

5.2 D. R. Bond, G. E. Jackson and L. R. Nassimbeni: S. Afr. J. Chem. 36, 19 (1983).

5.3 M. H. Moore, L. R. Nassimbeni, M. L. Niven and M. W. Taylor: Inorg. Chem. Acta. 115, 211 (1986).

5.4 M. H. Moore, L. R. Nassimbeni, and M. L. Niven: Inorg. Chem. Acta. 131, 45 (1987).

5.5 J. Lipkowski: J. Mol. Struc. 75, 13 (1981).

5.6 L. Lavelle: B.Sc. (Honours) Project, 1986, unpublished results.

5.7 L. R. Nassibeni, S. Papanicolaou and M. H. Moore: J. Incl. Phenom. 4, 31 (1986).

5.8 M. H. Moore: unpublished results.

5.9 G. H. Stout and L. H. Jensen: X-ray Structure Determination A Practical Guide, The Macmillan Company, London, (1968).

5.10 J. Lipkowski, K. Suwinska, G. D. Andreetti and K. Stadnicka: J. Mol. Struct. 75, 101 (1981).

5.11 M. H. Moore, L. R. Nassimbeni and M. L. Niven: J. Chem. Soc. Dalton Trans. 2125 (1987).

5.12 A. Guarino, G. Occhiucci, E. Possagno and R. Bassanelli: Spectrochimica Acta: 33A, 199 (1977).

5.13 F. Valach, P Sivy and B. Koren: Acta Cryst. C40, 957 (1984).

5.14 A. I. Kitaigorodsky: Molecular Crystals and Molecules, Academic Press, New York (1973).

CHAPTER 6

Thermogravimetric Analysis

6.1 Introduction.

Thermal analysis is the determination of a relationship between a physical property and temperature of a substance. In this study mass and thermal properties are measured. The change in mass of a sample is measured in two ways:

a) At a constant temperature, isothermal analysis and is therefore a function of time.

b) With a varying temperature, thermogravimetric analysis (TGA) with simultaneous differential thermal analysis (DTA).

With thermogravimetric analysis the weight of a substance is recorded as a function of temperature.

With differential thermal analysis the difference in temperature between a sample and a reference material is recorded while both are subjected to the same heating programme.

6.2 Previous work.

Previous work has shown thermal analysis as an informative tool in the study of Werner Clathrates. Quantitative thermal analyses on $[MX_2L_4]$ complexes have been reported since the mid 1960's[6.1, 6.2]. As the guest molecules are not chemically bound to the macrostructure (host molecules) they are easily removed and usually give a

characteristic weight loss peak at relatively low temperatures. Following this weight loss at higher temperatures is the subsequent decomposition of the host complexes. Previous work has shown the decomposition to proceed in four, three or two steps with each step giving the appropriate weight loss of the four bases[6.3, 6.4]. Clathrates which dissociate into host and guest before thermal decomposition of the host begins have been classified by Casellato and Casu[6.5] as thermally `unstable´ as opposed to the decomposition of `stable´ clathrates where chemical destruction of the host accompanies escape of the guest component. This terminology should not be confused with the usage of unstable and stable in an absolute sense. As discussed in chapter five there is usually very little binding interaction between the host and guest (this is dependent on the guest included as some halogenated guests have been shown to display secondary bonding[6.6]). This is characterised by structures with a high host to guest ratio being less stable, as shown by the layer-type structures which are less stable than the zeolite-like β-phases[6.5].

6.3 Visual observation and isothermal studies.

Visual observation of the crystals was briefly discussed in section 3.5.1 and is discussed in greater detail in conjunction with the isothermal studies. With the morphologies of crystals 1 and 2 (Pbcn) being the same, photographs of crystal 1 are shown for illustrative purposes. Similarly for crystals 3, 4 and 5 ($I4_1/a$) with photographs of crystal 5 being used for illustrative purposes. This does not imply that compounds which crystallise in the same space group show

the same morphology. Crystal morphology can be greatly altered by varying the conditions under which crystal growth occurs, with crystallisation in the same space group.

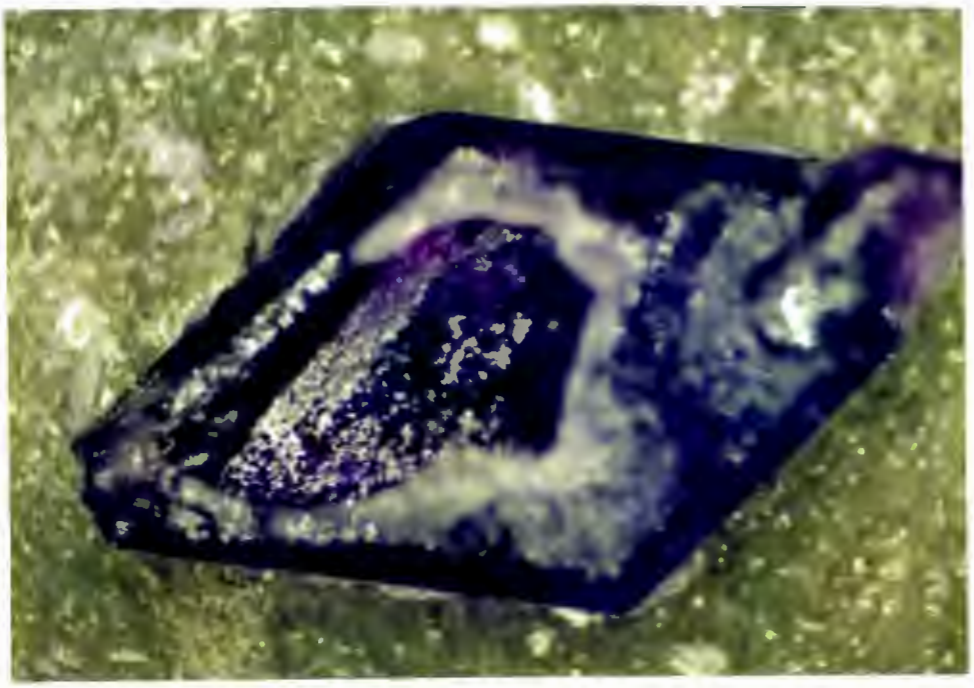

A) Crystal 1 HANE, before isothermal run.

B) Crystal 1 HANE, after isothermal run.

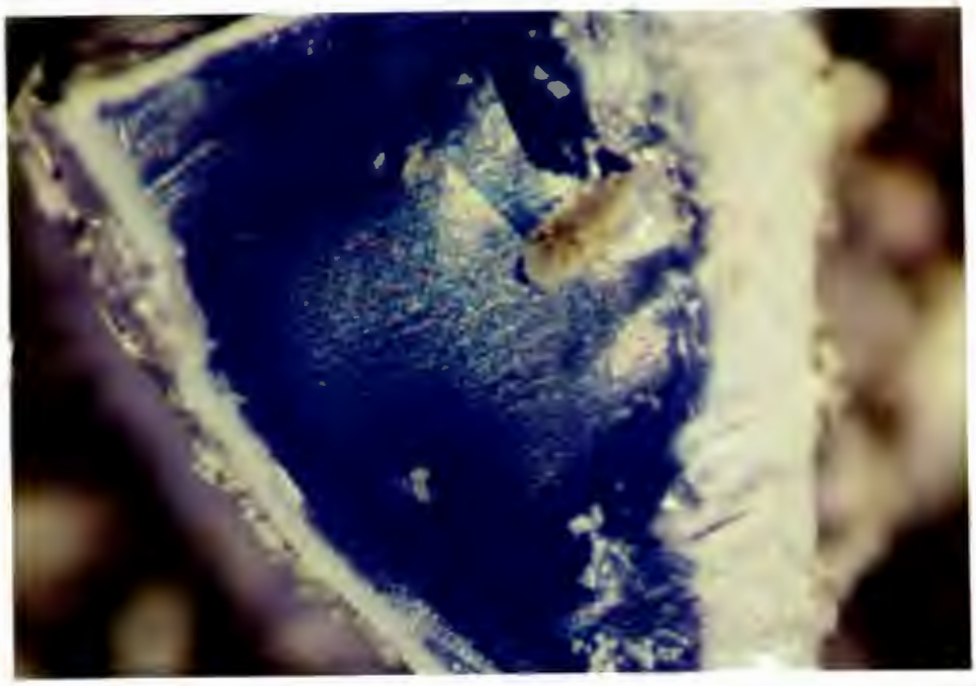

c) Crystal 6 BEN; cross section cut after being removed from mother liquor for 8 minutes

D) Crystal 6 BEN; after isothermal run.

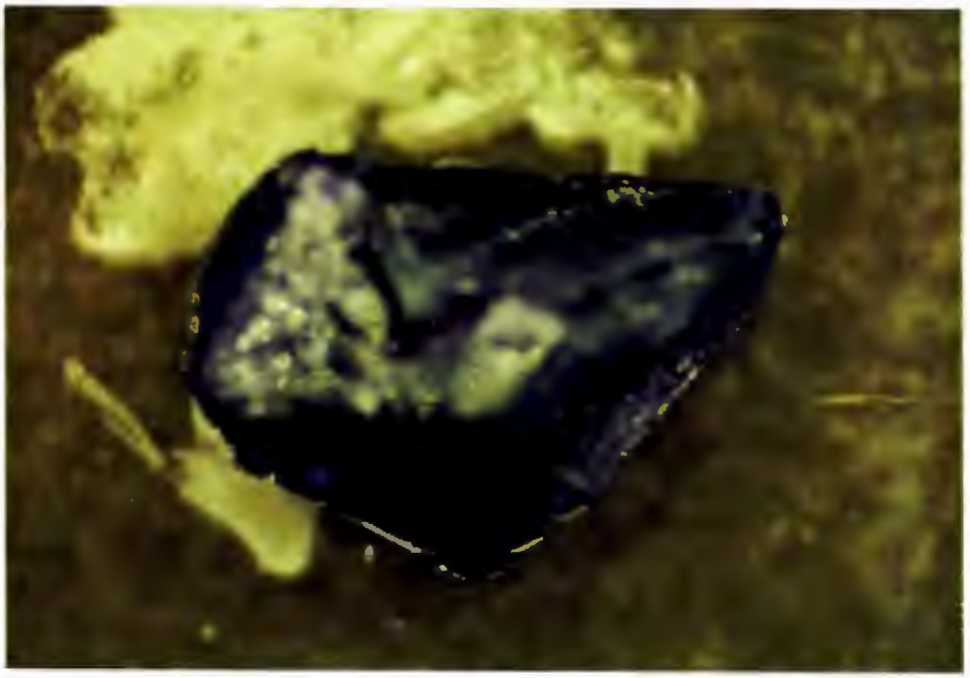

E) Crystal 4 DIEN4

F) Crystals of 7 PY (laths with rectangular cross section).

All isothermal runs were carried out at 25 °C with the flow rate of the inert carrier gas, N_2 at 60ml/min. The runs were performed with the furnace temperature at equilibrium (25 °C) at time zero. The crystals were sufficiently large to enable each sample to have comparable dimensions. That is, each sample (crystal) was cut, with a single crystal of approximatly 10mg being used for analysis. This is necessary in comparing rates of guest loss which may be diffusion controlled. The curves obtained are percentage weight loss versus time in minutes or hours. The isothermal runs for the clathrates clearly show the loss of guest to be independent of host decomposition at 25 °C.

The curves for structures 1 to 5 indicate no preferential loss of one guest over the other in the guest mixture. This may be expected as structural analysis show the guest sites as being indistinguishable within each structure. It is imprecise to relate the different rates of guest loss to the properties of the guests alone, as the type of guest sites (channel or cavity) and the host to guest ratio must also be taken into account. The rate of guest loss is unlikely to be strongly dependent on the breaking of host-guest bindings or host-host bindings as structural analysis show little indication of such bindings being present for these structures.

The curves for structures 1 and 2 have identical rate loss of the guests. The curves level off after 180 minutes with no weight loss attributable to host decomposition. Percentage weight loss is 19.5 and 18.8% for structures 1 and 2 respectively, with a calculated weight loss of 19.8% (total guest weight %) for both.

The curve for structure 3 levels off after 95 minutes at 15.4% (11.4% calc). The TG and DTA of this structure have an unusual host

decomposition which are different from the systematic host decomposition obtained for the other structures.

The curves for structures 4 and 5 have identical rate loss of the guests. After 18 hours the curves have not levelled off at 11.0% (15.5% calc and 15.3% calc respectively) indicating further guest desorption at a very slow rate.

With the guests being located in similar type channels for structures 1 to 5 the different rates of desorption may be attributed to the very high vapour pressure of THF (162 mmHg at 25 C). Structures 1 and 2 have 89 and 88 THF guest percent respectively, structure 3 with a different packing (to structures 1 and 2) contains 48%, and structures 4 and 5 with the same packing as structure 3 contain 26% and 25% respectively.

The curve for structure 6 levels off after 160 minutes at 26.2% (28.2% calc). With the benzene molecules localised in large interlinking cavities and a host to guest ratio of 1:3, it is difficult to campare with the previous structures.

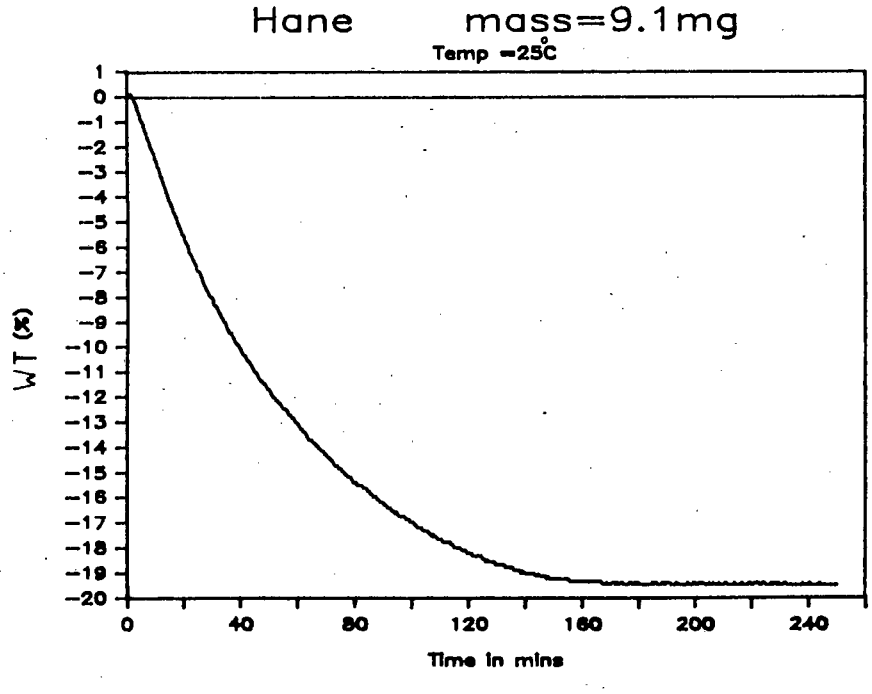

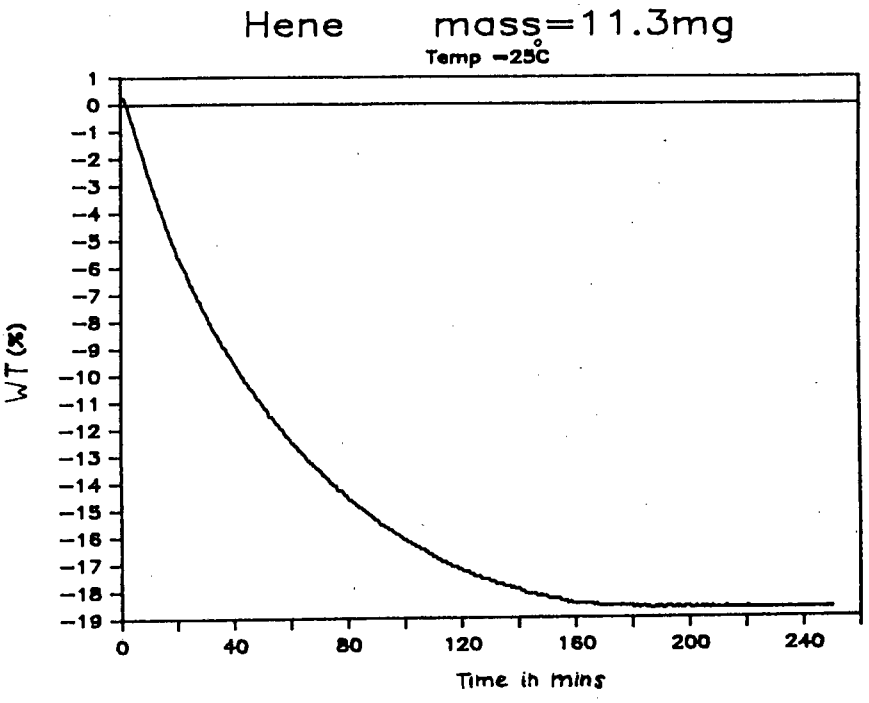
Hene mass=11.3mg
Temp =25C
WT (%)
1
0
-1
-2
-3
-4
-5
-6
-7
-8
-9
-10
-11
-12
-13
-14
-15
-16
-17
-18
-19
0
40
80
120
160
200
240
Time in mins

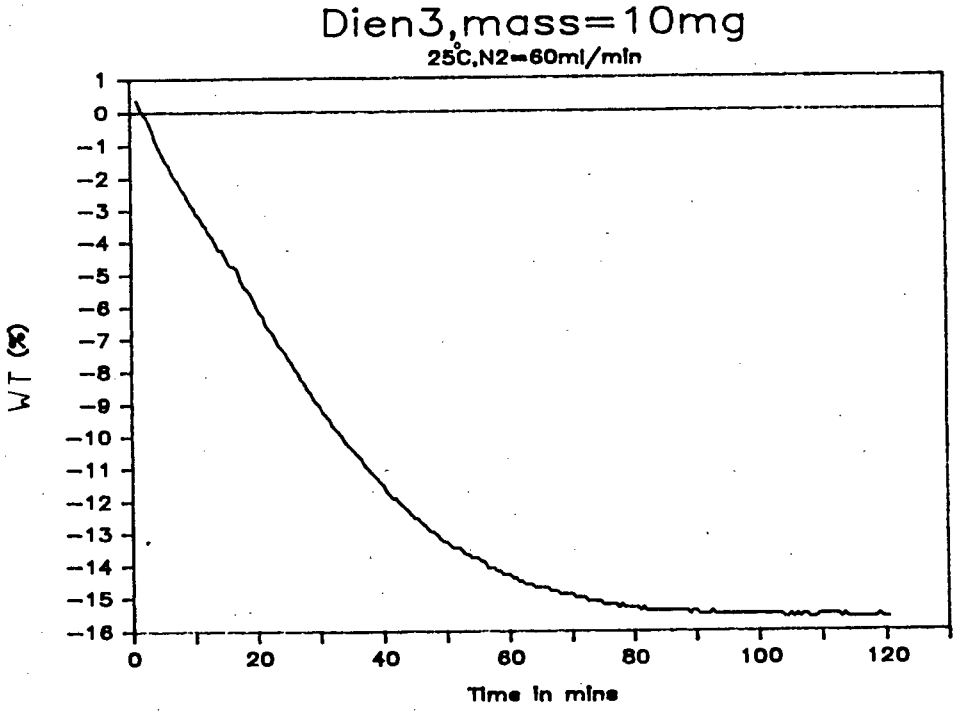
Dien3,mass=10mg
25C,N2=60ml/min
WT (%)
1
0
-1
-2
-3
-4
-5
-6
-7
-8
-9
-10
-11
-12
-13
-14
-15
-16
0
20
40
60
80
100
120
Time in mins

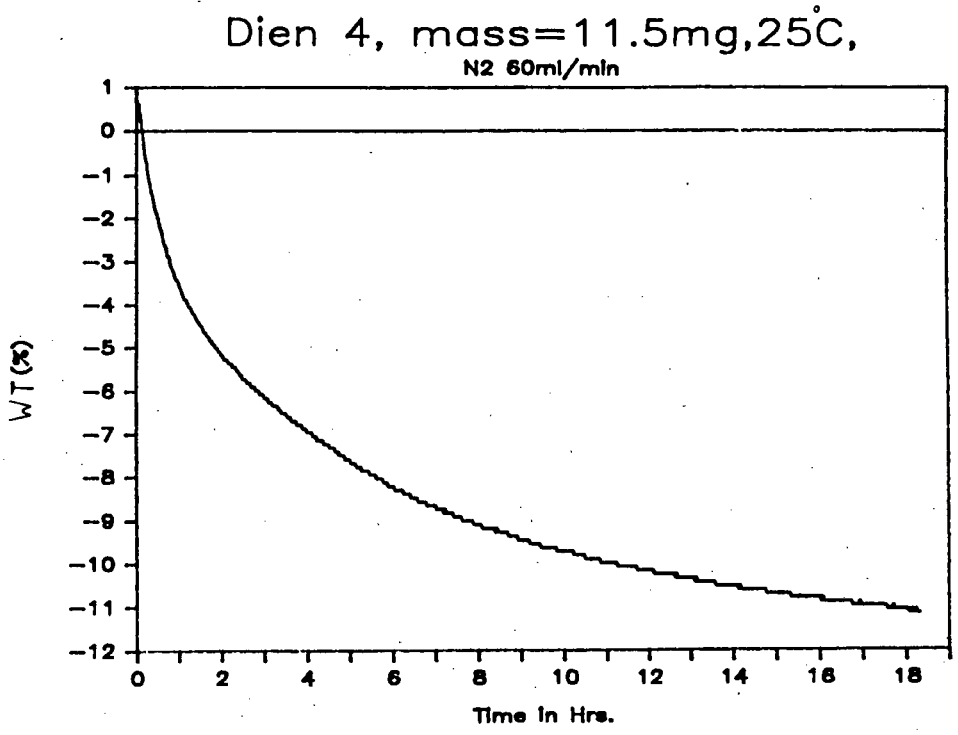
Dien 4, mass=11.5mg,25°C,
N2 60ml/min
WT(%)
1
0
-1
-2
-3
-4
-5
-6
-7
-8
-9
-10
-11
-12
0
2
4
6
8
10
12
14
16
18
Time in Hrs.

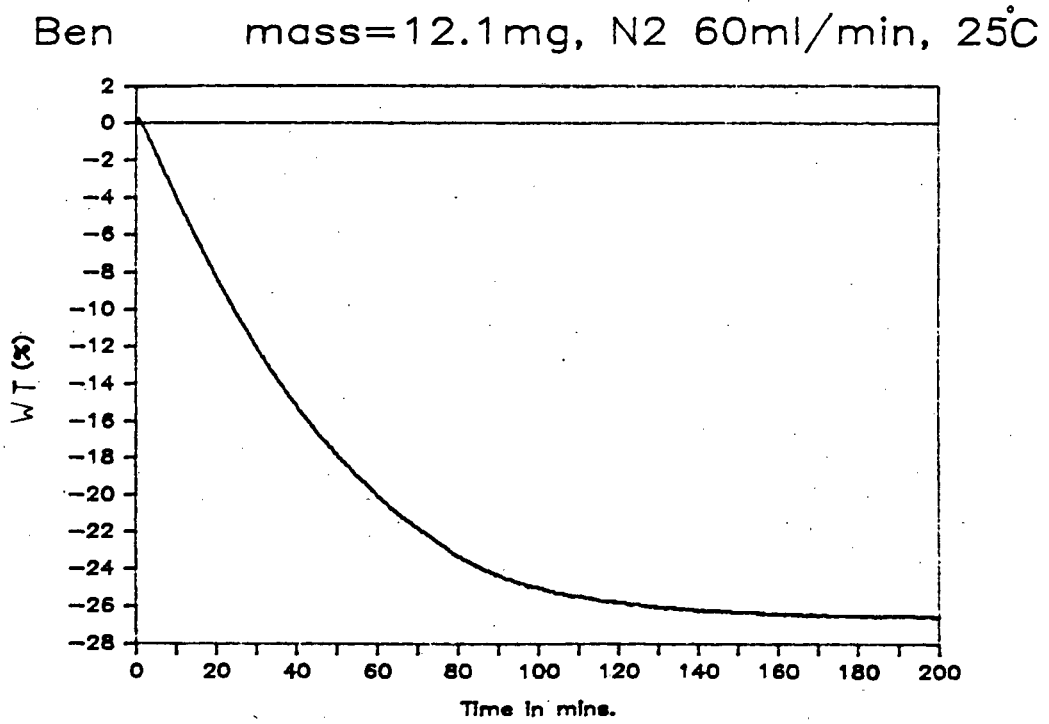
Ben mass=12.1mg, N2 60ml/min, 25°C
WT(%)
2
0
-2
-4
-6
-8
-10
-12
-14
-16
-18
-20
-22
-24
-26
-28
0
20
40
60
80
100
120
140
160
180
200
Time in mins.

6.4 Thermogravimetric and differential analysis.

6.4.1 Interpretation of curves.

During an endothermic event the temperature of the sample, T_s, lags behind the temperature of the reference, T_r (or the furnace temperature, $T_f=T_r$), which follows the heating programme.
With $\triangle T$ (T_s-T_r) recorded against T_r the resulting endothermic curve is obtained.

Each endotherm is characterised by its onset temperature, T_{onset}, which are marked by arrows on the abcissae of each curve in figures 6.4.1. As discussed in section 3.7 these T_{onset} values as obtained from figures 6.4.3 are corrected by I to obtain the sample temperatures quoted in table 6.4.1.

sample temperature = 1.05(furnace temperature) - 51.45 °C I

where furnace temperature is T_{onset}.

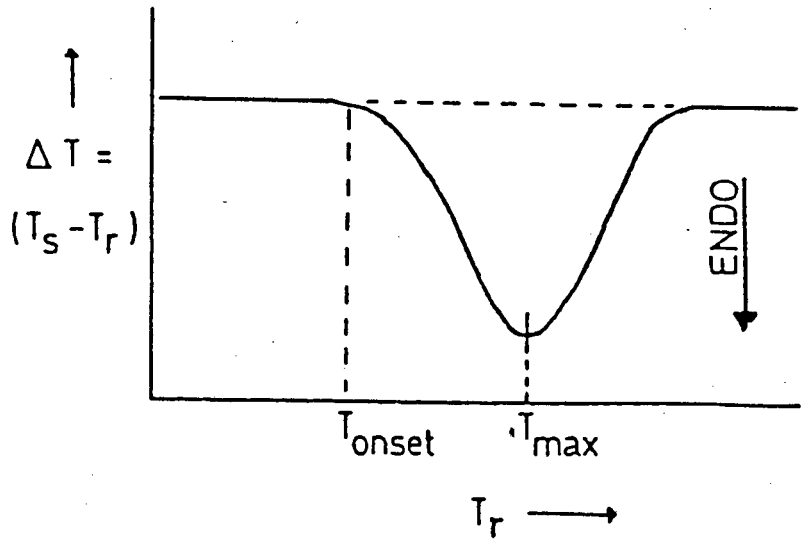

Figure 6.4.1 Differential thermal analysis curve showing an endothermic event.

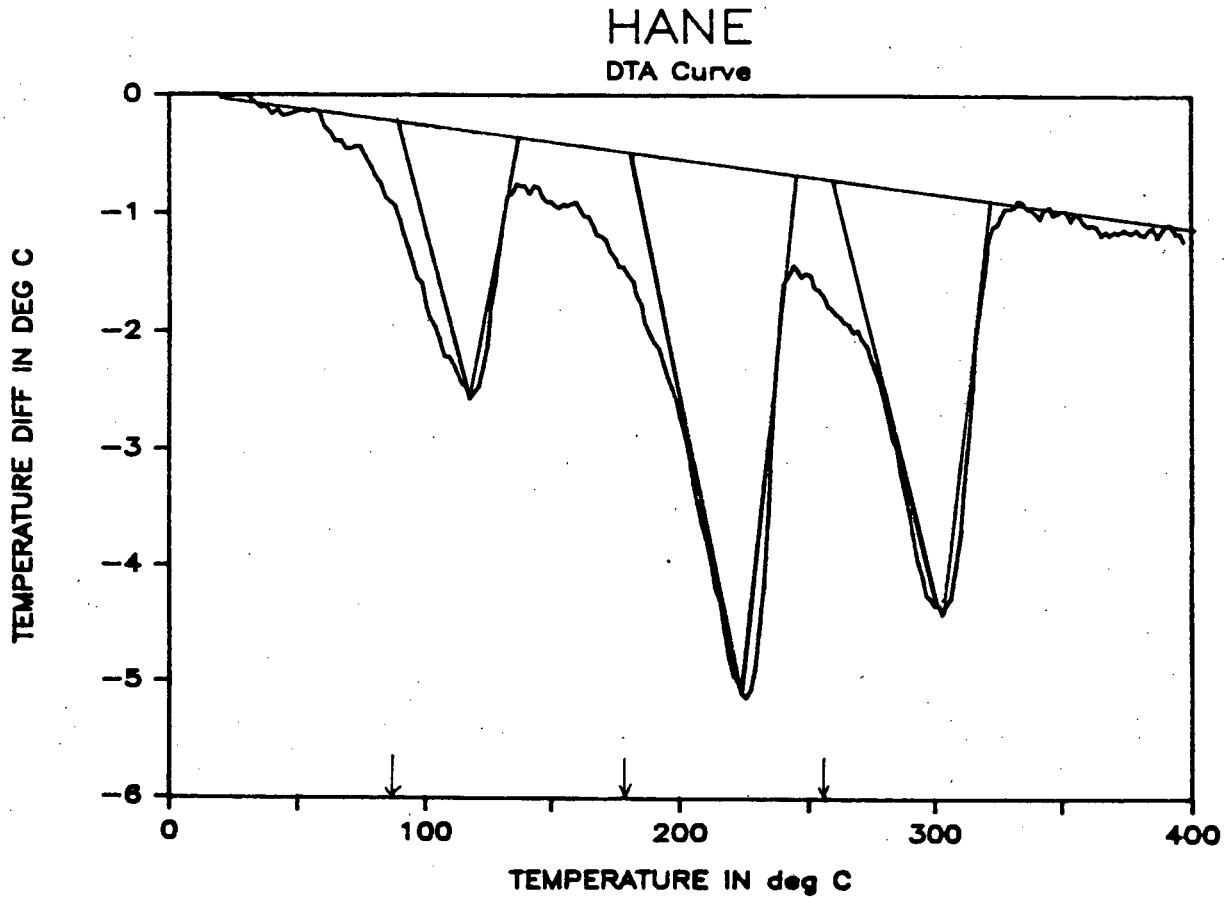

Figure 6.4.2 Construction of baseline.

The temperature at which the recorder response is at its maximum distance from the baseline (T_{max} in figure 6.4.1) is not reported because it is very dependent upon the heating rate and factors such as sample size and thermocouple position. In DTA curves the baseline may initially be displaced from zero owing to asymmetry in the sample and reference holders, and the mismatching in thermal properties of the sample and reference materials. Thus it is not always easy to determine the thermal events in the sample which are detected by deviations of the signal from the baseline. After decomposition was complete the response did not return to its original position because the thermal properties of $[Ni(NCS)_2]$ are different from those of the original sample.

For each sample the baseline was constructed as indicated in figure 6.4.2. Once a satisfactory baseline had been defined the area under each endotherm could be obtained. When two thermal events could not be separated the areas were estimated by extrapolation of the steepest slope to the baseline. Measurement of these chosen areas was carried out by the cutting and weighing method. The values obtained, A_s (cm^2), are listed in table 6.4.1. This measured sample area is then assumed to be proportional to the enthalpy changes, $\triangle H$, associated with structural changes and chemical reactions[6.7].

$$\triangle H = A_s \times K/m_s \qquad \text{II}$$

where m_s is the sample mass (g) and

K is a calibration factor (J/cm^2).

The calibration factor was determined by relating the known enthalpy change for the melting of pure naphthalene (naph) to the measured

peak area of this enthalpy change.

$$K = H_{melt,naph} \times \frac{mass_{naph}}{A_{naph}}$$

$$= 0.319 \text{ J/cm}^2$$

The heating rate used in the temperature programme and its sensitivity range do not enter the calculations as they are the same for all standards and samples. With the calibration factor K being temperature dependent samples with higher melting points and known enthalpy changes were used. Organic samples with melting points in the temperature range 150 °C to 450 °C were used as their thermal conductivity and heat capacity are similar to the clathrate samples with host decomposition in this temperature range. However the organic compounds used gave impurity peaks and/or additional peaks of phase changes which overlapped with the melting point peaks and/or had unknown enthalpy changes for the phase transitions. This resulted in naphthalene giving the only reliable calibration factor.
In this study the enthalpies associated with guest release are the most important, with the melting point of naphthalene (80-81 °C) falling within this range. The enthalpies of the host decomposition were also calculated using naphthalene as the standard, as only large differences in enthalpy change values can be considered as significant because of the inherent difficulties in establishing accurate areas under the endotherms.

6.4.2 Results and discussion.

The TG and DTA curves are shown in figure 6.4.3 with the results summarised in table 6.4.1.

The TG curves show that the mechanism of decomposition is:

$$[Ni(NCS)_2(4\text{-ViPy})_4].nG(s)$$

STEP 1 ↓

$$[Ni(NCS)_2(4\text{-ViPy})_4](s) + nG(g)$$

STEP 2 ↓

$$[Ni(NCS)_2(4\text{-ViPy})_2](s) + 2(4\text{-ViPy})(g)$$

STEP 3 ↓

$$[Ni(NCS)_2](s) + 2(4\text{-ViPy})(g)$$

where: nG = total guest molecules.

The DTA experiments were used to evaluate the sample temperatures and enthalpies of each step in the decomposition mechanism outlined above.

Structure 3 deviates from the above decomposition sequence with the third % weight loss step (step X) not accountable to any reasonable chemical intermediate. Structure I T has the lowest guest release temperature of 21 °C confirming the difficulty encountered when trying to mount a single crystal. According to the above mentioned classification all these clathrates are unstable with the guest

molecules being released before host decomposition. This confirms that the guests are not strongly enclosed by the host. The variation in sample temperatures and the values obtained for the areas under the endotherms representing the host decomposition indicate the varying amounts of damage caused by the guest release. The values obtained for the enthalpy associated with the removal of the first two bases is always higher than those obtained for the removal of the remaining two bases. This indicates that the two base intermediate is less stable than the four base complex. The dark, yellowish-brown powder left remaining at the end of each thermal analysis resembled that described for $[Ni(NCS)_2]$ as determined by the thermal analysis of $[Ni(NCS)_2(NH_3)_4]$ under N_2[6.8].

TABLE 6.4.1 THERMAL ANALYSIS RESULTS.

	% WEIGHT LOSS		SAMPLE TEMP[a]	AREA	△H	△H TOTAL
	calc	meas	(°C)	(cm^2)	(kJ/mole)	
1 HANE						
step 1	19.8	17.5	38	1.7	37	
step 2	48.1	45.0	137	3.9	86	
step 3	76.4	71.0	217	3.3	72	195
2 HENE						
step 1	19.8	13.0	47	1.1	26	
step 2	48.1	42.0	143	4.3	102	
step 3	76.4	68.0	217	3.9	92	220
3 DIEN3						
step 1	11.4	11.0	41	1.0	21	
step 2	42.7	44.0	137	4.4	92	
step X	-	67.0	223	2.4	50	
step 3	74.0	76.5	301	0.8	17	180
4 DIEN4						
step 1	15.5	14.0	64	1.5	33	
step 2	45.3	44.5	140	3.9	87	
step 3	75.2	72.0	232	2.6	58	178

5 THF/BEN						
step 1	15.3	13.0	49	2.4	52	
step 2	45.2	43.0	139	5.6	121	
step 3	75.1	69.5	232	3.9	84	257
6 BEN						
step 1	28.2	21.0	38	2.1	55	
step 2	53.6	48.0	121	3.6	94	
step 3	78.9	72.0	216	2.8	73	222
I T						
step 1	19.5	16.5	21	1.6	38	
step 2	47.9	45.0	137	4.5	107	
step 3	76.4	72.0	223	4.0	95	240

[a]As obtained from the DTA curves and corrected for by equation I.

Figure 6.4.3 Thermograms of structures 1 to 6 and I.

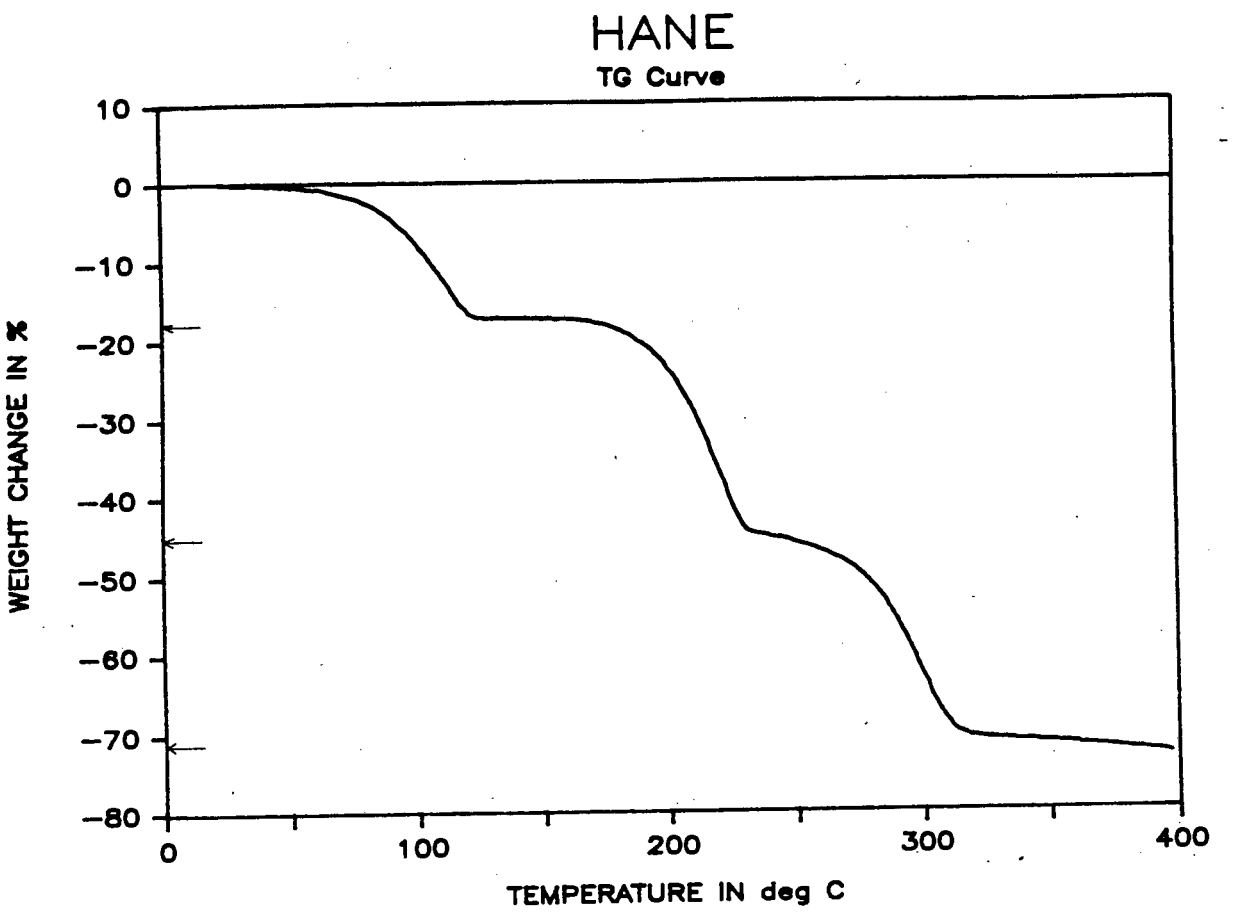

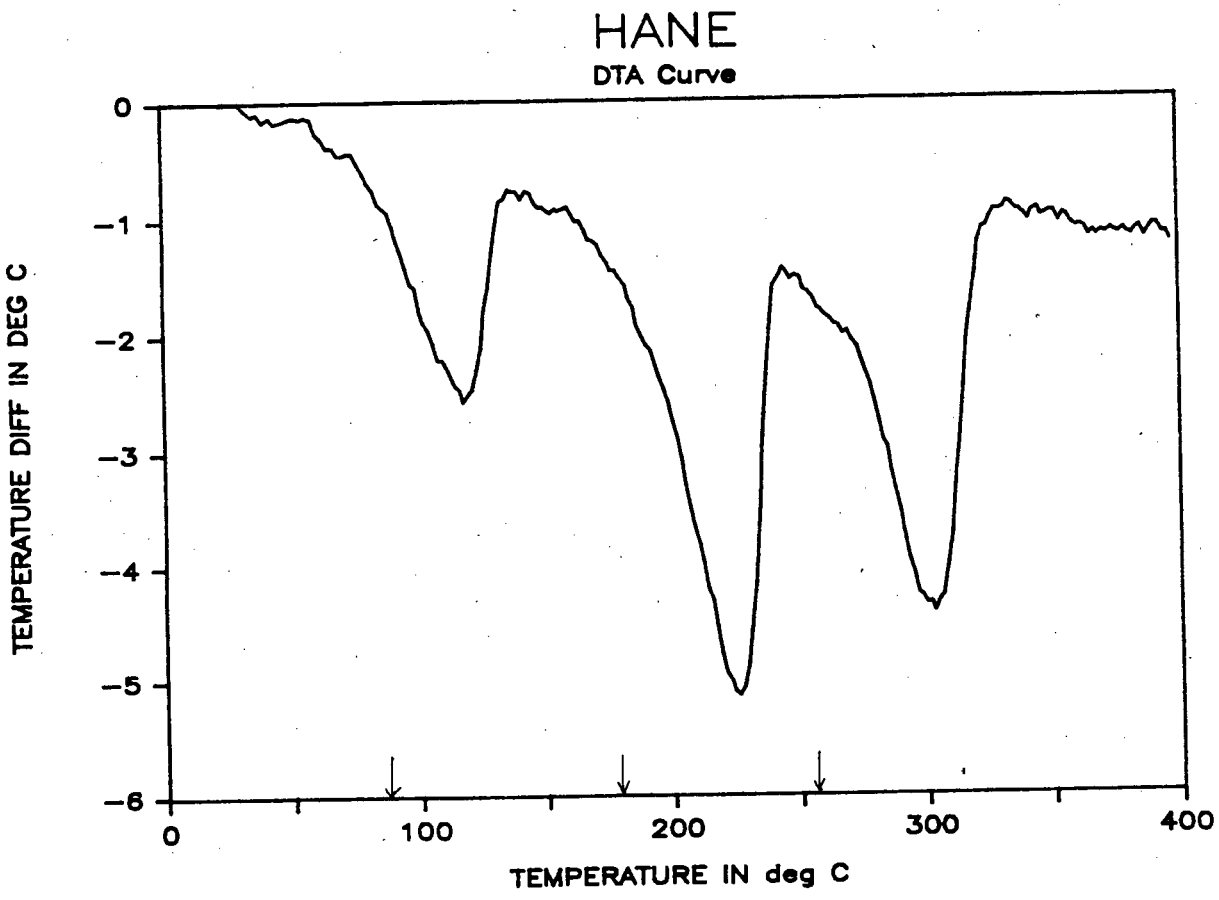

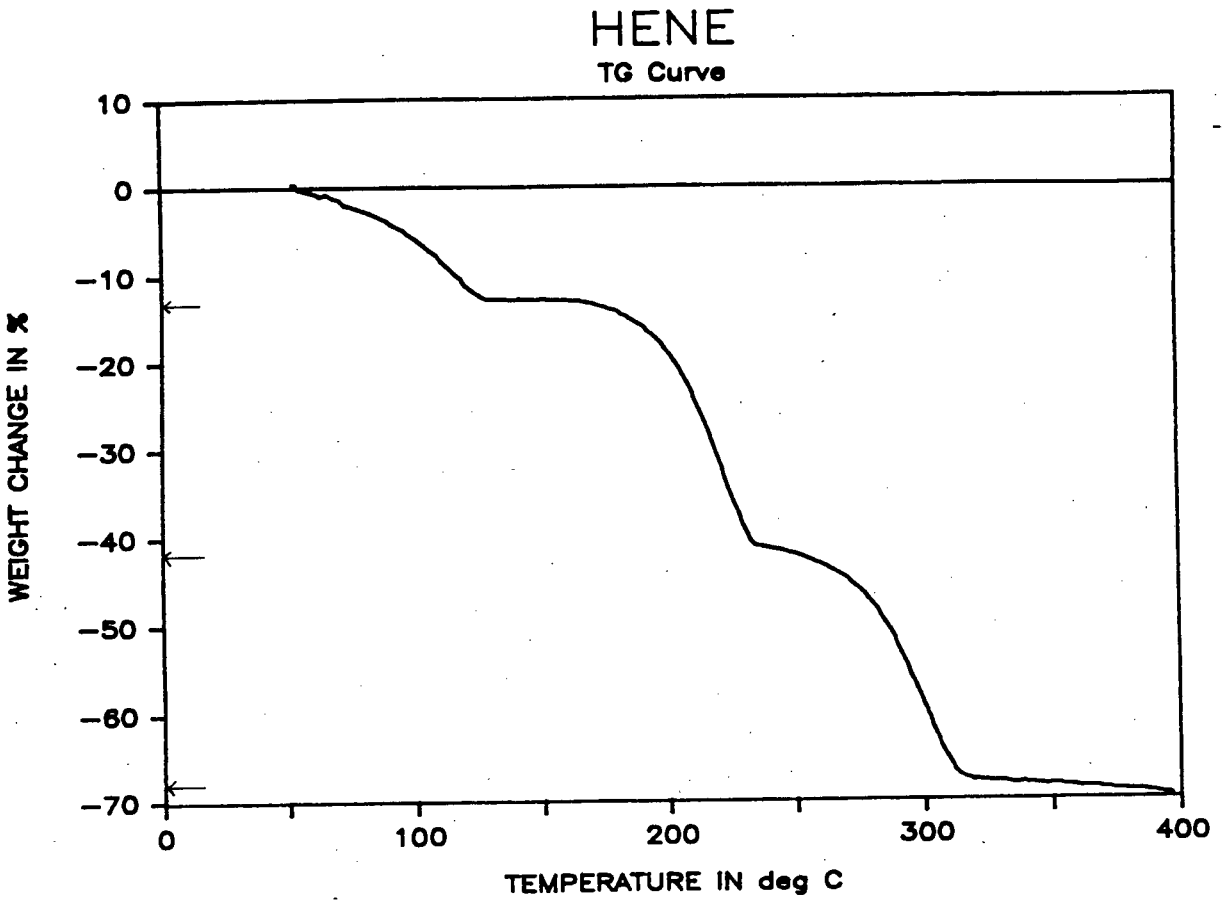
HENE
TG Curve
WEIGHT CHANGE IN %
10
0
-10
-20
-30
-40
-50
-60
-70
0
100
200
300
400
TEMPERATURE IN deg C

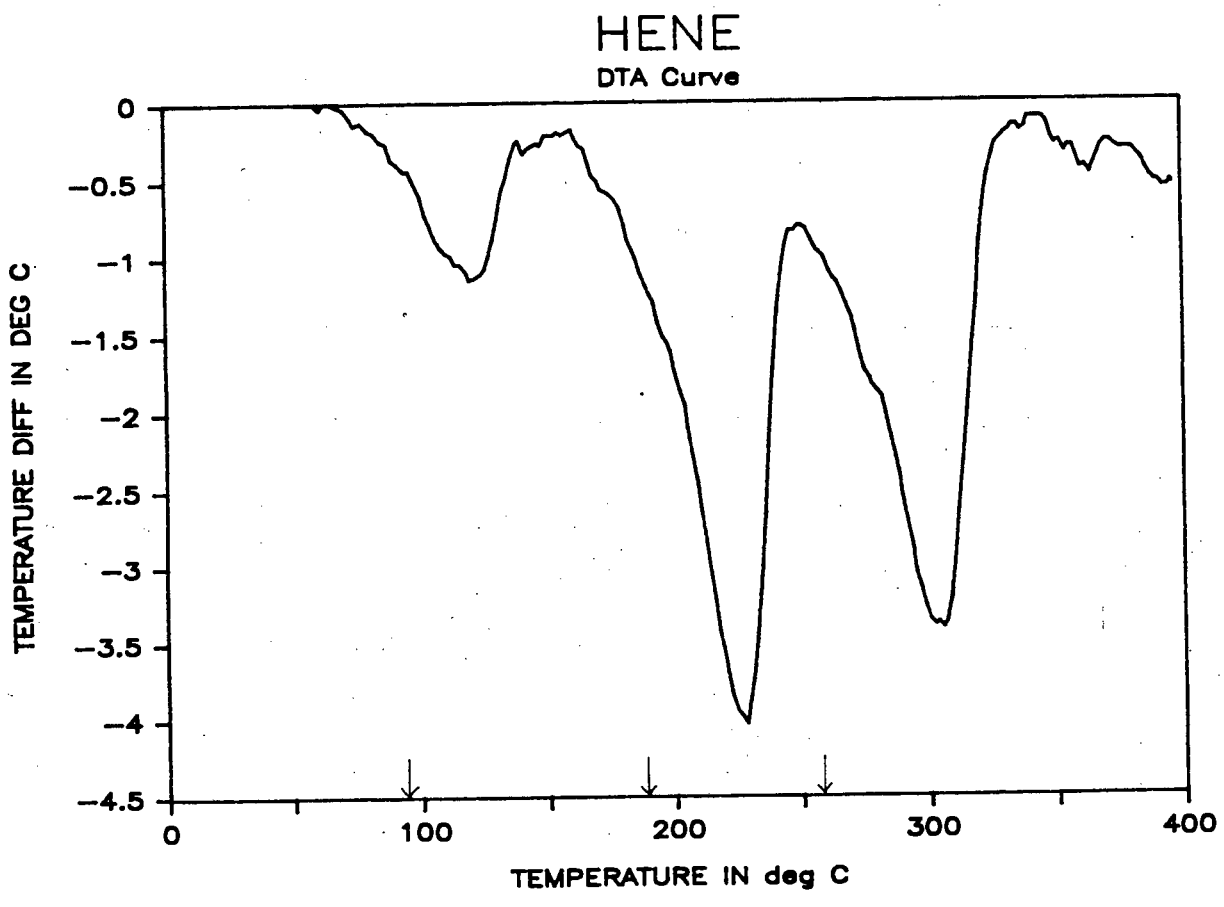
HENE
DTA Curve
TEMPERATURE DIFF IN DEG C
0
-0.5
-1
-1.5
-2
-2.5
-3
-3.5
-4
-4.5
0
100
200
300
400
TEMPERATURE IN deg C

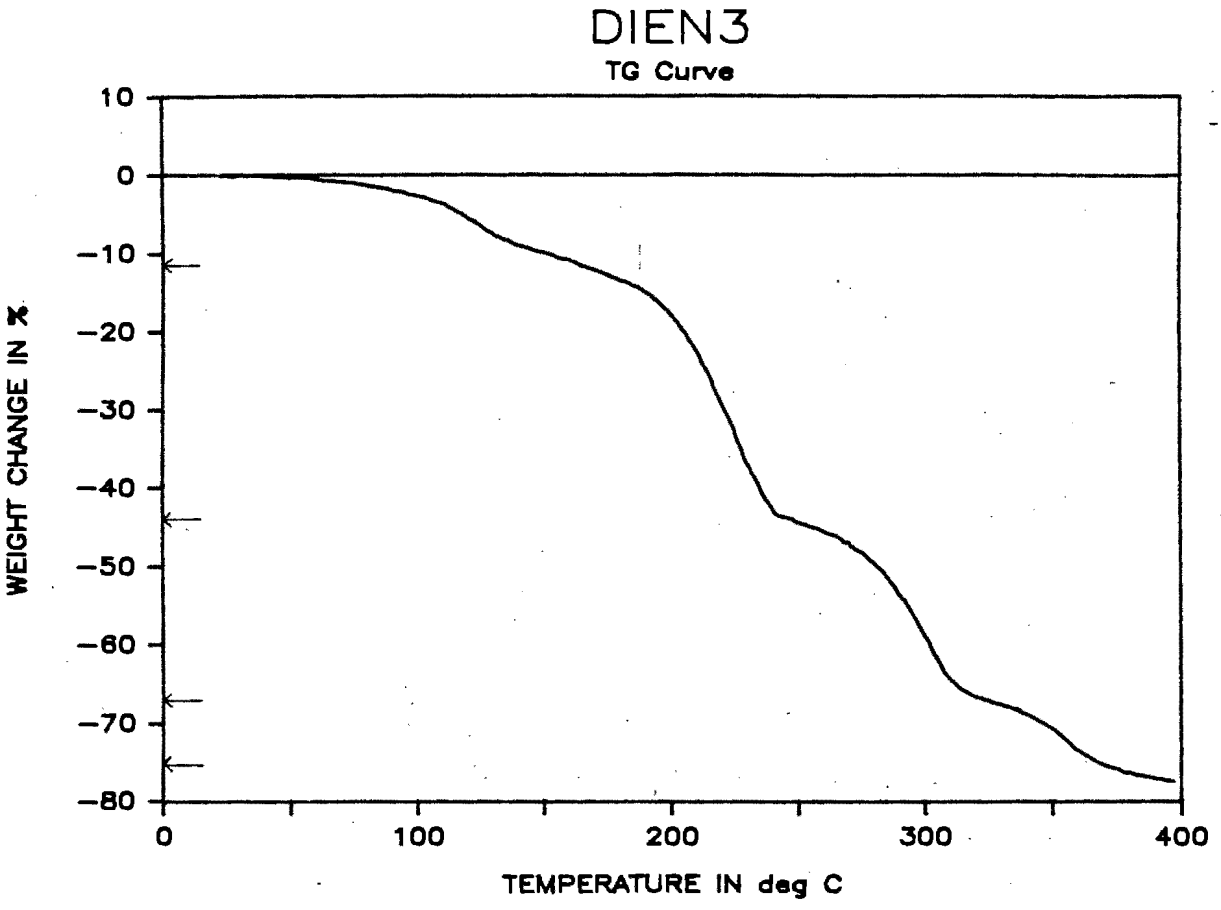
DIEN3
TG Curve
WEIGHT CHANGE IN %
10
0
−10
−20
−30
−40
−50
−60
−70
−80
0
100
200
300
400
TEMPERATURE IN deg C

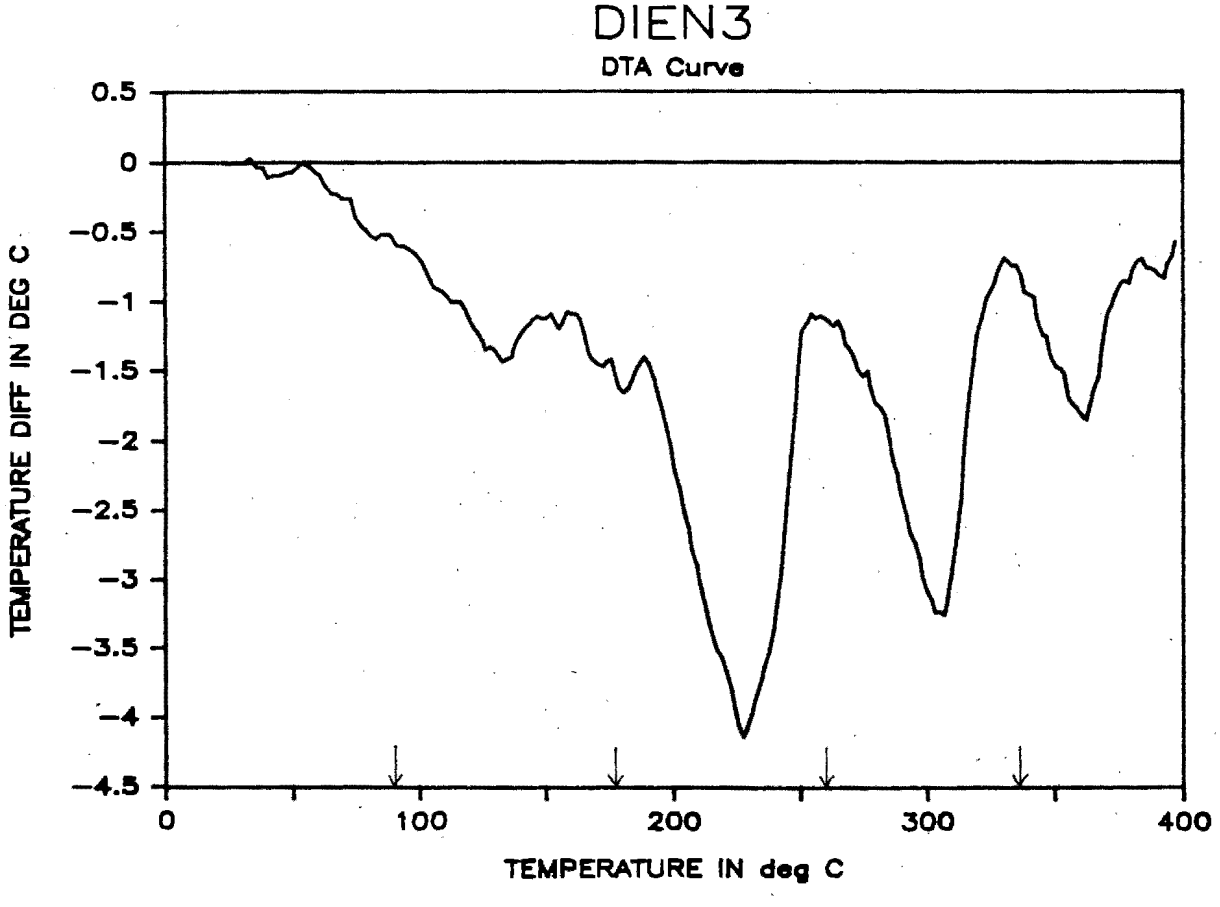
DIEN3
DTA Curve
TEMPERATURE DIFF IN DEG C
0.5
0
−0.5
−1
−1.5
−2
−2.5
−3
−3.5
−4
−4.5
0
100
200
300
400
TEMPERATURE IN deg C

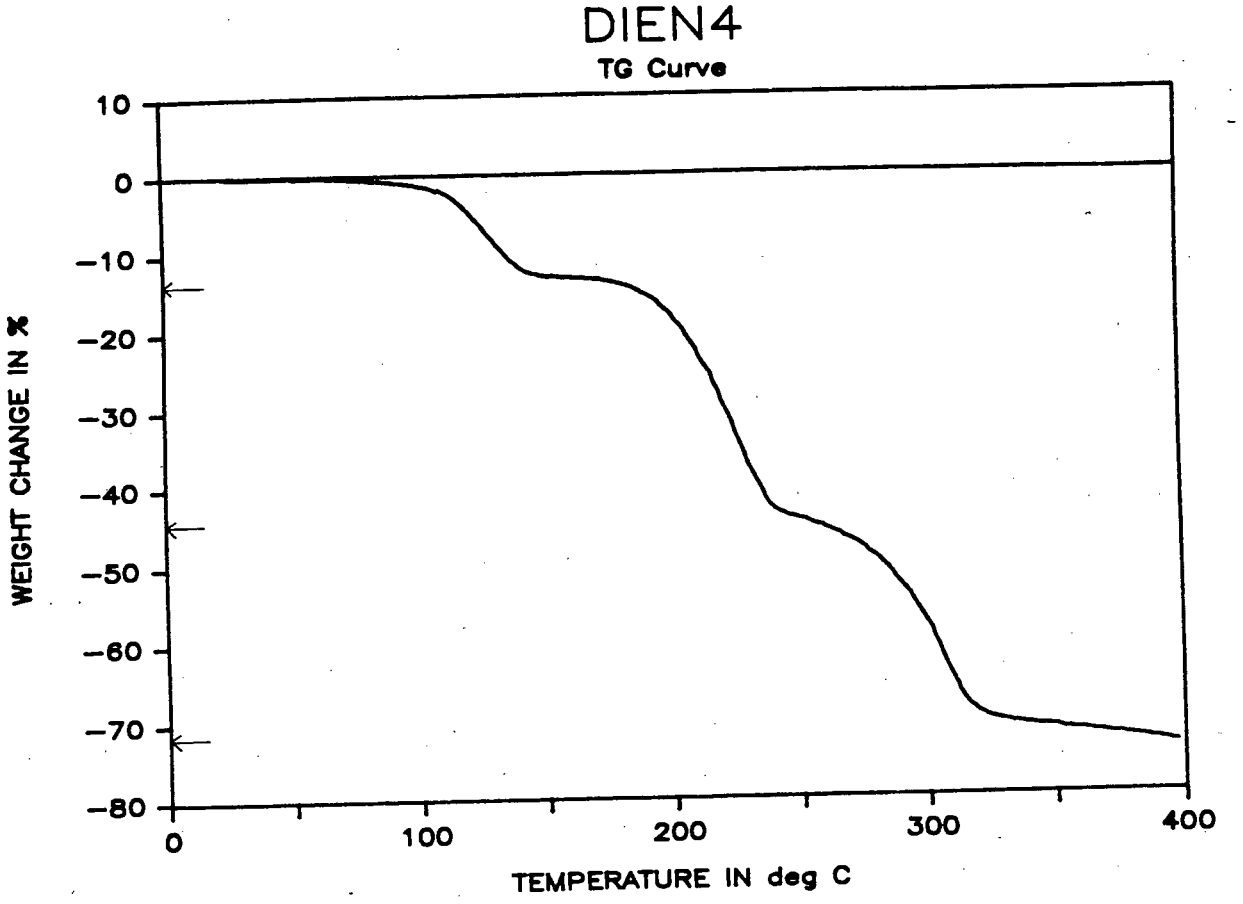
DIEN4
TG Curve
WEIGHT CHANGE IN %
10
0
-10
-20
-30
-40
-50
-60
-70
-80
0
100
200
300
400
TEMPERATURE IN deg C

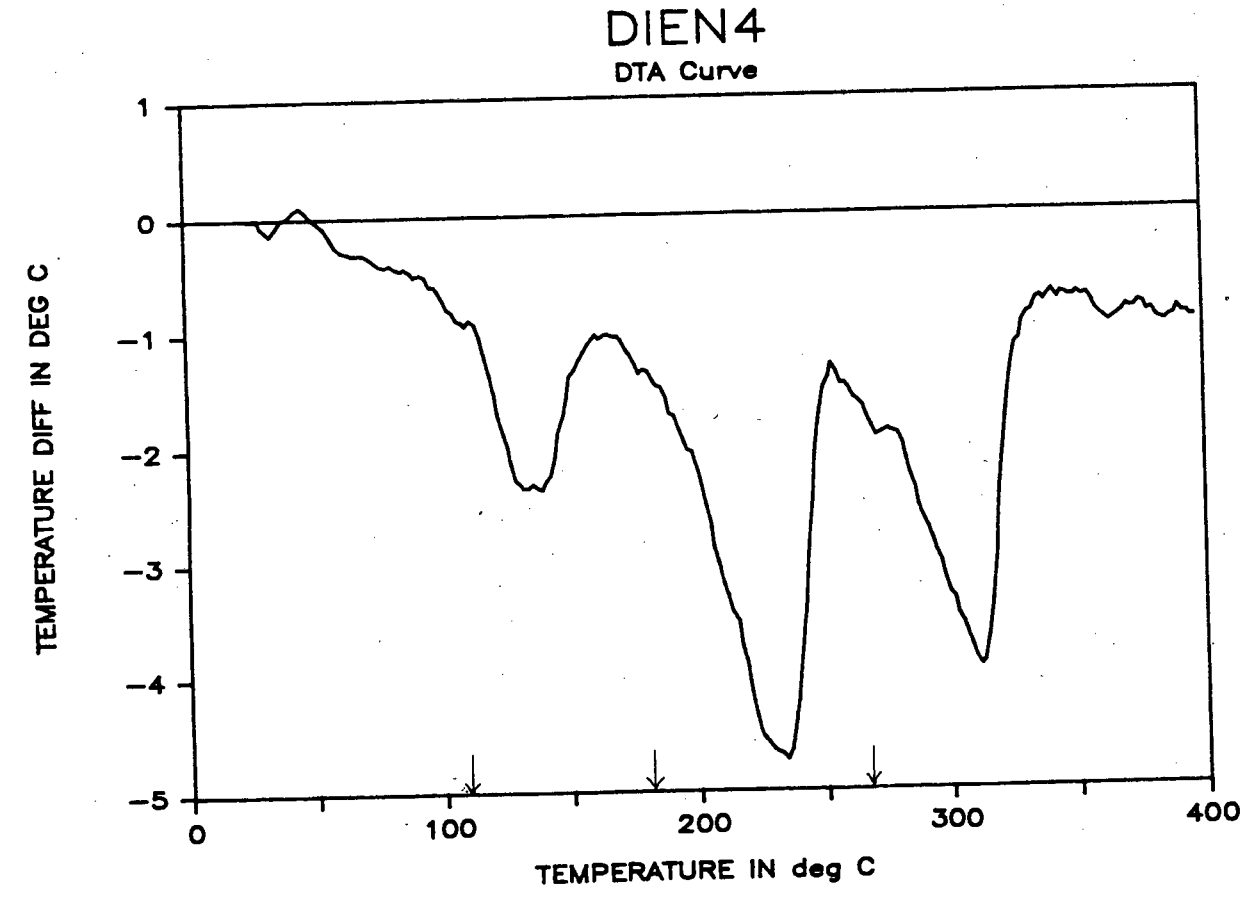
DIEN4
DTA Curve
TEMPERATURE DIFF IN DEG C
1
0
-1
-2
-3
-4
-5
0
100
200
300
400
TEMPERATURE IN deg C

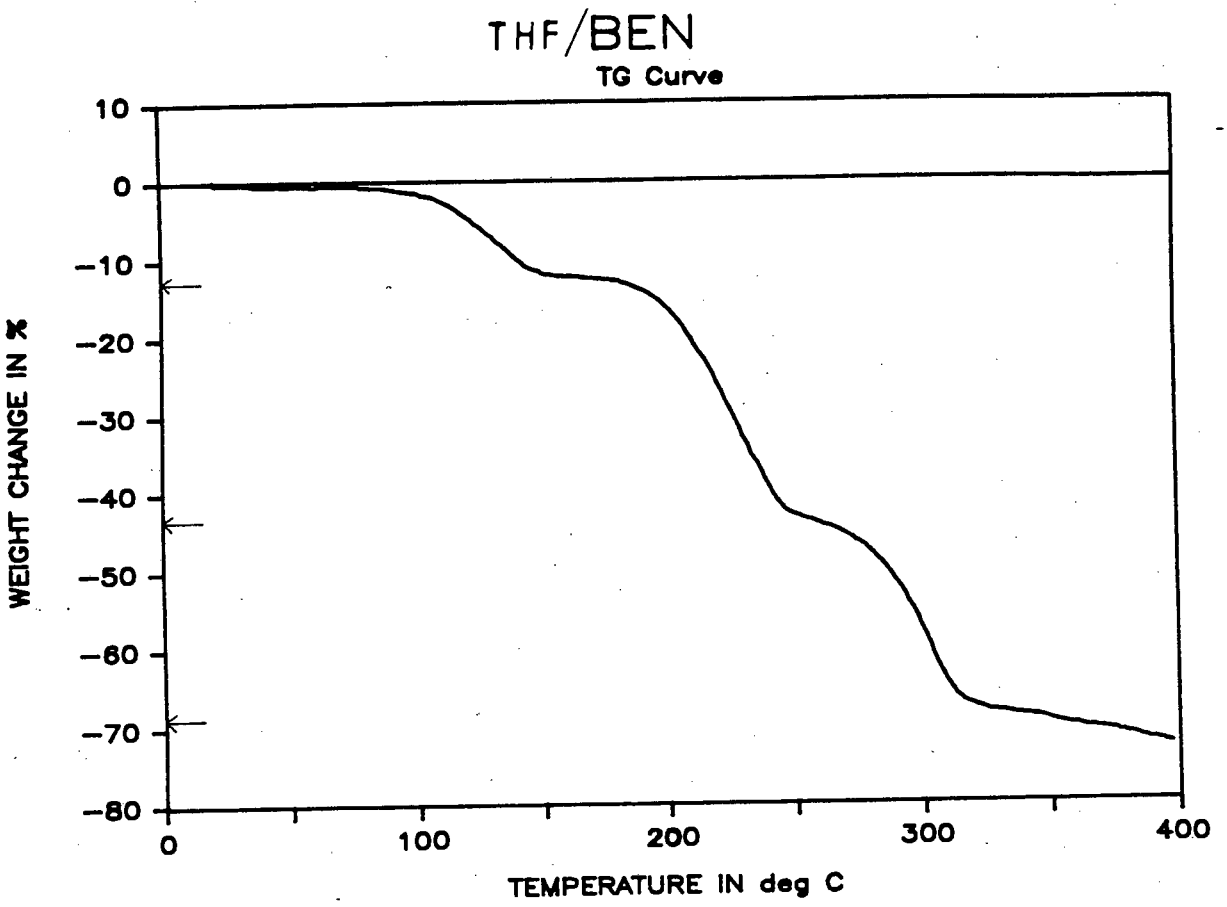
THF/BEN
TG Curve
WEIGHT CHANGE IN %
10
0
-10
-20
-30
-40
-50
-60
-70
-80
0
100
200
300
400
TEMPERATURE IN deg C

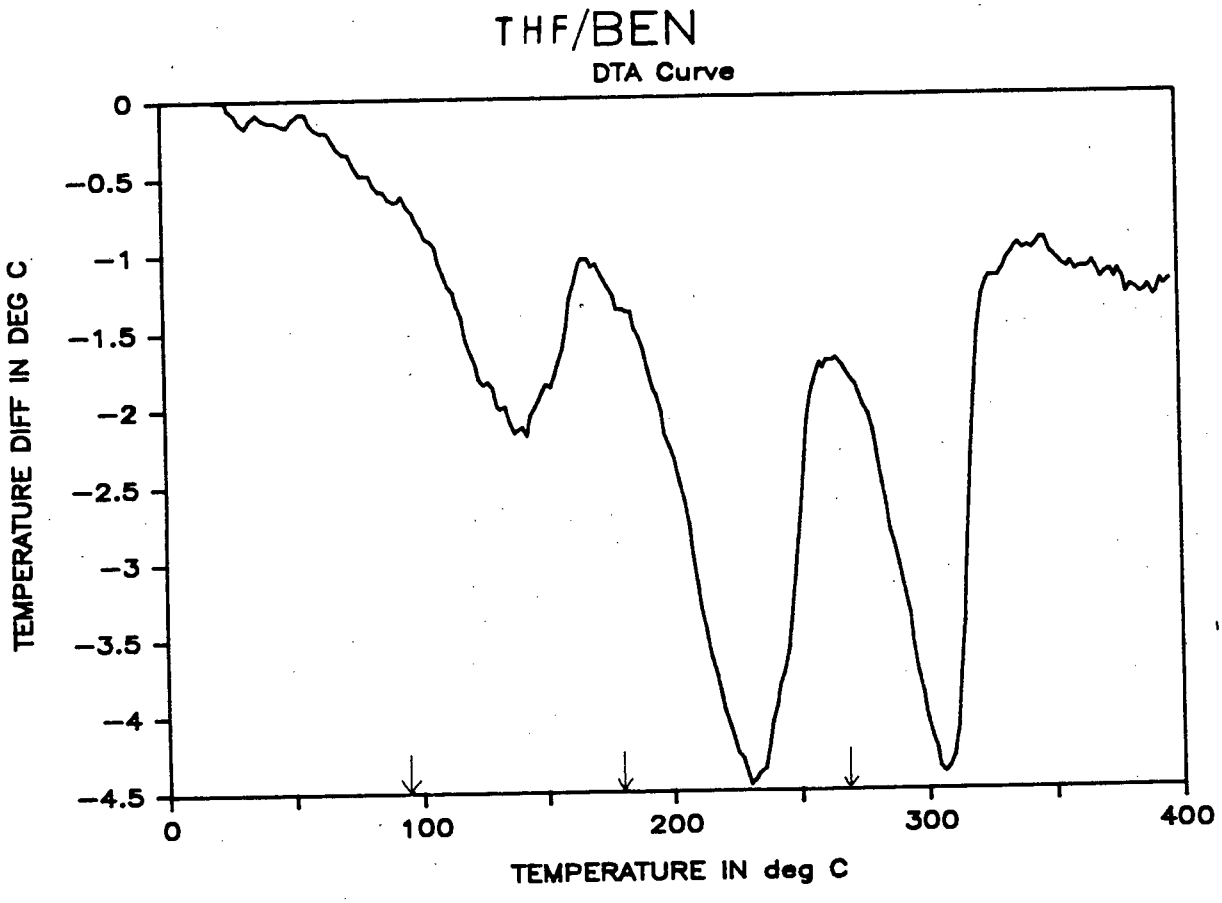
THF/BEN
DTA Curve
TEMPERATURE DIFF IN DEG C
0
-0.5
-1
-1.5
-2
-2.5
-3
-3.5
-4
-4.5
0
100
200
300
400
TEMPERATURE IN deg C

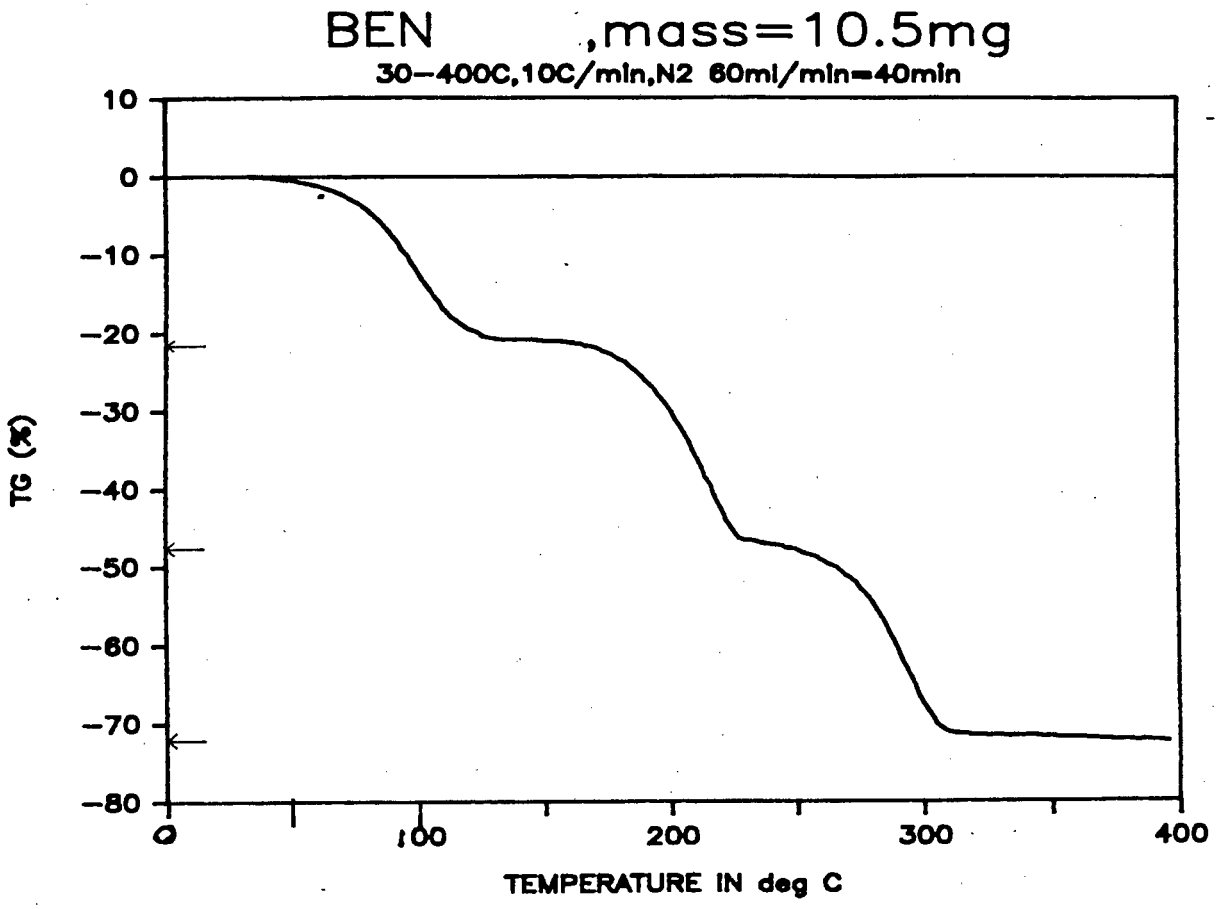
BEN ,mass=10.5mg
30-400C,10C/min,N2 60ml/min=40min
TG (%)
10
0
-10
-20
-30
-40
-50
-60
-70
-80
0
100
200
300
400
TEMPERATURE IN deg C

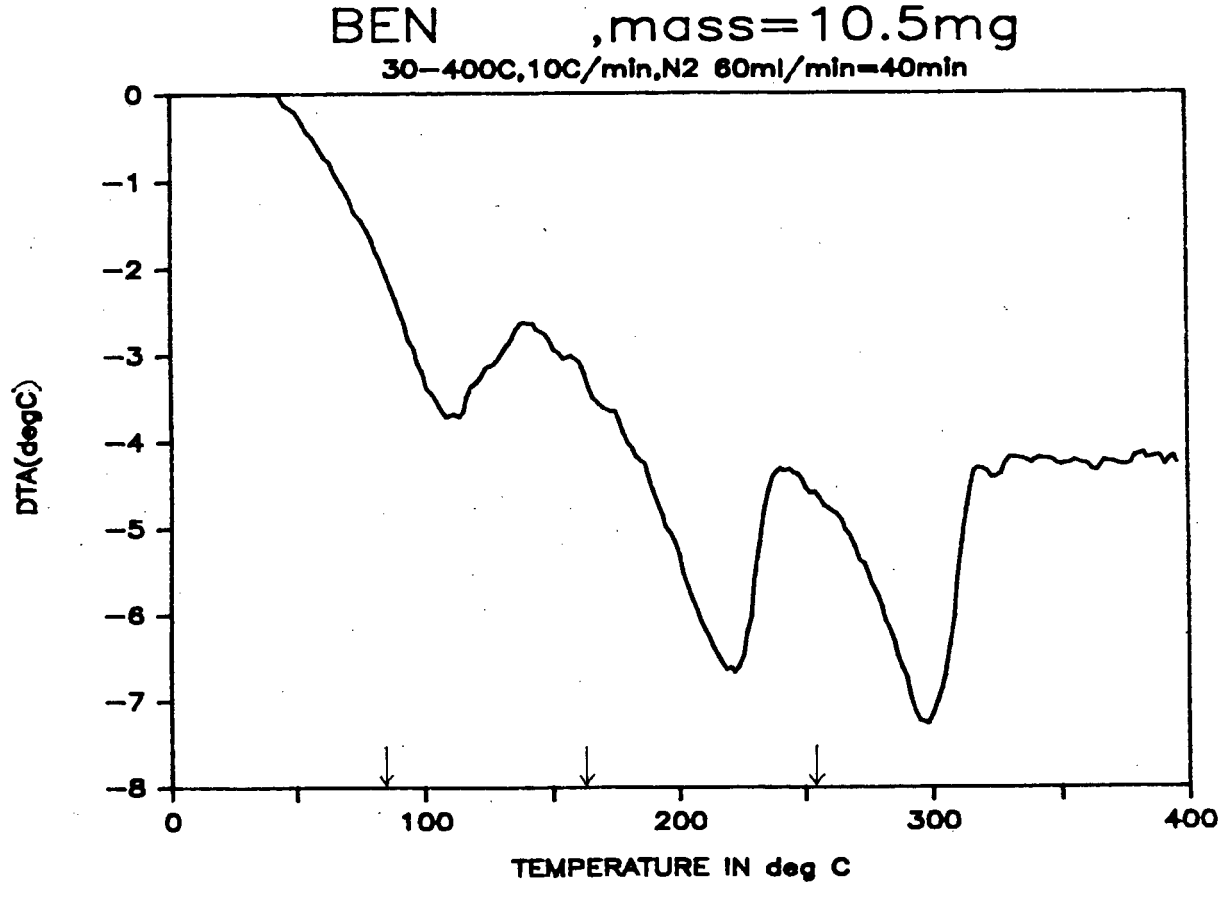
BEN ,mass=10.5mg
30-400C,10C/min,N2 60ml/min=40min
DTA(degC)
0
-1
-2
-3
-4
-5
-6
-7
-8
0
100
200
300
400
TEMPERATURE IN deg C

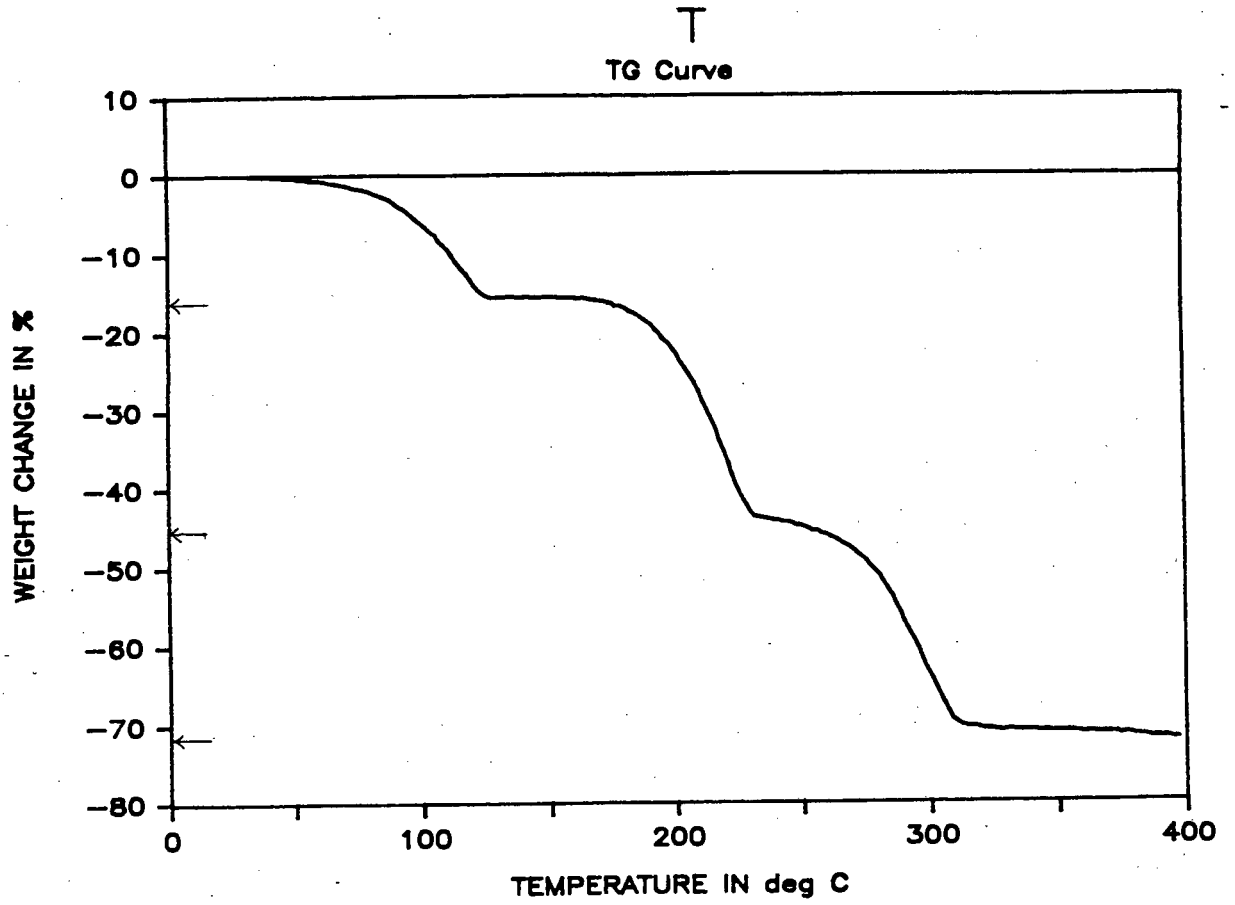
T
TG Curve
10
0
−10
−20
−30
−40
−50
−60
−70
−80
WEIGHT CHANGE IN %
0
100
200
300
400
TEMPERATURE IN deg C

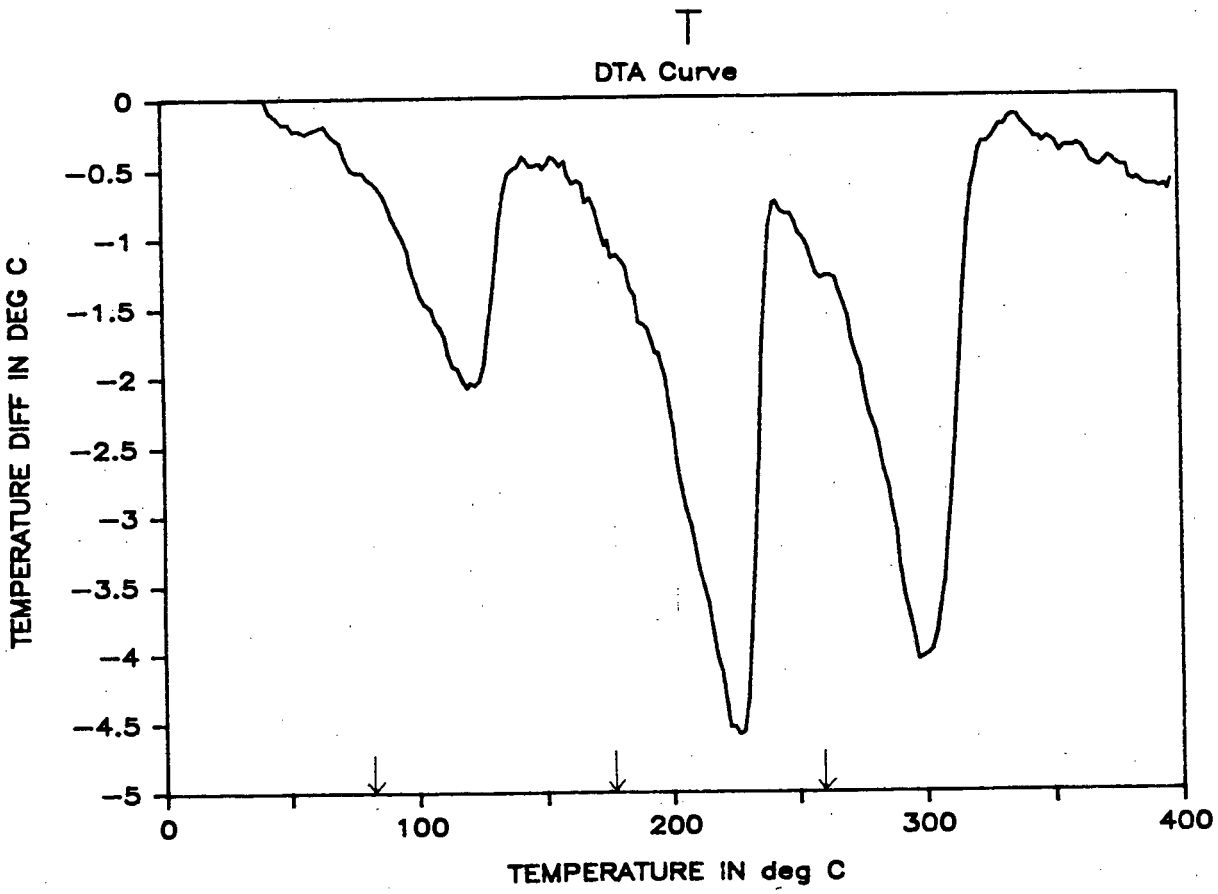
T
DTA Curve
0
−0.5
−1
−1.5
−2
−2.5
−3
−3.5
−4
−4.5
−5
TEMPERATURE DIFF IN DEG C
0
100
200
300
400
TEMPERATURE IN deg C

6 REFERENCES

6.1 W. W. Wendlandt and J. P. Smith: The Thermal Properties of Transition Metal Amine Complexes, Elsevier, New York (1967).

6.2 G. Beech, C. T. Mortimer and E. G. Taylor: J. Chem. Soc. A, 925 (1967).

6.3 E. Jona, T. Sramko and J. Gazo: Chem. Zvesti 27, 145 (1973).

6.4 M. H. Moore, L. R. Nassimbeni and M. L. Niven: Inorg. Chem. Acta. 131, 45 (1987).

6.5 F. Cassellato and B. Casu: Erdol Kohle Erdgas Petrochem 22, 71 (1969).

6.6 L. R. Nassimbeni, M. L. Niven and A. P. Suckling: Inorg. Chem. Acta., in publication.

6.7 M. E. Brown: Getting Started in Thermal Analysis, Rhodes Univ., Grahamstown (1985).

6.8 E. Dubler, A. Reller and H. R. Oswald: Zeitschrift fur Kristallographie 161, 265 (1982).

CHAPTER 7

Selective Criteria

7.1 Review of structures with [Ni(NCS)$_2$(4-ViPy)$_4$] as host.

For structures 1 to 5 the percentage of THF included decreased from 89% guest to 25% guest with a corresponding percentage increase of the second guest. Structures 1 and 2 with small amounts of the second guest and structure T with THF only, all crystallise in space group Pbcn. The decrease of included THF from 88% to 48% and inclusion of guests with the shape of an approximate hexagon causes the host to crystallise in a different space group, I4$_1$/a. For these structures the volume of the guests is a more significant characteristic as the guests are disordered. This space group remains for three structures with the percentage THF decreasing from 48% to 25%. The final structure (6) with benzene only crystallises in the space group P$\bar{1}$, with 6 guest molecules per unit cell.

For structures 1 to 5 and T they all have the guest THF in common and include approximately 8 molecules of guest per unit cell, with structures 4 and 5 deviating from this trend with 11 molecules of guest per unit cell.

In terms of maximum enclathrating ability the host to guest ratio of 1:3 is the highest observed with benzene as the only guest.

As originally stated, previous work with this host had shown THF to be a good solvent and not included as a guest. On this basis the

experimental work was undertaken to determine if the host $[Ni(NCS)_2(4\text{-}ViPy)_4]$ would enclathrate guests that varied systematically in one property only, that is THF would not be considered as a competitor. As part of the experimental procedure the tops of the crystal-containing vials (structures 4 and 5) were removed to facilitate crystal formation. In view of the results with mixtures of guests included, it is difficult to determine what effect this may have caused. If the preferential evaporation of the solvents has an effect on the ratio of guests included, this effect is consistent or possibly negligible, as nmr of structures 3, 4 and 5 were repeated some months later and were the same as the original results. These crystals were obtained by solvent evaporation for all three vials as opposed to the original crystals obtained where the vial containing crystal 3 had remained sealed.

A brief mention should be made concerning crystal formation with competition of two or more guests for one absorption center. In order to have a valid comparison of what may be called competition 'reactions' certain criteria should be met.

a) With prior knowledge of the possible number and shape(volume) of absorption sites (x) that are available to the competing guests there should be a minimum of x of each type of guest present in solution. That is for every x site there are two different guests competing. Alternatively a large excess ($\geq$x) of each guest in equal numbers would be considered an unbiased competition. Experimentally this may lead to solubility problems with the solution being too dilute to allow crystallisation.

b) Having satisfied a) crystallisation must occur without

evaporation. i.e. selective loss of one guest owing to its higher vapour pressure.

c) The host must be soluble in both guests (solvents) with the guests being miscible.

d) The property that is being selected should vary for the different guests with the other properties remaining constant, this being the hardest to fulfil with many properties being interrelated.

Taking structure 5 as an example inference cannot be made that the host is preferentially selective towards aromatic compounds. The volumes of THF and benzene used to dissolve the host powder did not take criterion a) into account. Crystal formation occurred after solvent evaporation. THF and benzene vary significantly in their dipole moments (1.63 D and 0.0 D, respectively) and aromatic nature and less significantly in their volumes 78.4 $Å^3$ and 88.2 $Å^3$.

In comparing structures 1 to 5 some inference may be made noting the experimental variations which were shown not to have an effect for structure 3. Obviously the reverse check for structures 4 and 5 could not be conducted as no crystals formed without solvent evaporation. In order to determine what property of the guests gave rise to the observed results, if any one property, the following properties of the guests in their pure state are listed and solubility studies of the host were performed.

dipole moments (μ) D; theoretical volume (Vol) $Å^3$ as calculated from reference[7.3]; density (ρ) $g.cm^{-3}$ at 20 °C; melting point (Mp) °C; boiling point (Bp) °C; vapour pressure (Pvap) mmHg at 25 °C [7.1, 7.2].

	πe^-	μ	Vol	ρ	Mp	Bp	P(vap)
cyclohexane	0	0.0	102.6	.778	6.5	81	98
cyclohexene	2	0.55	97.8	.810	-104	83	89
1,3-cyclohexadiene	4	0.44	93.0	.840	-98	80.5	-
1,4-cyclohexadiene	4	-	93.0	.847	-49	87	-
benzene	6[1]	0.0[2]	88.2	.877	5.5	80	95
tetrahydrofuran	0	1.63	78.4	.889	-108	66	162

[1] Forming an aromatic system with unique properties.

[2] On the grounds of molecular symmetry.

With the data available no systematic trend of the above properties could be correlated with the molecular ratios found in the crystals.

7.2 Solubility studies of the host $[Ni(NCS)_2(4\text{-ViPy})_4]$.

Solubility studies of the host in pure THF, cyclohexane, cyclohexene, 1,3-cyclohexadiene, 1,4-cyclohexadiene, benzene and 50% by volume mixtures of THF with cyclohexane, cyclohexene, 1,3-cyclohexadiene, 1,4-cyclohexadiene and benzene were performed. These solubility studies are illustrated in figure 7.1 as solubility curves. Each curve is a function of saturated solution (weight host powder per 100ml solvent) with temperature. The area below each curve represents

a two-phase system which contains saturated solution and undissolved host powder. Above each curve the solution is clear with no undissolved host powder and represents a one phase system. The temperature range is from 24 °C to approximately 64 °C with higher temperatures causing possible host breakdown as the solutions would change from their characteristic blue to a greenish colour.
The host was totally insoluble in pure cyclohexane and cyclohexene for the temperature range studied and is therefore not shown in figure 7.1. The host was insoluble in pure 1,3-cyclohexadiene and 1,4-cyclohexadiene at room temperature with the full temperature range not being studied owing to insufficient solvent. The host being insoluble in these liquids necessitated the use of THF as a solvent. Of all the guest properties the solubility curves show the only consistent characteristic which varies in the same manner as the guest ratios found in the crystalline state. As crystal formation occurred at approximately 25 °C (not temperature controlled) the solubility curves are studied in this region. For the 50% by volume mixtures the host is least soluble in THF/cyclohexane with increasing solubility for the series THF/cyclohexene, THF/1,3-cyclohexadiene, THF/1,4-cyclohexadiene and THF/benzene. In relation to the crystalline state it appears that as host solubility increases for each mixture, THF is excluded. It may be invoked that prior to crystallisation the more soluble solvents surround the host to a greater degree and are trapped by the host provided they have suitable molecular volumes. With the volume of THF remaining constant for each solubility curve the increased solubility can only be attributed to the second solvent. Thus in each crystallisation a greater number of the second solvent molecules surround the host and

are enclathrated to a greater degree in the process of crystallisation.

For the above experimental systems only, the interpretation invokes a 'gross' selection criterion with the ratio of solvent molecules surrounding the host molecules prior to crystallisation being enclathrated. However it is noted that structure 6 with pure benzene only has the highest host to guest ratio of 1:3 with the host being less soluble in pure benzene than pure THF which yielded a host to guest ratio of 1:2.

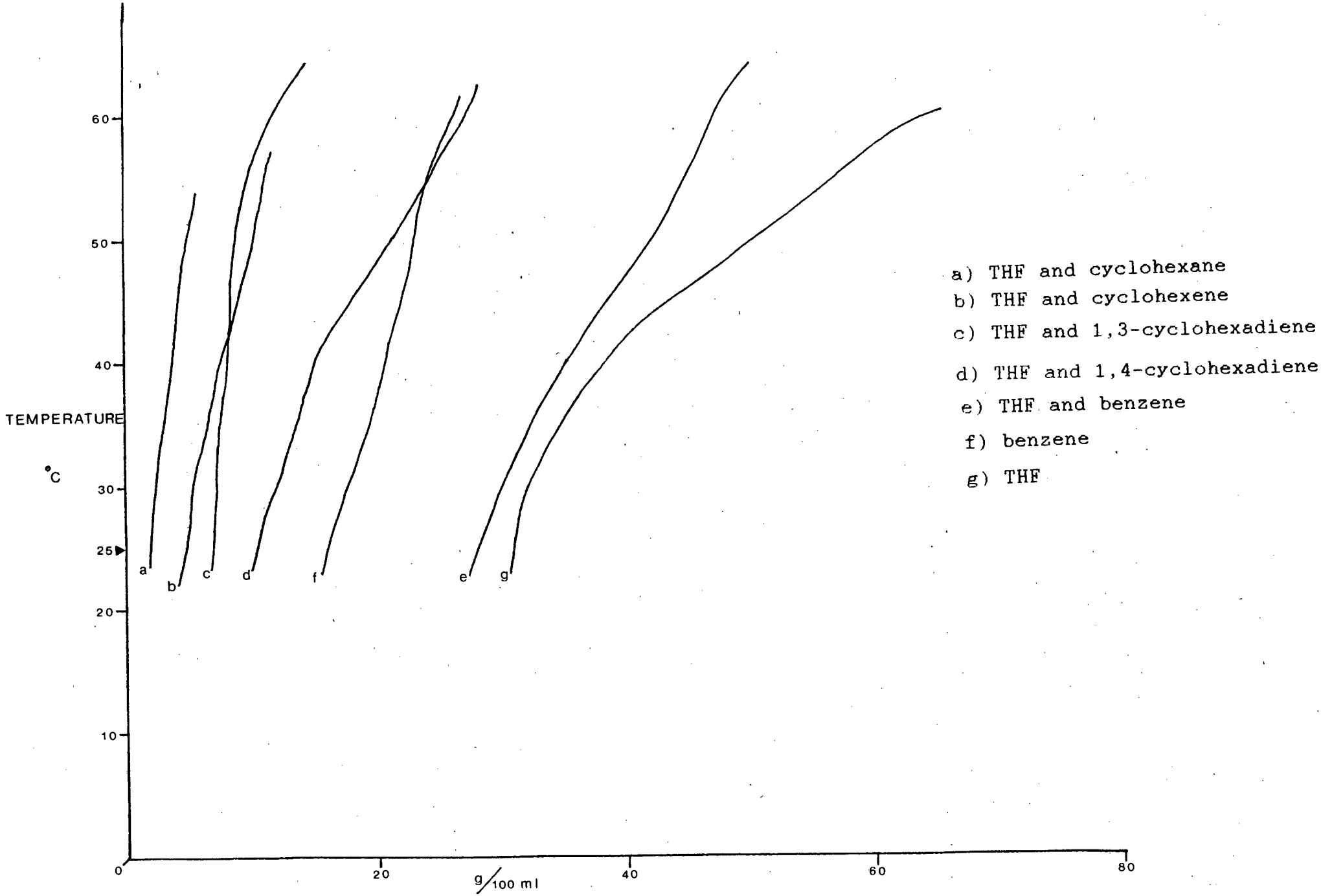

Figure 7.1 Solubility curves of $[Ni(NCS)_2(4\text{-ViPy})_4]$

7 REFERENCES

7.1 Lange's Handbook of Chemistry, Edited by J. A. Dean, 12th edition, McGraw-Hill Book Company, (1979).

7.2 CRC Handbook of Chemistry and Physics, 66th edition, CRC Press Inc. (1985).

7.3 A. I. Kitaigorodsky: Molecular Crystals and Molecules, Academic Press, New York, (1973).